International Society for the Advancement of Supercritical Fluids
(I.S.A.S.F.)

PROCEEDINGS

SEMINAR ON AEROGELS
Properties-Manufacture-Applications

6th – 7th December
2012

Université de Lorraine/ENSIC
NANC Y (France)

SEMINAR ON AEROGELS
Properties-Manufacture-Applications

DECEMBER 6-7, 2012

ENSIC-Nancy (France)

ORGANIZATION

CHAIRS

Prof. Irina SMIRNOVA
(TU Hamburg-Harburg, Germany)
e-mail : Irina.smirnova@tu-harburg.de
Dr. Michel PERRUT
(SEPAREX, Champigneulles, France)
e-mail : mperrut@separex.fr

CONTACT DETAILS

Secretary: Françoise BRIONNE
ISASF – ENSIC, 1 Rue Grandville – B.P. 451
F-54001 Nancy CEDEX – FRANCE
Phone/Fax : +33 (0) 3 83 17 50 03
e-mail: Francoise.brionne@ensic.inpl-nancy.fr
Website: http://www.isasf.net

CONFERENCE LOCATION

ECOLE NATIONALE SUPERIEURE DES INDUSTRIES CHIMIQUES (ENSIC)
1, Rue Grandville – F-54001 NANCY (France)

SCIENTIFIC PROGRAMME

THURSDAY 6 DECEMBER, 2012

9.00 – 13.30	**REGISTRATION** **ENSIC – AMPHI A**
9.00 – 11.00	**POSTER INSTALLATION** **ENSIC – Salle A1**
11.0 – 12.00	**POSTER SESSION** **ENSIC – Salle A1**
12 .00-13.30	**TIME FOR LUNCHEON**
13.30 – 14.00	**OPENING** **ENSIC – AMPHI A**
14.00 – 16.00	**SESSION 1 : ORGANIC AEROGELS** • **Cellulose/Polysaccharides-based :** **CO01 POLYSACCHARIDE-BASED AEROGELS AND THEIR AREAS OF APPLICATIONS.** **Smirnova I. and Garcia-Gonzalez C., TU Hamburg-Harburg** **CO02 AEROCELLULOSE, AEROGEL-LIKE CELLULOSE MATERIAL : PREPARATION, PROPERTIES AND POTENTIAL APPLICATIONS.** **Budtova T., CEMEF, MINES PARIS TECH, Sophia Antipolis (France)** **CO03 CELLULOSE AEROGELS CROSS-LINKED WITH GLYOXAL.** **Karadagli I., Milow B. and Ratke L., Institut für Materialphysik im Weltraum, Köln (Germany)** **CO04 SYNTHESIS AND CHARACTERIZATION OF MONOLITHIC *Kappa*-CARRAGEENAN AEROGELS.** **Ganesan K. and Ratke L., Institut für Materialphysik im Weltraum, Köln (Germany)** **CO05 AEROGEL HOLLOW TUBES FROM NATURAL-ORIGIN POLYSACCHARIDES AS TAILOR- MADE URINARY STENTS.** **Barros A.-A, Duarte A.-R., Pires R.-A., Mano J.-F. and Reis R.-L., University of Minho, Taipas (Portugal)** **CO06 AEROGELS FROM REGENERATED CELLULOSE : PROS AND CONS OF SELECTED CELLULOSE SOLVENTS** **Pircher N., Schimper C., Potthast A., Rosenau T. and Liebner F., University of Natural Resources and Life Sciences, Vienna (Austria)**
	BREAK AND POSTERS
17.00-18.20	**SESSION 1 : ORGANIC AEROGELS (CON'T)** • **Other Organic :** **CO07 GELATIONS KINETICS : SIZE EFFECT AND OTHER ISSUES** **Ratke L. and Milow B., Institut für Materialphysik im Weltraum, Köln (Germany)** **CO08 ELABORATION OF MONOLITHIC ORGANIC AEROGEL FROM LOW MOLECULAR WEIGHT ORGANOGEL : TOWARDS THERMAL INSULATORS.**

	Jamart-Grégoire B., Allix F., Son S., Pickaert G., LCPM/ENSIC, Nancy, Barth D., LRGP/NANCY, Jeannot Y., Felix V. and Degiovanni A., LEMTA, Lorraine University, Nancy (France) **CO09 AEROGELS FROM LIGNIN OBTAINED BY LIQUID HOT WATER TREATMENT OF WHEAT STRAW.** **Perez-Cantu L., Smirnova I., Hamburg University of Technology and Liebner F., University of Natural Resources and Life Sciences, Vienna (Austria)** **SESSION 2: AEROGEL MODELLING** **CO10 MODELLING OF PROCESSES WITH AEROGELS USING CELLULAR AUTOMATA.** **Menshutina N., Mendeleev University, Moscow (Russia)**
18.20 – 18.30	**ARTIST USING AEROGELS** **CO11 ART & SCIENCE RESEARCH ON THE ETHEREAL NANOMATERIAL SILICA AEROGEL, FOR A SUSTAINABLE URBAN DESIGN.** **Michaloudis I, Curtin University, Perth (Australia)**
18.30 – 19.45	**WALK IN THE OLD CITY TOWARDS DINNER**
19.45	**DINNER**
FRIDAY DECEMBER 7, 2012	
8.30 – 9.50	**SESSION 3: INORGANIC AEROGELS** **CO12 EFFECT OF THE SOLVENT USED ON SURFACE MODIFICATION ON THE SYNTHESIS OF AEROGELS DRIED UNDER AMBIENT PRESSURE** **García-Torres B.-A., Alvarez-Contresas L., Aguilar-Elguezabal A., Centro de Investigacion en Materiales Avanzados, S.C., CIMAV, Chihuahua and Enriquez F., Universidad Autónoma de Chihuahua (Mexique)** **CO13 BATCH AND CONTINUOUS ADSORPTION OF ACTIVE MOLECULES ON SILICA AEROGEL FROM SUPERCRITICAL SOLUTIONS.** **Caputo G., University of Salerno (Italy)** **CO14 THERMAL STABILITY OF HYDROPHOBIC XEROGELS AND AEROGELS SYNTHESIZED FROM MTMS.** **Afonso S., Matias T., Portugal A., Durães L., University of Coimbra (Portugal) and Ochoa M., Active Space Technologies, Coimbra (Portugal)** **CO15 MINERAL AEROGELS FOR ENERGY APPLICATIONS** **Rigacci A. and Beauger C., CEP, Mines Paris Tech, Sophia Antipolis (France)**
9.50 – 10.40	**BREAK AND POSTERS**
10.40 – 12.00	**SESSION 4 : COMPOSITE AEROGELS**

	CO16 ORGANIC/INORGANIC HYBRID LOW DENSITY XEROGELS. **Noisser Th., Börner M. and Reichenauer G., Bavarian Center for Applied Energy Research, Würzburg (Germany** **CO17 INORGANIC-ORGANIC HYBRID AEROGELS.** **Ramaswamy A.-P., Ratke L., Institut für Materialphysik im Weltraum, Köln (Germany) and Soraru G.-D., University of Trento (Italy)** **SESSION 5: AEROGEL MANUFACTURE** **CO18 DRYING OF AEROGELS WITH SUPERCRITICAL CO_2.** **Lack E., Seidlitz H., Sova M. and Lang jr.-F., Natex Prozesstechnologie, Ternitz (Austria)** **CO19 A NEW CONCEPT FOR AEROGEL DRYING PROCESS SCALE-UP.** **Ruiz-Gonzalez F., Français E., Perrut M., SEPAREX, Champigneulles (France)**
	LUNCH BREAK
14.00 – 16.00	**INFORMAL TALKS**

ORAL COMMUNICATIONS

Session 1: ORGANIC AEROGELS

Session 2 : AEROGEL MODELLING

ARTIST USING AEROGELS

Session 3 : INORGANIC AEROGELS

SESSION 4 : COMPOSITE AEROGELS

SESSION 5: AEROGEL MANUFACTURE

Session 1: ORGANIC AEROGEL

Cellulose/Polysaccharides-based

CO01

POLYSACCHARIDE-BASED AEROGELS AND THEIR AREAS OF APPLICATIONS

C.A. García-González; I. Smirnova

[a] *Institute of Thermal Separation Processes, Hamburg University of Technology, Hamburg (Germany), email: irina.smirnova@tuhh.de*

ABSTRACT

In this paper an overview about the synthesis and application of polysscharides-based aerogels is given. Natural polymer-based (bio-based) materials have the great advantage of being a renewable and suitable feedstock for environmentally sustainable processes. Besides, these systems are biodegradable, biocompatible and biologically stable.

These properties make natural polymers, specially polysaccharides, promising for a wide range of life sciences applications, going from agricultural (e.g., pesticides) to pharmaceutical (e.g., drug delivery systems) including food and biotechnology industries. Focusing on delivery systems for chemicals, especial materials are needed with not only the aforementioned properties, but also with high loading capacities. Aerogels based on organic precursors have highly porous, light-weighted structures with large surface areas.

In this work, the preparation of aerogels from different natural polymer precursors, especially polysaccharides, (starch, lignin, pectin, alginate, chitosan) was carried out. Aerogels were produced from hydrogels obtained by the sol-gel technology, followed by the supercritical drying of the gels. The processing method was adapted to the different gelation mechanisms of the precursors (thermotropic, ionotropic, covalent binding). The end materials showed a porous structure with surface areas ranging from 100 to 700 m^2/g and densities from 0.05 to 0.5 g/cm^3.

This technique thus allows the development of tailor-made materials with controlled properties by the selection of the proper organic precursor. Emulsion techniques were coupled to the processing approach to obtain aerogels in the form of microspheres. Step-by-step (emulsion+gelation → solvent exchange → supercritical drying) process optimization led to light-weight ($\rho \approx 0.1$-0.5 g/cm^3), spherical aerogel particles (10-100 μm) with high specific surface areas (100-700 m^2/g). The obtained product was specifically assessed for its use as a drug carrier. Loading by supercritical CO$_2$-assisted impregnation of a model drug was attempted with excellent results (15-20 wt.% drug loaded using starch aerogel microparticles as the matrix). Further the modeling of the supercritical drying for these materials is discussed.

CO02

AEROCELLULOSE, AEROGEL-LIKE CELLULOSE MATERIAL: PREPARATION, PROPERTIES AND POTENTIAL APPLICATIONS

Tatiana Budtova*, Roxane Gavillon, Romain Sescousse, Cyrielle Rudaz

Center for Material Forming (CEMEF)[1], Mines ParisTech, UMR CNRS 7635

BP 207, 06 904 Sophia Antipolis Cedex, France

Tatiana.Budtova@mines-paristech.fr

Polysaccharides, being abundant natural polymers, are very promising candidates for the development of novel environmentally friendly porous bio-based materials. One way to synthesise highly porous polysaccharides is partly inspired by aerogel preparation route: polymer dissolution in a solvent followed by coagulation in a non-solvent and drying in supercritical CO_2.

We prepared and characterised cellulose-based aerogel-like materials, called “Aerocellulose” (Figure 1), with density around 0.05-0.2 g/cm^3 and specific surface of several hundreds of m²/g. Different solvents for cellulose dissolution were used: 8%NaOH-water /1-3/, ionic liquids such as 1-ethyl-3-methylimidazolium (EMIMAc) /4/ and EMIMAc mixed with co-solvent, dimethylsulfoxide. Cellulose was coagulated in water or in ethanol and dried in supercritical CO_2. Various shapes can be obtained (Figure 2).

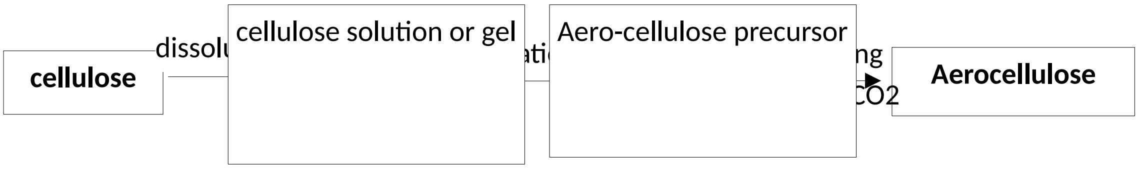

Figure 1. Schematic presentation of the main steps of Aerocellulose preparation

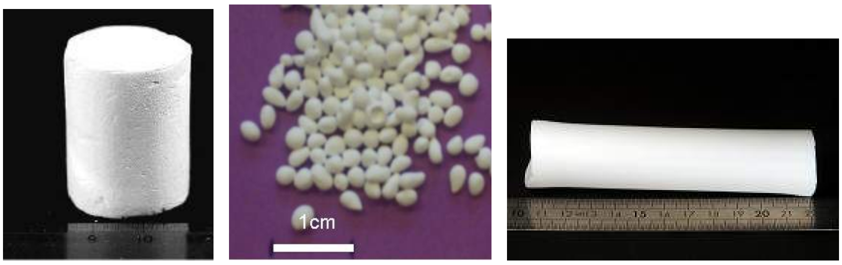

Figure 2. Aerocelluloses of various shapes: from cylinders to beads

The influence of cellulose concentration, solvent and type of non-solvent on aerocellulose morphology will be presented (Figure 3). The problems that arise during aerocellulose characterisation will be discussed.

---

[1] Member of the European Polysaccharide Network of Excellence (EPNOE), www.epnoe.eu

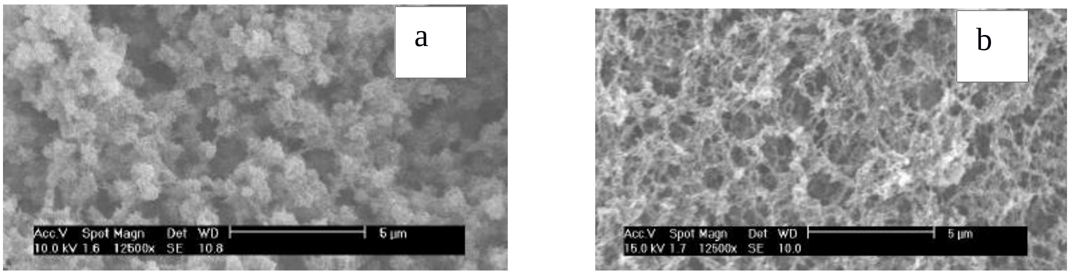

Figure 3. Aerocellulose morphology: (a) from cellulose-EMIMAc and (b) from cellulose-NaOH-water solutions

Aerogel-like materials made from another polysaccharide, pectin, will also be briefly presented and compared with Aerocellulose.

Acknowledgements

The research leading to these results has received funding from the European Union Sixth Framework Programme FP6 under grant agreement No. NMP3-CT2003-505888, “Aerocell” project; French National Research Agency (ANR), projects “Carbocell” N ANR-06-MAPR-0004 and “Nanocell” ANR-09-HABISOL-010 and national French competitive clusters Capenergie, Tenerrdis and Derbi.

We should like to thank P.Ilbizian (CEP, Mines ParisTech, Sophia-Antipolis, France) for supercritical drying.

REFERENCES

1 R. GAVILLON, T. BUDTOVA, “Aerocellulose: new highly porous cellulose prepared from cellulose-NaOH aqueous solutions”, *Biomacromolecules*, *9*, 269-277 (2008).

2 R. SESCOUSSE, T. BUDTOVA « Influence of processing parameters on regeneration kinetics and morphology of porous cellulose from cellulose-NaOH-water solutions”, *Cellulose*, 16(3), 417-426 (2009).

3 R. SESCOUSSE, R.GAVILLON, T. BUDTOVA “Wet and dry highly porous cellulose beads from cellulose-NaOH-water solutions: influence of the preparation conditions on beads shape and encapsulation of inorganic particles”, *Journal of Materials Science*, 46, 759-765 (2011)

4 R. SESCOUSSE.; R. GAVILLON, T. BUDTOVA, “Aerocellulose from cellulose-ionic liquid solutions: preparation, properties and comparison with cellulose-NaOH and cellulose-NMMO routes”, *Carbohydrate Polymers*, *83*, 1766-1774 (2011).

CO03

CELLULOSE AEROGELS CROSS-LINKED WITH GLYOXAL

Ilknur Karadagli, Barbara Milow and Lorenz Ratke

Institut für Materialphysik im Weltraum, Deutsches Zentrum für Luft- und Raumfahrt (DLR), Linder Höhe, 51147 Köln, Germany.

Abstract

This study explores the preparation of cellulose aerogels from microcrystalline cellulose and comparing structural modification with and without glyoxal as a cross-linker. The cellulose wet gels were synthesized by dissolving microcrystalline cellulose (1, 3 and 5 wt.%) in a calciumthiocyanate salt melt hydrate-$Ca(SCN)_2.4H_2O$ at 110˚C. Wet gels were washed and regenerated in an ethanol bath. The aerogels were dried supercritically with carbon dioxide ($scCO_2$). Crosslinking with an aqueous 40 wt.% glyoxal solution was performed using aluminum sulfate as a catalyst at various concentrations of glyoxal with respect to cellulose in the ethanol regeneration bath.

The morphology and structure of cellulose aerogels were characterized using scanning electron microscopy (SEM), nitrogen adsorption/desorption analysis and pore size distribution (BET) and thermogravimetric analysis (TGA). Mechanical behavior of cellulose aerogels was investigated in compression tests. Thermal conductivity of cellulose aerogels was determined at atmospheric pressure and room temperature. The envelope density of the samples varied between 20-140 g/cm^3. Nitrogen adsorption analysis gave specific surface areas of 150-297 m^2/g.

The microstructure can be described as an open porous nano-felt with pore sizes ranging from 10 to 100 nm and fiber diameters of around 10-20 nm (Figure 1). Thermal conductivity of cellulose aerogels varies linearly with cellulose concentration from 0.04 to 0.075 W/m.K. The mechanical behavior is typical for a porous material: after onset of deformation there is a long plateau at almost constant stress. The aerogels exhibit a Poisson ratio of around zero. The Young’s modulus is 8.4 MPa for the 3 % cellulose aerogel and cross-linking of cellulose aerogels with glyoxal improves the compression strength of cellulose aerogel by approximately 50 %.

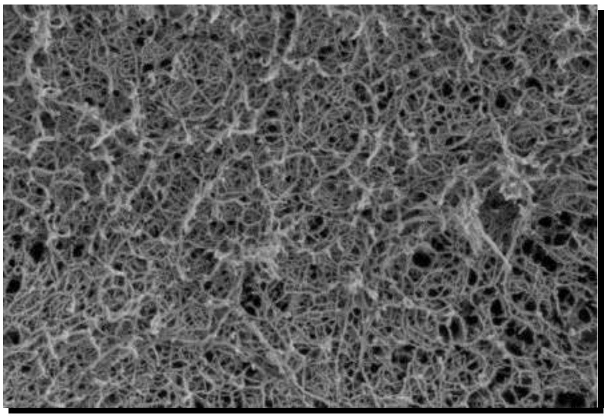

Figure1. SEM picture of a cellulose aerogel cross-linked with glyoxal

---

CO04

SYNTHESIS AND CHARACTERIZATION OF MONOLITHIC *K*-CARRAGEENAN AEROGELS

Kathirvel Ganesan and Lorenz Ratke
Institute of Materials Physics in Space, German Aerospace Center, Linderhöhe 51147, Cologne, Germany.

Abstract

Aerogels of *k*-carrageenan were synthesized and their properties were investigated by envelope density analyzer, scanning electron microscopy and N_2 adsorption-desorption analysis. The concentrations of *k*-carrageenan were varied between 0.5 and 3 wt %. Aerogels showed volume shrinkage, 55-65 %, depending upon the concentration of *k*-carrageenan. The envelope density was in the range between 42-160 $kg.m^{-3}$. For all concentrations, the specific surface area of aerogels was about 225 $m^2.g^{-1}$. The interconnected fibrillar structures of aerogel and fibre thickness were characterized by scanning electron microscope.

Introduction

Aerogels based on polysaccharides have attracted great attention in many research fileds including drug delivery cycle, separation techniques, textile applications, tissue engineering and catalysis due to their abundance in renewable natural source, ease of production, biocompatibility and biodegradability [1-7]. Among many aerogels based on polysaccharides, only few which have cationic or anionic functional groups could be used as host for applications where high chemical affinity to guest atoms/molecules is in demand. For instance, the carboxylate anion in alginate matrix coordinated to Pd metal can be used as catalyst for Suzuki reaction [2].

Carrageenans are a group of naturally available anionic polysaccharides having sulfate functional groups. Those are extracted from red marine algae. In their family, there are three major forms of carrageenans commercially available which are named as *kappa*- or *k*-, *iota*- or *i*- and *lambda*- or λ-carrageenan. They are widely used in food industries as thickening and stabilizing agent especially in dairy products [8] and can also be used in enzyme immobilization and catalysis [9].

The monomer unit in polymeric structure of *k*-Carrageenan is shown in Figure 1. It has a sulfate functional group per disaccharide unit and forms hard gel in the presence of potassium, rubidium or caesium ion. It is soluble in hot aqueous solution above 80 °C. After cooling below mid-point temperature T_m, depending upon the concentration of cation, it forms gel due to its structural transition from coil to helix and aggregation of helices [8, 10].

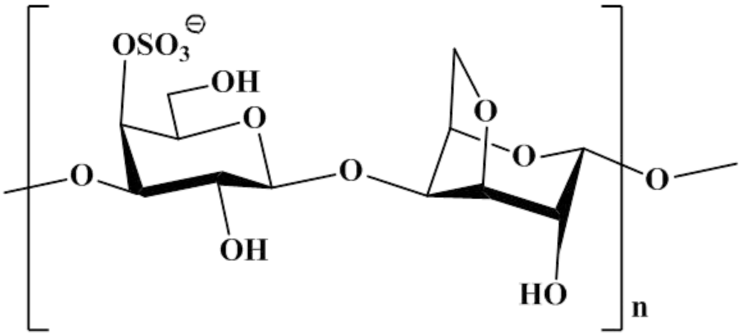

Figure 1: Chemical structure of *k*-carrageenan polymer.

Quignard et al. has reported *k*-carrageenan aerogels in the form of micro-beads, comprising the properties of mesoporous structure with narrow pore size distribution, having 95 % shrinkage from its gel volume [11]. Monolith form of *k*-carageenan aerogel could be of interests in industries, may provide a wide spectrum of applications like other polysaccharides calcium alginate and cellulose aerogels due to their renewable source, presence of anionic sulfate functional group and gelling nature. In this paper, we report preparation and characterization of monolith form of *k*-carrageenan aerogels.

Materials and methods

For the preparation of hydrogels, deionized water was used. All chemicals have been used as received. Organic solvents with a grade of Normapur were used for solvent exchange. Supercritical drying was carried out in an autoclave using pure carbon dioxide (CO_2), following the procedure reported by Hoepfner et al [12]. The following instruments were used to analyze the materials: envelope density by Micromeritics - GeoPyc 1360, BET nitrogen adsorption isotherm by Micromeritics - Tristart II 3020, scanning electron microscope images from Merlin – Carl Zeiss Microscope.

Synthesis of aerogels

Monolith form of *k*-carrageenan aerogels were synthesized by following three consecutive steps: 1) preparation of hydrogels; 2) solvent exchange; and 3) drying the gels under supercritical condition (**Fig. 2**).

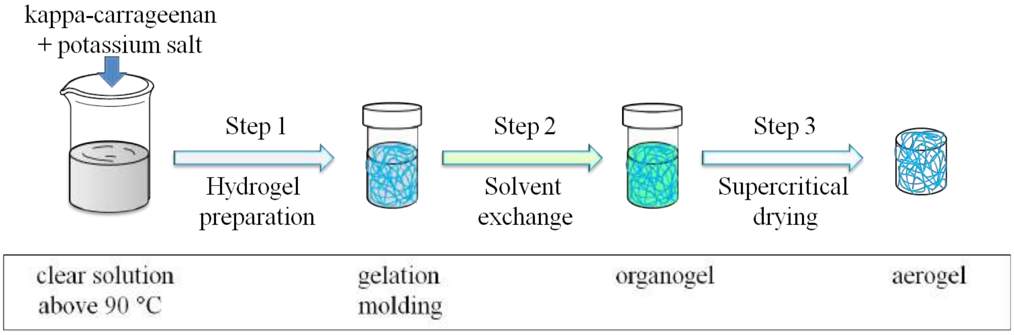

Figure 2: Schematic diagram illustrating the steps involved in synthesis of *k*-carrageenan aerogels.

Hydrogels were prepared by warming the aqueous solution of *k*-carrageenan in the presence of potassium ions above 90 °C, transferring the clear solution into the desired molds and cooling the solution to room temperature. After solvent exchange with polar organic solvents such as ethanol or acetone, the gels were dried under supercritical condition. The concentrations of *k*-carrageenan were varied from 0.5 to 3 wt %. The monolith form of aerogel is shown in Figure 3.

Figure 3: Image showing the monolith form of *k*-carrageenan aerogel (3 wt %).

Results and discussion

A linear plot was observed for the volume shrinkage of aerogels with respect to the concentration of *k*-carrageenan (**Fig. 4**). The higher concentration of *k*-Carrageenan (3 wt %) exhibits less shrinkage about 55 % after drying the gels whereas the lower concentration (0.5 wt %) showed maximum shrinkage of 65 %.

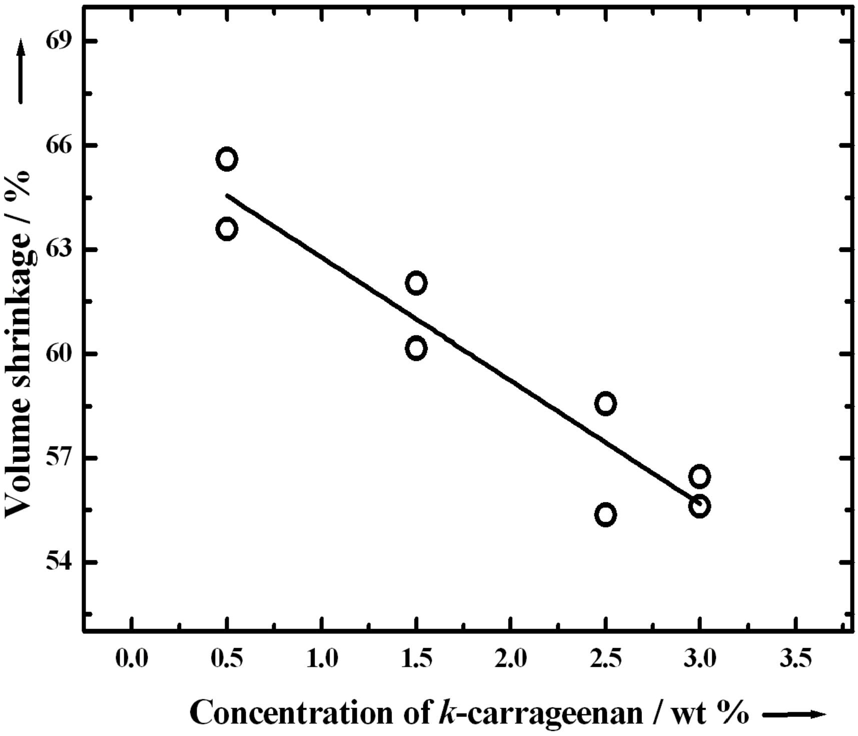

Figure 4: Volume shrinkage of aerogels with respect to the concentration of *k*-carrageenan

Scanning electron microscope images of the lower, 0.5 wt % and the higher, 3 wt % concentration of *k*-carrageenan aerogels are shown in **Figure 5**. The interconnected fibrillar structure was observed with a larger pore size distribution ranging from meso- to macropore. The fibre thickness was about 15 nm. Compared to the higher concentration of *k*-carrageenan aerogel (see **Fig. 5c and 5d**), the lower concentration, 0.5 wt %, showed loosely bound porous network (**Fig. 5a and 5b**).

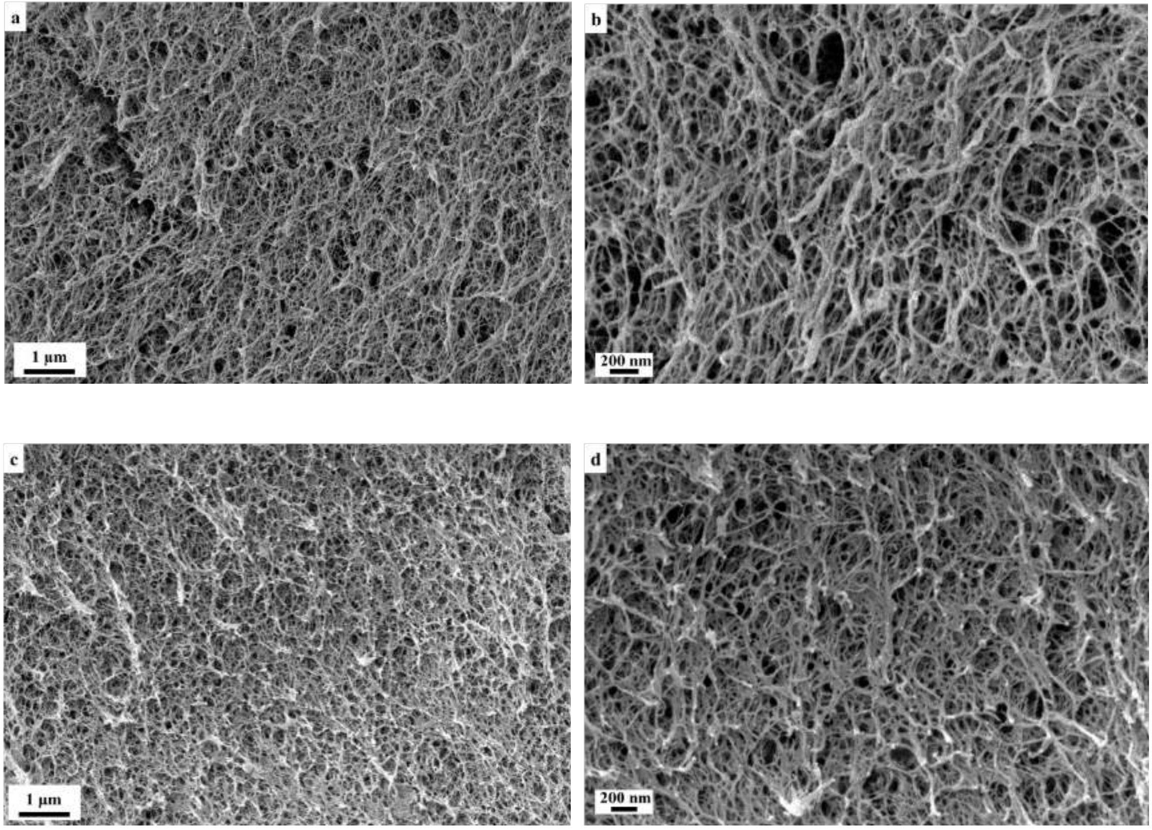

Figure 5: Scanning electron microscope images of *k*-carrageenan aerogels with a concentration of 0.5 wt % (5a and 5b) and 3 wt % (5c and 5d).

A linear relation of envelope density with concentration of *k*-carrageenan aerogels was observed (**Fig. 6**). The envelope density was in the range between 42 and 160 kg.m^{-3} depending upon the concentration of *k*-carrageenan. The decrease in amount of *k*-carrageenan in aerogel to zero gave intercept value, 1.29 kg.m^{-3} (almost close to zero value) i.e., the density of air, obtained from graph by extrapolating the line.

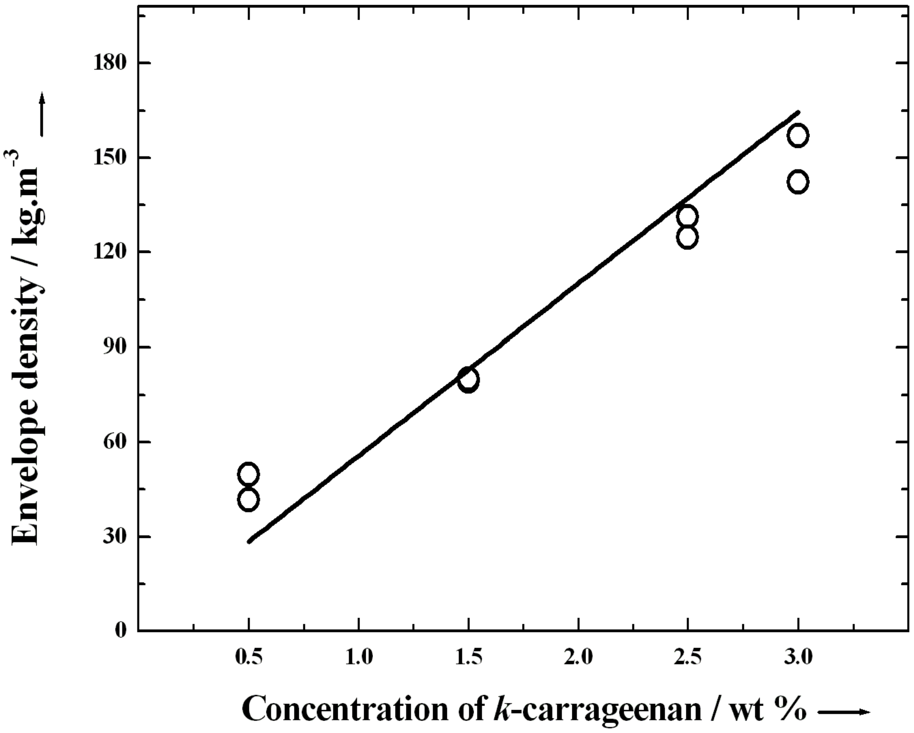

Figure 6: The envelope density of aerogels with respect to the concentration of *k*-carrageenan.

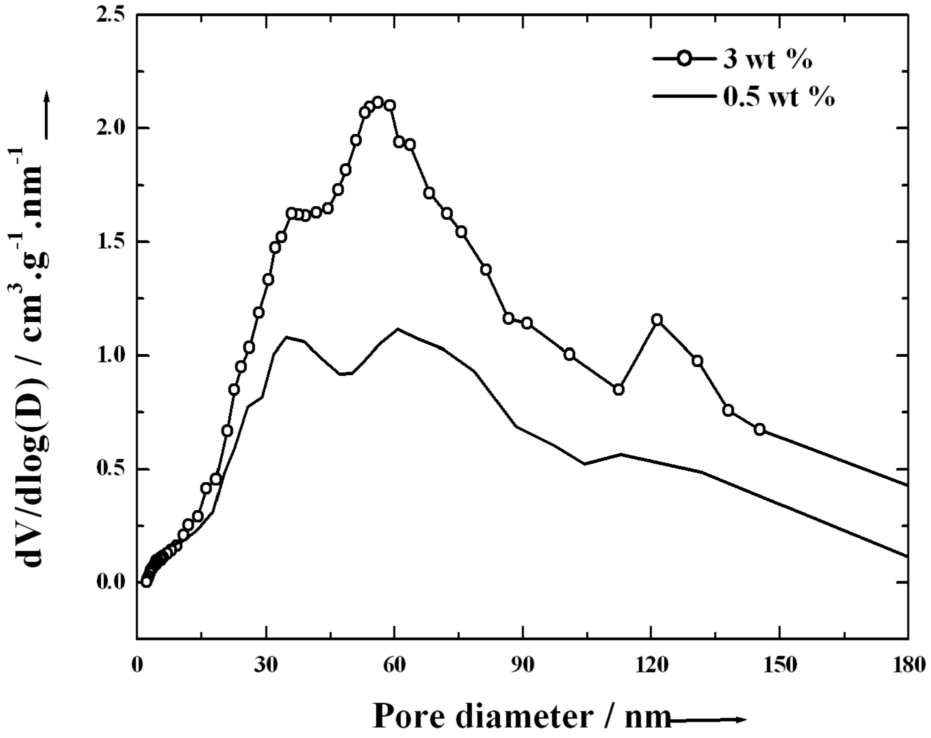

Figure 7: Pore size distribution of *k*-carrageenan aerogels with a concentration of 0.5 wt % (straight line) and 3 wt % (line with opened circles).

The porous structure and the specific surface area of aerogel were analyzed from N_2 adsorption-desorption isotherm. BET specific surface area, i.e., the specific surface area per mass was appeared to be almost independent of concentration of *k*-carrageenan, holding a value of 225 $m^2.g^{-1}$.
Figure 7 shows the pore size distribution of *k*-carrageenan aerogel. The plot shows broad peak ranging from mesopore to macropore, suggesting the broad pore size distribution, agreeing with the results obtained from scanning electron microscopy (see **Fig. 5**). The pore size distribution could be denser when higher concentration of *k*-carrageenan used than lower concentration 0.5 wt % that might be reflected in the peak maxima.

Conclusion

It is shown in this paper that monolith form of *k*-carrageenan aerogels can been prepared. The meso- and macroporous structure of the material was confirmed by scanning electron microscopy and BET isotherm. The envelope density (42–160 $kg.m^{-3}$) showed dependency on the concentration of *k*-carrageenan. Aerogels showed volume shrinkage of 65 % for lower concentration. As we understood from the literatures, there are several factors that can affect the shrinkage behaviour of aerogels. These results are contrast to the properties of aerogels obtained for microbeads form [11]. If we compare these results with monolithic cellulose aerogels [12], these materials are almost behaving like in the same way. To understand the system and solve the unanswered questions, still we need to go through more and more experiments. The well understood system of this open porous material may draw good attention in many applications.

Reference

1. Smirnova, I., Pharmaceutical applications of aerogels. In *Aerogels Handbook*, First ed.; Aegerter, M. A.; Leventis, N.; Koebel, M. M., Eds. Springer: New York, **2011**; p 695.

2. Primo, A.; Liebel, M.; Quignard, F., Palladium Coordination Biopolymer: A Versatile Access to Highly Porous Dispersed Catalyst for Suzuki Reaction. *Chemistry of Materials* **2009,** 21, (4), 621-627.
3. Mehling, T.; Smirnova, I.; Guenther, U.; Neubert, R. H. H., Polysaccharide-based aerogels as drug carriers. *Journal of Non-Crystalline Solids* **2009,** 355, (50-51), 2472-2479.
4. White, R. J.; Antonio, C.; Budarin, V. L.; Bergstroem, E.; Thomas-Oates, J.; Clark, J. H., Polysaccharide-Derived Carbons for Polar Analyte Separations. *Advanced Functional Materials* **2010,** 20, (11), 1834-1841.
5. Liebner, F.; Haimer, E.; Potthast, A.; Rosenau, T., Cellulosic Aerogels. In *Polysaccharide Building Blocks: A Sustainable Approach to the Development of Renewable Biomaterials*, First ed.; Habibi, Y.; Lucia, L. A., Eds. John Wiley & Sons, Inc.: New Jersey, **2012**.
6. Garcia-Gonzalez, C.; Alnaief, M.; Smirnova, I., Polysaccharide-based aerogels-promising biodegradable carriers for drug delivery systems. *Carbohydrate Polymers* **2011,** 86, (4), 1425-1438.
7. Ratke, L., Monoliths and fibrous cellulose aerogels. In *Aerogels Handbook*, Aegerter, M. A.; Leventis, N.; Koebel, M. M., Eds. Springer: New York, **2011**; p 173.
8. Piculell, L., Gelling Carrageenans. In *Food Polysaccharides and Their Applications*, Second ed.; Stephen, A. M.; Phillips, G. O.; Williams, P. A., Eds. CRC Press, Taylor & Francis Group: New York, **2006**.
9. Velde, F. v. d.; Lourenco, N. D.; Pinheiro, H. M.; Bakker, M., Carrageenan: A Food-Grade and Biocompatible Support for Immobilisation Techniques. *Adv. Synth. Catal.* **2002,** 344, (8), 815-835.
10. Rinaudo, M., Advances in Characterization of Polysaccharides in Aqueous Solution and Gel State. In *Polysaccharides. structural diversity and functional versatility*, Dumitriu, S., Ed. Marcel Dekker: New York, **2005**.
11. Quignard, F.; Valentin, R.; Renzo, F. D., Aerogel materials from marine polysaccharides. *New J. Chem.* **2008,** 32, 1300-1310.
12. Hoepfner, S.; Ratke, L.; Milow, B., Synthesis and characterisation of nanofibrillar cellulose aerogels. *Cellulose* **2008,** 15, 121-129.

CO05

AEROGEL HOLLOW TUBES FROM NATURAL-ORIGIN POLYSACCHARIDES AS TAILOR-MADE URINARY STENTS

Alexandre A. A. Barros[1,2], Ana Rita C. Duarte[1,2], Ricardo A. Pires[1,2],
João F. Mano[1,2] Rui L. Reis[1,2][1] 3B's Research Group - Biomaterials, Biodegradables and Biomimetics,
University of Minho, Headquarters of the European Institute of Excellence on Tissue Engineering and Regenerative Medicine, AvePark, 4806-909 Taipas, Guimarães, Portugal
[2] ICVS/3B's - PT Government Associate Laboratory, Braga/Guimarães, Portugal

Abstract

A urinary stent is defined as a thin tube which is inserted in the ureter to prevent or treat the obstruction of urine flow from the kidney. Silicone, latex, polyvinylchloride and polyurethanes are the most widely used materials for the preparation of the stents. Nonetheless, major drawbacks still concern urologists regarding their application. Severe clinical complications may result from the use of these materials such as fracture, encrustation and infection. Particularly serious are bacterial infections which represent the cause of several morbidity and mortality cases. The indwelling time for stent depends on the nature of the obstruction of the ureter. In some of the cases, the ureteral stents are temporary and it is often required a second surgery to remove the stent.

In this work, the possibility to prepare aerogel hollow tubes from natural origin polysaccharides, in particular alginate, k-carragenaan, gellan gum and a blend of these with gelatin was evaluated. Hollow tubes (stents), with a diameter between 1.5 and 6 mm, were prepared following conventional aerogel processing steps. The stents were characterized by different techniques: scanning electron microscopy (SEM) was used to evaluate their surface morphology; water uptake and polymer degradation were followed by weigh measurements at predetermined timeframes, using an artificial urine solution as immersion medium. *In vitro* assessment of possible encrustation,

i.e. the deposition of magnesium and/or calcium salts on the developed stents was also carried out. SEM coupled with energy dispersive x-ray spectroscopy (EDS) and Fourier transform infrared spectroscopy (FTIR) were used to evaluate inorganic encrustation. *In vitro* performance demonstrated that, despite the high water uptake ability (approximately 1000%), the developed aerogels/hydrogels do not present an extensive swelling behavior, i.e. they are able to maintain their shape and integrity upon immersion in simulated body fluids. The degradation of the materials in solution can be tuned, depending on the biomaterial, between 14 and 60 days. Additionally, no encrustation was observed for the tested time periods (up to 28 days). These data reveals that the studied aerogels/hydrogels are able to promote major breakthroughs in the development of biocompatible and biodegradable urinary stents.

CO06

AEROGELS FROM REGENERATED CELLULOSE: PROS AND CONS OF SELECTED CELLULOSE SOLVENTS

Pircher, N., Schimper, C., Potthast, A., Rosenau, T., Liebner, F.*
Department of Chemistry, University of Natural Resources and Life Sciences Vienna,
Konrad-Lorenz-Straße 24, A-3430 Tulln, Austria, E-mail: falk.liebner@boku.ac.at

Research on cellulose aerogels, as a new sub-class of lightweight, open-porous functional materials, has virtually undergone a boom since its early days some ten years ago. In the meantime cellulose-based aerogels are considered to be promising materials for a wide variety of applications such as high-performance heat and sound insulation, gas sorption, magnetic devices, anode materials for lithium ion batteries, controlled release of bioactive compounds for withdrawal, wound and skin treatment, or tissue engineering.

Apart from aerogels composed of nano- or microfibrillated cellulose, the preparation of aerogels from non-derivatized plant cellulose ideally comprises a) molecular-dispersing dissolution of the biopolymer under full preservation of its chemical integrity, b) subsequent coagulation ("regeneration") of cellulose, aiming at the formation of a homogeneous yet hierarchical network of open micro-, meso- and macropores, and c) conversion of the lyogels into aerogels under full preservation of the pore features, commonly accomplished by drying with supercritical fluids.

The cellulose solvent is one of the key factors which largely affect the properties of the final aerogels as differences in cellulose dissolving performance, mechanism of dissolution and gel formation, or side reactions can cause significant variations in density, morphology, mechanical stability, homogeneity, porosity, pore geometry, pore size distribution, chemical integrity or surface characteristics of the final aerogels. The current paper therefore discusses the pros and cons of selected direct cellulose solvents in this respect and illustrates that the choice of cellulose solvent is an important tool for tailoring the properties of aerogels for certain applications.

INTRODUCTION

In light of the recent extensive search for advanced functional renewable materials to substitute their synthetic equivalents, research on cellulosic aerogels offers a promising field.

Pronounced properties like very low density and an open pore structure which is accessible to modification, provide a broad basis for investigations regarding fundamental chemical and material scientific, as well as application oriented and product characteristic considerations.

The preparation of aerogels from regenerated cellulose comprises various steps of material processing, each one containing a range of parameters tuning the properties of the final product. However, the solvent system constitutes a major influence on the properties of the final product. Differences in dissolution power, dissolution and gelation mechanisms as well as possible side reactions cause significant variations in the supramolecular assembly of the cellulose II polymorph and therefore the morphology of the obtained network structure. In some cases, even the chemical integrity of the material is jeopardized.

Despite a number of alternative approaches, cellulosic aerogels are usually prepared by dissolving cellulose in an appropriate cellulose solvent, shaping and subsequent regeneration of the cellulose II polymorph by means of a cellulose antisolvent. After removing the solvent by several washing steps, the obtained lyogels are finally converted into an aerogel aiming at a far-reaching preservation of the highly porous network structure, as the latter is a prerequisite to many aerogel applications. At present, supercritical CO_2 drying is regarded the most effective technique to accomplish this task.

DISSOLUTION OF CELLULOSE

Dissolution of cellulose strongly depends on some molecular and supramolecular features of the raw material. In particular, the extensive hydrogen bond network, which is based on a large number of polar hydroxyl groups, can be seen as a key factor, as it stabilizes intra- and intermolecular conformations. Therefore, the ability of a given solvent to disrupt hydrogen bonding considerably attributes to its dissolution power towards cellulose. Lindman et al. underline that non-polar regions within the glucopyroanose rings lead to amphiphilic overall properties, which explains solubility of cellulose in solvents exhibiting mixed polarity such as ionic liquids and NMMO [1].

In addition to general aspects in the field of polymer dissolution such as chain degradation or undesired side reactions, choosing a solvent system aiming at the preparation of cellulosic aerogels requires additional considerations. Important product properties such as pore size distribution and surface area are largely influenced by both, the dissolution and gel forming processes.

Furthermore, a variety of continuative factors such as toxicological concerns, difficulties with removing the solvent system, with preparing shaped monoliths of complex geometry, or laborious and insufficient recovery of expensive solvents have to be accounted for.

In the following, a selection of solvent systems, used in the preparation of aerogels from nonderivatized cellulose is compared with regard to the aforementioned aspects.

SELECTED CELLULOSE SOLVENTS

N-Methylmorpholine-N-oxide

The monohydrate of N-Methylmorpholine-N-oxide (NMMO·H_2O) is used in industrial scale to dissolve cellulose via the Lyocell route. To facilitate dissolution, the original cellulose hydrogen bond network is disrupted and replaced by a new one, interconnecting cellulose macromolecules and solvent molecules [2-5].

The process is economically feasible and environmentally benign, as NMMO·H_2O is biodegradable, can be recovered in high rates and features low toxicity in production and further handling. It enables the direct dissolution of a wide variety of cellulosic raw materials and due to its high dissolution power, up to 15 wt% of cellulose can be dissolved, provided high shearing.

A potentially disadvantageous aspect is the comparatively high oxidation potential of the tertiary amine oxide NMMO. Side reactions can cause discoloration as well as cellulose degradation and eventually even result in severe effects, such as deflagrations or blasts [6,7]. Fortunately, these adverse effects can be repressed by the usage of stabilizers. Phenolic antioxidants, such as propyl gallate, prevent homolytic side reactions, whereas heterolytic side reactions, caused by the presents of carbenium–iminium ions, can be avoided using *N*-benzylmorpholine-*N*-oxide as a sacrificial stabilizer [8,9].

As a cellulose solvent in the preparation of aerogels, NMMO·H_2O has the advantage of melting at temperatures above 80°C and being solid at room temperature, which allows molding and accelerates regeneration of the shaped NMMO/cellulose bodies. Furthermore, due to its very low vapor pressure, a far-reaching constant solvent/solute ratio can be maintained throughout cellulose dissolution (100–120°C).

Because NMMO exhibits a high affinity towards cellulose, a considerable amount remains confined to fibrillary interstices of the lyogel, even if several washing steps are applied. As NMMO is also highly hygroscopic, remaining traces can thus absorb considerable amounts of water that finally lead to pore collapsing. This effect and the crystallization behavior of NMMO cause intensive shrinkage (10% for regeneration and 20% for $scCO_2$ drying in case of 3 wt% cellulose) of the bodies [10-12].

The morphology of the regenerated cellulose II polymorph obtained from $NMMO \cdot H_2O$/cellulose solutions can be controlled to a certain extend by the regeneration procedure. Regeneration from molten NMMO yields a globular structure, whereas regeneration of solidified Lyocell dopes results in a net of cellulose strands. It is assumed that latter is caused by phase separation (free solvent/cellulose-bound solvent) upon solidification [13].

Liebner et al. prepared cellulose aerogels containing 3 and 6 wt% of different commercial pulps by dissolving cellulose in molten NMMO at about 100–120°C, molding, extracting the solidified castings with an organic cellulose antisolvent, and drying of the obtained lyogels by supercritical carbon dioxide. The density of the obtained aerogels was in the range of 46–69 mg/cm^3 (3 wt% cellulose) and 106–137 mg/cm^3 (6 wt% cellulose). Scanning electron microscopy (SEM) pictures and nitrogen sorption experiments revealed a largely uniform, mesoporous structure with an average pore size of 9–12 nm and a specific surface area of 190–310 m^2/g. Doubling the cellulose content of Lyocell dopes slightly increased the BET surface areas [12, 14].

Amongst other factors, density depends on the extent of shrinking during the regeneration, washing and drying steps. The mechanical response profiles upon application of uniaxial compression stress have been found to be largely independent of the solvent used for cellulose dissolution. Young's moduli E describing the stiffness of isotropic elastic materials are comparatively low for aerogels from nonderivatized cellulose and mainly depend on density, and therefore on the cellulose content of the already prepared cellulose lyogel as well as on the shrinkage rate.

Although aerogels obtained from 3% cellulose containing Lyocell dopes had Young's moduli between 5 and 10 N/mm^2, doubling the cellulose content increased the E values by about one order of magnitude [12]. Similar values were reported by Innerlohinger et al. who prepared a large set of aerogels from 0.5 to 13 wt% cellulose containing NMMO dopes [11]. This is due to the increased resistance to cell wall bending and pore collapsing (higher plateau stress). On the other hand, an increasing cellulose content reduces the strain at which densification begins as the cell walls can touch each other at lower stress due to the presence of smaller pore radii. A similar trend was found for cellulose aerogels that were obtained by regenerating microcrystalline cellulose from corresponding solutions in aqueous sodium hydroxide and the ionic liquid EMIM acetate [15].

Ionic Liquids

Within the last decade, ionic liquids (ILs) such as 1-butyl-3-methyl-imidazolium (BMIM) and 1-ethyl-3-methyl-imidazolium (EMIM) chlorides and acetates have found increasing attention with regard to their potential to dissolve cellulose. Some ILs facilitate direct dissolution of up to 20 wt% of cellulose at comparably low temperatures [16-18]. They are not oxidizing, largely stable, chemically inert and have no vapor pressure, which, as for $NMMO \cdot H_2O$, enables control of the cellulose concentration throughout the dissolution process.

On a technical scale, latter argument also constitutes a drawback, since it excludes distillation of the comparatively expensive solvent. Recovery is further complicated since C-2 of imidazolium-based ILs can react with aldehyde/hemiacetal functions, resulting in the accumulation of considerable amounts of ILs in the cellulose by covalent binding [19-21]. However, this side reactions can be easily prevented by the presence of an alkyl group at the very C-2 position [21].

Morphologically, a globular structure is obtained for cellulose II regenerated from BMIMAc or EMIMAc/cellulose solutions. As for regeneration from molten NMMO, cellulose is spatially homogeneously distributed and phase separation occurs in one step, via spinodal decomposition, creating regular small spheres [13,15,22,23].

Deng et al. prepared 4 wt% highly nanoporous cellulose foams from BMIM chloride. Dissolution was carried out at room temperature, followed by coagulation of cellulose in water and subsequent rapid freeze-drying using liquid N_2. The resulting open fibrillar network structure consisted of cellulose II crystalline structure and had a specific surface area of up to 186 m^2/g [24].

Sescousse et al. reported a pore size distribution in the nanometer range peaking at about 10-20 nm for cellulosic aerogels prepared by dissolution of microcrystalline cellulose in EMIM acetate and subsequent supercritical CO_2 drying, which is in agreement with the values obtained by Liebner et al. for aerogels from Lyocell dopes. SEM pictures evidenced the presence of open pores sizing from few hundred nanometers to a few microns. The obtained surface areas were 230 m^2/g for 5 wt% aerogels, but only 130 m^2/g for double cellulose content. The authors furthermore suggested a linear approximation of density (16.8·cellulose wt% in mg/cm^3), which yields similar values to those listed by Liebner et al. for NMMO-derived aerogels [12,15].

Salt Hydrate Melts

A variety of salt hydrate melts, such as $ZnCl_2 \cdot nH_2O$, $Ca(SCN)_2 \cdot nH_2O$ or $LiSCN \cdot nH_2O$ are known solvent systems for cellulose. They are obtained either by heating salt hydrates which are solid at room temperature or from salt/water solutions with a water content corresponding to the coordination number of the respective cation. During diffusion of the melt into the cellulose fibers, the original cellulose hydrogen bonds are replaced by complexes containing single polymer chains and salt melt ions, yielding a colloidal system. While cooling the cellulose solution down to about 80°C, the cluster size increases until a gel is formed [25,26].

Salts hydrates melts are a cost-effective and environmentally benign option and can be recovered in good quantities.

For the preparation of cellulosic aerogels, the solvent system calcium thiocyanate tetrahydrate was employed with varying amounts of water [26,27]. The solvent allows for the preparation of low-density aerogels (ca. 10 mg/cm^{-3}) whose geometry is much better preserved during the drying procedure compared to aerogels obtained from $NMMO \cdot H_2O$ or TBAF/DMSO.
A drawback is the limit regarding the achievable cellulose content of the solutions, which is located around 3.5 wt% [26].

Jin et al. prepared 0.5-3.0 wt% cellulosic aerogels from calcium thiocyanate tetrahydrate solution. Freeze drying after solvent-exchange to t-butyl alcohol was an effective tool to preserve a uniform network structure with a nitrogen adsorption surface area of 160–190 m^2/g, slightly increasing with cellulose content. Densities were found to be about 20-100 mg/cm^3 [27].

The same cellulose concentration range was covered by Hoepfner et al. using the solvent system $Ca(SCN)_2 \cdot 4H_2O$ + 6–10 H_2O molecules and supercritical CO_2 drying. The resulting aerogels exhibited densities of 10-60 mg/cm^3 and specific surface areas of 200–220 m^2/g. SEM pictures illustrate pore sizes ranging from about one hundred nanometer to a micron, with the pores becoming smaller, the pore size distribution more regular and the network structure finer with increasing cellulose concentration [26].

Alkali Hydroxides

Precooled aqueous solutions consisting of NaOH and urea can rapidly dissolve cellulose. It is supposed that at low temperature, NaOH “hydrates” such as $[OH(H_2O)_n]^- Na^+$ are formed by dynamic supramolecular assembly, which in turn are able to reorientate and cleave hydrogen bonds. Urea is assumed to self-assemble at the surface of the chains, forming a water-soluble inclusion complex with cellulose/NaOH hydrate encaged. An even better dissolution behavior for cellulose was reported for the system LiOH and thiourea [28].

Regarding the preparation of aerogels, limitations of the achievable cellulose content of the solutions and the processable molecular weight of cellulose are disadvantageous.
Regeneration of the cellulose II polymorph from gelled cellulose in aqueous NaOH yields a net of cellulose strands. Gelation for this system is accompanied by a microphase separation, leading to agglomeration of cellulose molecules and the formation of macroscopic network forming particles, even before any antisolvent is added. Different from cellulose solutions in ILs and NMMO, the comparatively low concentrated NaOH freely diffuses inside this network but is increasingly hampered at higher cellulose content [15].
Gavillon et al. prepared aerogels from 3-7 wt% cellulose/NaOH/water gelled solutions at a temperature of -6°C, followed by gelation at higher temperatures, regeneration and supercritical CO_2 drying. It was found that the preparation and in particular the regeneration conditions strongly influence both, the density as well as the porosity of the obtained material. The pore size distribution of the bodies reached from a few tens of nanometers to a few tens of micrometers. For 5 wt% cellulose containing gels densities between 120 and

140 mg/cm^3, BET surface areas ranging from 240 to 280 m^2/g, and mean pore diameters of about 0.9 µm were obtained for different types of cellulose [13].

Cai et al. prepared aerogels by gelation of cellulose from aqueous alkali hydroxide/urea solution and supercritical CO_2 drying, featuring very high surface areas of 400–500 m^2/g [29].

CONCLUSION

In this paper, pros and cons of selected cellulose solvents are discussed with regard to the preparation of cellulosic aerogels. To this end, important characteristics of aerogel bodies obtained from cellulose, dissolved in $NMMO \cdot H_2O$, ionic liquids, salt hydrate melts or aqueous mixtures of urea with alkali hydroxides are compared. Density, shrinkage of the shaped bodies, specific surface area, pore size distribution and mechanical stability parameters constitute such factors. Besides product properties, process related, as well as ecologic and economic considerations are discussed.

ACKNOLEDGEMENT

The financial support by FWF - Austrian Science Fund (Austrian-French Project CAP-Bone), OeAD - Austrian Agency for International Cooperation in Education and Research (Amadee-Project FR10/2010), and by the University of Natural Resources and Life Sciences Vienna (BOKUDOC grant C. Schimper) is thankfully acknowledged.

REFERENCES

[1] LINDMAN, B., KARLSTRÖM, G., STIGSSON, L., Journal of Molecular Liquids, Vol. 156, 2010, p. 76-81

[2] HARMON, K. M., AKIN, A. C., KEEFER, P. K., SNIDER, B. L., Journal of Molecular Structure, Vol. 269, 1992, p. 109

[3] IOLEVA, M. M., GOIKHMAN, A. S., BANDURYAN, S. I., PAPKOV, S. P., Vysokomol. Soedin., Ser. B, Vol. 25, 1983, p. 803

[4] KHANIN, V. A., BANDURA, A. V., NOVOSELOV, N. P., Russian Journal of General Chemistry, Vol. 68, 1998, p. 305

[5] ROZHKOVA, O. V., MYASOEDOVA, V. V., KRESTOV, G. A., Khim. Drev., Vol. 2, 1985, p. 26

[6] ROSENAU, A., POTTHAST, A., SIXTA, H., KOSMA, P., Progress in Polymer Science, Vol. 26, 2001, p. 1763

[7] ROSENAU, A., POTTHAST, A., ADORJAN, I., HOFINGER, A., SIXTA, H., FIRGO, H., KOSMA, P., Cellulose, Vol. 9, 2002, p. 283

[8] ROSENAU, A., SCHMID, P., KOSMA, P., Tetrahedron, Vol. 61, 2005, p. 3483

[9] ROSENAU, A., SCHMID, P., POTTHAST, A., KOSMA, P., Holzforschung, Vol. 59, 2005, p. 503

[10] INNERLOHINGER, J., WEBER, H. K., KRAFT, G., Lenzinger Berichte, Vol. 86, 2006, p. 137

[11] INNERLOHINGER, J., WEBER, H. K., KRAFT, G., Macromolecular Symposia, Vol. 244, 2006, p. 126

[12] LIEBNER, F., HAIMER, E., POTTHAST, A., LOIDL, D., TSCHEGG, S., NEOUZE, M.-A., WENDLAND, M., ROSENAU, T., Holzforschung, Vol. 63, 2009, p. 3

[13] GAVILLON, R., BUDTOVA, T., Biomacromolecules, Vol. 9, 2008, p. 269

[14] LIEBNER, F., POTTHAST, A., ROSENAU, T., HAIMER, E., WENDLAND, M., Holzforschung, Vol. 62, **2008**, p. 129

[15] SESCOUSSE, R., GAVILLON, R., BUDTOVA, T., Carbohydrate Polymers, Vol. 83, 2010, p. 1766

[16] HERMANUTZ, F., GÄHR, F., UERDINGEN, E., MEISTER, F., KOSAN, B., Macromolecular Symposia, Vol. 262, 2008, p. 23

[17] SWATLOSKI, R. P., JACS, Vol. 124, 2002, p. 4974

[18] ZHU, S., WU, Y., CHEN, Q., YU, Z., WANG, C., JIN, S., DINGA, Y., WUC, G., Green Chemistry, Vol. 8, 2006, p. 325

[19] EBNER, G., SCHIEHSER, S., POTTHAST, A., ROSENAU, T., Tetrahedron Letters, Vol. 49, 2008, p. 7322

[20] LIEBNER, F., PATEL, I., EBNER, G., BECKER, E., HORIX, M., POTTHAST, A., ROSENAU, T., Holzforschung, Vol. 64, 2010, p. 161

[21] SCHREMS, M., EBNER, G., LIEBNER, F., BECKER, E., POTTHAST, A., ROSENAU, T., Cellulose Solvents: For Analysis, Shaping and Chemical Modification, American Chemical Society, 2010, p. 149

[22] BIGANSKA, O., NAVARD, P., Cellulose, Vol. 16, 2009, p. 179

[23] GAVILLON, R., BUDTOVA, T., Biomacromolecules, Vol. 8, 2007, p. 424

[24] DENG, M., ZHOU, Q., DU, A., VAN KASTEREN, J., WANG, Y., Materials Letters, Vol. 63, 2009, p. 1851

[25] FISCHER, S., Ph.D. thesis, TU Bergakademie Freiberg, Freiberg, Germany, 2003

[26] HOEPFNER, S., RATKE, L., MILOW, B., Cellulose, Vol. 15, 2008, p. 121

[27] JIN, H., NISHIYAMA, Y., WADA, M., KUGA, S., Colloids and Surfaces A: Physicochemical and Engineering Aspects, Vol. 240, 2004, p. 63

[28] LUE, A., ZHANG, L., Cellulose Solvents: For Analysis, Shaping and Chemical Modification, 2010, American Chemical Society, 2010, p. 67

[29] CAI, J., KIMURA, S., WADA, M., KUGA, S., ZHANG, L., ChemSusChem, Vol. 1, 2008, p. 149

Session 1: ORGANIC AEROGEL

Other Organic

CO07

GELATION KINETICS: SIZE EFFECT AND OTHER ISSUES

Lorenz Ratke und Barbara Milow
Institut für Materialphysik im Weltraum, DLR Köln, 51147 Köln, Germany

Abstract

One essential step in the production of aerogels is the gelation of the colloidal solution starting from molecular precursors. Gelation is most often thought as being a consequence of aggregation and coalescence of nanometer to micrometer sized particles. Gelation is thought to have occurred once the colloidal particles build a spanning cluster. Aging of the gels leads to further growth of particles, aggregation and stiffening of clusters by curvature dependent solution and re-precipitation.

A kinetic description of gelation needs a source for particle motion and thus aggregation, like Brownian motion or some type of fluid flow. Such ideas of gelation always suggest that there is a volume or size dependence of gelation: the larger the container is, in which a gel shall form, the greater the gelation time. There is only one experimental investigation reported in the literature using base or neutral catalyzed silica aerogels, finding a small size dependence.

We experimentally and theoretically investigated the size effect of gelation using Resorcinol-Formaldehyde aerogels. We find a clear dependence of gel time on the sample size under mild shear conditions. We developed a theoretical model based on Smoluchowski’s aggregation model adding, however, a growth term which accounts for the continuous growth of the colloidal particles while clustering happens.

The model is solved analytically and agrees very well, even quantitatively with our experimental observations for base catalyzed RF-gels. Applying the same model to describe gelation of acid catalyzed RF-aerogels yields also an excellent agreement for the gel-time dependence on catalyst concentration.

CO08

ELABORATION OF MONOLITHIC ORGANIC AEROGEL FROM LOW MOLECULAR WEIGHT ORGANOGEL / TOWARDS THERMAL INSULATORS

B. Jamart-Grégoire*,[1] **D. Barth,**[2] **F. Allix,**[1] **S. Son,**[1] **G. Pickaert,**[1] **Y. Jeannot,**[3] **V. Felix,**[3] **A. Degiovanni**[3]
[1]*LCPM, Lorraine university, CNRS, 1 rue Grandville BP 20451, 54001 Nancy, France*
[2]*LRGP, CNRS, 1 rue Grandville BP 20451, 54001 Nancy, France*
[3]*LEMTA, Lorraine University, CNRS avenue de la forêt de Haye, 54504, Vandoeuvre-lès-Nancy, France*

brigitte.jamart@ensic.inpl-nancy.fr

ABSTRACT

A family of low molecular weight organogels obtained from amino acid derivatives *via* an easy and inexpensive way has been studied. The removal of the solvent by supercritical CO_2 drying process leads to the corresponding aerogel in a monolithic form. The supramolecular organization of gelator molecules has been elucidated by using X-ray diffraction, NMR and IR spectroscopies. This new kind of aerogel possesses a very low density and a high specific surface. Moreover, regarding the aprotic character of the solvent contributing to the organogel formation, the corresponding aerogel possesses a very important hydrophobiccharacter. More interestingly and newly, these new organic aerogels can be handled without cracking. This property let us to undertake thermal conductivity measurement and to conclude that this new material could be useful for thermal insulation.

INTRODUCTION

Low molecular weight organogelators are small organic molecules (molecular weights less than 2000 g mol^{-1}) able to gelify organic solvents and prevent them from flowing. 1 The self-assembly of low molecular weight organogelators leads to thermoreversible physical gels which trap the solvent by forming a three dimensional network through non covalent cross-linked interactions. Many applications have been described in the literature for organogels.2 However, a few works have been devoted to their conversion into corresponding aerogel. To the best of our knowledge, only one publication describesthe formation of aerogel using a supercritical CO_2 drying process from the corresponding Low Molecular Weight organogel (LMWO). So, DDOA aerogel was described by Placin and al.3 as a piece of cotton wool.

Aerogels are defined as dry solids with very low apparent densities, large specific surface areas, and in most of the case, they exhibit amorphous structure.4 Depending on their aspect after drying, it is common to divide aerogels in two categories: 1) aerogel monoliths obtained without cracking by drying wet gel and 2) those obtained as fluffy aerogel powders. Concerning the chemical structure, the former are mostly inorganic or polymeric compounds, the latter are oxides, such as alumina, which for instance are more considered as xerogel because of a specific pore volume much lower than silica aerogel monoliths. Because of their highly divided solids characters, aerogels can develop very attractive physical and chemical properties and can contribute to high added value technical solutions not achievable by other means of low temperature soft chemical synthesis.5 As example, aerogels can be used in high degree of technology, in space exploration and electronics. Some of them have been considered as thermal super-insulators.67 Inorganic aerogels (nanoporous silica) 8910 exhibit very interesting thermal properties (thermal conductivity less than 0.030 $W.m^{-1}.K^{-1}$ at atmospheric pressure and lower than 0.008 $W.m^{-1}.K^{-1}$ at 1 mbar). Some conductivities of the same order of magnitude have also been obtained for polymer aerogels.

Here, we report the first Low molecular weight aerogel (LMWA) obtained in a monolithic form. The supramolecular organization of organogelator responsible of the gelation phenomenon has been elucidated. The high porosity of this material let us to undertake thermal conductivity measurements.

MATERIALS AND METHODS

Preparation of Organogelators and corresponding Organogels

Organogelators and Organogels were prepared following the protocol described in references [11] and [13]

Aerogels Preparation See reference [20]

Aerogels were prepared using a supercritical CO_2drying process

Description of the Supercritical CO_2 drying process

Materials

Installation for supercritical CO_2 drying is composed of three main systems (**Figure 1**):

A **supply line** with CO_2:

– A CO_2 cylinder which provides the system with CO_2 gas at a pressure of 50-60bar;

– A cold heat exchanger (Element I) with T_1 = 4°C which allows to liquefy the CO_2;

– A CO_2 tank (Element II) which recovers excess CO_2 at the outlet of the weir;

– A high pressure membrane pump (Lewa, type EK1);

– A damper (Element III) which reduces the fluctuations of the pump;

– An overflow (Element IV) for attaching the pressure at which it is desired to supply the circuit (TESCOM);

– A exchanger (Element V) which varies the temperature simultaneously with the increase of temperature in the autoclave;

– A mass flowmeter (Element VI) (Micromotion RFT9739) which provide the mass of CO_2 and the instantaneous flow, with a bath of T_2 = 60°C, at whose output is CO_2 supercritical. CO_2 flow-rate varied from 300 g/h to 1200 g/h, depending of the experiments.

An **autoclave** (Element IV: φi= 6 cm, height = 6 cm) which gives place for occur the drying. The temperaturewithinthe autoclaveis controlledbya thermostatic bathat T_3 andthe pressureis readon a gaugeBourdonof precision2bar.

An **evacuation line** of CO_2/solvent consisting of three cyclone separators (Elements VIII to X). The temperature of the first two cyclones is regulated by a bath at T_4 = 20°C. These separators are used to separate the solvent from the CO_2. The solvent is recovered in a liquid form through the leaving valves of the separators while the gaseous CO_2 passes through each separator to be discharged just through the top of the third separator.

Method for the preparation of Aerogels.

The drying of organogels by supercritical CO_2 was performed using the following procedure: a sample of organogel (around 5 to 7 g.) is introduced in the autoclave.Supercritical drying is performed following two steps according to the thermodynamic data : a static step followed by a dynamic or continuous supercritical drying. The conditions of the first step for a toluene organogel was those of liquid CO_2 (T=15°C, P= 90 bars with a contact duration between organogel and $CO_2$of

15 minutes). Then the temperature was increasing at 45°C (P=90 bars, solvant:toluene, duration: 20 minutes). In the second step, the system is in supercritical state and the solvent extraction can be performed. According to a CO_2 flowrate near 350 g/h, the drying need 210 minutes. At the end of the procedure, the pressure is first released to atmospheric pressure and the aerogel is extracted out of the autoclave.

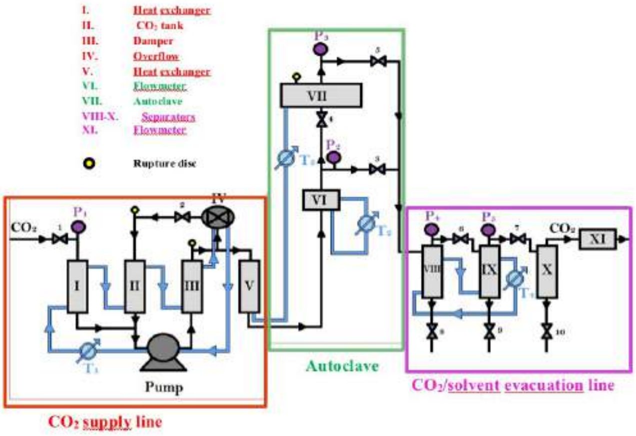

Figure 1 :CO_2 supercritical drying process

Characterization of organogels and aerogels.

NMR spectra were recorded on a BRUKER AVANCE spectrometer operating at 300 MHz or 600 MHz, in deuterated ($CDCl_3$), deuterated dimethylsulfoxide (*d6*-DMSO) or deuterated toluene (*d8*-Toluene). Chemicals shifts are given in ppm regarding tetramethysilane (TMS) as internal standard in $CDCl_3$ (δ=0 ppm for TMS). Infrared spectra were recorded on a BRUKER TENSOR 27 spectrometer equipped with a thermostated cell compartment and a liquid nitrogen cooled MCT detector over 32 scans. The samples were analysed in a 500 µm optic path length CaF_2 cell and the resolution of spectra is 2 cm^{-1} or with an ATR Pike Miracle bearing germanium crystal. Powder X-Ray diffraction (PXRD) measurements have been performed using a Panalytical X'Pert PRO diffractometer equipped with a Cu tube, a Ge(111) incident beam monochromator (λ = 1.5406Å) and an X'Celerator detector. MEB pictures have been obtained from High resolution MEB Hitachi FEG S4800 coupled with a dispersion spectrometer by the service of microscopy of the Faculty of Sciences and Technics of the University of Lorraine Nancy, France.

RESULTS

Preparation of organogelators and organogels.

During the last few years, our research group has studied a family of new (*L*)-amino acid type gelators bearing carboxybenzyl (Z) as amine protecting group and a naphthalimide moiety as fluorescent chromophore. 1112These compounds are highly versatile as they contain a lateral chain, a chiral center and protecting groups which allow the synthesis of a large number of analogs. We demonstrated that compounds 1 and 2 derived respectively from *L*-Phenylalanine and *L*-Leucine can trap a large variety of aromatic solvents and some chlorinated one(**Figure 2**).

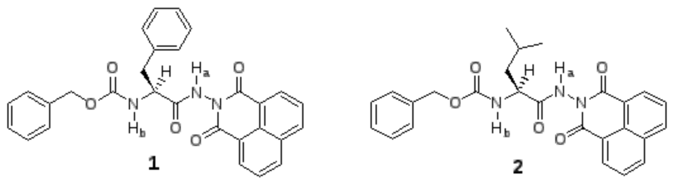

Figure 2 : Respective molecular structure of phenylalanine and leucine based gelators **1** and **2**

The physico-chemical organogelation properties, such as critical gelation concentration (CGC) and sol-gel phase transfer temperature (T_g) of these gels showed that strong gels can be obtained from a very low concentration of amino acids derivatives in aromatic solvents such as toluene. (**Table 1**)

Table 1: Gelation properties of **1** and **2** in toluene

Gelator	CGC at 4°C		T_g at 1 wt%	
	(wt %)	(mM)	(°C)	
1	0.17	2.99	63[a]	70[b]
2	0.30	5.68	40[a]	50[b]

[a] Determined by the “falling ball” method14

[b] Determined by NMR spectroscopy

Preparation of Aerogels.

Starting from the previously obtained organogels, we have shown that the corresponding aerogelscould be obtained using supercritical CO_2 drying process. Aerogel can be obtained for example, starting from a 1%wt organogel in toluene.Interestingly and newly, this new organic aerogel was obtained in a monolithic form and can be handled without cracking (**Figure 3**).

Figure 3: Pictures of an aerogel obtained from an organogel of gelator **1** 1 wt% in toluene

MEB analyses let us to determine that aerogel is composed of entangled fibers of 40-130 nm diameter. Structures of xerogel (dried materials obtained by evaporation of the solvent in the open air) and corresponding aerogel (obtained by supercritical CO_2 drying process), both obtained from of the same organogel (gelator **1**, 1wt% in toluene), were compared. The pictures (**Figure 4**) showed that aerogel is composed of fibers having a diameter between 40 and 130 nm, while xerogel fibers have a bigger diameter between 100 and 200 nm. This difference could be explained by a phenomenon of aggregation of small fibers during evaporative drying which does not occur during the supercritical drying.19

Same kind of aerogel can also be obtained starting from gelator **1** 0.5wt% in tetraline. A closer look at MEB pictures revealed helicoidal fibers (**Figure 4**).

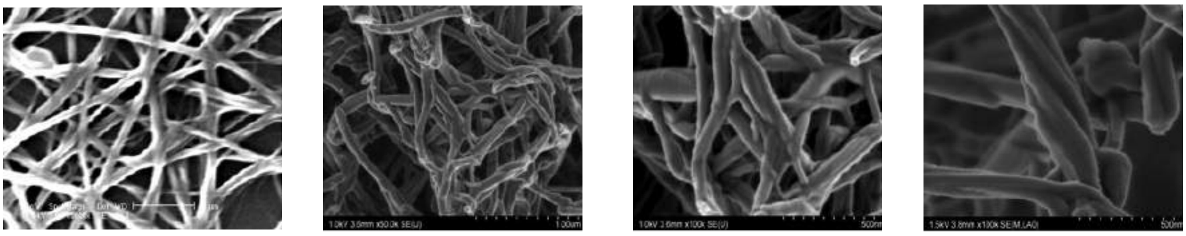
a b c d

Figure 4 : MEB pictures of (a) : a xerogel obtained from an organogel of gelator **1** 1 wt% in toluene ; (b) : an aerogel obtained from an organogel of gelator **1** 1 wt% in toluene, Magnification x5,000 ; (c) : an aerogel obtained from an organogel of gelator **1** 1 wt% in toluene, Magnification x50,000and (d) : an aerogel obtained from an organogel of gelator **1** 0.5 wt% in tetraline, Magnification x50,000.

Supramolecular arrangement of organogelator molecules.

Different spectroscopic techniques such as NMR, FT-IR, fluorescence and circular dichroism (CD) have been used to elucidate the detailed structures of supramolecular organogels obtained.1213 First of all, the comparison of the IR spectra of the gel and the isotropic solution of 1 in *d8*-Toluene demonstrated that intermolecular H-bonds were involved in the 3D network formation. (Same kind of results was obtained for organogel obtained from 2). As we can see in **Figure 5**, in the gel state, the NH vibrators located at 3311 and 3198 cm^{-1}correspond to hydrogen bonded ones. Heating the *d8*-toluene gels **1** from 30 to 100°C leads, as shown in **Figure 5**, to a gradual collapse of hydrogen bonded NH and CO groups in favour of the free ones. This indicates a disruption of the intermolecular hydrogen bonded network responsible for the gel formation. These observations suggest that both NH and CO groups are involved in intermolecular hydrogen bonding which stabilizes the gel-fiber organization.

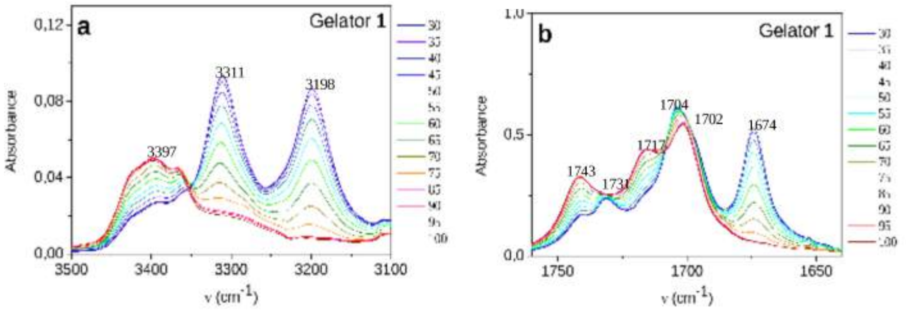

Figure 5 : Variable temperature (from30 to 100°C)FT-IR of gelator **1** in *d8*-toluene

These observations were confirmed by ^{1}H NMR analyses. In fact, in contrast of most of the organogels cases reported in the literature 15, our gelator molecules **1** and **2** in *d8*-toluene (1 wt%) at 25°C still keep a good thermal motion in the fibers and are still visible in NMR as very sharp signals. This observation allowed us to compare NMR spectra of isotropic solution and gel in *d8*-toluene. As shown in **figure 3a**, the NH signals of gelator **2** at 1 wt% (gel state), are shifted downfield (from 8.32 to 8.70 ppm for H_a and from 4.77 to 5.00 ppm for H_b) and become broader compared to those observed at 0.05 wt% (free molecules state). These observations indicate that H_a and H_b are involved in a hydrogen bond network in the gel state.

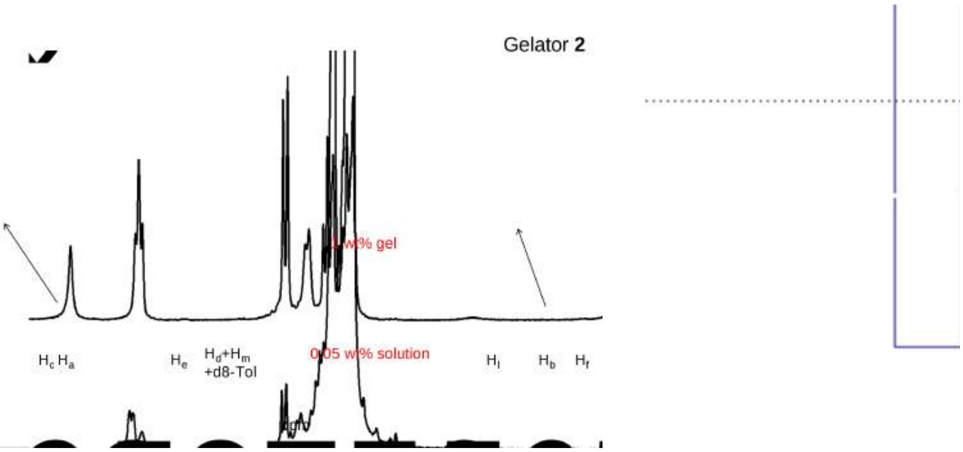

Figure 6 : (a-left) ^{1}H NMR spectra in *d8*-toluene of gelator 2 in solution state (bottom, 0.05 wt%) and in gel state (top, 1 wt%). (b-right) Variable temperature (from 25 to 100°C) ^{1}H NMR of gelator 2 in d8-toluene: coalescence of H_C proton

At this state of our research, two stacking modes can be considered for intermolecular association: the stacks parallel or head-to-head16and antiparallel stacks or head-to-tail 1718(**Figure 7**).

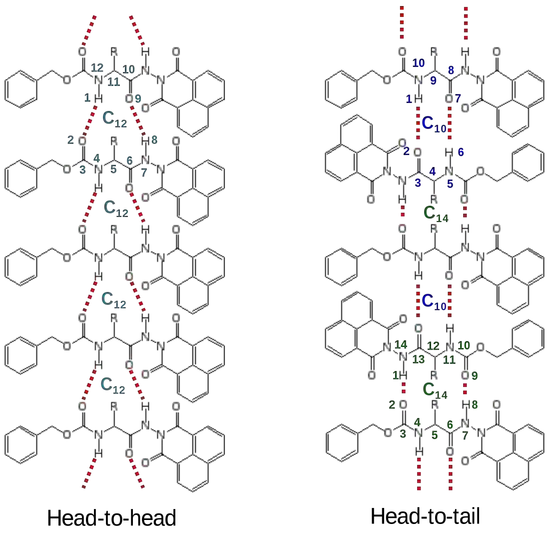

Figure 7 : Two possible primary intermolecular self-assembly processes

An interesting observation can be made about H_c, the *ortho* naphthalimide protons. In the case of gelator **2**(**Figure 6b**),we observed a coalescence of naphthalimide H_c protons by turning from gel to dilute solution during heating process of gels. In fact, the H_c protons in the gel state are not equivalent and appear at 8.28 ppm as a two overlapping doublets. On the contrary, at higher temperature (corresponding at the Tg) these protons become equivalent and appear as a doublet at 8.32 ppm. We can then conclude that the observed signals in gel state correspond to aggregates where the naphthalimide units are not anymore free of rotation probably because of π–π stacking interactions. We noticed that this phenomenon appeared to Tg, this means that naphthalimide moieties are free of rotation prior gelation. In other words, the stacks existing before gelation does not prevent the free rotation of this group. Head-to-Head stacking-up is not suitable for the free naphthalimide rotation, the groups would be too close from one to another. This hypothesis has been confirmed by a 2D NMR analysis which pointed out closed contacts between phthalimidic and benzylic protons. All these results demonstrate that the self-assembly of the gelator molecules in the gel state follows a Head-to-Tail arrangement.

In contradiction with this observation, the X-Ray (**Figure 8)** analyses performed at the monocrystalline state (which is obtained from slow evaporation of methanol solution) demonstrated a parallel molecular self-assembly.

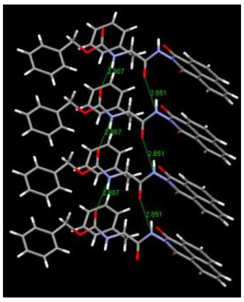

Figure 8 : Molecular self-assembly of gelator **1** obtained by X-Ray monocrystal analysis

We decided to compare FT-IR spectrum of both crystal and gel state. ATR spectra of monocrystals gives a specific signature in the amide A (NH stretching vibration) and amide I (CO stretching vibration) region which can be attributed in accordance to X-Ray analyses, to a Head-to-

Head arrangement (**Figure 9a-b**). In contrast, the ATR spectra of tetraline organogel (4% wt, (**Figure 9a-b**) give a striking different infrared signature with two well separated bands at 3315 and 3179 cm^{-1} in the amide A region. These results showed that, the gelling molecules can adopt different supramolecular arrangements depending on the state in which they are (single crystal or gel).

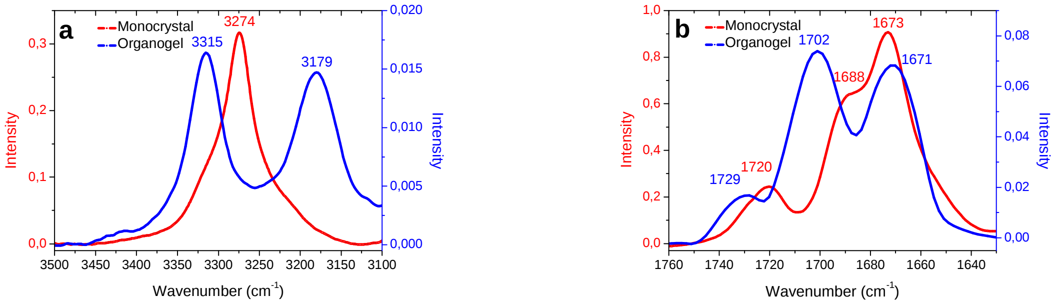

Figure 9 : Comparison of infrared ATR spectra, (a) amide A region and (b) amide I region, of monocrystal state (red) and 4% wt tetraline organogel (blue)

In conclusion of this first part, we demonstrate that gelators **1** and **2** can be self-assembled into a network able to trap organic solvent. The first step of this assembly consists of the formation of hydrogen bonded Head-to-Tail primary columns of gelator molecules, followed by the assembly of those columns *via* intercolumnar π–π stacking interactions. The **Figure 10** represents schematically this molecular association.

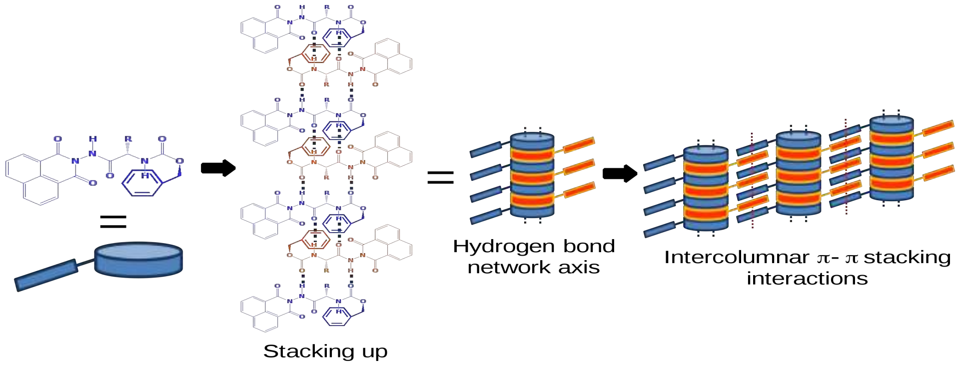

Figure 10 :Schematic representation of primary molecular self-assembly into columns and secondary intercolumnar association

SAXS experiments performed on a 6 wt% tetraline organogel of **1** (**Figure 11**) showed respectively four reflections in ratios of 1, 1/√3, 1/√4 and 1/√7 and the corresponding *d* spacing are 27, 15, 13 and 10Å. These spacings, attributed to (10), (11), (20), (21) reflections, are typical of a

2D hexagonal lattice18 which indicates that fibers are constituted of cylinders arranged in hexagonal fashion. The diameter D and section S of a cylinder can be calculated out of the d_{10} spacing as followed: D = (2xd_{10})/√3 = 31Å, S = Dxd_{10} = 840Å^2(**Figure**). As the maximum diameter found for a primary Head-to-Tail column (**Figure 7**) is of 18Å, the 31Å cylinders must correspond to a hexagonal arrangement of several primary columns. The projection along hydrogen bonds axis can be cartooned as shown in **Figure 12.** In this schematic representation, the blue molecule is the top one (in the front), the red one is right behind (in the back) and the next one would be hidden by the blue one, and so on. Thanks to that angle, six primary columns will self-assemble via π–π stacking interactions to give a nanotube which diameter is of 31Å. The last self-assembly step leads to the hexagonal arrangement of the nanotubes.

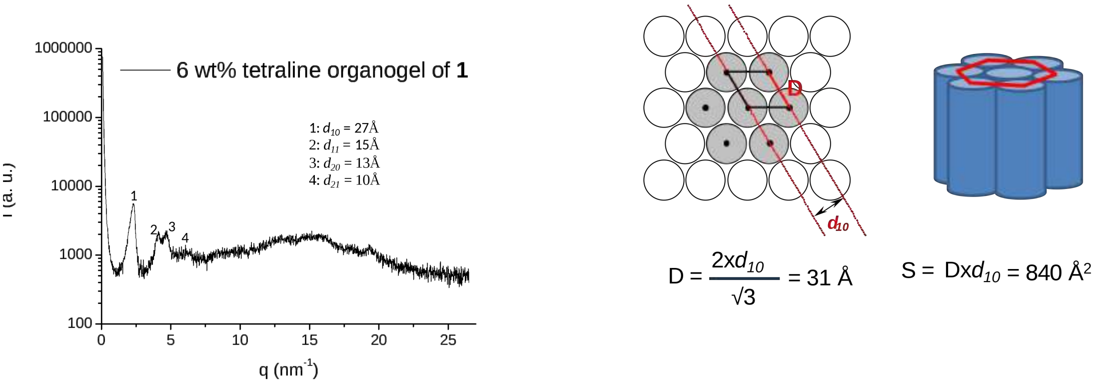

Figure 11 : (left) SAXS of 6 wt% tetraline organogel of **1**. (right) 2D hexagonal lattice

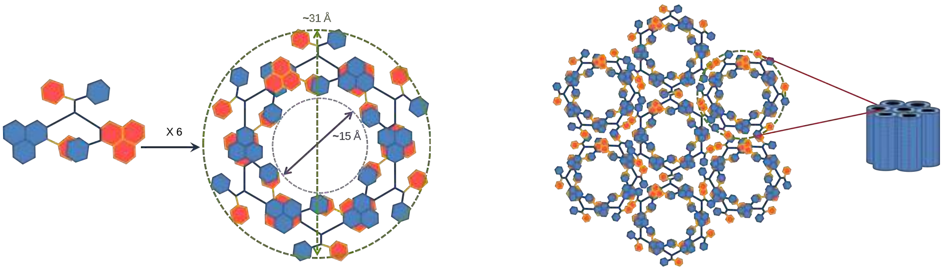

Figure 12 : (left) Schematic representation of six primary columns self-assembly into 31 Å diameter nanotube. (right) Schematic representation of six nanotubes self-assembly

Comparison of the molecular arrangements of organogel and aerogel.

Comparative infrared and SAXS studies between organogel and aerogel show unambiguously that supercritical CO_2 drying do not affect the fiber structure. First, the infrared ATR spectra of both materials are almost identical as shown in **Figure 13.** This means that at molecular level, the Head-to-Tail self-assembly of gelator molecules into primary columns is exactly the same for oganogel and aerogel. Second, the SAXS spectra of aerogel show (**Figure 14**) also, as in the case of organogel, that fiber is made of cylindrical objects arranged in a hexagonal fashion. Indeed, in the small angle region, seven sharp reflections in ratios of 1, 1/√3, 1/√4, 1/√7, 1/√9, 1/√12 and 1/√13 are observed. The spacings and attribution of those reflections as well as the parameters D and S of the cylinders are gathered in **Table 2**. In the case of aerogel, the characteristic reflections of 2D hexagonal lattice are much sharper than in the case of organogel. This indicates that in the aerogel state, the size and the organization of nanotubes are much more precise. By looking at D and S parameters, we can also notice that solvent removal leads to a little contraction of nanotubes size from 31 to 28.6 Å for diameter D and from 840 to 710 Å^2 for section S. In conclusion, the CO_2 supercritical drying allows a highly selective extraction of solvent keeping intact the molecular organization with only a kind of crystallization effect on fibers.

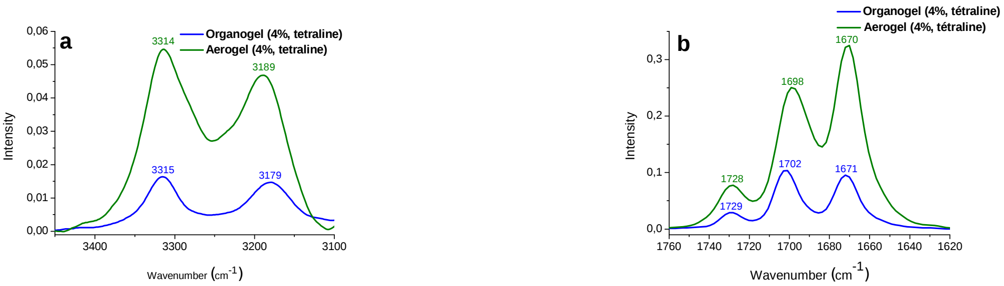

Figure 13 : Comparison of infrared ATR spectrum of organogel in tetratline and the corresponding aerogel

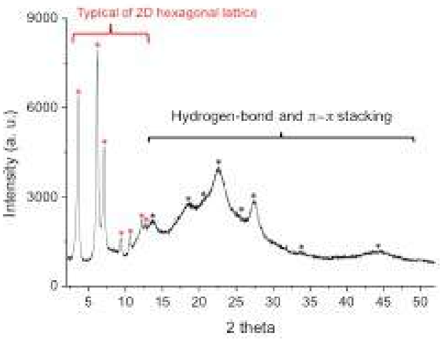

Figure 14 : SAXS spectra of aerogel obtained from gelator **1**

Table 2 : Spacings, diameter D and section S derived from SAXS spectrum of organo and aerogels

	d_{10} ^{a}	d_{11} ^{a}	d_{20} ^{a}	d_{21} ^{a}	d_{30} ^{a}	d_{22} ^{a}	d_{31} ^{a}	D ^{a}	S ^{b}
Aerogel	24.8	14.3	12.5	9.5	8.3	7.2	6.9	28.6	710
Organo gel	27	15	13	10	N.O.	N.O.	N.O.	31	840

unit: Å, (b) unit: Å^2, (c) Not Observed

Properties of aerogels.

This new aerogel presents very interesting properties [20]: a) A density estimated to 8.7kg.m^{-3} which is very low compared to this of silicate aerogels (3-350kg.m^{-3}) 222324or extruded polystyrene (35kg.m^{-3}), b) a skeleton density of 1346 kg.m^{-3} c) A high specific area of 90.5m^2/g. Moreover, regarding the aprotic character of the solvent contributing to the gel formation, the corresponding aerogel possesses also a very important hydrophobic character.

Thermal properties of aerogels.

Considering the intrinsic characteristics of the aerogels, a potential application is their use in the field of thermal insulation. However, none of the existing methods for the measurement of thermal conductivity could be applied to aerogels because of their very low density making imprecise the surface temperature measurements.

- Development of the "Three layers " method

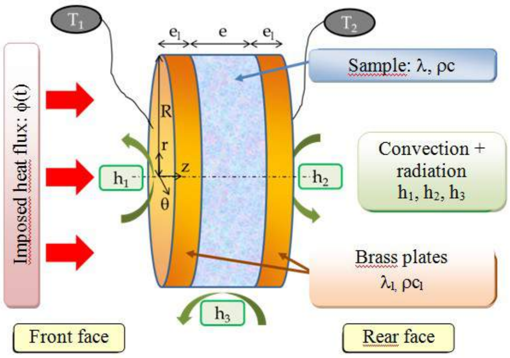

Figure 15: Schema of the « Three layer» method

The new measuring device 24, developed for lightweight insulators and super insulators, consists of a stack of three layers: a brass plate - a sample - a brass plate (**Figure 15**). A thermal disturbance is imposed on one brass plate and the transient temperature variations of the two plates are recorded. This enables us to identify the transfer function between the two temperatures and to estimate the thermal conductivity (and in some cases the volumic heat capacity) of the sample using an inverse method. Transfer model is purely analytical and takes into account the bidirectional transfer in the sample.

The validation of the method was carried out in two stages: the analytical model was first validated by comparison with a numerical 3D simulation and then the experimental device **(Figure 16**) and the estimation methods were validated on insulators and super insulators with a thermal conductivity between 0.018 and 0.18 $Wm^{-1}K^{-1}$ measured by other methods. Measurement accuracy is estimated at 5%. The complete device consists of a sealed chamber and a vacuum pump for performing measurements at room temperature at pressures ranging from 10^{-3}mbar to 10^{3} mbar.

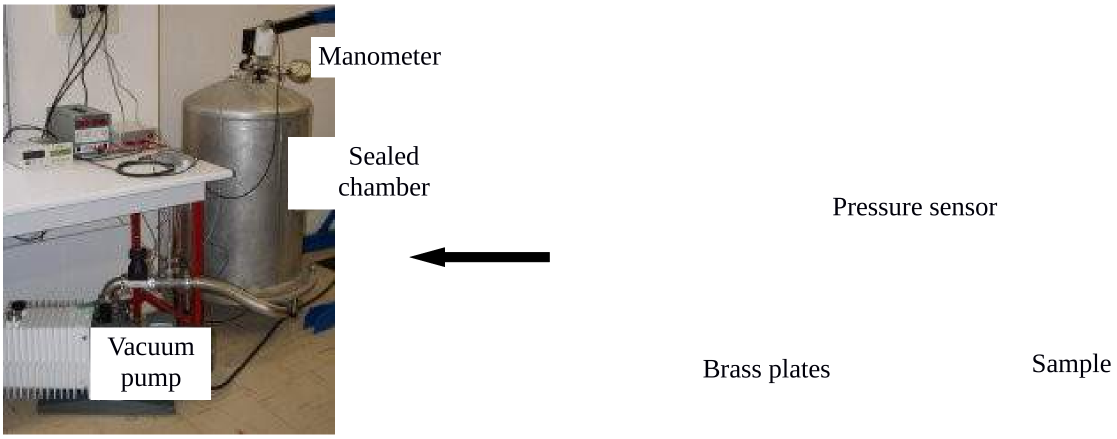

Figure 16 : The « Three layer» method: experimental device

- Measurement results at atmospheric pressure

Three aerogels obtained from corresponding organogels in toluene were thermally characterized by three-layer method, which is particularly difficult because they behave almost like still air. The experimental results are presented in and in **Table 4**.

Table 3 : Characteristics of aerogels samples

Material	Thickness (mm)	Density ($kg.m^{-3}$)	Porosity (%)
Aerogel 1 (3%)	3.55	26.8	98.0
Aerogel 2 (3%)	4.90	26.8	98.0
Aerogel 3 (2%)	4.90	17.7	98.7

Table 4 : Estimated parameters (conductivity, heat density, " exchange coefficient", parallel resistance)

Material	λ ($W.m^{-1}.K^{-1}$)	ρ_c ($J.m^{-3}.K^{-1}$)	h ($W.m^{-2}.K^{-1}$)	R ($K.W^{-1}$)
1	0.0265	50400	5.8	310
2	0.0268	47300	5.4	400
3	0.0269	48600	5.8	370

- Thermal Porosimetry

The establishment of an equivalent thermal conductivity model suitable for lightweight insulators associated with measures of thermal conductivity for air pressures ranging from 10^{-3} mbar to 10^{3} mbar allowed us to estimate a pore sizes distribution in aerogels Error: Reference source not found **Figure 17** and **Figure 18** show the results for the aerogel **1**.

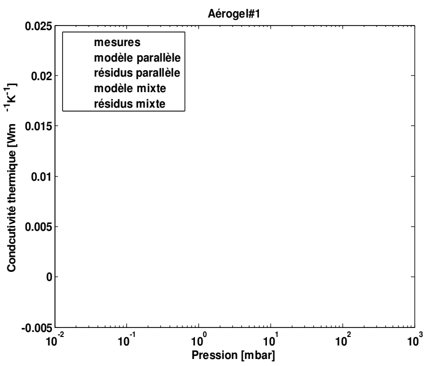

Figure 17 : Thermal conductivity

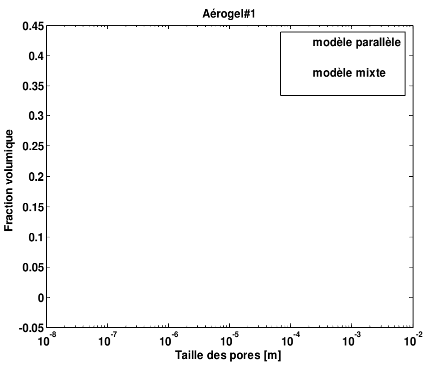

Figure 18 : Pore size distribution

An Helium pycnometer has been used for the measurement of the porosity. The difficulties in obtaining a reliable value of the volumic heat capacity (values obtained by the Three-layer method are much too high) led us to perform a measurement by calorimetry (dSc Evo of Setaram) ($Cp = 1210\ J.Kg^{-1}K^{-1}$). Due to the virtual absence of matter, X-ray tomography cannot reach the structure of the aerogel. A study by polarized light scattering has highlighted a structure consisting of rods with an average diameter of 300 nm. Finally transmission measurements in the infrared (between 5 et 25 μm) allowed us to reach a value of the radiative conductivity at room temperature (**Table 5**).

Table 5 : Radiative properties

Material	Transmission rate (%)	Radiative conductivity($Wm^{-1}K^{-1}$)
Aerogel 3%	0.094	0.0029
Aerogel 0.5%	0.189	0.0028

CONCLUSION

Monolithic aerogel can be obtained from low molecular weight organogels using a supercritical CO_2 drying process. Hydrogen bonds and $\pi-\pi$ stacking interactions are responsible of the gelation phenomenon. Thanks to a new measuring device using a tri-layer stack we could measure a thermal conductivity of about 0.027 W / m / K for our aerogels. Given their remarkable properties, low thermal conductivity, scattering in the infrared and hydrophobic character, these new materials can be used in the field of thermal insulation. Studies of developing composite materials formed of silica aerogel and our aerogels are being studied.

ACKNOWLEDGMENT The authors thank the National Research Agency (ANR) for financial support (MULOWA Blan08-1_325450).

REFERENCE

1 Terech, P.; Weiss, R. G. Low Molecular Mass Gelators of Organic Liquids and the Properties of Their Gels. *Chemical reviews***1997**, *97,* 3133–3160.

2 Van Esch, J. H. We can design molecular gelators, but do we understand them? *Langmuir : the ACS journal of surfaces and colloids***2009**, *25,* 8392–4.

3 Placin, F.; Desvergne, J.-P.; Cansell, F. Organic low molecular weight aerogel formed in supercritical fluids. *Journal of Materials Chemistry***2000**, *10*, 2147–2149

4 Pierre, A. C.; Pajonk, G. M. Chemistry of aerogels and their applications. *Chemical reviews***2002**, *102,* 4243–65.

5 Nicola, H.; Schubert, U. Aerogels – Airy Materials : Chemistry , Structure , and Properties.

6 Sangeetha, N. M.; Maitra, U., Supramolecular gels: Functions and uses. *Chemical Society Reviews* **2005,** 34, (10), 821-836.

7 Vintiloiu, A.; Leroux, J.-C., Organogels and their use in drug delivery -- A review. *Journal of Controlled Release* **2008,** 125, (3), 179-192.

8 Ayabe, M.; Kishida, T.; Fujita, N.; Sada, K.; Shinkai, S., Binary organogelators which show light and temperature responsiveness. *Organic & Biomolecular Chemistry* **2003,** 1, (15), 2744-2747.

9 J. H. Hafkamp, R.; P. A. Kokke, B.; M. Danke, I.; P. M. Geurts, H.; E. Rowan, A.; C. Feiters, M.; J. M. Nolte, R., Organogel formation and molecular imprinting by functionalized gluconamides and their metal complexes. Chemical Communications 1997, (6), 545-546.

10 Liang, G.; Yang, Z.; Zhang, R.; Li, L.; Fan, Y.; Kuang, Y.; Gao, Y.; Wang, T.; Lu, W. W.; Xu, B., Supramolecular Hydrogel of a d-Amino Acid Dipeptide for Controlled Drug Release in Vivo. Langmuir 2009, 25, (15), 8419-8422.

11 N. Brosse, D. Barth, B. Jamart-Grégoire, Tetrahedron Lett. 2004, 45, 9521-9524;

12 Q. N. Pham, N. Brosse, C. Frochot, D. Dumas, A. Hocquet, B. Jamart-Gregoire, New J. Chem. 2008, 32, 1131-1139;

13 F. Allix, P. Curcio, Q. N. Pham, G. Pickaert, B. Jamart-Grégoire, Langmuir 2010, 26, 16818-16827

14 Terech, P.; Rossat, C.; Volino, F., On the Measurement of Phase Transition Temperatures in Physical Molecular Organogels. *Journal of Colloid and Interface Science* **2000,** 227, (2), 363-370

15 Cassin, G.; de Costa, C.; van Duynhoven, J. P. M.; Agterof, W. G. M., Investigation of the Gel to Coagel Phase Transition in Monoglyceride-Water Systems. *Langmuir* **1998,** 14, (20), 5757-5763.

16 Yabuuchi, K.; Tochigi, Y.; Mizoshita, N.; Hanabusa, K.; Kato, T., Self-assembly of carbazole-containing gelators: alignment of the chromophore in fibrous aggregates. *Tetrahedron* **2007,** 63, (31), 7358-7365

17 Iqbal, S.; Miravet, J. F.; Escuder, B., Biomimetic Self-Assembly of Tetrapeptides into Fibrillar Networks and Organogels. *European Journal of Organic Chemistry* **2008,** 2008, (27), 4580-4590

18 Laschat, S.; Baro, A.; Steinke, N.; Giesselmann, F.; Hägele, C.; Scalia, G.; Judele, R.; Kapatsina, E.; Sauer, S.; Schreivogel, A.; Tosoni, M. Discotic liquid crystals: from tailor-made synthesis to plastic electronics. *Angewandte Chemie (International ed. in English)* **2007**, *46*, 4832–87.

19 Mizoshita, N.; Kutsuna, T.; Kato, T.; Hanabusa, K., Smectic liquid-crystalline physical gels. Anisotropic self-aggregation of hydrogen-bonded molecules in layered structures. *Chemical Communications* **1999**, (9), 781-782

20 Jamart-Grégoire, B.; Brosse, N.; Quoc Nghi, P.; Barth, D.; Scondo, A.; Degiovanni, A. Utilisation d'aérogels pour la préparation de matériau pour isolation thermiqueINPL, Br. Fr. n°09/53363 du 20 mai 2009. Jamart-Grégoire, B.; Brosse, N.; Quoc Nghi, P.; Barth, D.; Scondo, A.; Degiovanni A. Utilisation d'aérogels pour la préparation de matériau pour isolation thermique*PCT Int. Appl. (2010), WO 2010133798 A2 20101125.Al AT BE BG CH CZ DE DK EE ES FI FR GB GR HR HU IE IS IT LI LT LU LV MC MK MT NL NO PL PT RO SE SI SK SM TR*

21 Placin, F.; Desvergne, J. P.; Cansell, F., Organic low molecular weight aerogel formed in supercritical fluids. *Journal of Materials Chemistry* **2000,** 10, (9), 2147-2149.

22 Gesser, H. D.; Goswami, P. C., Aerogels and related porous materials. *Chem. Rev.* **1989,** 89, 765-788.

23 Tang, Q.; Wang, T. Preparation of silica aerogel from rice hull ash by supercritical carbon dioxide drying. The Journal of Supercritical Fluids 2005, 35, 91–94.

24 Novak, Z.; Habulin, M.; Krmelj, V.; Knez, Ž. Silica aerogels as supports for lipase catalyzed esterifications at sub- and supercritical conditions. *The Journal of Supercritical Fluids***2003**, *27*, 169–178.

25 Jannot, Y.; Degiovanni, A.; Payet, G. Thermal conductivity measurement of insulating materials with a three layers device, *International Journal of Heat and Mass Transfer* **2009**,*52*, 1105-1111.

Félix, V.; Jannot, Y.; Degiovanni, A. A thermal porosimetry method to estimate pore size distribution in highly poro

AEROGELS FROM LIGNIN OBTAINED BY LIQUID-HOT-WATER TREATMENT OF WHEAT STRAW

L. Perez-Cantu[*a], **F. Liebner**[b], **I. Smirnova**[a]
[a] Institute of Thermal Separation Processes, Hamburg University of Technology, Eißendorfer Str. 38, D-21073 Hamburg (Germany)
[b] Department of Organic Chemistry, University of Natural Resources and Life Sciences (BOKU), Konrad-Lorenz-Str. 24, A-3430 Tulln (Austria)
E-mail: lilia.perez@tu-harburg.de
Tel/Fax: +49 40 42878 2688 / 4072

ABSTRACT

Aerogels can be principally synthesized from any material that can form a gel. This includes natural organic polymers, such as starch, alginate, cellulose, and other polysaccharides, which have a clear advantage of being biocompatible, biodegradable and renewable. The aim of this work is to apply this technique to lignin, another biopolymer but of phenolic nature, in order to obtain aerogels.

Lignin is a natural polymer found in lignocellulosic material and represents the largest by-product in the manufacturing of lignocellulose-based ethanol. The lignin used in this work was obtained after enzymatic saccharification of liquid-hot-water-pretreated wheat straw from a second generation biorefinery. This phenolic biopolymer has been used as a renewable and biodegradable organic backbone for the production of porous materials. Due to its highly branched, three dimensional structure, lignin can form a colloidal solution with the appropriate selection of a crosslinker. In this work, alkaline aqueous solutions of lignin were chemically crosslinked with oligooxyalkylene diglycidylethers of different chain length and dried under scCO2 after solvent exchange.

The porous materials obtained in this way exhibit high surface area, high porosity, small density and good mechanical properties, which allow their use in different industrial applications, such as a natural product based insulation material, due to their relatively low thermal conductivity, which lies around the higher end of common insulation materials.

INTRODUCTION

The production of lignin based gels has been reported sporadically in literature. Highly reswellable gels could be prepared with the reaction of lignin with formaldehyde, glyoxal, glutaric dialdehyde at elevated temperatures [1,2]. Other lignin gels could be obtained by crosslinking lignin with bifunctional organic agents such as epichlorohydrin in the presence of any alkali as a catalyst [3]. Another source produced hydrogel films by copolymerization of lignin with acrylamid and polyvinyl alcohol [4].

Aerogels containing lignin have been mentioned in literature as well. By solving cellulose-lignin-xylan mixtures in ionic liquids at higher temperatures stable gels that were supercritically dried could be obtained [5]. Another author produced organic aerogels from a mixture of lignin, resorcinol and formaldehyde in water at ambient temperature [6]. The crosslinking of lignin products with the epoxide polyethylene glycol diglycidyl ether (PEGDE) has been reported in literature before [7, 8, 9]. PEGDE is particularly well suited for the crosslinking of lignin, because of its very reactive nature due to its heterocyclic C-O-C units with two polar C-O bonds leading to a high local tension in the epoxide ring [7, 10]. Under these conditions, the molecule is highly susceptible towards nucleophilic ring-opening reactions with nucleophiles such as phenolate ions [9]. Through the described crosslinking reaction with PEGDGE highly swellable, mechanically stable hydrogels could be obtained [8, 9, 10]. The analysis of their mechanical properties as well as their swellable character was performed as well. The further processing of the lignin-PEGDE hydrogels to obtain aerogels has not been yet reported in the literature.

MATERIALS AND METHODS

Materials

The lignin products used in this work were obtained in-house according to the Aquasolve process, described elsewhere [11, 12], consisting of the liquid hot water (LHW) pretreatment and an enzymatic hydrolysis. For the preparation of hydrogels only the Aquasolve solid lignin fraction of the process, referred to as AS lignin, was used.

Ethylene glycol diglycidyl ether (EGDGE) and polyethylene glycol diglycidyl ether (PEGDE) were used as crosslinking agents. The molecular weight of the monomer EGDGE was 174.19 g/mol and the density 1.19 g/ml. The average number of the repeating unit in the polymeric PEGDGE molecule was nine, resulting in a molecular weight of 526 g/mol and a density of 1.14 g/ml.

Methods

The preparation of crosslinked lignin hydrogels was performed similarly to [8, 9]. A certain percent by weight per volume of lignin was dissolved in aqueous sodium hydroxide and the solution was stirred for overnight. The crosslinking agent was added continuously while stirring at a previously defined amount in mmol/g lignin for PEGDGE. The solution was then further stirred until an increase in viscosity due to the gelation was observed. The solutions were poured into syringes, in order to allow the gels to age.

After aging, the content was then pressed out of the syringes and suitable products were prepared to proceed with the solvent exchange. The procedure described was performed under different conditions and temperature. Lignin and crosslinker concentration were also varied.

The resulting stable hydrogels were subjected to different solvent exchange procedures at ambient conditions with organic solvents. After this, the lignin hydrogels were dried with supercritical carbon dioxide according to the procedure described elsewhere [13]. For solvent removal from the gel structure, the samples were dried for 4 hours at 40 °C with a continuous supercritical carbon dioxide flow at 120 bar. At the end the flow was stopped and the autoclave was slowly depressurized for unloading the samples.

RESULTS

Gelation of the prepared solutions was the first analyzed response variable. As shown in Table 6, the most important parameter for gelation is the lignin concentration in solution. For successful gelation, this amount was found to be minimum 20%w/v of AS lignin in solution. Solutions with lower concentrations did not gelated at all. Temperature increase can decrease the amount of crosslinker needed for structure formation. In any combination of parameters, there is a higher need of the monomer than of the polymer in mmol/g lignin for a successful gelation of the solutions.

Table 6 Parameter values for succesful gelation of lignin solutions

Lignin [%w/v]	T [°C]	PEGDE [mmol/g]	EGDE [mmol/g]
20	25	1	2
	40	1	2
	60	0.5	1

Temperature has a positive influence in gelation time as well, shortening the time needed for obtaining stable gels. This may be explained through an increase in the rate of reaction between the crosslinker and lignin. As shown in Figure 8 the effect is higher for EGDE as for PEGDE, which could indicate an increase of mobility of the monomer crosslinker due to the higher temperature of the solution.

Figure 8 Effect of temperature on gelation time of lignin solutions

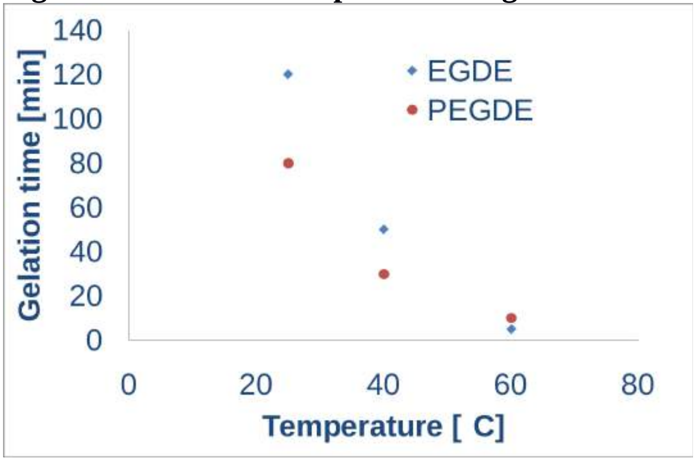

After gelation of the lignin solutions was successful, the stable aged gels were given a solvent exchange process for replacing the aqueous solution in the gel for a solvent that can be extracted with $scCO_2$. Solvent content in the solvent exchange baths was gradually increased until 100% solvent was achieved. During this process, the gels suffered shrinkage in their volume, and as shown in Figure 9, there is little relationship between the crosslinker amount and the volumetric change. The shrinkage of the aerogels represented around 20% of the original volume of these monoliths.

After successfully exchanging water for an appropriate solvent, the lignin gels are dried under scCO2 conditions (40°C, 120 bar) for several hours, in order to remove the solvent from the pores. The purpose of the supercritical drying procedure is to reduce the mechanical stress in the pores in order to preserve the internal open structure of the gel. Shrinkage is mostly related to destruction of internal structure and thus reducing of the surface area available. Figure 9 shows the shrinkage of the aerogels after scCO2 drying. It can be seen that the largest shrinkage occurs during this process and comes to an overall value of 40 to 50% of the original volume of the monoliths. This is relatively high compared to shrinkage of inorganic aerogels, but within the range for organic-based materials [14].

Figure 9 Shrinkage of lignin monoliths before (after solvent exchange) and after drying with scCO2 (for 20% w/v lignin concentration, PEGDE and 40°C)

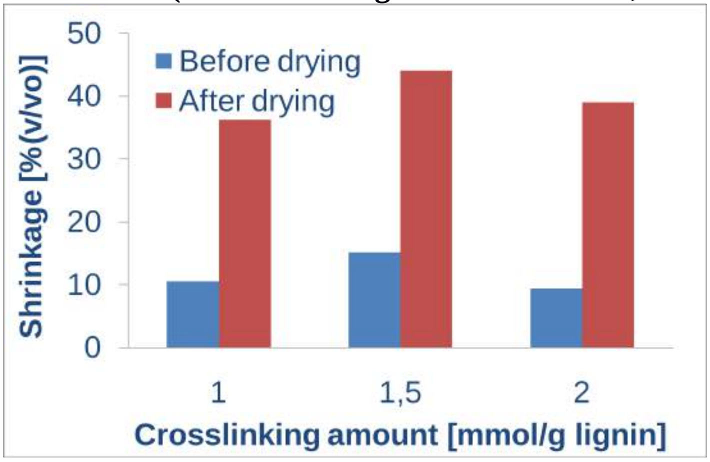

Once dried, the lignin aerogels were tested for their internal surface area, measured with BET analysis. As seen in Figure 10, larger surface areas can be obtained with the crosslinker in its monomer form as with the larger chain length. This may indicate the formation of mesopores due to the size of the monomer molecule in comparison of the 9-times longer polymer, which may create larger pore sizes and lower the BET area.

Figure 10 BET Area of lignin monoliths of different EGDE/PEGDE concentrations (20%w/v lignin concentration)

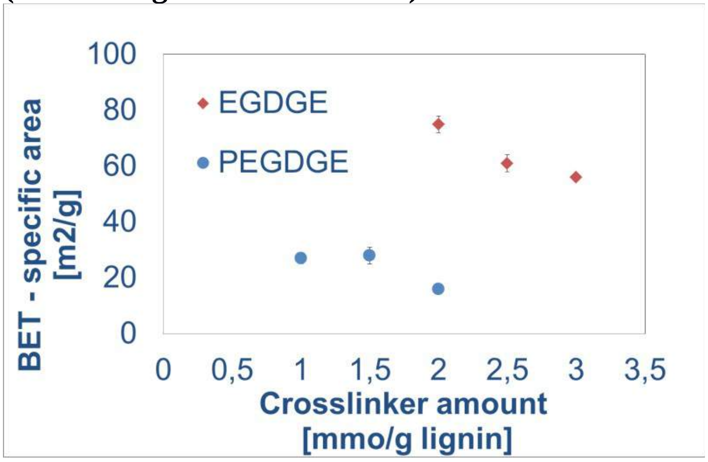

In the same way, larger amounts of crosslinker reduce this value as well, possibly forming compacter structures with less surface area in the mesopore range. It is to be evaluated if these materials exhibit larger surface areas in the micropore range. The densitiy of the obtained materials are relatively low for the amount of lignin added and directly proportional to the crosslinker amount added as expected.

Table 7 Material properties of lignin aerogels obtained from a 20%w/v lignin solution

Crosslinker	Amount [mmol/g]	Specific surface [m^2/g]	Density [g/m^3]	Shrinkage [%]
M	2	75.7±3.4	0.233±0.031	22.5±4.9
	2.5	61.3±3.1	0.227±0.001	23.8±0.0
	3	56.3±1.9	0.248±0.012	41.2±4.2
P	1	27.7±1.2	0.266±0.010	34.3±3.5
	1.5	28.6±1.4	0.320±0.003	38.9±19.7
	2	16.3±0.1	0.332±0.011	33.1±2.8

CONCLUSION

Organic aerogels based on a crosslinking reaction of lignin with epoxides of ethylene glycol have been produced. It was found that a minimum amount of lignin is required to produce stable hydrogels. The same can be said for the crosslinkers. The need of crosslinker for gelation at higher temperatures was lower and shorter gelations times could be also achieved with the increase in temperature. Shrinkage occurred during solvent exchange and after scCO2 drying of the materials. The structural properties of the obtained aerogels have been the subject of analysis. According to these properties, the best resulting aerogels were prepared by crosslinking 20% (w/v) lignin with the monomer EGDE in alkaline solution at room temperature.

REFERENCES

[1] DELLICOLLI, H.T., DILLING, P., FALKEHAG, S. I., US-Pat. 4,244,728, **1976**.
[2] DELLICOLLI, H.T., DILLING, P., FALKEHAG, S. I., DE-Pat. 27 03 812, **1977.**
[3] BROWN, W., US-Pat. 4,131,573, **1977**.
[4] EL-ZAWAWY, W.K. Polym. Adv. Technol., Vol. 16, **2005**, p.48.
[5] AALTONEN, O., JAUHIAINEN, O., Carbohydrate Polymers, Vol. 75, **2009**, p. 125.
[6] CHEN, F., XU, M., WANG, L., BioResources, Vol. 6, **2011**, p. 1262.
[7] URAKI, Y., ISHIKAWA, N., NISHIDA, M., SANO, Y., *J Wood Sci*., Vol. 47, **2001**, p. 301.
[8] NISHIDA, M., URAKI, Y., SANO, Y., Bioresource Technology, Vol. 88, **2003**, p. 81.
[9] PASSAUER, L., FISCHER, K., LIEBNER, F., Holzforschung Vol, 65, **2011**, p. 309.
[10] PASSAUER, L., Dissertation, Technische Universität Dresden, **2008**.
[11]INGRAM, T., WÖRMEYER, K., LIMA, J.C.I., BOCKEMÜHL, V., ANTRANIKIAN, G., SMIRNOVA, I., Bioresource Technology, Vol.102, **2011**, p. 5221.
[12] WÖRMEYER, K., INGRAM, T., SAAKE, B., BRUNNER, G., SMIRNOVA, I., Bioresource Technology, Vol.102, **2011**, p. 4157.
[13] INNERLOHINGER, J., WEBER, H.K., KRAFT, G., Macromol. Symp 244, **2006**, p. 126.
[14]KAYSER, H., MÜLLER, C.R., GARCIA-GONZALEZ, C.A., SMIRNOVA, I., LEITNER, W., MARIA, P.D., Applied Catalysis A, General, **2012,** in Press**.**

Session 2: AEROGEL MODELLING

CO10

SYSTEM APPROACH FOR MODELING OF AEROGELS AND PROCESSES IN SC REACTORS

Professor N. Menshutina

D. Mendeleyev University of Chemical Technology of Russia, CAPE Faculty, chemcom@muctr.ru,
tel./fax.: 7 (495) 495-00-29

INTRODUCTION

Aerogels - an innovative material which in recent years increasingly used in the industry of developed countries as heat insulation, noise insulation and filter material in aircraft and rocket production, construction and engineering. Aerogels are promising as a drug delivery system of active drugs in the pharmaceutical industry, etc. [1-3].

At the present time it becomes an urgent task to simulate the drying process, diffusion, adsorption in aerogels and composite materials based on organic and inorganic aerogels. In addition, an important task is to simulate the equipment for production or use of aerogels. Computational experiment which is based on the models will reduce the time of new developments and reduce the cost of the experiment [4].

APPROACH OF MODELING

System approach for modeling processes of obtaining aerogels and aerogel compositions in SC reactors was suggested, including consideration of processes from nano to macro scale.

Approaches for modeling of aerogel’s nanostructure are discussed on the first level. The following processes are discussed on the second level: drying of aerogels, diffusion and adsorption. On the third level the influence of hydrodynamics in the reactor on these processes is considered.

System approach allows considering the influence of various parameters (sol composition, structure of aerogels, heat and mass transfer, hydrodynamics) on final characteristics of composites based on aerogels and thus, on the quality of the prepared material. Full consideration of various phenomena on nano and micro scale, together with recommendations, concerning process organizing in the apparatus require parallel computing. It involves creation of parallel computing, fast processing and reliable data storage.

Modeling approaches that are used in each level are discussed below.

First level: modeling of aerogel’s structure, determination of its characteristics.

Aerogel is a highly porous, nanostructural material. It refers to three-dimensional nanomaterial that is based on a matrix or crystal with nanometer-sized grains. Based on a number of studies, it was found that inorganic aerogels have chaotic structure. For modeling, or more precisely, for computer generation of aerogel’s structure and its visualization, two approaches were used:

- model and algorithm of slightly overlapping spheres.
- multi DLA model – model of aggregation, diffusion limited.

Model of slightly overlapping spheres suggests filling of nano volume with spheres with certain overlapping and then their consistent removal until two conditions are achieved: certain porosity and existence of links between spheres (fig. 1).

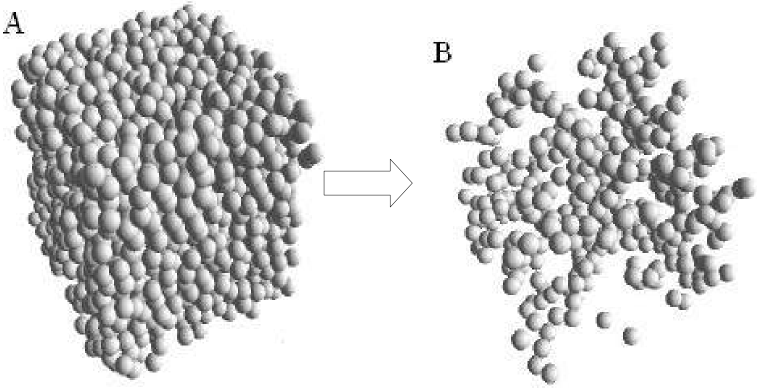

Figure 1. Weakly overlapping spheres method

Algorithm of Hoshen-Kopelman was used in this model. It allows checking the existence of links between spheres. When no sphere can be removed without destroying the cluster and given porosity is still not achieved it’s necessary to return to the original close-packed structure and try to remove other spheres. Suggested model was checked on nano and micro scales and can be used for 3D models (fig. 2).

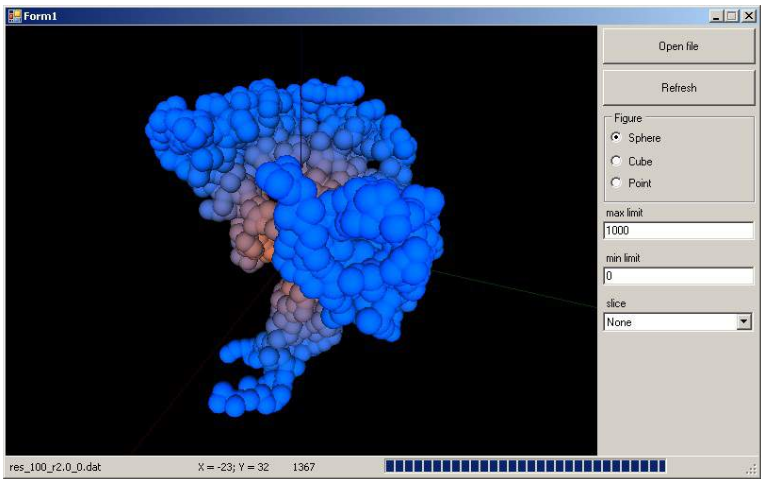

● Sphere

max limit 1000

min limit 0

slice None

res_100_r2.0_0.dat X = -23; Y = 32 1367

Figure 2. Weakly overlapping spheres method. Visualization

Diffusion-limited aggregation model is the second approach for generation of chaotic structures of aerogels. In this approach structures of aerogels are similarity and fractals may be used. The condition of formation of aerogel’s structure is determined by drying or diffusion (replacement of the solvent with scCO2 with a subsequent decrease in pressure). That’s why the use of Multi DLA model can be perspective. The main difference of this model is presence of several initial centers, that can speed up calculations (fig. 3).

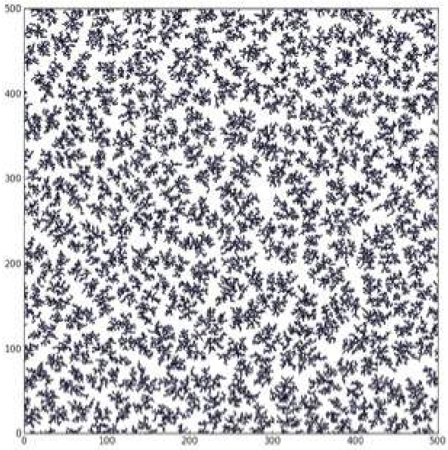

Figure 3. Diffusion Limited Aggregation (DLA)

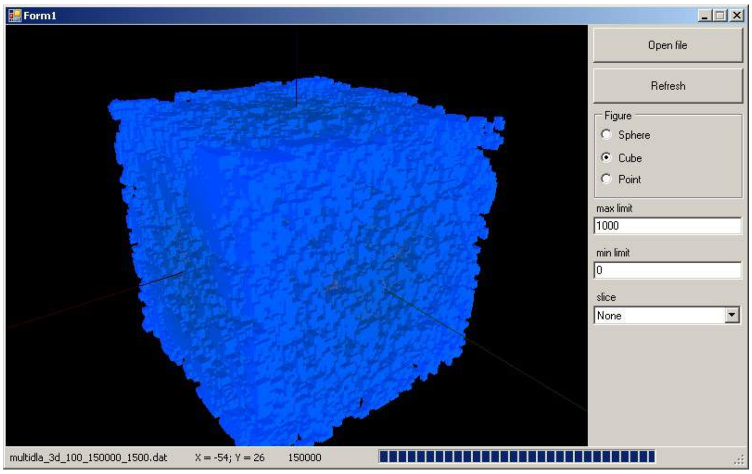

Figure
○ Sphere
● Cube
○ Point

max limit
1000

min limit
0

slice
None

multidla_3d_100_150000_1500.dat X = -54; Y = 26 150000

Fig. 4. Diffusion Limited Aggregation. Visualization

Computer generation of aerogel’s structure (fig. 4) and ability to create 3D aerogel’s structure allow evaluating:

- characteristics of “created” aerogels (pore size distribution, specific surface);

- possibility of modeling diffusion, drying and adsorption processes in them;
- research heat transfer e.t.c.

Calculation of pore size of generated chaotic structures was performed, using the developed algorithm. It is based on geometric constructions the main idea of which is consistent attempts to fill the free space of a given structure with spheres of certain radius. Filling starts with spheres of the largest diameter, that is getting reduced by a certain amount on each step until its minimum.

Filling of generated structure is carried out after sampling of area. To make the sampling, three-dimensional network consisting of equal cubes is imposed on the investigated structure. For the structure with linear sizes 600 nm it’s necessary to make around $2{,}5\cdot10^{15}$ operations. Obviously, it takes a lot of time to process such array. Parallel computing can reduce it. For the above three models, parallel computing was performed using CUDA technologies on graphic card nVidia. Moreover, based on the proposed approaches and models, software system “Nanostruct” was implemented.

The structure of this software is shown on fig. 5. It consists of 5 modules, that are connected between each other: calculation module, that includes all models and algorithms; module of the initial data (experimental and reference); visualization and output module in form of tables; module of additional software; information module for users.

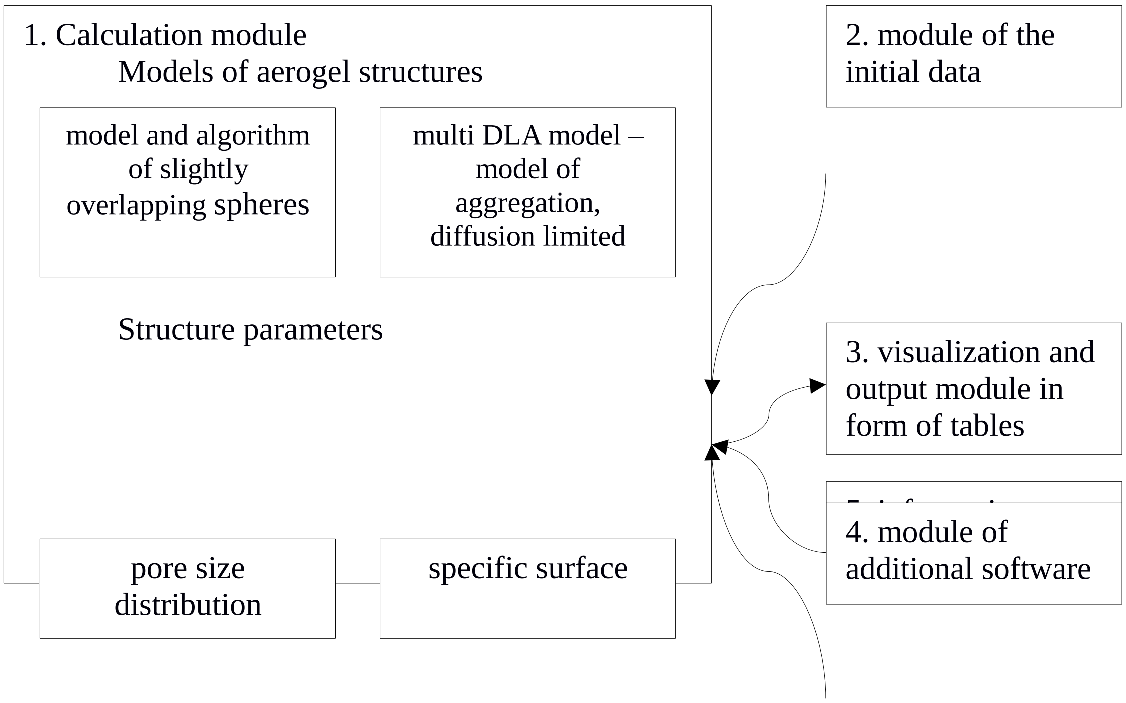

Figure 5. Structure of software "Nanostruct"

Second level: modeling of physico-chemical processes (diffusion, drying, adsorption, heat transfer) in aerogels. The main approach of this level is the use of cellular automata. CA is modeling, where simple transition rules on a periodic lattice, that divides area on elementary volumes, are used. Transition levels can have fundamental basis or can be in the form of static dependencies. Models that use CA are attractive because they allow creation of algorithms of parallel computing.

CA with Margolus neighborhood is probabilistic and is well used to solve diffusion problems, where each cell is associated with individual system component, and transitions between cells with individual processes. Unlike other CA, where all actions are performed with one cell, in Margolus CA they are performed with 2*2 blocks (for 2D case, fig. 6). On each step the block can be rotated or maintain its position. This method allows achieving high degree of parallelism.

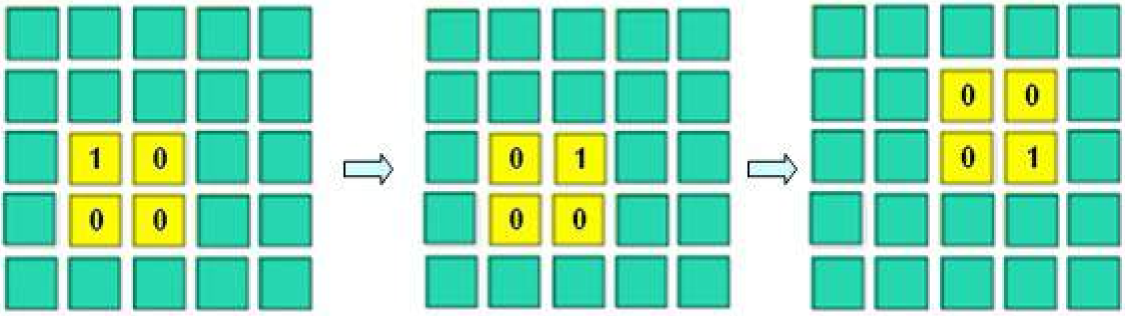

Figure 6. Cellular automata in physicochemical modeling

Third level: modeling of the processes in SC reactor.

The main modern approach, that is used for modeling of processes in chemical and industrial equipment is a complex description of the behavior of a heterogeneous system inside the reactor at each point in time. This approach can be performed using CFD software, for example Fluent. Optimal parameters of the process (flow rate, pressure, concentration), scaling, design characteristics of industrial equipment can be determined, using this approach, together with appropriate software. The use of Fluent 6.0 software for determination of optimal flow rates is shown on fig.7. Moving of SCF (CO_2) in lab reactor with aerogels inside is shown.

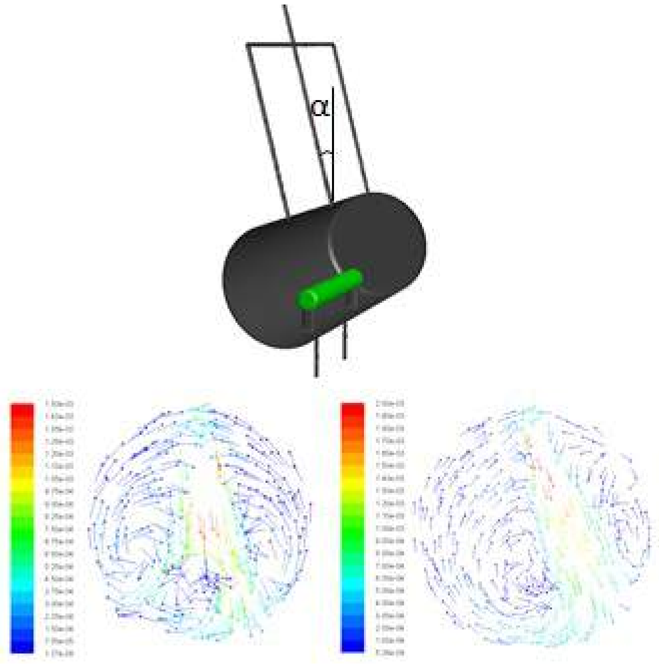

Figure 7. Moving of SCF (CO_2) in lab reactor

Joint use of models for generation aerogel’s structure, CA models for description diffusion processes in them and hydrodynamic models in heterogeneous media, allows achieving complex mathematical description of all phenomena and processes in SC reactors and opens new horizons in the transition to continuous technology and creation of unique equipment for certain uses.

CONCLUSION

System approach for modeling of aerogels and processes in supercritical reactor was presented. Highlighted different scales for modeling: nano (model structure), micro (local object modeling and physico-chemical processes in it) and macro (simulation equipment). The numerical methods and models that can be used were presented.

REFERENCES

[1] AKIMOV, Y.K. Fields of application of aerogels (review). Instruments and Experimental Techniques, 46(3), **2003**, p.287-299

[2] ALNAIEF, M., SMIRNOVA, I. In Situ Production of Spherical Aerogel Microparticles. The Journal of Supercritical Fluids, In Press, Accepted Manuscript. **2011**

[3] LEVENTIS, N. et. al. Aerogels Handbook, NY: Springer. **2010**

[4] MENSHUTINA, N.V., GURIKOV, P.A., KOLNOOCHENKO, A.A. 3D Reversible Cellular Automata for Simulation of the Drug Release from Aerogel-Drug Formulations. Proceedings of 19th European Symposium of Computer Aided Process Engineering (ESCAPE 2009), **2009**, p.943-947

ARTIST USING AEROGELS

CO11

AEROGELIC LIGHT: ART & SCIENCE RESEARCH ON THE ETHEREAL NANOMATERIAL SILICA AEROGEL, FOR SUSTAINABLE URBAN DESIGN.

Authors: **Dr. Ioannis MICHALOUdiS*, Miik Green**
Speaker: **Dr. Ioannis MICHALOUdiS**

Address: 2A, David street, Mount Pleasant, 6153 W. Australia
Telephone: + 61 420 892 919
Fax: + 61 8 9266 2971
e-mail: michalou@alum.mit.edu
Ioannis.MICHALOUDIS@curtin.edu.au

ABSTRACT

This paper aims to present Aerogels as materials that can be considered as sustainable works of art & design as well as concepts for sustainable urban design. Typically, aerogels are amongst the world's lightest solids and have some of the best insulation qualities known to man. These inherent material characteristics make them important candidates in future urban ecological strategies. These physical properties are as pivotal to an environmental awareness as the aesthetic properties embodied in aerogels. In combining art and science, these works have the ability to visually represent our surrounding natural world in a unique, aerogelic way. A cosmic material that is almost immaterial, we merge two words here, 'angel' and 'aerogel' to reference the ethereal and the unseen.

Sustainable urban design is at the forefront of international discussion, as the issues of changing weather patterns, arctic shelf ice depletion and global warming (amongst other topics) has reinvigorated dialogue on the subject. Materials that have the ability to withstand acute temperatures, or to insulate – both of which are inherent properties of aerogel – are currently in high demand - the extreme insulation properties inherent in silica aerogels have wide ranging

possibilities, from architectural applications to garment design within the fashion industry. We seek to present aerogels as materials that not only inform us about the world around us, but also to help create a sustainable future, opening new avenues for dialogue, specifically in regards to green design.

‘To feel that we are apart from nature is our greatest conceit’

James Turrell

INTRODUCTION

Art and science have the ability to inspire and transform when combined. The synthesis of these two disciplines is important, as each field can draw from their shared knowledge. What this paper aims to achieve is a new way of viewing our surrounding environment and future ecological prospects: not just as concepts, but also as tangible objects. Materialising these concepts may involve a combination of art, design, science and technology: through the medium of silica aerogel, new possibilities can be revealed regarding the way we interact with our atmosphere as well as the function of future green design, from fields as divergent as fashion and architecture.

Aerogels are derived from a variety of materials including zirconia, silica and alumina. NASA initially developed aerogel as a means of stellar dust collection, using the material as a means to protect the integrity of the particles, cushioning against impact and heat. These materials have the lowest sound velocity of any known solids, containing extremely low dielectric constants. They have the ability to support up to 1500 times their gross weight and contain exceptional internal surface areas; (a small cube of aerogel may contain up to two basketball courts). Typically, aerogels are slighty hazy, as light scatters through the material, giving these solids a smokey-blue appearance. This pale blue colouring operates in a similar way to earth’s atmospheric functions. Ie., as the sun takes on an orange hue, so does the shadow from a vial of aerogel. This phenomenon is due to ‘Rayleigh Scattering’ and ‘Mie Scattering’, the way in which the colour is perceived depends on the sunlight angle and size of the particles.

Fig 1: *'Eclipse'*, dimensions variable. Silica aerogel, trimmed glass bottles. ©Michalou(di)s 2005.

TYNDALL EFFECT

The works pictured in (Fig 1) are half-filled bottles containing silica aerogel. The work is illuminated to highlight the 'Tyndall Effect' of the bluish/orange tint to the material dependant on the light source. 'This color comes from a reflective transparent sheet on which the sculpture rests. We can clearly see the shape of the torso, its reflection. But if this is the torso's mirror image, why is its color not a blue one but an orange one? Only the phenomenon of Mie scattering can explain this visual enigma. This orange light is the light that transpierced the sculpture, traveled to the plastic sheet, where it reflects to our eyes as an orange color. In fact, if we keep the sculpture between our eyes and a light, the sculpture has an orange and not blue hue. These blue and orange colors are why if you have a piece of silica aerogel in your hand, it is as though you hold a piece of sky between your fingers'. [1]

The works are suspended, appearing to float in space, seemingly as light as the material they contain. The works are representative of man's unceasing production and the need to produce and consume. The bottles are crude, and while the work is about our collective impact due to manufacturing, it is evident that the bottles are produced from recycled glass. This adds another dimension to the artwork, as, like a recycled product, these bottles have seemingly been through the machine that initially manufactured them. The contrasting substance of the aerogel with the bottles is evident, yet this is another aspect that links the work back to production – the bottles and the aerogel are derived from silica (sand), and while there are different grades of silica, the products still share the same base mineral.

Silica production accounts for many skyscraper windows: these windows allow unwanted heat and light to enter many of these buildings, on a massive scale. What if windows were treated with nanomaterials and became highly efficient insulators? This addition/incorporation would drastically reduce emissions and make for more comfortable city spaces. Aerogel technology has already been trailed in double panel windows to great effect, deadening sound and offering superb insulation. Could biotechnology allow us the possibility to produce aerogel cultures? Could these cultures be synthesized with our built environments to create self-establishing green spaces?

AEROGELS AND URBAN DESIGN

In ‘Design for a Sustainable World’, Victor Margolin argues that a renewed push towards using sustainable products and processes is pivotal if we are to save our environment, and create attitudes that centre on responsible product choices and materials. He writes ‘The challenge of creating a sustainable world has moved from the realm of idealism to that of necessity. Our survival as a human race depends on it’. [2] The important question to be asked, then, is: “if the atmosphere can be understood as a protective garment invisibly draping our planet, then could aerogels provide practical solutions to aid this veil?”

Fig 2: ‘*Sky surrounded by lava,* melted brass, aerogel, dimensions variable, ©Michalou(di)s 2004.

This experiment (Figs 2-5) is the first attempt to combine the classic heavy sculptural medium of brass with the contemporary medium of silica aerogel. At Shivaji University, (Maharashtra, India) Dr. Manish Kulkarni and Dr. Sharad Bhagat were impressed, as the combination of these materials resembled molten lava encasing a piece of sky.

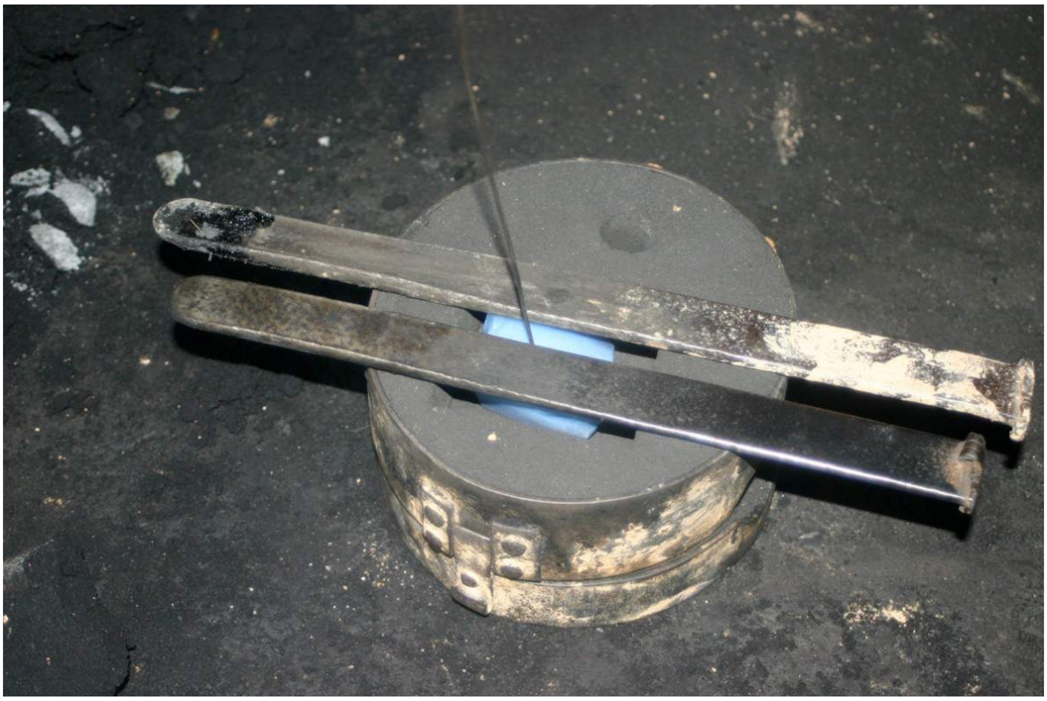

Fig 3: ‘*Sky surrounded by lava,* melted brass, aerogel, dimensions variable, ©Michalou(di)s 2004.

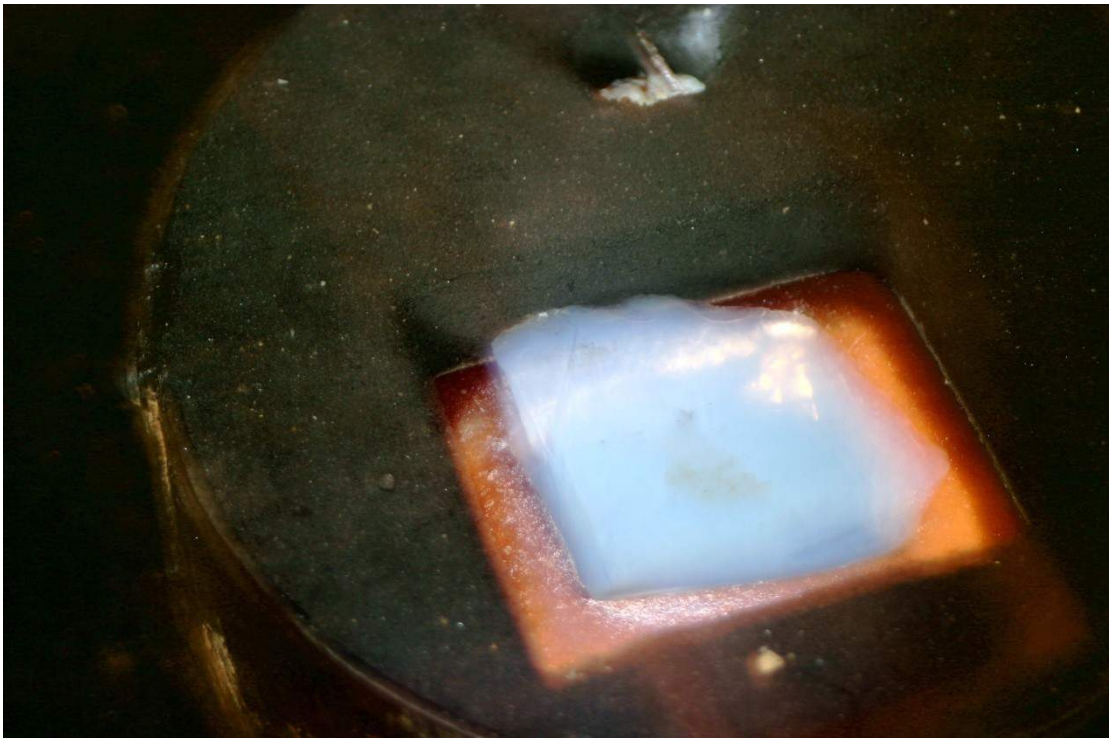

Fig 4: ‘*Sky surrounded by lava,* molten brass, aerogel, dimensions variable, ©Michalou(di)s 2004.

The work in (Fig 4) highlights the light play within the material, the sunset and sunrise phenomenon. While the colouring is a significant element of the aerogel, the heat contained within the metal plate, in this instance, provides the orange glow. These aesthetic interventions represent the physical properties of the aerogel and its ability to withstand heat up to, and in excess of, 1200 degrees. The extreme example seen here references our atmosphere, and the barrier of the ozone layer represented as the aerogel. The importance of this image is that the visible heat contained in the metal is enough to combust many materials, referencing also the furnace and the refining of steel and molten metals. The ghostly aerogel, in stark contrast to the orange heat of the foundry, remains visually unchanged, almost softer and lighter against the radiation – seemingly ice-like and cool.

While the resistance between the materials is physically evident in the image, the broader picture presented here is in relation to the ephemeral, the protection the invisible ozone provides the human race. While it shields earth from the sun’s ultraviolet rays, it is also a barrier that can be degraded and destroyed if we underestimate the negative impact of our products and processes, ie. the manufacture of chlorofluorocarbons. This work, similarly, points to material applications of aerogel that can mimic the function that the ozone layer plays in protecting the earth, creating a second layer of defense. What the work posits is the following scenario: if our ozone layer was depleted to a critical level, would a need for physical barriers arise, and if so, could these physical barriers be manufactured from silica aerogel? Sustainable urban design is necessary for these propositions.

SKY DOMES – FUTURE HOUSES?

Margolin provides R. Buckminster Fuller as an example of a designer who was concerned about the earth’s future, and who, in the 1920s, began to propose green products and architecture that challenged the then current methods of production and manufacture. The geodesic dome brought him public attention, Margolin stating that the ‘economy of materials as well as their durability, flexibility, and ease of construction were quickly recognized by the United States Marine Corps, and then were widely adopted by the industry’. [3]

While Fuller had grasped the necessity of planning for a sustainable future that incorporated the latest technologies and materials, he was also willing to realise these ideas in the form of prototypes and projects. His visionary initiatives culminated in an electronic display that would provide an ongoing, updated representation of the world’s global resources as part of the World Design Science Decade. He also published ‘A Comprehensive Anticipatory Design Science’ in which he raised concerns about depleting resources and the importance of designing for the future’. [4] What if Fuller had aerogel at his disposal when he was engineering these structures, though? He most certainly would have realised the potential of the nanomaterial, perhaps as a substitute for the triangular panes of glass in his geodesic domes. This could create a structure that is strong, lightweight and self-supporting, capable of eliminating heat, cold and sound: namely, a *Sky Dome*. Sharing Fuller’s perspective, we are able to envision a new world that combines art, science and technology to allow for the creation of new spaces for human habitation.

Artist James Turrell also recongnises the importance of a relationship with the natural world, utilising his art installations as a means of establishing this connection. As he puts it: ‘There was a time when men were very much aware of the solar movements, the stars, the sun… and one can say that the calendars of different civilizations such as the Mayans, the Egyptians and even the Christians were related to the positions and movements of the planets. We live in a time where we have lost this connection with the earth and the sky’. [5]

UNIQUE MATERIAL COMBINATIONS

Fig 5: *‘Sky Surrounded by Lava’* molten brass, aerogel, dimensions variable, ©Michalou(di)s 2004.

The image (Fig 5) is one that shows the combination of molten brass with silica aerogel. In this process, brass is poured into a mold, then mixed and set with the aerogel to create a final form combining the two materials, albeit in an unlikely composition. While bronze is a traditional artistic sculptural material, silica aerogel is a relatively new one. Additionally, the brass is very dense while the aerogel is lightweight and translucent. In this material exchange, the artist becomes a material alchemist, merging old processes with new technologies. This heterogeneous material combination is reminiscent of one of silica aerogel’s original uses: namely cosmic dust collection.

NASA researchers have analysed the comet-dust fragments embedded in the aerogel from various crafts over a period of years. They found not only grains that yielded surprising results, but also information from the samples challenged traditional understanding of the particles location. Comet grains are comprised of isotopes evident throughout the solar system: Olivine was also found in one particle: (A component of Hawaii’s green sand – magnesium olivine is believed to have been amongst the materials that formed around our young sun.) The same grain contained calcium-aliminium: a mineral that only forms in extreme heat, when in close proximity to the sun. Of the samples the researchers analysed, all came (contrary to popular belief) from the inner solar system. [6] The microscopic sample images from the mission show the comet grains embedded in the aerogel pockets, each particle seen with a unique static trajectory, as the force has left the entry points visible in the material. These grains appear to still be moving, captured in motion.

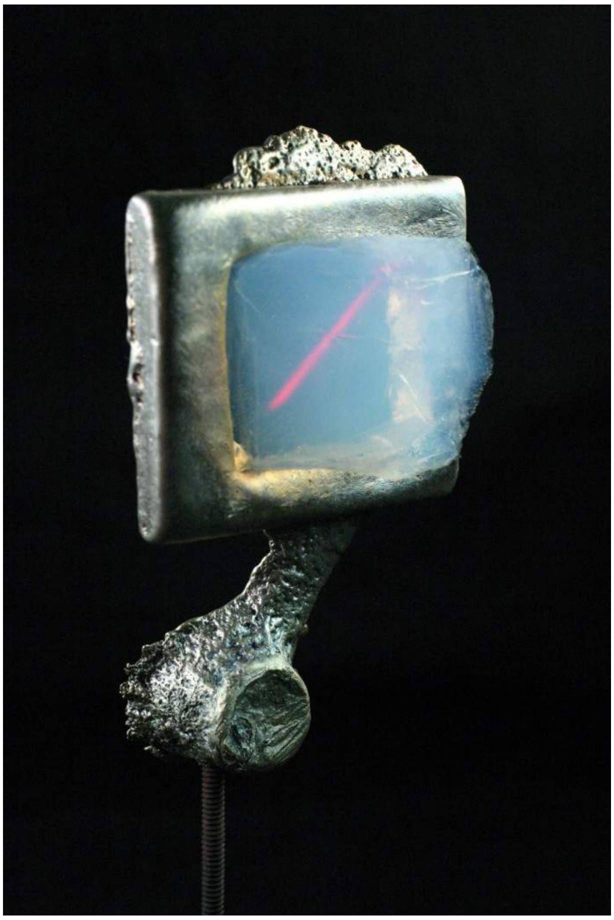

Fig 6: ‘*Framed Sky*’ mixed media, dimensions variable, ©Michalou(di)s 2004.

While the capturing of interstellar particles and pouring of brass in a foundry seem polar opposites, both demonstrate our need to challenge existing theories and extend preconceived material notions. The brass/aerogel casting synthesizes two unlikely materials, creating an uneasy relationship between the two. Unlike the functional aerogel from the Stardust mission, which exists to display the mineral results, (Fig 6) appears to be the centerpiece of the work, the surrounding mineral existing as a housing or vehicle for display of the cosmic material. Juxtaposing densities, the physicality of these solids and heterogeneous pairing allow us to reconsider aerogels as aesthetic forms, not just as functional products.

Presenting aerogel in this manner privileges its form over function, subverting industry’s expectation of the product. In this case, the form and appearance are the focus rather than its insulating properties. The work is placed in the context of a gallery rather than a laboratory. This platform allows the public to engage with it, firstly, through aesthetic means, before looking into its scientific credentials. Buckminster Fuller captured the public’s imagination via the prototypes of his geodesic domes – industry and production followed. He had realised that scientific concepts alone would not bring about the change he was predicting. While the domes are at the forefront of sustainable urban design, they were initially appreciated and embraced on the basis of their form and structure – (one that also contains fractal dimensions and is found in the natural world.)

The brass works also position these pieces as art objects to be considered in terms of aesthetics; of beauty and form. The inbuilt laser within the work adds visual intrigue, revealing both a solid with a non-solid appearance.

ILLUMINATION: LED LIGHT

‘Illumination’ generally refers to the power of light to reveal: to enlighten or elucidate. This definition plays out in these works in a similar way. The physicality of the aerogel is examined through direct light/laser interaction, while the hidden qualities are also revealed during this intervention, similar to the effect of light moving through smoke. The viewer is confronted with an object of beauty that appears to contain within it a physical improbability.

Light has been used in works of art for centuries. The way the LED light illuminates the disc of aerogel in the work ‘Noli Me Tangere’ (Fig 7); makes the viewer privy to a visual revelation. James Turrell speaks of the revealing power of light: ‘we use light to illuminate things. I am interested in the thinness of light. I am not so much interested in those things the light illuminates as I am in the revelation of light itself. Using light in a manner as seen in a lucid dream helps connect the material with the immaterial, the seen with the unseen’. [7] What is evident in these works is the immaterial being made visible. As the light enters the disc, we are able to see, through the illumination, the materiality of the artwork.

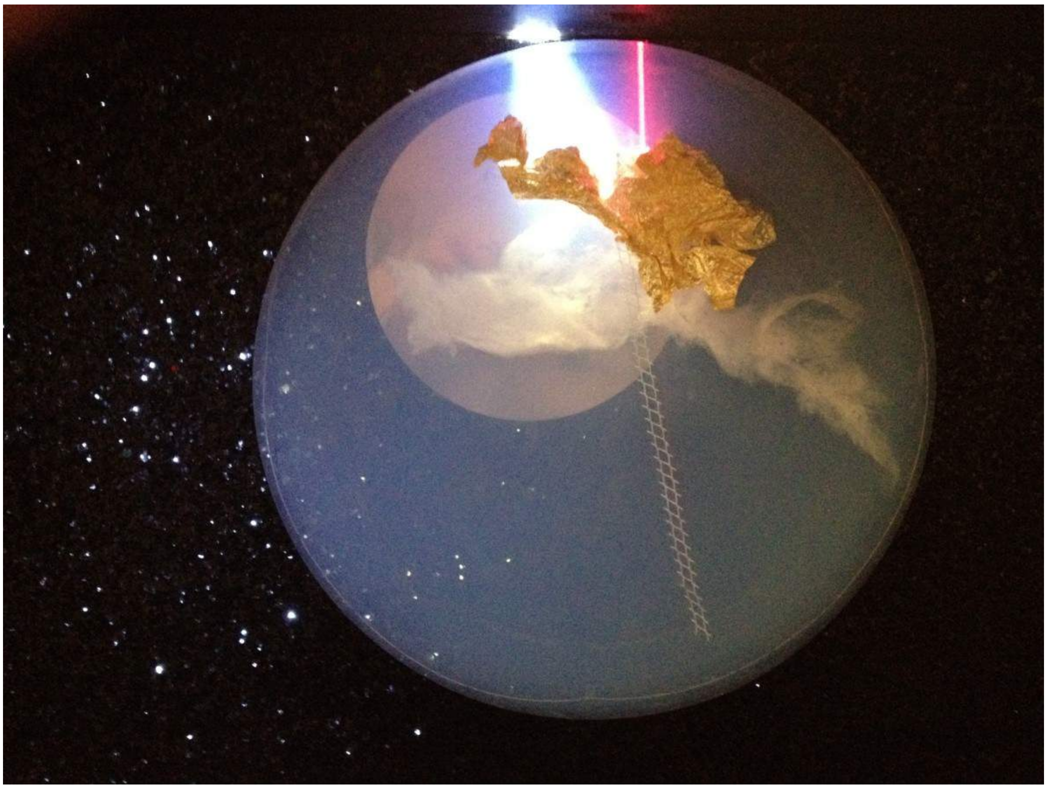

Fig 7: *‘Noli Me Tangere’* dimensions variable, silica aerogel, laser, crystal, breath, LED lighting, motor, ©Michalou(di)s 2010.

ILLUMINATION: LASERS

The use of lasers in art was initially promoted by Gyorgy Kepes, a Hungarian artist who ‘wished to contribute to the successful reunification of man and nature’. [8] While Kepes used the laser to inform us directly about the natural world, the works in (Figs 6 – 10) function using silica aerogel as the conduit. In (Figs 7 and 8), the laser passes through a rotating Swarovski© crystal, causing the laser light to amplify and scatter dynamically.

This direct intervention with material in real-time, draws attention to the phenomenon of scattering that is a natural occurrence. The mechanics of a motor that turns and illuminates a crystal are representative of man’s efforts to replicate the natural, the ephemeral and the invisible. Again, we have reference to the importance of maintaining our skies, and the sobering message that any attempts to imitate natural phenomena are ultimately inconsequential. This is an SOS (save our skies), the laser can be imagined here (Fig 8) as a pure beam of heat, puncturing through a hole in the ozone layer and destroying random areas with it’s focused rays.

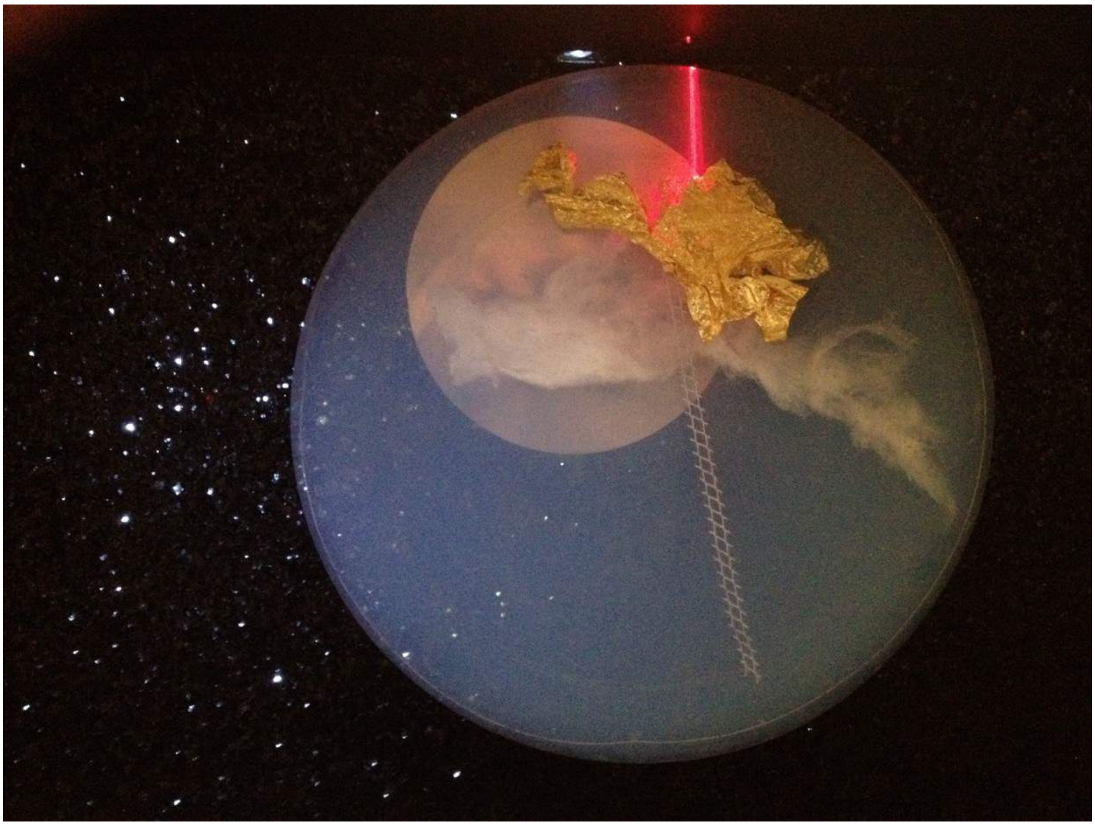

Fig 8: *‘Noli Me Tangere’* dimensions variable, silica aerogel, laser, crystal, breath, LED lighting, motor, ©Michalou(di)s 2010.

‘This project aims to defamiliarise the way in which we view, and interact with the sky, the atmosphere and ultimately the world that surrounds us. Viewing sky from an alternate perspective prompts an aesthetic re-engagement that is visual in nature. Re-presenting the sky/cloud works as both a symbolic gesture and a tangible form, thereby creating a synthesis of science and art’. [9]

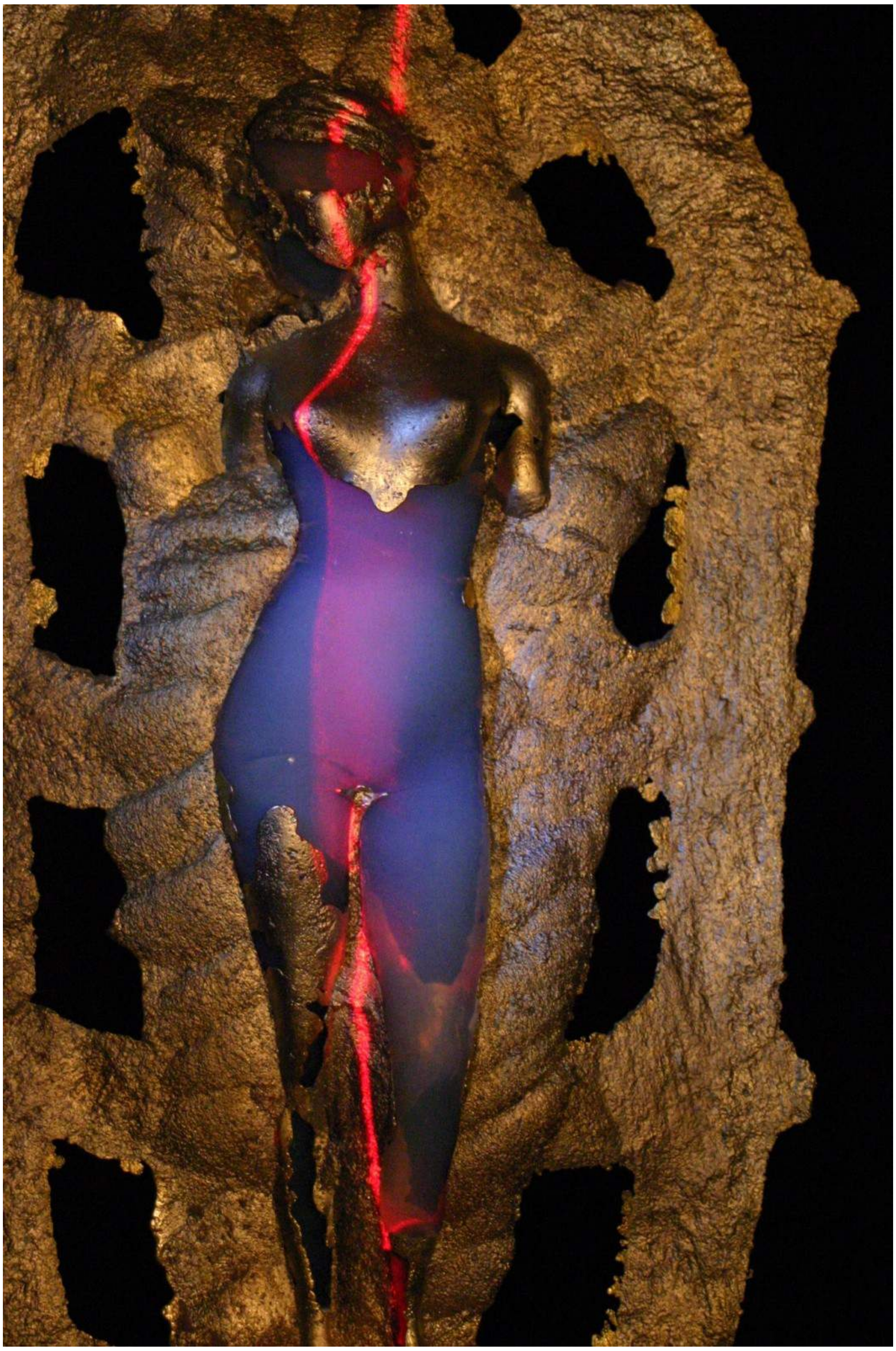

Fig 9: ‘*Veria Girl’*, 35 x 200 x 10cm, silica aerogel, brass, laser. ©Michalou(di)s 2006.

While the use of lasers in art is a relatively recent phenomenon, industry has, over a much longer period, commercialised many functions for laser, from measuring and marking, to delicate eye surgery and large-scale industrial laser cutting. The work ‘*Veria Girl’* seen in (Fig 9) approaches these notions, referencing formal sculpture and traditional approaches to figurative representation. The line that dissects the figure is included as an element within the work, although its interaction is limited solely to defining the exterior of the brass

sections that compose the work. Where the aerogel is touched, light scatters throughout the substance: at these points it becomes absorbed into the work rather than simply functioning as a marker.

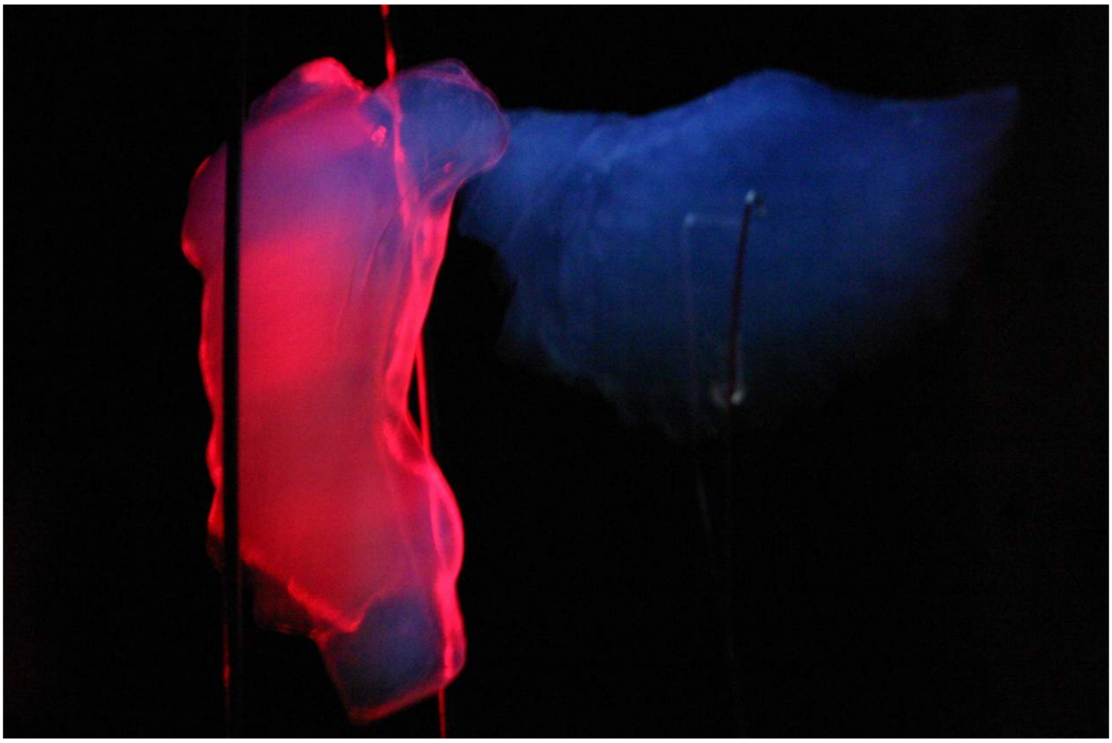

Fig 10: *'Icare, I care…'* Installation. Silica aerogel, red laser, stainless steel rods. ©Michalou(di)s 2005.

The use of the laser as a method to illuminate the form in (Fig 10) shows the ability of art to reveal what may otherwise remain hidden or undiscovered. While this paper has discussed the ephemeral properties of aerogels, and their applications for a sustainable future, the exotic nature of silica aerogel is not to be underestimated. Many new materials have been produced since aerogels were discovered, but none have the translucency or appearance of silica aerogel. The ability of the laser to fully illuminate the cast figure reveals the extent to which light is able to scatter throughout the structure, giving the work an almost holographic appearance.

'Icare, I care' is a work that conjures up images of a future that appropriates light/laser technology, an existence that is less tactile than our current (that relies on wiring and physical connections). The use of lasers to transmit information without the aid of cables may become a reality as the material/immaterial boundaries are challenged through evolving technology. If we extend these ideas (which the medium of aerogel allows,) can matter, as well as information, be passed via laser/light, and could these light beams have the ability to enable teleporting? The figure appears to be bathed in a laser beam, with colour operating like an ethereal garment. Perhaps this is how the artist views the future – as light through the lens of nanomaterial.

AEROGELS – NATURAL GEOMETRY

Mathematician Benoit Mandelbrot formulated the idea of fractals in the 1970s, refining the idea further over many years to create a better understanding of natural geometry. Mandelbrot proposed that all natural forms had a 'fractal dimension' having self-similar shapes that, upon investigation, revealed the same configuration, at all scales. In 'The Fractal Geometry of Nature' he states: 'both their regularities and their irregularities are statistical. Also, the shapes described here tend to be scaling, implying that the degree of their irregularity and/or fragmentation is identical at all scales'.[10] Throughout nature, these forms are evident, from the self-repeating nautilus shells to dendritic drainage patterns found in river systems. Unveiling these forms gives us a clearer understanding of nature, and the systems that exist in the seeming chaos, one that is characterised by symmetry. These forms are evident in the silica aerogel, a mineral derivative that exhibits these traits.

Stanislas Teichner states that the thermal qualities of aerogels have a direct correlation with their fractal dimension: ‘The exceptional thermal properties of aerogels depend on their fractal structure and fractal dimensions.’ [11] It is easy to forget that these mysterious products are derived from something as commonplace as sand, but their fractal nanostructures betray this history.

CONCLUSION:

These works aim to encourage dialogue about humanity’s impact on the natural world. There is hope for a better, more sustainable, mode of living, if we are willing to consider the impact of existing materials on our atmosphere, and to embrace new products and their potential application to our urban environment.

Space technology’s nanomaterial, silica aerogel, is the central material used throughout these works. The work in (Fig7 and 8), ‘*Noli me tangere’* translates as ‘*Touch Me Not’*, its etymology stemming from Christ’s appearance to Mary Magdalene post-resurrection. Ascension followed soon after this encounter, and a physical separation ensued. The 2004 ‘*Sky Cloning project*’ saw clouds encapsulated in aerogel: conceptually, these works maintain similar parallels with this story. Mary now becomes an onlooker, able to observe remotely, like the viewer of this artwork. These untouchable cloud-forms only permit visual investigation yet can be connected with in a tactile manner.

The tension between the physical and the untouchable here is a constant reminder of the unseen spheres that surround us. The protective veils that surround our planet may be ephemeral but offer us physical defense, substantial screens composed of minimal substance. These artworks serve to remind us that these transient screens may only offer us temporary protection, yet provide hope for a sustainable future.

IOANNIS MICHALOUDIS

BIOGRAPHY: Dr. Ioannis MICHALOUdiS received his Ph.D in Visual Arts at the University of Paris I, Panthéon-Sorbonne in 1998. His artistic work till then was characterised by the use of elastic fabric in site-specific installations (*in situ*), environmental art and public art projects. In 2001 had received the Fulbright Award in order to achieve a postdoctoral research titled *(Nephele)3* at the Center for Advanced Visual Studies of Massachusetts Institute of Technology. The *aer( ) sculpture* project is an art & science research concerning the creation of sculptures using silica aerogel, a material used by NASA in space exploration, an immaterial material having the appearance of a fragment of sky.

MIIK GREEN

BIOGRAPHY: Green is a multidisciplinary artist living and working in Western Australia, and is represented by Stella Downer Fine Art (NSW) and Linton & Kay Contemporary (WA). As the recipient of an *Australian Postgraduate Award Scholarship,* Green is currently undertaking a M.Phil. at Curtin University of Technology. Green has completed a Bachelor of Arts (Hons, 1st Class), a Bachelor of Visual Arts, Painting and has an Advanced Diploma of Industrial Design – *miikgreen.com*

REFERENCES

[1] Michaloudis, I., Journal of Non-Crystalline Solids**,** 350, **2004**, p.63.

[2] Margolin, V. “Design for a Sustainable World” *Design Issues* 14 (2): **1998**, p. 84.

[3] Ibid.

[4] Ibid.

[5] Moscatelli, F., James Turrell, Charta Books Ltd, **2009**, p. 43.

[6] Cowen, R., Science News, 170, **2006**, p. 387.

[7] Moscatelli, F., James Turrell, Charta Books Ltd, **2009**, p. 43.

[8] Csaji, A., and Kroo, N., Leonardo, 25, **1992**, p. 23-28.

[9] Michaloudis, I., Miik G., The 3rd Art and Science International Symposium, (Paper being published), China, **2012**

[10] Mandelbrot, B., The Fractal Geometry of Nature, W.H. Freeman and Co, **1982**, p.1

[11] Teichner, S., Chemtech, 21, **1991**, p. 372-377.

Session 3: INORGANIC AEROGELS

CO12

EFFECT OF THE SOLVENT USED ON SURFACE MODIFICATION ON THE SYNTHESIS OF AEROGELS DRIED UNDER AMBIENT PRESSURE

B.A. García-Torres a, Fernando Enríquez b, L. Álvarez-Contreras a, A. Aguilar-Elguezabal*a
a Centro de Investigación en Materiales Avanzados, S.C., CIMAV, Miguel de Cervantes 120,
Complejo Industrial Chihuahua, 31109 Chihuahua, Chih., México
bFacultad de Ciencias Químicas, b Universidad Autónoma de Chihuahua – UACh, Campus
Universitario, Chihuahua, Chih. 31200, México
*Corresponding author: alfredo.aguilar@cimav.edu.mx

Abstract

Aerogel is also known as solid smoke due to is low density, since more than 85 % of its volume is air [R. Baetens et.al., (2011)], for this reason aerogels present a high potential as thermal and

acoustic isolation materials, with the advantage over organic materials of its high stability at high temperatures and the absence of the release of toxic sub products when exposed to fire.
Kistler developed the method of synthesis of SiO_2 based aerogel in 1931 [S.S. Kistler (1932)], in a process that required the use of supercritical conditions for the removal of the water after gelation of SiO_2 precursor. Main challenge to spread the use of this material in ordinary applications like isolation in construction is to lower the production cost. For this purpose the drying of the aerogel under ambient conditions has been exhaustively studied, since the collapsing of structure occurs when water is removed from the SiO_2 matrix by evaporation due to capillary forces. After wet gel is obtained, water must be substituted before drying, and to aid this process, surface hydrophilic nature is changed by means of the exchange of polar –OH groups on surface by non-polar groups, like the obtained with trimethylchlorosilane. Surface modification is made under a non-polar solvent, being hexane the most common solvent.
In this work we report the results of the use of several solvents and steps on the silanol groups substitution from alcogel surface, with the aim to obtain an aerogel monolith free of cracks. Aerogels obtained presented typically as best results, a density around 0.18 g/cc, thermal conductivity of 0.04 W-m/K and surface area higher than 800 m^2/g.

Introduction

Aerogels were synthesized by the first time around 80 years ago by Samuel Kistler, and only recently during last decades significant advances have been made to develop applications of this material [L. W. Hrubesh et.al., (1990)]. These materials are amorphous and porous solids, and are constituted by a meso and macroporous tridimensional network of silica nanoparticles. Aerogel due to its low density which could be from 0.1 to 0.3 g/cm^3 [Sung-Woo Hwang et al., (2008)] [Sharad D. Bhagat et al., (2007)], have a wide diversity of applications like thermal [M. Schmidt et.al., (1998)], acoustic [Lawrence W. Hrubesh, et.al., (1998)] and electric isolation [GunS. Kim, Hyung H. Park et.al., (2001)] [Rubén Baetens et al., (2011)]. Thermal conductivity could be lower than 0.06 W/mK [P.B. Wagh et al., (1999)], and surface area values are high, typically from 470 to more than 800 m^2/g [Sharad D. Bhagat et al., (2007)] [P.B. Wagh et al., (1999)]. The industrial aerogel synthesis concerns a sol-gel process where the bottle-neck consist of the elimination from porosity of the solvent used during preparation, since for this purpose is necessary to use a drying step on an autoclave under critical conditions. Many efforts have been made recently to found an alternative process to dry the aerogel under ambient conditions. The key to develop such process consist on the modification of hydrophylic surface after gel aging step to transform to hydrophobic surface and then displace the polar solvents used during synthesis, outside of the porosity, avoiding thus the capillary forces that the interaction of polar solvent and polar walls of porosity generates during the evaporation of solvent. For this purpose a non polar solvent is used as vehicle to transport the reactive, trimethychlorosilane (TMCS) to internal surface of the pore system and change the polar exposed HO-Si groups at surface by the non-polar $(CH_3)_3$-Si groups. After this change the evaporation under ambient condition of solvent becomes less destructive.

In this work the modification of surface is made using three different solvents, hexane, heptane and acetone and the resulting aerogels are characterized to determine the effect of each solvent to produce an aerogel monolith with best properties.

Materials and Methods

The synthesis of aerogel was made by sol-gel method. For this purpose tetraethylorthosilicate (TEOS, Aldrich al 98%) was used as precursor, as well as isopropyl alcohol (IPAFaga Lab 99.5%), distilled water, hydrochloric acid (HCl 36-38% J.T. Baker), ammonium hydroxide (NH_4OH_28-30% J.T. Baker), n-heptane(99.5% Analytical), Acetone (99.6% Acros Organics) and Hexane (99.977% CTR Scientific).

Precursors were used at the molar ratio TEOS: IPA: H2O: HCl: NH_4OH = 1:3:4:1.8x10^{-3}: 8.12x10^{-3} according to Gun S. Kim, Hyung H. Park et al., (2001). Solution was maintained under stirring for 90 min, and the sol thus prepared was kept at 30 °C for one day without stirring to obtain the gel.

The second step was the aging using solvents. Initially the gel was maintained under a mixture of water/IPA (molar ratio 0.55:0.65), with this treatment the removal of unreacted precursors is expected, as well as the increase of crosslinking. Subsequently, solvent mixture was changed to a TEOS/IPA solution (molar ratio 0.022:0.327) and kept at 30 °C for a day, this treatment has as main objective to improve mechanical properties of gel. Previously to the surface modification treatment, TEOS/IPA solvent was changed to non-polar solvents (n-heptane, hexane or acetone) and maintained during one day at 30 °C, this treatment was made to avoid a fast reaction in the next step, which could damage the structure of the gel.

The third step consist of the modification of surface, for this purpose a mixture of TMCS: IPA: Solvent (molar ratio 0.75: 3.17:0.83) was used. This mixture was added at a rate of 10.6 ml/h, thereafter the gel was maintained on the resultant solution and reactive mixture during one day, after this treatment the hydrophobicity of surface was obtained. Later gel was washed with solvents (n-heptane, hexane and acetone), to eliminate the formed HCl and the unreacted TMCS. Drying of gel was made under solvents atmosphere at 50 °C.

Characterization

Monoliths of silica aerogel were characterized by nitrogen adsorption (-196 °C) to determine textural properties on an equipment model Autosorb 1C from Quantachrome. Surface area was calculated by the method of Brunauer Emmett and Teller (BET) and pore size distribution was made by Barret-Joyner-Halenda (BJH) method. Aerogel structure was characterized by field emission scanning electron microscopy (FE-SEM) in a Jeol JSM-7401 equipped with energy-dispersed spectroscopy (EDS) to determine elemental composition and dispersion of elements. To determine the hydrophobicity of aerogel surface the contact angle was measured by FTA200 dynamic contact angle analyzer, and Infrared spectra were taken with a Perkin Elmer FTIR, model Espectrum GX. Thermal conductivity was measured with an equipment Thermal Conductivity 2022 from Unitherm.

Results and Discussion

The solvent change from TEOS/IPA to non-polar solvent has as objective to reduce the amount of water that is occluded at porosity of aerogel in order to minimize the damage that could occur during the step of surface modification, since IPA and water during the drying process induces the cracking of structure due to capillary forces on porosity.

The surface modification treatment begins with the transformation of the hydrophilic surface of aerogel to hydrophobic by changing the silanol groups by trimethylsilyl (TMS) groups as is shown in reaction 1, and thus by this way is promoted the removal from porous of water and other polar compounds formed during reaction as co-products.

(1)

One of the main side reactions consists on the formation of isopropoxytrimethylsilane (IPTMS), which results from the reaction of the solvent IPA and TMCS according to 2.

(2)

The formation of IPTMS also lead to the hydrophobization of surface, since this compound reacts with the silanol groups of surface to form a trimethylsilyl group, and IPA is released as is shown:

(3)

As the internal walls of pores are covered by TMS groups, the surface became hydrophobic and the water, HCl and IPA of cavities are displaced by the non-polar solvent used as vehicle for this surface modification. Some reactions of TMCS produce non-desirable products like hexamethyl-disiloxane, and the same could occur for IPTMCS

(4)

(5)

These reactions are exothermic, and tend to increase local temperature, which can damage the integrity of the monolith, for this reason reaction was controlled to keep system at 30 °C.

Figure 1 shows the image of the monoliths after drying. As can be seen the sample obtained using acetone broken into pieces, which could be associated to a partial modification of surface on internal pores, being present the mechanism of fracture during drying which consist on the collapse of pores due to capillary forces due to the attractive forces of solvent and pore walls. Best results were obtained for hexane, which has the lower boiling point temperature (69 against 98 °C of heptane), and also lower surface tension (18.4 and 20.4 N/m for heptane), these two properties made easiest the release of solvent during drying of monoliths.

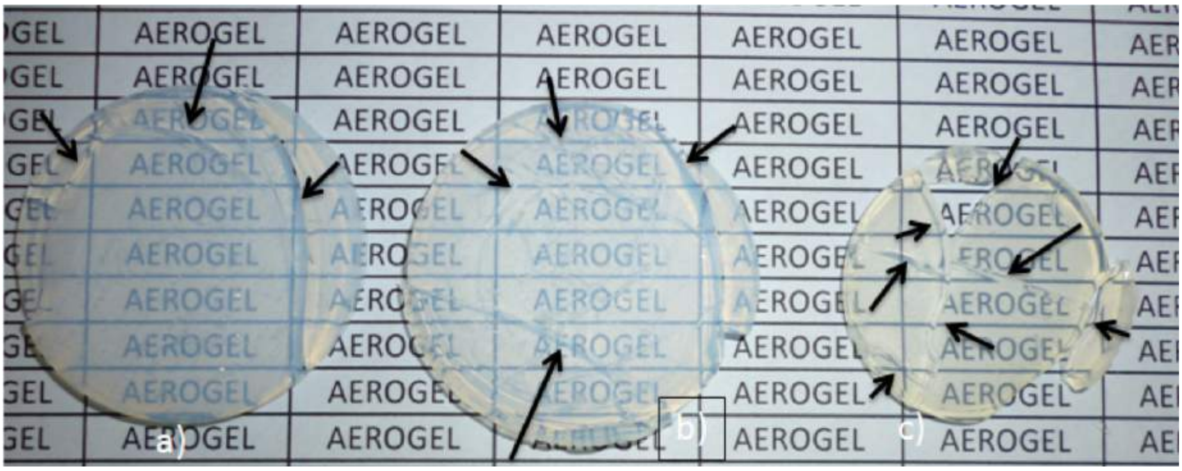

Figure 1. Aerogel monoliths obtained with surface modification treatment and solvent pre-treatment with a) Hexane, b) Heptane; and c) Acetone.

As was mentioned before three solvents were studied as vehicle to aid during the modification of surface. The non-polar solvents hexane and heptane shown best results. The use of acetone, an aprotic solvent lead to a poor surface modification probably due to the miscibility of acetone and water, thus water remains on porosity and reversibility of reactions could cause rehydroxilation of the surface of aerogel. With the use of acetone as solvent a higher cracking and contraction is observed on the monoliths after drying. The higher contraction is explained by the uncompleted modification of surface, which restricts the spring-back process of structure. For samples treated with the non-polar solvents a lower density was obtained as can be seen in Table 1. Difference of density is more than twice for acetone treated sample when compared with samples made with hexane and heptane.

Surface area is almost the same for the three samples, a little increase is observed for sample treated with acetone, probably due to the cracking of structure, which produced formation of dust of aerogel. Pore volume was higher for sample prepared with hexane, which was the sample that preserved better the integrity, i.e. these materials presented the lower cracking of the monoliths.

Table 1. Comparison of aerogel properties prepared with different solvents for surface modification.

Sample	Density (g/cm^3)	Surface Area (m^2/g)	Pore Volume (cm^3/g)	Contact angle	Thermal Conductivity (W/mK)
Hexane	0.22	836	3.05	126	0.054
Heptane	0.18	851	2.18	136	0.046
Acetone	0.51	901	2.63	119	0.062

The isotherms obtained from nitrogen adsorption characterization were of type IV according to IUPAC classification [Rouquerol et al., (1994)], and not big differences were found among the samples. Pore size distribution results indicated that mean pore size is around 7 nm for the samples.

Figure 2a and 2b shows typical microstructure of aerogel samples, and as can be seen, particle size of spherical units are from 5 to 12 nm. Micrograph 2b allows to observe the pores of diameter around 7 nm determined by nitrogen adsorption, and also the presence of well-structured macropores which are not in the range of evaluation with that technique. Image 2c shows a structure with high agglomeration found with higher frequency for the aerogel obtained with the use of acetone, which explains the higher density of this sample.

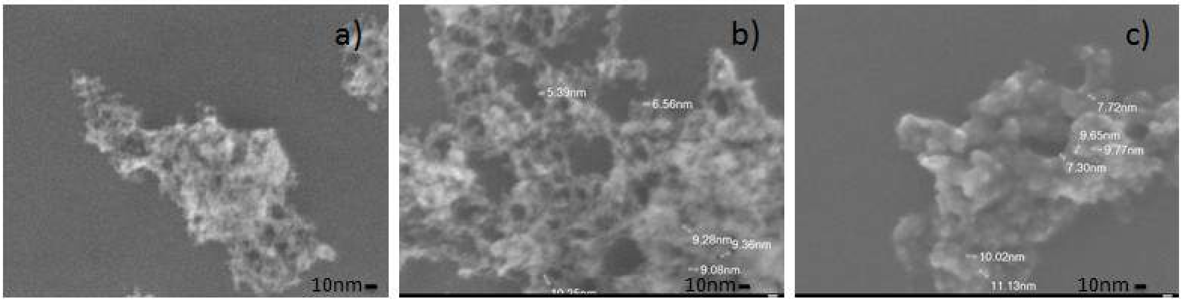

Figure 2. Micrographs of aerogel, a) and b) correspond to typical structures found for aerogels with low density, and c) to material obtained from the synthesis where acetone was used as solvent.

The contact angle of a water drop on surface of aerogel is an index of the amount of hydrophobization. As was shown in Table 1, the lower contact angle corresponds to sample synthesized with the use of acetone. Difference from the other samples is lower than 15%, this could be explained considering that the exchange of –OH groups by trimethylsilyl groups on exposed surface is highly probable, and main difference on surface modification degree must be at the internal surface of pores. The use of heptane lead to the higher hydrophobicity value, this result could be due to a favorable condition of this solvent to promote the reaction of TMCS with –OH groups from aerogel surface.

Infrared spectroscopy made to aerogel samples corroborates the surface nature modification. As can be seen at figure 3, there are signals of C-H groups (stretching vibration 2900-3000 cm^{-1}) that correspond to the trimethylsilyl group attached to surface. Besides the signals associated to aerogel structure (1050-1100 and 560 cm^{-1}), the absorption bands at 1240-1250 and 840-850 cm^{-1} corresponding to $Si\text{-}CH_3$ groups from TMCS are also present.

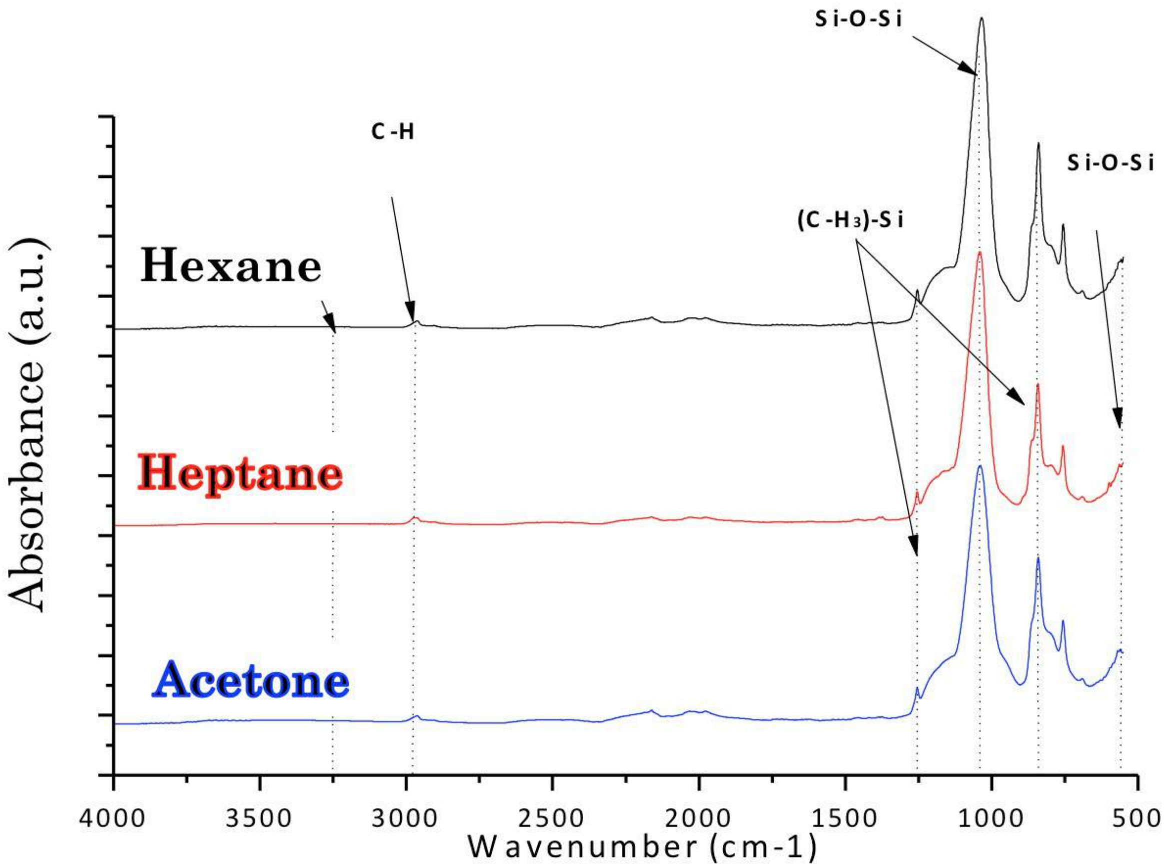

Figure 3. Infrared spectra of aerogel samples obtained with the use of the solvents hexane, heptane and acetone.

Results of thermal conductivity are associated to density of aerogels, since the highest conductivity was obtained for the aerogel with the highest density (where acetone was used) and the lower conductivity (0.046 W/m K) was obtained for the material with the lower density (0.18 g/cm^3). The thermal conductivity of air is the half of the best value obtained for this materials, thus these monoliths are adequate for application as thermal insulation materials, however more research must be done to optimize their synthesis in order to obtain monoliths free of cracks.

Conclusions

In the synthesis of aerogel monolith with the drying at ambient pressure process, with an intermediate step where surface is modified to obtain a non-polar surface, best results on integrity (monolith with only few cracks) was obtained when hexane was used as solvent for surface treatment, which has lower boiling temperature and surface tension, however best value on density, thermal conductivity and hydrophobicity (contact angle) was obtained for samples prepared using heptane as solvent, despite the higher amount of defects on structure. Thus a compromise result on the selection of solvent, where the low density, low viscosity, low boiling temperature and low surface tension of hexane could help to dry the aerogel with minor damage on the structure, and a better compatibility of TMCS and heptane allows a higher surface modification degree and higher water elimination during hydrophobization step, that gives a better spring back result and so, lower density and lower thermal conductivity, but with a monolith with visible cracked structure. The use of acetone, a polar solvent was non-adequate to promote the complete modification of aerogel surface, which was detrimental to the synthesis of the monolithic structure of aerogel.

Bibliography

Gun S. Kim, Hyung H. Park. and Sang H. Hyun : "Synthesis of low-Dielectric Silica Aerogel films by ambient Drying.". *J.Am. Ceram. Soc.*, 84 (2) 453-55 (2001)

Rouquerol J, Avnir D., Faitbridge C.W., Everett, D.H., Haynes J.H., Pernicone N, Ramsay J.D.F., Sing K.S.W., Unger K.K, IUPAC Recommendations for the characterization of porous solids " *Pure Appl. Chem*. 1994, 66 1739

L. W. Hrubesh, "Aerogels: the world's lightest solids," *Chemistry and Industry*, no. 24, pp. 824–827, 1990

Lawrence W. Hrubesh: "Aerogel applications". *Journal of Non-Crystalline Solids* 225 1998. 335–342.

M. Schmidt , F. Schwertfeger: "Application for silica aerogel products". *Journal of Non-Crystalline Solids* 225 1998. 364–368

P.B. Wagh, R. Begag, G.M Pajonk, A. Venkateswara Rao, D. Haranath; " Comparison of some physical properties of silica aerogel monoliths synthesized by different precursors" *Materials Chemistry and Physics* (1999) 214-218.

Ruben Baetens**, Bjørn Petter Jelle, Arild Gustavsen: "Aerogel insulation for building applications : a state of the art review". Energy and buildings 43 (2011) pag. 761-769**

Sharad D. Bhagat, Yong-Ha Kim, Myung- Jun Moon, Young-Soo Ahn, Jeong- Gu Yeo; "A cost-effective and fast synthesis of nanoporous SiO2 aerogel powders using water-glass via ambient pressure drying route" ***Solid State Sciences*** **9 (2007) 628-635**

Sung-Woo Hwang , Tae-Youn Kim, Sang-Hoon Hyun: "Optimization of instantaneous solvent exchange/surface modification process for ambient synthesis of monolithic silica aerogels". *Journal of Colloid and Interface Science* 322 (2008) 224–230 S.S. Kistler, Coherent expanded a

CO13

BATCH AND CONTINUOUS ADSORBTION OF NIMESULIDE ONN SILICA AEROGEL FROM

SUPERCRITICAL CARBON DIOXIDE SOLUTIONS

Giuseppe Caputo*, Mariarosa Scognamiglio, Iolanda De Marco
Dipartimento di Ingegneria Industriale, Università degli studi di Salerno,
Via ponte don Melillo, 1– 84084, Fisciano (SA), Italy
*e-mail: gcaputo@unisa.it; mrscogna@unisa.it; idemarco@unisa.it
Tel. +39-089-964091 fax: +39-089-964057

Abstract

The high adsorption capacity of silica aerogels is exploited in the aim of incorporating poor water soluble drugs into silica aerogel. Adsorption takes place from a fluid solution of the drug in supercritical CO_2 and ethanol as co-solvent. A new fixed bed adsorption plant has been developed to allow fast mixing of fluid phase and effective contact in the adsorption column. Adsorption isotherms were measured for one model substance, nimesulide, at 40 °C and breakthrough curve was experimentally obtained. The drug loading of the drug into silica aerogel was up to 9 wt%. The drug composite was characterized using scanning electron microscopy and release kinetics of the adsorbed drug were also evaluated by in vitro dissolution tests. The dissolution of nimesulide from loaded aerogel is much faster than dissolution of crystalline nimesulide. Around 80% of nimesulide dissolves from the aerogel within 6 minutes, whereas dissolving 80% of the crystalline drug takes about 90 min.

Keywords: adsorption, supercritical fluids, carbon dioxide, silica aerogel, drug delivery system, breakthrough.

1 Introduction

The poor water solubility of some drugs limited their bioavailability. A fast dissolving system can be defined as a dosage form for oral administration, which when placed in mouth, rapidly dispersed or dissolved increasing compliance and efficacy of the therapy. Fast dissolving and fast dispersing drug delivery system may offer a solution to these problems. A possible approach for ensuring maximum bioavailability is the increase of drug dissolution rate and/or solubility. To improve the dissolution rate of drugs, different techniques have been developed [1]. The most common approach is based on particle size reduction that can be achieved by processes based on micronization or nanosuspension. In the field of supercritical fluids, various promising techniques of micronization of drugs and excipients with SC-CO_2 have been developed [2]. An alternative way to improve the availability of a drug is its dispersion on a biocompatible substrate [3]. Silica based materials used as substrate are widely employed as additives, free flow agents and drug carriers also in commercial products. A special class of silica materials are silica aerogels (SA). They are low density nanoporous solids with a fine open-pore structure that exhibits unique properties, such as high porosity (90–99%), high surface area (400–1000 m^2/g), extremely low density (0.003–0.15 g/cm^3).

These properties allow them to be used as host matrix for drug delivery. Silica aerogels were recently shown to be a potential candidate for oral drug delivery systems [4, 5, 6]. A promising method to adsorb a drug into porous substrates is supercritical (SC) deposition or adsorption [4, 5, 7, 8, 9]. Essentially, the process involves the dissolution of the active molecules in a supercritical fluid and the impregnation of the substrate by its exposure to this solution. Supercritical carbon dioxide (SC-CO_2) is commonly used due to its relatively good solvent power for various drugs, mild critical temperature (31 °C), low critical pressure (7.4 MPa) and inertness. After the removal of the supercritical fluid (SCF) by expansion, a drug-loaded matrix free of solvent residues is obtained. This method takes advantage of the unique properties of SCFs. Indeed, a SCF possesses a unique combination of gas-like and liquid-like properties, that can be adjusted by small changes in temperature or pressure.

Low viscosity and high diffusivity of SC-CO_2 allow a rapid equilibration and micropore penetration of the fluid phase within the matrix. SCFs also have zero surface tension that not only facilitates the rapid permeation and diffusion into porous substrates, but also avoids the pore collapse of SA that occurs using organic liquids, due to capillary stresses caused by the liquid-vapour menisci within pores.

Until now, SC adsorption within SA has been studied using simple batch vessels in which SA and active molecules are loaded and equilibrated until equilibrium is reached. Because pure SC-CO_2 is used as solvent, the maximum amount of active compound that can be loaded on SA is limited by its solubility in SC-CO_2 at given condition of temperature and pressure. One way to increase the solubility is the increase of pressure of SC-CO_2; an alternative is the use of a compatible and benign co-solvent which increase the solubility of the active compound in the fluid phase. The fluid phase composed by SC-CO_2 and co-solvent must satisfy the condition that the mixture is supercritical at the operating pressure and temperature. Indeed, if a liquid phase is formed, the aerogel structure could be damaged and polluted by the cosolvent.

In this work, the adsorption of a model drug on SA was studied using a new experimental apparatus properly designed for this purpose. The best way to deal with SC-fluid mixture is to use a continuous process in which the fluid phase is continuously pumped in an adsorption column containing the SA matrix. Because, a fundamental stage of the process is the formation of the ternary mixture SC-CO_2/organic solvent/active compound, a mixing stage has been provided that allows a fast and effective solubilization of the components.

The new experimental plant has been tested with nimesulide as active compound and ethanol as solvent. Nimesulide has been choosen for comparison purposes because in a previous study its adsorption using a batch mode apparatus was studied. Adsorption isotherm and breakthrough curve of the column at 40 °C were determined. Loaded SA were characterized by in vitro dissolution test to study the properties of the composite material and its potentiality for industrial applications.

2. Materials and methods

Materials

Hydrophilic Silica Aerogel (SA) in form of monolithic blocks was purchased from Merketech Int. (USA). The nominal density is 0.1 g/cm^3 and the surface area is 800 m^2/g and the mean pore size is about 20 nm. Deposition experiments were performed using cubic blocks of 1 cm obtained by cutting SA monoliths with a knife. Nimesulide (purity 98%) was purchased from Sigma-Aldrich (Italy). CO_2 research grade 4.8 was purchased from SON (Italy). All products were used as received.

Methods

Samples of the loaded SA were observed by Field Emission Scanning Electron Microscopy (FE-SEM) (LEO 420, USA) operating at 5 kV. Crushed fragments of the sample were dispersed on a carbon tab previously stuck to an aluminium stub and coated with gold-palladium (layer thickness 250Å) using a sputter coater (mod. 108A; Agar Scientific, UK). Several FE-SEM images from different parts of the sample were taken for each run to verify the powder uniformity.

Drug Dissolution profiles were obtained with a USP apparatus 2, consisting of Varian 7025 paddle dissolution tester (Varian, Agilent Technologies Italia s.p.a, Italy). All studies were run according to the USP 25 paddle method: 150 rpm, 900 mL of dissolution medium, T=37.2 ± 0.1 °C, sink conditions ($c < 0.2\ c_s$). The adsorbed SA monoliths were coarsely crushed in a mortar and suspended in water. Then, the aqueous solution was continuously pumped to a flow cell in a spectrophotometer and absorbances were recorded at 396 nm. The composition of the dissolution medium was 0.2 M KH_2PO_4/0.2 M NaOH (ph 7.4) according with USP 25, plus 0.5 % w/v of Tween 80.

3. Apparatus

The laboratory plant is described in figure 1. It is made by 316 SS tested for a maximum pressure of 300 bar at 200 °C. It mainly consists of two feed lines, used to deliver the CO_2 and the liquid solution, and three main vessels: mixer, adsorption column and condenser. CO_2, stored in a vessel (V), is delivered to the mixer by a volumetric pump (P1) (Milroyal tipo MD140G6M35/J) through a one way valve (V'-1) and on/off valve (V4). The head of the pump is cooled by a thermostatic bath

(C) to avoid cavitation of CO_2. The liquid solution is delivered by a membrane pump (P2) (Lewa, Germany, type LDB) from a graduated cylinder.

The mixer is a stainless steel autoclave (NWA GmbH, Germany) having an internal volume of 100 mL, closed on the bottom and on the top with two finger tight clamps. The top cap holds three 1/8" ports. Mixing is provided by an impeller mounted on the top cap and driven by a variable velocity electric motor. The autoclave is heated by thin band heaters (H) (Watlow, USA mod.*STB4E3A9*) whose thermal control is guaranteed by a PID controller (Watlow, USA). The temperature inside the cylinder is measured by a K-type thermocouple with an accuracy of ± 0.1 °C. Pressure is measured by a digital gauge manometer (Parker, USA). Mixer was designed to provide a contacting volume and a residence time sufficient to allow the dissolution of SC-CO_2 in the liquid solution up to the saturation conditions.

The adsorption column (P) is a 316 SS cylindrical vessel with an internal volume of 50 cm^3. It is packed with a silica aerogel bed. The pressure inside the column is maintained by a micrometric valve MV2 heated by electric heaters to avoid clocking during CO_2 expansion. From the exit of the column the gaseous flow of CO_2 and solvent is sent to a gravimetric gas/liquid separator, that is a Pyrex® element properly designed for the separation of the solvent from the gas stream. At the inlet port of the separator an impact surface is provided to improve separation. The liquid is collected at the bottom of the cylinder where a probe connected to an UV-spectrophotometer allows the continuous measurement of the liquid composition. The separator has been designed to condense ethanol. At the exit of the separator a rotameter (FE) is used to measure CO_2 flow rate.

The design of the separator has been based on the method proposed by Treybal [10]. The input data were liquid density, gas density at given temperature and their flow rates. The design procedure has been the following: 1) the limit velocity is calculated on the base of the ratio between the density of the gas and the liquid; 2) the surface of the separator is calculated from the limit velocity and the volumetric flow rate of the gas; 3) a tentative residence time is assumed and the volume of the separator is calculated.

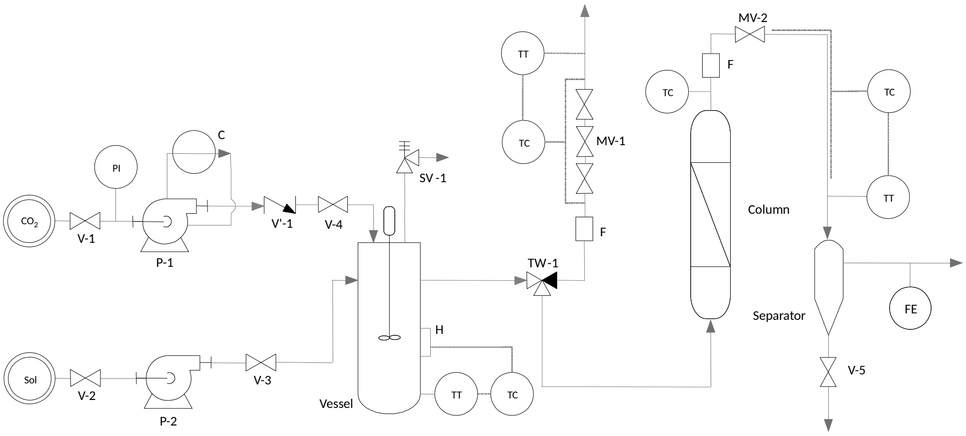

Figure 1. Continuous plant for the adsorption of drugs from supercritical carbon dioxide solutions.

Results and discussion

Supercritical adsorption has been carried out in a continuous mode until saturation of the SA bed is reached. SC-CO_2 and a liquid solution (ethanol+nimesulide) after mixing are continuously delivered to the high pressure adsorption column. Results have been compared with batch experiments obtained in a previuos work [8].

Because the phase behavior of the ternary system CO_2/EtOH/Nime is not available, our analysis is based on the binary system CO_2/EtOH. It is thus assumed that the effect of nimesulide on the phase behavior is negligible. This assumption is reasonable considering the low concentration of nimesulide (< 0,25 wt%). The temperature and pressure conditions (40 °C and 10 MPa) have been selected considering the following factors: a) thermolability of the drug; b) formation of a single fluid phase between CO_2 and ethanol. The miscibility curve of the binary system CO_2/EtOH is shown in **figure 2**.

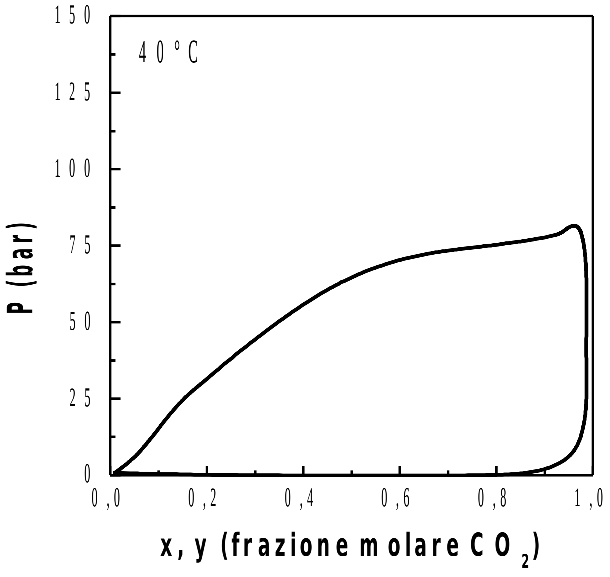

x, y, CO2 mole fraction

Figure 2. Phase behaviour diagram of the system CO$_2$/EtOH at 40° C

At this condition of temperature and pressure the effect of the weight ratio CO$_2$/EtOH (R) on the drug loading has been studied. Experiments have been carried out using a SA bed with a L/D of 9.4, and pumping 150 mL of EtOH solution with nimesulide concentration of 3 mg/mL. All the operating points comprised between 0.38-0.88 CO$_2$ mole fraction fall in the one phase region of the phase diagram. In **table 1** the obtained drug loadings are reported.

R	**X_{CO2}**	**W_{nime}**	**Loading, %**	**time**
7.2	0.88	0.000047	0.48	94
3.4	0.78	0.000856	1.0	75

1.5	0.61	0.0015	2.8	50
0.9	0.48	0.00197	5.4	60
0.6	0.38	0.00245	8.9	37

Table 1. Adsorbtion data of nimesulide on silica aerogel at different values of the CO_2/EtOH weight ratio (R). $W_{nime}$is the mass fraction of nimesulide in the solution, time is the duration of the experiment until bed saturation is reached.

The variation of nimesulide loading on SA with respect to the concentration of nimesulide in the fluid solution is reported in figure 3. Because each experiment has been carried out for a time corresponding to the saturation of the bed, loading represents the maximum quantity of nimesulide that can be absorbed on SA at the given conditions. As a consequence, the curve of figure 3 represents the absorption isotherm of nimesulide on SA at 40 °C.

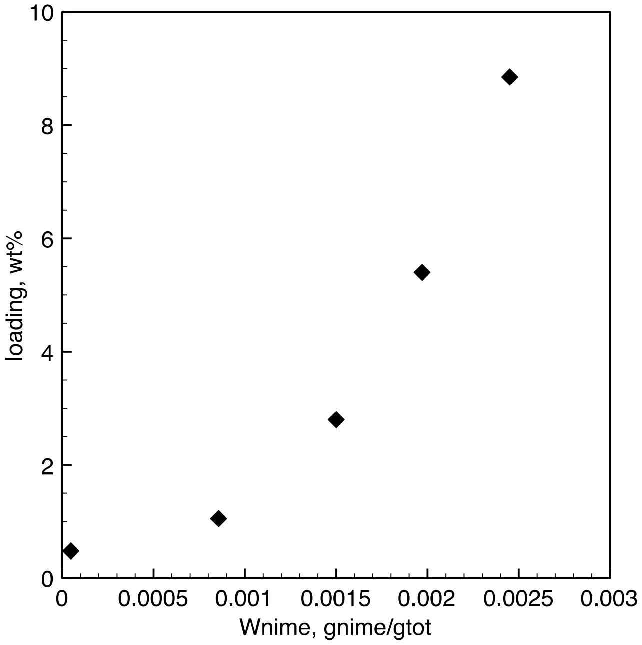

Figure 3. Adsorption isotherm for nimesulide on silica aerogel at 40 °C/100 bar

As expected, the loading of nimesulide on SA increases with increasing concentration of nimesulide in the fluid phase. The maximum loading obtained is 8.85 wt%, corresponding to 227.7 mg of nimesulide adsorbed in the bed. Brunauer et al. [11] classified the isotherms that are convex upward throughout (type I) as “favorable” to uptake of solute, whereas the ones that are concave upward throughout (type III) as “unfavorable” to uptake of solute. According to this classification, the isotherm obtained at 40 °C is favorable.

These data must be compared with the loading of nimesulide on SA reported by Caputo et al. [8] obtained using batch adsorption and pure CO_2 as solvent. At 40 °C, the maximum loading was merely 1.4 %, six times lower than that obtained using EtOH as co-solvent. Moreover, adsorption with pure CO_2 were carried out at a much higher pressure (22.5 MPa) to increase the solubility of nimesulide.

From the table 1 it is clear that an increase of ethanol fraction, increases the nimesulide loading. This result is due to two concomitant effects: a) increase of the concentration of nimesulide in the fluid phase; b) the competitive adsorption of CO_2 on SA is reduced and more adsorption sites are available for nimesulide molecules.

Breakthrough curve

The most important criterion in the design of fixed-bed adsorption systems is the prediction of column breakthrough curve which determines the operating life of the bed and regeneration time. When the fluid phase starts flowing in to the bed, the top of the adsorbent in contact with the gas stream quickly adsorbs the solute during first contact. The gas stream leaving the bed is practically free from the solute. As the volume of fluid getting from the bed increases, an adsorption zone of mass transfer gets defined. In this zone, adsorption is complete and it moves downwards through the bed in relation to time until the breakthrough occurs. When this zone reaches the end of the bed, the solute cannot be adsorbed any longer. This moment is called “breakpoint”. The plot obtained after this point gives the concentration history and is called breakthrough curve. When the mass transfer zone leaves the bed, the bed is completely saturated, adsorption does not occur and the outlet stream has the same concentration as one enters.

The breakthrough curve for the adsorption of nimesulide on SA at 40 °C and 10 MPa is shown in figure 4. This figure shows the relative effluent concentration against the elution time. The general pattern of the breakthrough curve was as expected. The effluent concentration first increased gradually and then increased sharply before reaching the value of the inlet concentration.

The starting point of the curve is shifted of 15 min. This time corresponds to the dead time of the process due to residence time of the fluid phase in the mixer. After 35 min. the concentration of nimesulide in the effluent stream starts to increase significantly (0.114 mg/mL). This point, corresponding to 10% of inlet concentration, can be assumed as breakpoint. Indeed, after this time the concentration increased sharply and reached a value of 50% of the inlet concentration after only 3 minutes. 38 min. represents the apparent half-time of the bed. Taking in to account the dead time of the plant, the real half-time is 23 minutes.

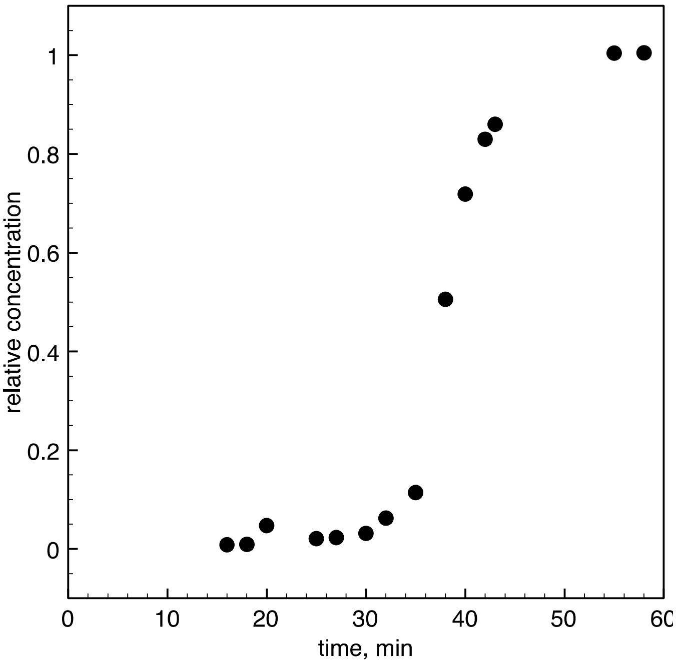

Figure 4. Breakthrough curve for adsorption of nimesulide on silica aerogel bed from a stream of CO_2 and ethanol at 40 °C, flow rate= 6.89 mL/min, X_{CO2}=0.378, C_{0nime}=0.00174 mg/mL, bed L/D=9.7.

Mass balance

In the transition regime all the solute fed to the column is used to saturate the bed. So the mass balance can be written as:

$$IN = ACC$$

with

$$IN = QC_0(t^* - t_0)$$

$$ACC = (W^{sat} - W_0)\rho_{bed} SL$$

where Q is the volumetric flow rate of the fluid phase (mL/min), C_0 is the concentration of adsorbate in the fluid phase (g/mL), t^* is the ideal half-time, t_0 is the mixing time, W^{sat} is the saturation concentration of adsorbate in the solid phase (mg_{ads}/mg_{sol}), W_0 is the concentration of the adsorbate in the solid phase at time t_0, ρ_{bed} is the density of the bed (g/cm^3), S and L are the cross-section and the length of the bed, respectively.

The mass balance is thus:

$$QC_0(t^* - t_0) = (W^{sat} - W_0)\rho_{bed} SL$$

from which

$$(t^{*}-t_{0})=\frac{(W^{sat}-W_{0})\rho_{bed}SL}{QC_{0}}$$

by substituting the following values W^{sat}-W_0=0.0885, ρ_{bed}=0.1 g/cm^3, S=2.0096 cm^2, L=15 cm, Q= 6.89 mL/min, C_0 =0.00174 g/mL, an half time of 37.23 min. is obtained a very good agreement with 38 min obtained experimentally.

Adsorption efficiency

The efficiency of the adsorption is one of the main parameter of the process. It is an expression of the quantity of drug adsorbed with respect to the drug fed to the column.

$$Eff\%=\frac{nime_{ads}}{nime_{fed}}\times 100$$

with

$$nime_{fed}=C_{0}\times Q\times (t^{*}-t^{0})$$

by substituting the following values, relating to experiment at R=0.58 (see table 1): Q= 6.89 mL/min, C_0 =1.74 mg/mL, t^*-t_0=20 min, a value of 240 mg of nimesulide is obtained. Thus, the efficiency is

$$Eff\%=\frac{227.7}{240}= 94.8\%$$

Very similar values were obtained for other experiments.

Characterization of silica aerogel after adsorption

Silica aerogel samples were analyzed by FE-SEM to observe the morphology of the material before and after loading. FE-SEM images taken at the same magnification (60K magnification) for samples obtained at 1, 5.4 and 8.9 wt% are reported in Figure 5. Also a FE-SEM image of SA before loading is reported.

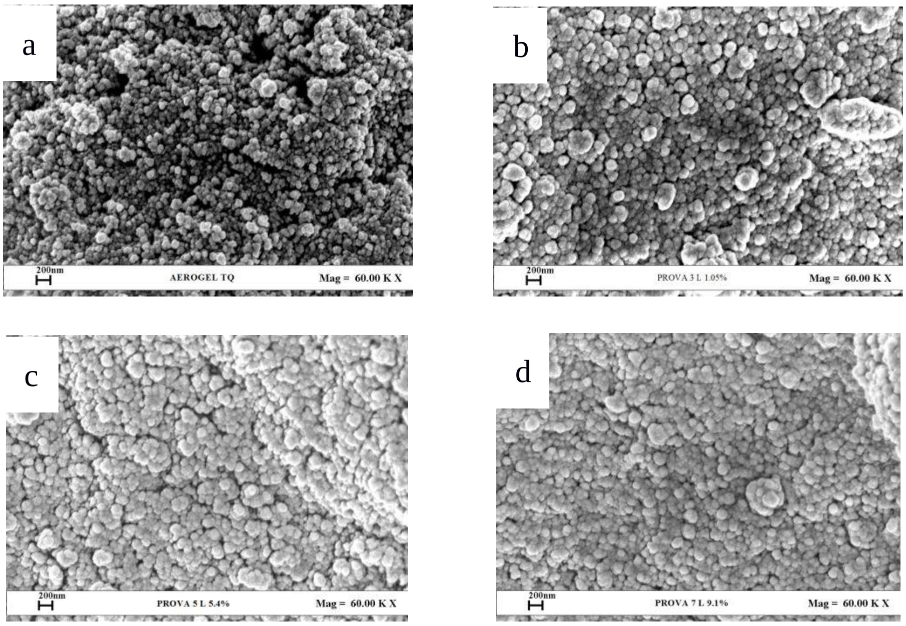

Figure 5. FE-SEM photographs of a) not treated SA and SA samples loaded with different amount of nimesulide: b) 1.0 wt %, c) 5.4 wt %, d) 8.9wt%.

FE-SEM images reveal that all samples have the same morphology and no nimesulide crystals were formed on the SA surface also at the higher loading. The presence of nimesulide within SA matrix is clearly revealed by EDX spectrum. In Figure 6 EDX of SA sample adsorbed at 5.4 wt% is shown. The spectrum contains Si peak characteristic of the aerogel and S peak characteristic of nimesulide. Therefore, we can conclude that the drug is adsorbed on the interior of the pores of SA at molecular level.

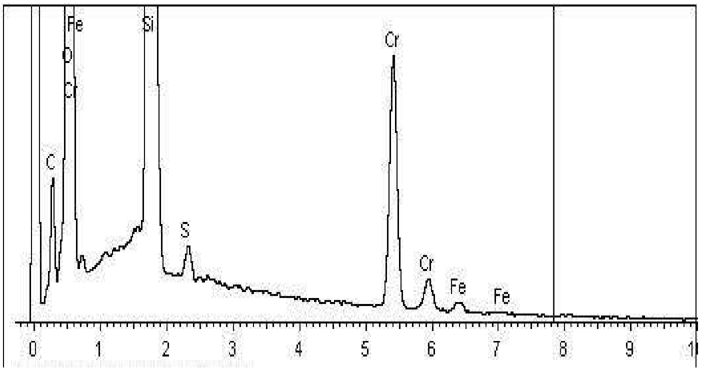

Figure 6. EDX spectrum of nimesulide/silica aerogel.

We studied also the dissolution rate of the drug in vitro. Solutions of phosphate buffer at pH = 7.4 was chosen as dissolution media following the recommendation US Pharmacopeia. The dissolution profile of the drug from the powdered loaded aerogel was compared with that of the pure crystalline drug. Release kinetics are shown in figure 7. The dissolution of nimesulide from loaded aerogel is much faster than dissolution of crystalline nimesulide. Around 80% of nimesulide dissolves from the aerogel within 6 minutes, whereas dissolving 80% of the crystalline drug takes about 90 min. Thus, the use of hydrophilic aerogels as a carrier promotes fast release of the drug. This effect can be explained by both an increase of specific surface area of the drug adsorbed on the aerogel and its non-crystalline structure in this state. In the case of the crystalline drug, even with a very small particle size, the crystal should be destroyed before the drug can be actually dissolved. If the drug is adsorbed on the aerogel, this step is eliminated and the dissolution process is accelerated. Another important effect is the partial collapse of aerogel structure in water. Hydrophilic aerogels are rapidly wetted with water, so the drug molecules are surrounded with water allowing a fast dissolution of drugs [5].

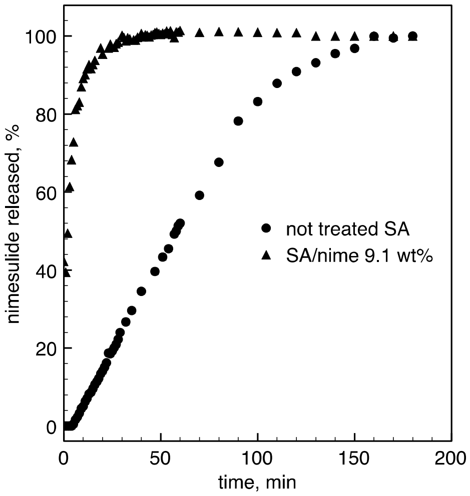

Figure 7. Release kinetics of nimesulide in buffer phosphate at pH= 7.4.

Conclusions

In this study, it was demonstrated that the supercritical fluid adsorption is an effective way to incorporate low water soluble drugs into a microporous silica aerogel.

The use of a fixed bed adsorption column fed with a supercritical CO_2 solution with ethanol co-solvent allows to obtain a pure drug delivery system at high drug content. Indeed, it was possible to prepare SA samples containing up to 9 wt% of nimesulide. Moreover, the process is highly efficient in term of quantity of drug adsorbed with respect to the drug fed to the column (>94%).

The SA/nimesulide composite has an enhanced dissolution rate that can be explained by both the increase in the specific surface area of the adsorbed drug and its non-crystalline structure in the formulation. These results encourage the development of industrial application of the proposed process.

References

[1] S. Pinnamaneni, N. G. Das, and S. K. Das, ″Formulation approaches for orally administered poorly soluble drugs″, *Pharmazie,* vol. 57, pp. 291–300, 2002.

[2] P.York, U. B. Kompella, and B. Y. Shekunov, *Supercritical fluid technology for drug development*, Marcel Dekker, New York, 2004.

[3] A. M. Hillery, A. W. Lloyd, and J. Swarbrick, ″Delivery und Targeting,” Taylor & Francis, London and New York, 2001.

[4] I. Smirnova, S. Suttiruengwong, and W. Arlt, ″Feasibility study of hydrophilic and hydrophobic silica aerogels as drug delivery systems″, *J. non Cryst. Solids*,vol. 350, pp. 54–60, 2004.

[5] I. Smirnova, S. Suttiruengwong, M. Seiler, and W. Arlt, ″Dissolution rate enhancement by adsorption of poorly soluble drugs on hydrophylic silica aerogels″*Pharm. Dev. Technol.*, vol. 9, pp. 443–452, 2005.

[6] U. Guenther, I. Smirnova, and R. H. H. Neubert, ″Hydrophilic silica aerogel as dermal drug delivery systems-dithranol as a model drug″*Eur. J. Pharm. Biopharm.*, vol. 69, pp. 935–942, 2008.

[7] I. Smirnova, J. Mamic, and W. Arlt, ″Adsorption of drugs on silica aerogels″, *Langmuir*, vol. 19, pp. 8521–8525, 2003.

[8] G. Caputo, M. Scognamiglio, and I. De Marco, ″Nimesulide adsorbed on silica aerogel using supercritical carbon dioxide″, *Chemical Engineering Research and design*, vol. 90, no. 8, pp. 1082-1089, 2012.

[9] G. Caputo, I. De Marco, and E. Reverchon, ″Silica aerogel–metal composites produced by supercritical adsorption″, *J. of Supercritical Fluids*, vol. 54, pp. 243–249, 2010.

[10] R. E. Treybal, ″Mass-Transfer Operations″, 3rd Edition, McGraw-Hill Book Company, 1980.

[11] S. Brunauer, L. S. Deming, W. E. Deming, and E. Teller, ″On a theory of the van der Waals adsorption of gases″, *J. Am. Chem. Soc.* vol. 62, pp. 1723–1732, 1940.

CO14

THERMAL STABILITY OF HYDROPHOBIC XEROGELS AND AEROGELS SYNTHESIZED FROM MTMS

Sónia Afonso[1], Telma Matias[1], Marta Ochoa[2], António Portugal[1], Luisa Durães[1,*]

[1]CIEPQPF, Department of Chemical Engineering, Faculty of Sciences and Technology, University of Coimbra, Pólo II, Rua Sílvio Lima, 3030-790 Coimbra – Portugal

[2]Active Space Technologies, Rua Coronel Júlio Veiga Simão, 3025-307 Coimbra, Portugal

*Corresponding author. Tel.: +351 239798737; fax: +351 239798703. E-mail address: luisa@eq.uc.pt

Abstract

Silica aerogels are excellent candidates to be applied in thermal insulation of Space devices. Their unique properties are known, such as a highly porous structure that results in very low thermal conductivity and density. When hydrophobic, they are suitable for insulation of electrical/electronic devices and are more durable. However, for Space harsh environment, they must present stable properties up to 200-300ºC. Thus, the aim of this work is to study the influence of increasing temperature in the properties of hydrophobic silica based xerogels/aerogels synthesized from methyltrimethoxysilane (MTMS) precursor. The samples were exposed to heat treatments at different temperatures – 300-800°C – and the chemical, physical and structural characterization of the as prepared and heat-treated materials was performed.

As-prepared xerogels exhibited low density (~80 kg/m^3), high porosity (93%), low thermal conductivity (0.040 W/(m K)) and high hydrophobicity (146º). They have lost their hydrophobic nature at 450ºC, where a sharp density increase to 105 kg/m^3 was also observed. After the highest temperature treatment, the density achieved 119 kg/m^3 and the thermal conductivity changed to 0.046 W/(m K). These changes were a consequence of a progressive densification of the material and the loss of methyl groups with the temperature increase.

The untreated aerogels show even higher porosity (97%), lower density (50 kg/m^3) and thermal conductivity (0.036 W/(m K)). They have lost their high hydrophobicity (149º) at 450ºC. Although not as significant as in xerogels, chemical and structural changes occurred in the aerogels samples with temperature. The material heat-treated to 800ºC exhibited higher density and the thermal conductivity changed to 0.042 W/(m K).

MTMS-derived xerogels/aerogels revealed excellent heat insulation potential that do not change significantly with the temperature increase. Additionally, they remain hydrophobic up to 300ºC and preserve their monolithicity up to at least 800ºC.

Keywords: Silica xerogels/aerogels; Thermal treatments; Thermal conductivity; Hydrophobicity; Space applications

1 INTRODUCTION

Silica based xerogels and aerogels are highly porous three-dimensional solid networks. This type of materials have gained special attention in the last decade due to their amazing properties, namely high porosity (80-99.8%), low density (50-150 kg/m^3), very low thermal conductivity (~0.02 W/(mK)) and high surface area (500-1200 m^2/g) [1]. These properties are ideal for several applications as thermal or acoustic insulators, catalysts, dielectric materials, sensors and others. More specifically, in the aerospace industry these nanostructured materials have been used as thermal insulators for re-entry and Mars vehicles, spacecraft components, spacesuits, cryogenic tanks, space station buildings [2-5]. A major requirement for applications in Space is the thermal stability of these materials, which should be kept until 200-300 ºC.

The thermal behaviour of hydrophobic silica based materials produced from MTMS was successfully studied by Rao *et al.* [6] by thermal analysis (TGA-DTA) and, in this study, the authors concluded that the tested aerogels would preserve their hydrophobicity up to 480ºC. Three years later, Rao *et al.* [5] produced by a two-step sol-gel procedure super hydrophobic and flexible aerogels that would remain hydrophobic up to a temperature of 253ºC. In a later study Nagardi and Rao [7], the same research group, studied the viability of obtaining xerogels by using MTES (methyltriethoxysilane) as precursor and detected a considerable mass loss at 200ºC, explained by solvent release from the porous structure, and at 450ºC due to the oxidation of methyl groups responsible for the hydrophobicity of the gels.

In 2012, Ochoa *et al.* [2] produced xerogels from different mixtures of MTMS and ETMS (ethyltrimethoxysilane) and by thermal gravimetric analysis detected a significant mass loss at 400 ºC due to the oxidation of methyl and ethyl groups. In addition, Durães *et al.* [4] studied the effect of the drying conditions in MTMS-derived xerogels/aerogels and concluded that the drying conditions do not show a significant effect in the chemical structure of the material but a clear change in bulk density was detected. In this study, the samples displayed good thermal stability with the oxidation of the methyl groups occurring in between 540 and 625ºC. Recently, Liu *et al.* [8] evaluated the influence of the thermal treatments in the physical and structural properties of aerogels produced from sodium silicate and concluded that the hydrophobicity was lost at a temperature of 430ºC. Although the aerogels had lost their monolithicity after being subjected to the thermal treatment at 500°C, they maintained their insulation properties until 800°C. A surface area of 466 m^2/g, a bulk density of 0.113 kg/m^3, a porosity of 91 % and a thermal conductivity of 0.091 W/(m K) were obtained for the heat-treated aerogels, after having been submitted at 800°C.

In this work, we monitored the relevant properties in MTMS-derived xerogels/aerogels subjected to heat-treatments from room temperature up to 800 ºC, and recorded the concomitant changes. In this way, we aim to study the influence of the heat treatments in the chemical, physical and structural properties of these flexible and hydrophobic materials, being the bulk density and thermal conductivity the most important properties considering the goal of their use for insulation systems in Space. The study was confined to highly hydrophobic xerogels/aerogels for the sake of their robustness and weathering resistance, important complementary properties that determine their use in Space applications.

2 MATERIALS AND METHODS

2.1 Gels synthesis and drying

Silica xerogels/aerogels were obtained by a two-step acid–base catalyzed sol–gel process using MTMS precursor. The production of these nanomaterials was based on the synthesis and drying procedures described by Durães *et al.* [4, 9] and early proposed by Rao, Baghat and co-workers [5, 10].

Summarily, MTMS was mixed with methanol and, then, an acid oxalic solution (0.01 M) was added to promote the hydrolysis of the precursor. After one day, an ammonium hydroxide solution (10 M) was slowly joined to raise the pH of the solution. The alkaline conditions favoured the combination of the silanol species by condensation reactions at a faster rate, resulting in the formation of a sol and, some hours later (4-6 h), an alcogel. A temperature of 25ºC was used in the steps until the end of the base addition and the gelation period occurred in an oven at 27ºC. The used molar ratios of MTMS:solvent:water were 1:35:8. The gel was then maintained at 27ºC during 2 days for aging, in order to increase the structure cohesion.

Finally, the prepared gels were dried by Ambient Pressure Drying (APD) or by Supercritical Fluids Drying (SFD) to produce xerogels and aerogels, respectively. In APD, the gels were put in a ventilated oven, and submitted to the following temperature cycles: 24 h at 60ºC, and three stages, at 100ºC, 150ºC and 200ºC, of one hour each. To perform SFD, the gels were placed in an autoclave where the temperature was increased at a heating rate of 80ºC/h and isochoric conditions, causing an increase in the pressure. Beyond the critical point of the methanol (239.4ºC, 8.09 MPa), the pressure was relieved at constant temperature (∼250ºC) and the aerogels were taken from the autoclave after flushing with nitrogen.

2.2 Xerogels/aerogels heat-treatments and characterization

The physical, chemical and structural characterization of the as-prepared samples was performed. Then, the samples were heat-treated in a furnace under ambient atmosphere at various temperatures – 300ºC, 450ºC, 600ºC or 800ºC – during 2 hours. After this time, the furnace was turned off and the materials were maintained therein until reaching room temperature. The heat-treated samples were stored in water-free conditions and, finally, characterized again. Three sample replicates were performed. The used characterization methods are described below.

Thermogravimetric analysis – TGA (*TGA Q500, TA Instruments*): used to study the thermal stability of xerogel/aerogel samples and to select the furnace plateaus. The samples were placed in an aluminium pan and heated from room temperature to 600ºC, at a constant rate of 10ºC/min, under a nitrogen flow.

Infrared spectroscopy – FTIR (*FT/IR-4200, Jasco*): used to evaluate the changes in the chemical structure of the samples. A small amount of each sample was milled with KBr and allowed to dry at 60° C during 24 h. For the analysis, this mixture was pressed in a mold and thin and circular pellets were obtained. The applied range of wave numbers was 400-4000 cm^{-1}, with a spectral resolution of 4 cm^{-1} and 64 scans per sample.

Elemental analysis (*EA 1108 CHNS-O*, Fisons Instruments): in order to determine the C, H, N and O elemental composition of the samples. For C, H and N determination, the sample combustion was undertaken in the equipment oven at 900ºC, and using a stream of He enriched with oxygen. The evaluation of the oxygen was done by sample pyrolysis at 1060ºC.

Apparent density measurement: regular sample pieces were measured (to obtain their volume) and weighted with an electronic digital micrometer and a balance, respectively, in order to calculate the apparent density.

He picnometry (*Accupyc 1330, Micrometrics*): to measure the skeleton density of xerogels/aerogels. The analysis was performed by pressurizing the sample cell to ∼1.25 bar above the ambient pressure and allowing the gas pressure to equilibrate. From the difference in the pressure readings of the sample cell and the reference cell, the actual volume of the sample skeleton is obtained.

N_2 gas adsorption (*ASAP 2000, Micrometrics*): to estimate the specific surface area and the pore size distribution of the materials. Before analysis, the samples were degassed at 200ºC in vacuum for 24 h to remove adsorbed species. In the analysis, volumes of the adsorbed nitrogen at different relative pressures (0.05-0.3) were taken at 77 K to obtain the specific surface area by the BET theory. The desorption isotherm was used (relative pressures from 1 to 0.5) to obtain the pore size distribution by the BJH theory.

Contact angle measurement (*OCA 20, Dataphysics*): used to evaluate the hydrophobic/hydrophilic character of the samples. Water drops of 10 µl were dropped on the horizontal surface of parallelepipedic sample pieces. The contact angle was measured directly from the obtained photograph of the water drop and its contour fit.

Thermal conductivity measurement (*TPS 2500S, Hot Disk*): used to access the thermal conductivity of the materials. A sensor was fitted between two pieces of the sample and was then heated by a constant electrical current for a short period of time. The generated heat dissipated into the material, causing a rise in temperature of the sensor and surrounding sample material. The obtained temperature profiles were mathematically treated to obtain the thermal properties of the sample.

Scanning electron microscopy – SEM (*JMS-5310*, *Jeol*): to observe the microstructure of the xerogels/aerogels. An Au film was deposited on the samples surface, using the PVD technique, to improve their electrical conductivity. The deposition time was 30 s. After metallization, the sample was analysed in the microscope under high vacuum.

3 RESULTS AND DISCUSSION

In Figure 1 and Table 1, the thermal stabilities of silica based xerogel and aerogel are presented, based on the thermogravimetric analysis. The first weight loss of the xerogel sample occurs at 164.4°C and corresponds to the evaporation of impurities (solvent, catalysts), which were trapped in the structure of material and were not removed during drying. The second weight loss corresponds to the oxidation of methyl groups and begins at 315.5ºC. This phenomenon develops due to the existence of residual oxygen in the analysis atmosphere and sample voids. The last weight loss starts at 529.1ºC and doesn't end to 600ºC (temperature limit of the analysis). It corresponds to a second stage of the oxidation of –CH_3 groups, probably reaching those groups that are more inside the structure.

In contrast to the xerogel, the aerogel exhibited only two significant weight losses in the temperature range of analysis. The first weight decrease occurs at 311.4ºC and corresponds to oxidation of –CH_3 groups by residual oxygen, as before. The second weight loss begins at 543.3ºC and also corresponds to the oxidation of methyl groups, now in a higher extent. This phenomenon continues to temperatures above 600ºC.

Figura Erreur ! Il n'y a pas de texte répondant à ce style dans ce document.**.1: Análise termogravimétrica: a) Xerogel e b) Aerogel**

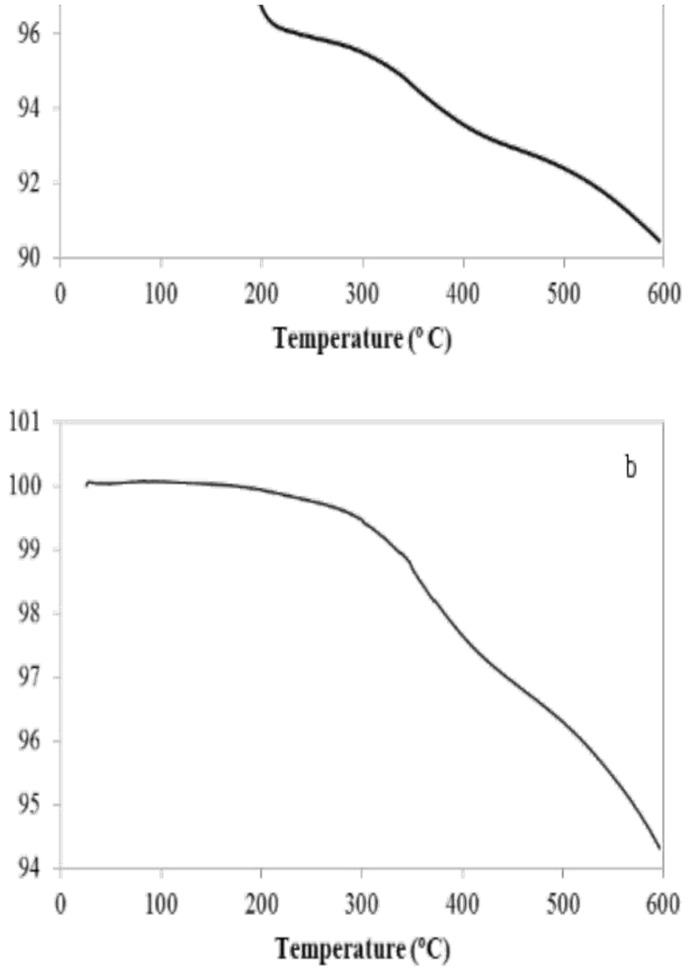

Figure 11: Weight loss profiles of a) xerogel and b) aerogel samples with temperature increase at a heating rate of 10ºC/min.

Table 8: Weight losses and temperatures of the corresponding thermal phenomena identified in the TGA of the synthesized xerogels and aerogels.

Sample	**Weight loss (%); [T_{ini}; T_{end}] (ºC)**	**T_{onset} (ºC)**	**T_{end} (ºC)**
Xerogel	- 3.92%; [25ºC; 228.1ºC]	164.4	228.1
	- 3.09%; [228.1ºC; 446.2ºC]	315.5	446.2
	- 2.53%; [446.2ºC; 600ºC]	529.1	-
Aerogel	- 3.17%; [25ºC; 457.0ºC]	311.4	457.0
	- 2.52%; [457.0ºC; 600ºC]	543.4	-

From these results it is evident that the aerogel has a negligible amount of impurities and, thus, only a very slight decrease in the curve is observed up to 300ºC. This shows the high effectiveness of the used supercritical drying method for impurities removal, which is due to the high final temperatures achieved during drying. In fact, the SFD method needs a final temperature of ∼250ºC whereas the used APD method only uses temperatures up to 200ºC.

The thermogravimetric analysis allowed the definition of the levels of temperature to be used in the furnace. Four levels of temperature were defined, 300ºC, 450ºC, 600ºC or 800ºC, corresponding to the limits of the steps of weight loss observed in the TGA, although for the last step there was uncertainty about its end temperature. Thus, temperatures of 600ºC and 800ºC were considered. The weight losses of materials subjected to the heat-treatments in the furnace are shown in Table 2.

Table 9: Weight losses of xerogels/aerogels at the several temperature levels in the furnace.

Temperature (ºC)	**Xerogels weight loss (%)**	**Aerogels weight loss (%)**
300	10.3 ± 3.1	3.9 ± 1.9
450	16.0 ± 4.0	21.4 ± 5.6
600	17.9 ± 2.9	24.0 ± 17.8
800	26.9 ± 4.3	24.9 ± 7.4

The xerogel samples treated at 300°C lost 10.3% of its initial weight. This phenomenon corresponds to the first step observed in TGA and attributed to the evaporation of impurities. In the next levels of temperature (450ºC and 600ºC), the methyl groups were in part oxidized, as it was also observed in TGA results. This caused an increase of 5.7%+1.9% in weight loss of the samples when compared to the first temperature level. When the xerogels are submitted at 800ºC, more 9% of their weight is lost, due to a higher extent of oxidation of $–CH_3$ groups (or probably complete oxidation).

For the aerogels, the phenomenon involved in each level of temperature is similar to that observed for the xerogels. However, the weight loss is lower at 300ºC, only 3.9%, in agreement with TGA results and discussion. In addition, the weight losses in intermediate levels are higher in aerogels than in xerogels, what can be explained by the more open structure of the aerogels that enables an easier diffusion of oxygen inside the structure and, consequently, a higher extent of oxidation of methyl groups at lower temperatures. It is worth noting that the standard deviations of the mean values presented in Table 2 are significant, and this can be explained by the extreme lightness of the samples what enhances the effect of the experimental errors.

The FTIR analysis may provide knowledge of the changes in the chemical structure of the studied materials. Figures 2 and 3 show the obtained spectra for the as-prepared and heat-treated xerogel and aerogel samples, respectively, as well as the identification of the observed bands according to the literature [11, 12].

The analysis of the FTIR spectrum of the untreated xerogel sample (200°C) shows the existence of a peak at 400-500 cm^{-1}, corresponding to the deformation vibration of the O-Si-O bonds (Figure 2). In the range 550-600 cm^{-1} appear the bands resulting of stretching vibrations of the Si-O bonds. The bands between 650 and 800 cm^{-1} and between 1000 cm^{-1} and 1200 cm^{-1} are due to symmetric and antisymmetric stretching vibrations of Si–O bonds, respectively. The hydrophobicity of the sample is observed through the existence of methyl groups, originating the symmetric and antisymmetric stretching vibrations of the C-H bonds that are found between 2800 and 3000 cm^{-1} and the stretching vibrations of the Si-C bonds near ~850 cm^{-1}. The symmetric and antisymmetric deformation vibrations of C-H bonds are also observed at ~1270 cm^{-1} and ~1400 cm^{-1}, respectively. The broad band existent at 3400-3500 cm^{-1} corresponds to the overlapping of the O–H stretching vibrations of hydrogen-bonded to water molecules and Si–OH stretching vibrations of the silanol hydrogen-bonded to water molecules.

The bands related with C-H and Si-C bonds that exist in the untreated xerogel, lose their intensity with increasing temperature of the heat-treatments, some fading up until 600ºC, while others disappear only at 800ºC. Thus, spectrum of the xerogel heat-treated at 800ºC shows only the presence of the deformation and stretching vibrations (simetric and antisymmetric) of Si-O bonds, which appear near 500 cm^{-1}, at ~800 cm^{-1} and between 1000 and 1200 cm^{-1}.

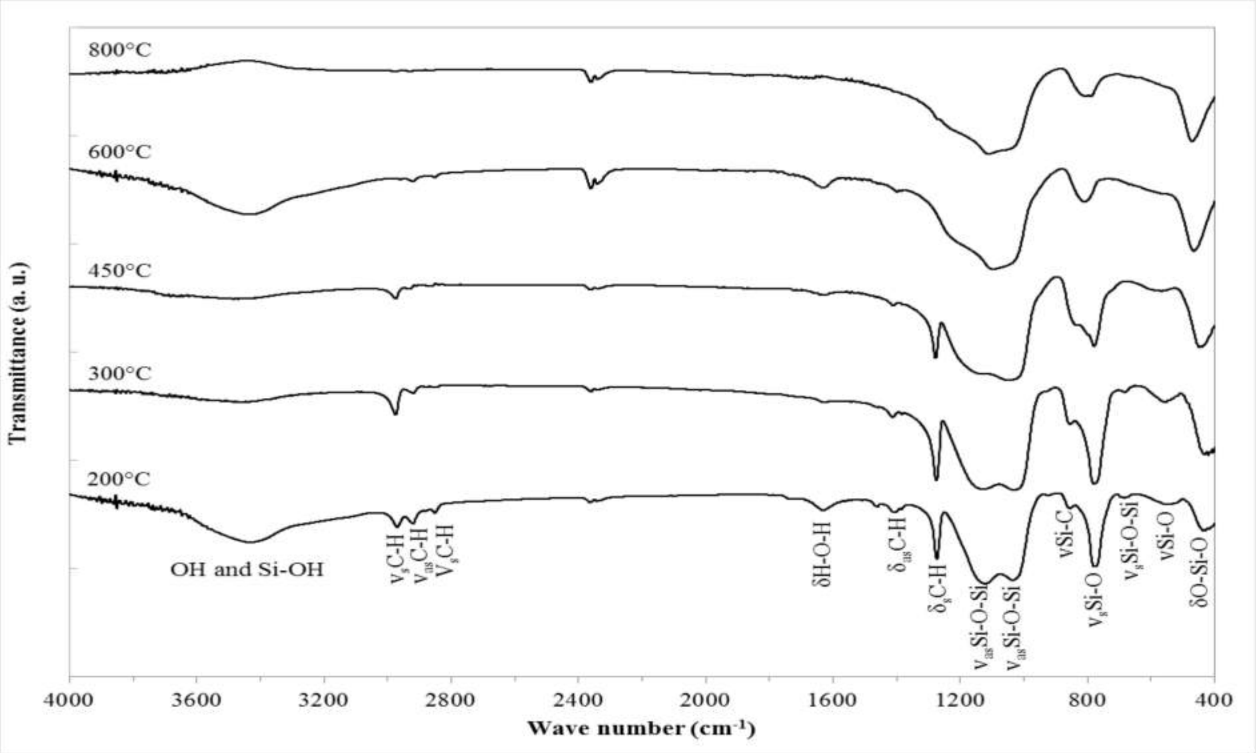

Figure 12: FTIR of untreated (200ºC) and heat-treated xerogel samples.

By the analysis of Figure 3, it is possible to conclude that the as-prepared aerogels have almost the same chemical structure of the as-prepared xerogels, being only noted the less amount of OH bonds. It is also verified that changes in the chemical structure of the materials with the increase in the heat-treatment temperature are identical to those occurring in the xerogels, although in aerogels the total disappearance of the C-H bonds occurs at a lower temperature (600ºC). This result is in agreement with the conclusions drawn from the weight losses in the furnace.

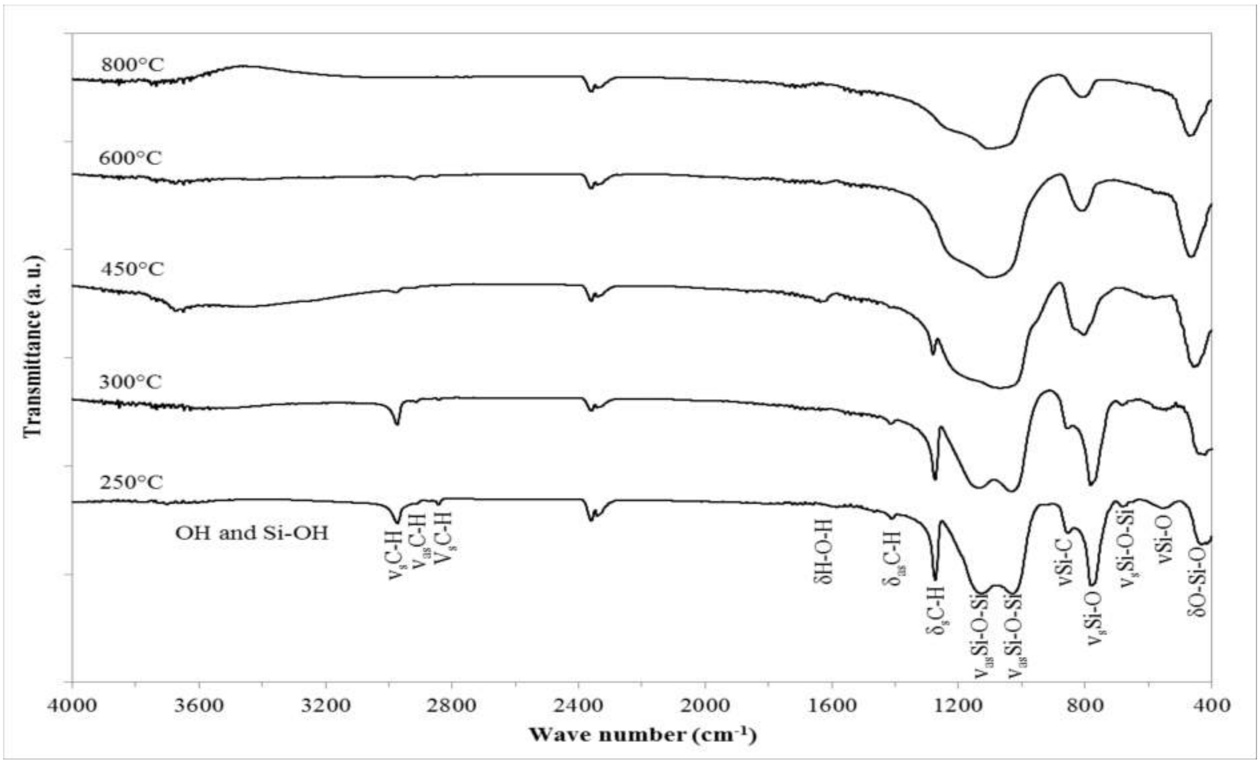

Figure 13: FTIR of untreated (250ºC) and heat-treated aerogel samples.

The elemental analysis provides the mass percentages of the elements carbon, hydrogen, nitrogen and oxygen in the samples. The elemental analysis experimental results obtained for the synthesized xerogels/aerogels are presented in Table 3. The theoretical estimates for these percentages may be obtained, considering the complete condensation of the hydrolyzed species and neglecting the OH groups at the structure ends. The theoretical elemental ratios calculated for complete condensation are Si:1C:3H:1.5O and 41.8Si:17.9C:4.5H:35.8O in molar and wt% base, respectively.

Table 10: Experimental mass percentages of C, H, O and N elements(a) for untreated and heat-treated samples.

Sample	**Temperature(°C)**	**C (%)**	**H (%)**	**O (%)**	**N (%)**
Xerogel	200	16.005	4.836	1.571	0.011
	450	1.008	1.417	5.126	0.005
	800	0.533	0.18	0.568	0.008
Aerogel	250	18.218	4.978	1.838	0.188
	450	0.533	0.914	2.664	0.008
	800	0.02	0.108	0.521	0.201

(a) The wt% errors associated with the measurements are ±0.43, ±0.20, ±0.15 and ±0.25 and for C, H, O and N, respectively.

A comparison between the theoretical and experimental wt% of C for the as-prepared xerogels/aerogels reveals that the condensation reactions were near complete since the values are in good agreement (Table 3). The values for H and O are affected by many factors, more specifically: existence of residues in the material; the OH terminal groups of the network were not considered in the theoretical estimates; lastly, the used temperature in the elemental analysis furnace (1060°C) is not enough to break the Si-O bonds. The existence of residues is confirmed by experimental values obtained for the wt% N. The very low wt% O (1.5-4.3) is justified by the low temperature of the furnace, as referred.

According to Table 3, the increase of the heat-treatments temperature causes a significant decrease of the amounts of C and H due to the oxidation of CH_3, and these elements almost disappear at 800°C. Some reduction of the OH groups in the structure of the materials may also have occurred. In addition, it is observed a greater reduction in the percentage of carbon and hydrogen at 450°C for aerogels than for xerogels, what confirms the FTIR results (Figures 2 and 3) and discussion.

Bulk and skeleton densities, porosities, surface areas and pore sizes of as-prepared and heat-treated xerogels/aerogels are presented in Table 4. Their thermal conductivities and contact angles are shown in Table 5 and Figure 4.

Table 11: Bulk and skeleton densities, porosities, surface areas and pore sizes of untreated and heat-treated samples of xerogels and aerogels.

Sample	**Temperature (°C)**	**Bulk density (kg/m^3)**	**Skeleton density (kg/m^3)**	**Porosity (%)**	**BET surface area (m^2/g)**	**BJH desorption pore size (nm)**
Xerogel	200	80.3 ± 2.0	1183.0 ± 59.7	93.2	579.3 ± 14.2	2.4
	300	71.0 ± 4.1	-	-	-	-
	450	105.1 ± 22.7	2331.7 ± 299.5	95.5	16.8 ± 0.3	4.7
	600	111.2 ± 7.1	-	-	-	-
	800	118.8 ± 5.2	2397.3 ± 239.9	95.0	6.4 ± 0.2	5.9
Aerogel	250	50.3 ± 3.4	1547.6 ± 81.9	96.8	271.0 ± 5.5	3.7
	300	58.0 ± 19.6	-	-	-	-
	450	58.0 ± 9.3	2563.0 ± 519.6	97.7	8.2 ± 0.1	15.9
	600	88.6 ± 15.6	-	-	-	-
	800	89.6 ± 29.6	2233.4 ± 248.4	96.0	9.0 ± 0.2	11.0

Table 12: Thermal conductivities and contact angle values of untreated and heat-treated xerogels and aerogels.

Sample	**Temperature (ºC)**	**Thermal conductivity (W/(m K))**	**Contact angle (º)**
Xerogel	200	0.0401 ± 0.0002	146.1 ± 2.1(a)
	300	0.0442 ± 0.0008	141.8 ± 6.2
	450	0.0608 ± 0.0014	-
	600	0.0596 ± 0.0009	-
	800	0.0463 ± 0.0008	-
Aerogel	250	0.0363 ± 0.0004	148.6 ± 1.7(a)
	300	0.0414 ± 0.0005	152.5 ± 4.1
	450	0.0494 ± 0.0006	-
	600	0.0448 ± 0.0025	-
	800	0.0423 ± 0.0006	-

(a) See Figure 4.

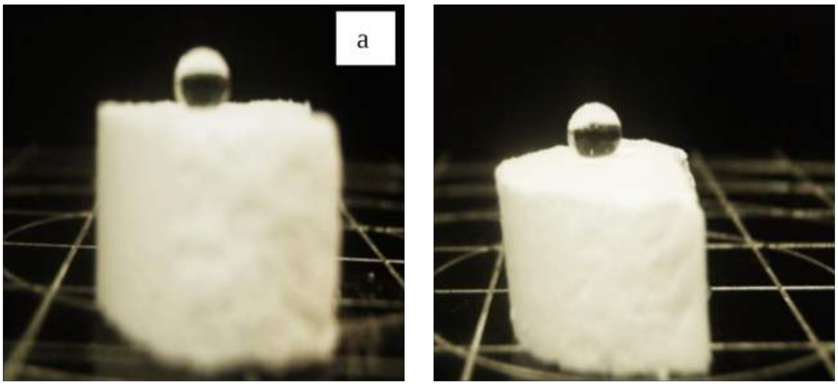

Figure 4: Contact angle of a) 146º for the xerogel and b) 149º for the aerogel.

As-prepared silica xerogels (200ºC) exhibited low density (80.3 kg/m^3), high porosity (93%), low thermal conductivity (0.0401 W/(m K)), high surface area (579 m^2/g) and high hydrophobicity (146º). After the heat-treatment of 300ºC, the bulk density decreases due to the evaporation of impurities, as observed in TGA results. The xerogels lose their hydrophobic behaviour at 450ºC, as expected, due to oxidation of methyl groups. The nonexistence of contact angle proves the change of hydrophobic to hydrophilic character. For the heat-treatment of 450ºC, the density of the sample increases to 105 kg/m^3 and the surface area decreases to 17 m^2/g. After the high temperature treatment (800ºC), the density of the final product increased to 119 kg/m^3, the thermal conductivity changed from 0.040 to 0.046 W/(m K) and the surface area decreased to 6.4 m^2/g. These changes were a consequence of a progressive densification of the material with the increase of temperature.

The untreated silica aerogels shown even higher porosity (97%), lower density (50 kg/m^3) and low thermal conductivity (0.036 W/(m K)) than xerogels. However, their specific surface area is lower probably due to the larger pore size. The aerogels maintained high hydrophobicity (~150º) up to 300ºC, since the oxidation of the methyl group occurs extensively only at 450°C, where the material becomes hydrophilic. As in xerogels, structural changes occurred in the aerogels samples with temperature. After the high temperature treatment (800ºC), the density of the final product increased, the thermal conductivity changed from 0.036 to 0.042 W/(m K), the specific surface area decreased to 9 m^2/g and the pores size increased.

It is worth noting that, for both samples, the thermal conductivity increases up to 450ºC, however it decreases for higher temperature treatments. This decrease beyond 450 ºC was not expected, considering the increase in density and in the pores size. Thus, the explanation for this may be related to the formation of some microfissures in the materials structure, invisible by eye inspection.

SEM micrographs of the as-prepared and heat-treated xerogels can be found in Figure 5. It is clear the highly porous three-dimensional silica network, formed by interlinked structural units with nanometric size. It is also observable that the porous structure includes pores with a wide range of sizes, from micro to macropores. The monolithicity of the samples is maintained with the increase in the temperature of heat-treatments, but the structural units become more linked/agglomerated, being notorious a densification of the structure.

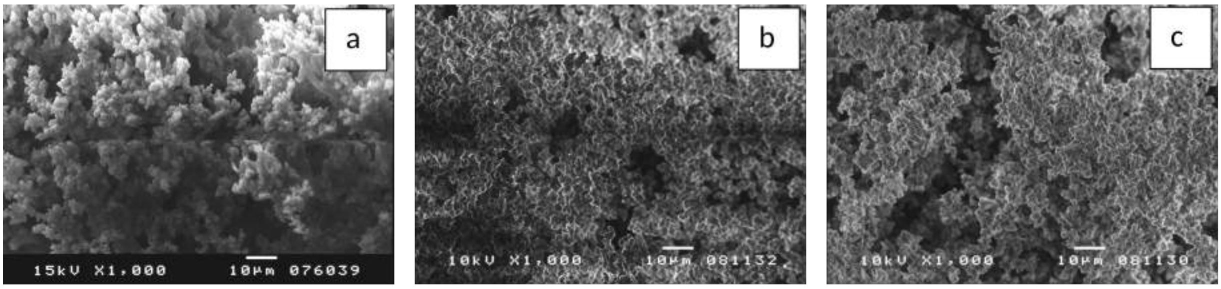

Figure 5: SEM micrographs of xerogels: a) untreated, b) heat-treated at 450ºC, c) heat-treated at 800ºC.

The structural characteristics of the as-prepared aerogels are similar to those of xerogels, although the first present a more open structure (Figure 6). The densification of the aerogels occurs with the increase of the temperature of heat-treatments, due to the agglomeration of the structural units. However, the three-dimensional network maintains its high porosity and monolithicity up to 800ºC, as was already observed for xerogels.

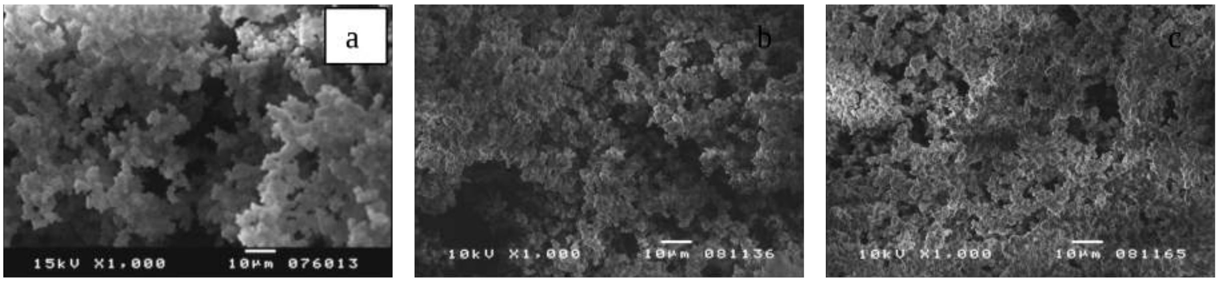

Figure 6: SEM micrographs of xerogels: a) untreated, b) heat-treated at 450ºC, c) heat-treated at 800ºC.

4 CONCLUSIONS

Monolithic silica based xerogels and aerogels were synthesized from methyltrimethoxysilane precursor and their thermal stability was studied. Thus, the effect of heat-treatments (300-800ºC) on the chemical, physical and structural properties of these materials was evaluated by characterizing the as-prepared and heat-treated samples with several techniques: TGA, FTIR, elemental analysis, He picnometry, N_2 adsorption, thermal conductivity and contact angle measurements and SEM.

The as-prepared xerogels and aerogels exhibited low density (80 and 50 kg/m^3, respectively) and thermal conductivity (~ 0.04 W/(m K)), high porosity and specific surface area and very high hydrophobicity (~150º), although the aerogels presented a more porous structure (97% porosity) than xerogels that resulted in higher insulation performance.

With the increase in the temperature of the heat-treatments, these materials lose their hydrophobic and flexible behaviours at 450ºC, due to the oxidation of methyl groups by the environmental air. They also suffered structural densification, achieving ~120 kg/m^3 in the case of xerogels and ~90 kg/m^3 for aerogels. However, the materials remain monolithic and the thermal conductivity values remain with the same order of magnitude, between 0.035 and 0.060 W/(m K), revealing their excellent heat insulation potential for Space applications.

ACKNOWLEDGMENT

This work was funded by FEDER funds through the Operational Programme for Competitiveness Factors - COMPETE and National Funds, through FCT - Foundation for Science and Technology under the project PTDC/EQU-EPR/099998/2008 – *GelSpace – Silica Based Aerogels for Insulation of Spatial Devices*.

REFERENCES

[1] AEGERTER, M. A., LEVENTIS, N., KOEBEL, M. M., Aerogels Handbook, 1st Ed., Springer, New York, **2011** (Chapter 2)

[2] OCHOA, M., DURÃES, L., BEJA, A.M., PORTUGAL, A., Journal of Sol-gel Science and Technology, Vol. 61, **2012**, p.151

[3] DORCHEH, A.S., ABBASI, M.H., Journal of Materials Processing Technology, Vol. 199, **2008**, p.10

[4] DURÃES, L., OCHOA, M., ROCHA, N., PATRÍCIO, R., DUARTE, N., REDONDO, V., PORTUGAL, A., Journal Nanoscience and Nanotechnology, Vol. 12, **2012**, p.6828

[5] RAO, A.V., BHAGAT, S.D., HIRASHIM, H., PAJONK, G.M., Journal of Colloid and Interface Science, Vol. 300, **2006**, p.279

[6] RAO, A. V., KULKARNI, M. M., AMALNERKAR, D. P., SETH, T., Journal of Non-Crystalline Solids, Vol. 330, **2003**, p.187

[7] NADARGI, D.Y., RAO, A.V., Journal of Alloys and Compounds, Vol. 467, **2009**, p.397

[8] LIU, G., ZHOU, B., Ni, X., SHEN, J., WU, G., DU, A., ZU, G., Journal of Sol-gel Science and Technology, Vol. 62, **2012**, p.126

[9] DURÃES, L., OCHOA, M., PORTUGAL, A., DUARTE, N., DIAS, J.P., ROCHA, N., HERNANDEZ, J., Advances in Science and Technology, Vol. 63, **2010**, p.41

[10] BHAGAT, S.D., OH, C.-S., KIM, Y.-H., AHN, Y.-S., YEO, J.-G., Microporous and Mesoporous Materials, Vol. 100, **2007**, p.350

[11] AL OWEINI, R., EL-RASSY, H., Journal of Molecular Structures, Vol. 919, **2009**, p.140

[12] BECKER, H.G.O., BERGER, W., DOMSCHKE, G., FANGHANEL, E., FAUST, J., FISCHER, M. GENTZ, F., GEWALD, K., GLUCH, R., MAYER, R., MULLER, K., PAVEL, D., SCHMIDT, H., SCHOLLBERG, K., SCHWETLICK, K., SEILER, E., ZEPPENFELD, G., Organikum, 2nd Ed., Fundação Calouste Gulbenkian, Lisboa, **1997** (C

CO15

MINERAL AEROGELS FOR ENERGY APPLICATIONS

Arnaud Rigacci*, Christian Beauger

Center for Energy and Processes (CEP), Mines ParisTech

BP 207, 06 904 Sophia Antipolis Cedex, France

arnaud.rigacci@mines-paristech.fr

Abstract

Silica aerogels have been studied for long regarding applications for thermal superinsulation. Nowadays, some products are developed at industrial levels. However, some improvements are still to be achieved. Within this frame, first of all, we present in this paper some of the brand new advances in this sector based on literature examples (organic/inorganic hybrids and composites, nanodispersions, coatings, …). To illustrate our contribution to this sphere, we also detail some of our most illustrative realizations on superinsulating monolithic, granular and blanket-types materials, paying a particular attention to the famous “spring-back” effect based on silylation of the silica pore walls (Figure 1) [1].

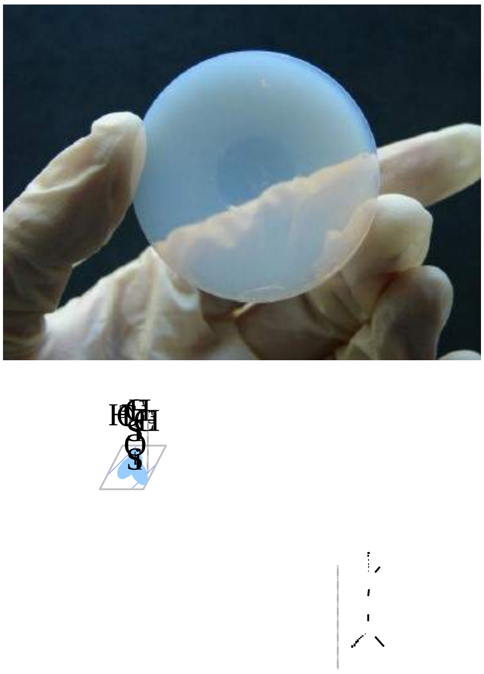

Figure 1. View of a superinsulating silica aerogel sample (top) and the schematic representation of the trimethylsilyl functionalization of silica used for hydrophobization

Regarding the energy sphere, silica aerogels are not the only ones intensively studied. To illustrate this point we present our works in emerging domains like watersplitting (or “how to produce hydrogen from water and sun without electricity inputs”). For this purpose, we have developed some platinised TiO_2 aerogels showing very promising efficiency compared to the standard commercial reference [2] (Figures 2 and 3).

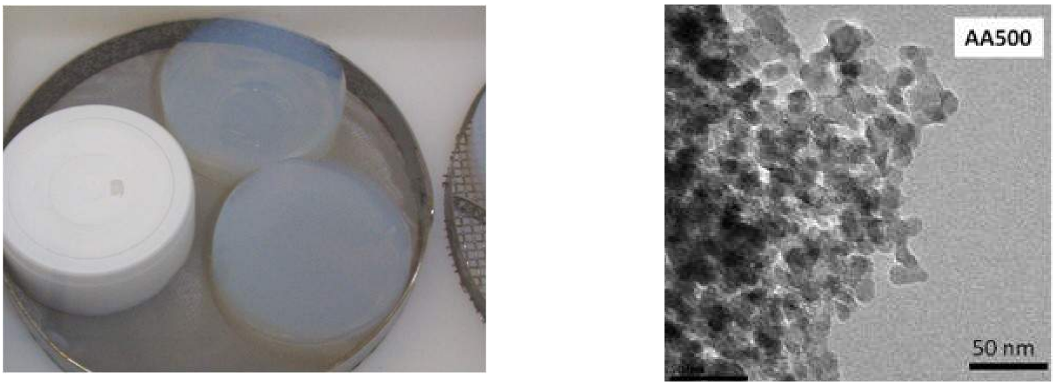

Figure 2 : view of representative wet TiO_2-based gels before drying (left) and their TEM micrograph after supercritical CO_2 drying and calcinations at 500 °C (right)

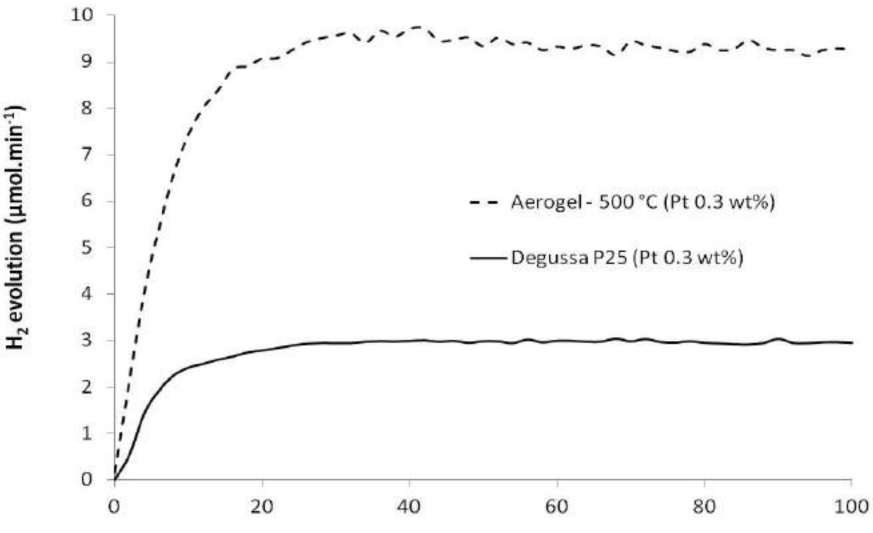

Figure 3 : H_2 evolution on TiO_2 Pt loaded samples: aerogel calcined at 500 °C and P25 – 150 W metal halide lamp, 0.9 l water + 0.1 l MeOH, 0.7 g samples, 0.3 wt% Pt/TiO_2, room temperature - Strasbourg, France.

Finally, we complete the picture with our native studies on tin dioxide (SnO_2) aerogels for Proton Exchange Membrane Fuel Cells (PEM-FC) electrodes. These brand new materials appear very exciting to try to replace more classical but highly corrodible carbonaceous materials classically used in this kind of systems. The first step consisted in preparing nanostrucured SnO_2 aerogels starting from home made tin alkoxide (Figures 4 and 5). Doping has then been performed with vanadium or niobium to make the materials electronic conductive. These first results will thus soon be enriched with conductivity measurements.

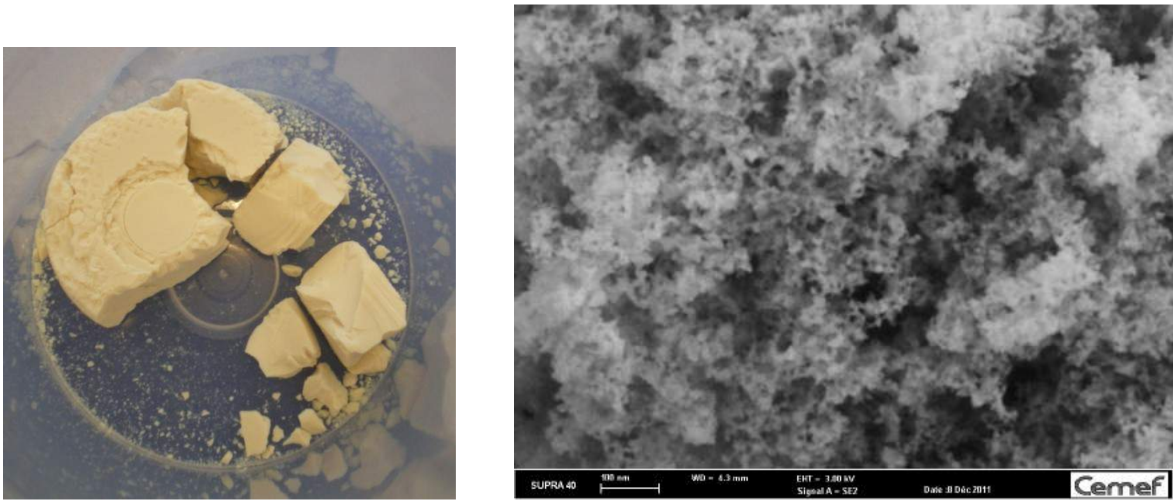

Figure 4 : view of a representative SnO_2 aerogel (left) and its SEM micrograph showing mean particle size of about 10 nm (right).

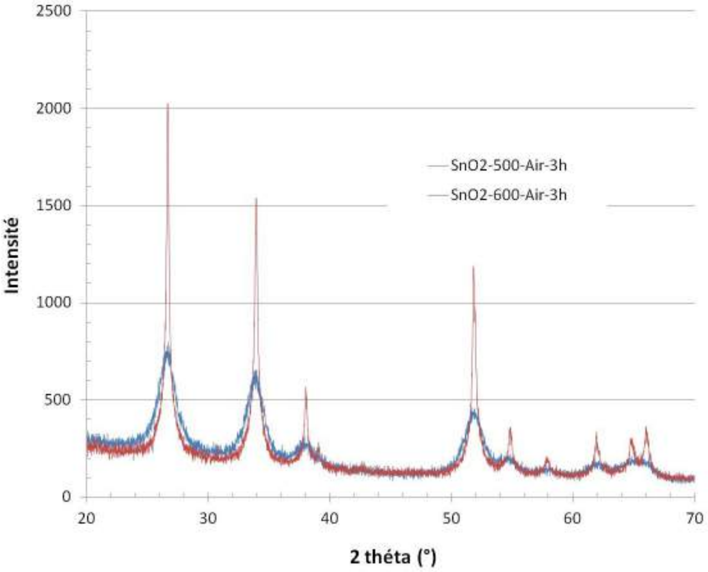

Figure 5 : XRD spectra of SnO_2 aerogels calcined at 500 and 600 °C under flowing air during 3 h.

Acknowledgements : The authors greatly acknowledge Nicolas Keller and Valérie Keller-Spitzer for water splitting measurements and ADEME and Carnot M.I.N.E.S as well as the NANOMINES Group for financial supports and fruitful discussions, respectively.

REFERENCES

1. A. BISSON, A. RIGACCI, D. LECOMTE, P. ACHARD, “Effective thermal conductivity of divided silica xerogel beds”, *Journal of Non-Crystalline Solids*, 350, 379-384 (2004)
2. D. D’ELIA, C. BEAUGER, J.F. HOCHEPIED, A. RIGACCI, M.H. BERGER, N. KELLER, V. KELLER-SPITZER, Y. SUZUKI, J.C. VALMALETTE, M. BENABDESSELAM, P. ACHARD, “Impact of three different TiO_2 morphologies on hydrogen evolution by water-splitting: nanoparticles, nanotubes and aerogels”, *International Journal of Hydrogen Energy,* 36 14360-14373 (2011)

Session 4 : COMPOSITE AEROGELS

CO16

ORGANIC/INORGANIC HYBRID LOW DENSITY XEROGELS

Theresa Noisser, Markus Börner, Gudrun Reichenauer
Bavarian Center for Applied Energy Research (ZAE Bayern), Am Hubland, 97074 Würzburg, Germany

Abstract

Xerogels, i.e. ambient pressure dried sparse gels, are considered to provide an alternative scalable approach to aerogels, if aerogel type properties can be provided. However, it is a fine line to walk between the reduction of drying shrinkage upon ambient pressure drying and the preservation of the application directed properties; this holds in particular, when high porosity in combination with small pore sizes are required.

To provide improved thermal insulations for elevated temperatures, i.e. above 250 °C, we used two different hybrid sol-gel based approaches for the synthesis of monolithic xerogels; in both processes the particle and thus the pore sizes were deliberately increased above the typical values achieved in the classical silica aerogel routes, thus reducing the capillary forces while drying the gels at ambient conditions:

1. *Stöber – approach:* To increase the particle size, the particle growth process and the formation of the interconnected network were separated into two independent process steps. First, uniform silica nanoparticles of about 20 nm in diameter were synthesized by a Stöber process and then crosslinked in a subsequent process step. To strengthen the gel network additional treatments were applied including an organic coating of the gel structure.

2.

3. *Molecular hybrid – approach:* Hybrid organic-inorganic xerogels were synthesized from TEOS and a bifunctional precursor. In the resulting materials the organic mojeties are incorporated in the primary particles. These hybrid particles are larger than their inorganic counterparts in classical silica gels.

After calcinations, both approaches provide monoliths with densities around 200 kg/m^3 and thermal conductivities of about 25 mW/(mK) at ambient conditions.

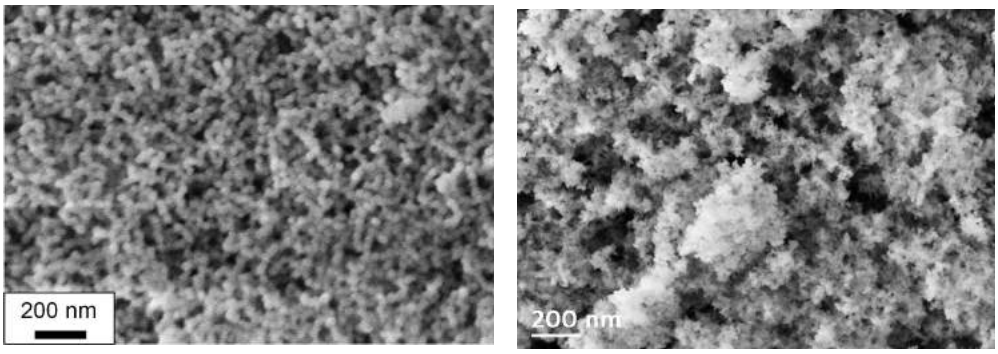

Figure : SEM images of the xerogels derived by a Stöber (left) and the inorganic/organic molecular hybrid (right) approach.

CO17

INORGANIC-ORGANIC HYBRID AEROGELS

Aravind P. Ramaswamy[1], Lorenz Ratke[1], Gian Domenico Soraru[2]

[1]Institut für Materialphysik im Weltraum, Deutsches Zentrum für Luft- und Raumfahrt, DLR, 51147 Köln, Gemany
[2] Department of Materials Engineering and Industrial Technology, University of Trento, Italy

ABSTRACT

Aerogels can be imagined as a huge amount of air dispersed in a nanostructured solid network and hence they possess very low density and high porosity. These materials with fascinating properties like low thermal conductivity, low dielectric strength, high surface area etc. have attracted researchers ever since their discovery by Kistler [1].

The incorporation of an organic part into an inorganic one is already known to be resulting in materials for special applications [2]. It is also reported that an organic part gives strength to the aerogel network which can withstand the capillary pressure while ambient drying [4]. In our work, we have prepared aerogels with various compositions of MTMS-GPTMS. To make a comparison study we prepared gels under supercritical and also under ambient conditions. The density of the supercritically dried hybrid aerogels lies between 0.16 to 0.31 g/cm^3, while the density of the ambient dried one ranges between 0.41 to 0.35 g/cm^3. The surface area of MTMS-0.25 GPTMS was found to be 464 m^2/g with a pore volume and pore diameter of 1.26 cm^3/g and 11.78 nm resp. It is interesting to note that MTMS-0.25 GPTMS composition dried under ambient conditions has surface area and pore volume almost similar to the supercritically dried ones. By tuning the composition of GPTMS and also playing with the sol-gel chemistry we were able to produce flexible aerogels.

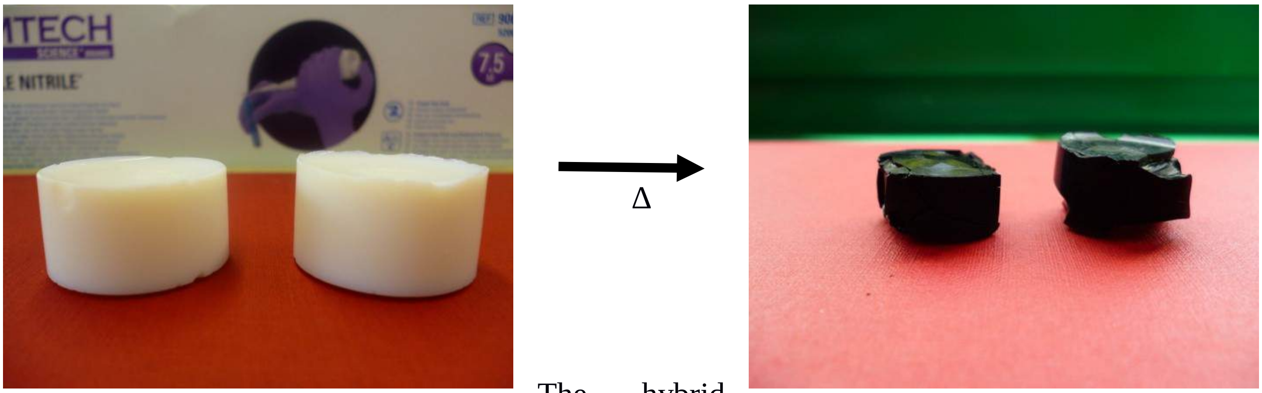

The hybrid gels were also pyrolysed in inert atmosphere to yield porous oxycarbide aerogels, where they may also find possible applications in catalyst support, molecular sieves, gas adsorbants, sensors and ceramics.

[1] Kistler SS (1931) Nature 127:741
[2] H. Schmidt, J. Non-Cryst. Solids 73 (1985) 681.
[3] Shajesh et al. J. Colloid and Interface Sci. 336 (2009) 691.

The hybrid gels were also pyrolysed in inert atmosphere to yield porous oxycarbide aerogels, where they may also find possible applications in catalyst support, molecular sieves, gas adsorbants, sensors and ceramics.

References

[1] Kistler SS (1931) Nature 127:741

[2] H. Schmidt, J. Non-Cryst. Solids 73 (1985) 681.

[3] Shajesh et al. J. Colloid and Interface Sci. 336 (2009) 691.

Session 5:
AEROGEL MANUFACTURE

CO18

DRYING OF AEROGELS WITH SUPERCRITICAL CO_2

Lack E.*, Seidlitz H., Sova M., Lang-jr. F.
NATEX Prozesstechnologie GesmbH
Werkstrasse 7, 2630 Ternitz, AUSTRIA
Phone: +43-2630-32120, Fax: +43-2630-38163, contact e-mail: office@natex.at

Abstract

Aerogels have already been known for 70 years, but due to the difficulties to remove the liquid from the porous structure and to avoid the collapse of the open structure during the drying process, the production of dry Aerogels is quite limited till now. By removing the liquid of the porous structure the surface tension in the solid liquid interfaces creates strong capillary forces and these forces destroy the porous structure. To freeze the liquid following by freeze-drying was not successful; the formation of ice crystals destroyed the porous structure as well. Currently the supercritical drying process is the best solution to avoid such capillary forces. Most of the Aerogels are produced from inorganic materials, like silica or metal oxides, but in the last years Aerogels from cellulosic materials are more and more investigated.

The most important gelation liquid is water, which causes an additional cost factor in the drying process. As the solubility of water in supercritical CO_2 and CO_2 in water is quite limited, it is necessary to remove the water out of the wet Aerogels and to replace the liquid by an organic solvent suitable for supercritical drying, mainly acetone and ethanol. In the EC supported project AEROCELL - contract no. NMP3-CT2003-505888 - mainly Aerogels from cellulosic materials were investigated. The production of the wet gels is different to the silica gels, which are mainly produced out of water solutions. As cellulose with higher DP (degree of polymerisation) is not soluble in water, we used solutions with NaOH or NMMO (N-methyl-morpholine-N-oxid) and the carbamate path to produce the wet gel. After gelation NaOH and NMMO has to be washed out to get a micro-porous or even nano-porous structure of cellulose filled with water. As most of the cellulose solutions are solid at room temperature, it was possible to transfer such solutions into different shapes, like cylinder, spheres, films or powder.

To start the supercritical drying it is necessary to replace the water by a solvent, suitable for supercritical drying, which was necessary for all kind of Aerogels. The supercritical drying process is a very delicate procedure and any surface tension has to be avoided in each step of the process. During the mentioned EC project and by our own research afterwards, a lot of different drying methods were developed in order to get an optimal solvent recycling and to keep the shrinking of the Aerogel bodies as low as possible, results and experience enabled plant design and economical consideration. The gelation, the solvent change and the supercritical drying process are quite expensive processes and still ongoing optimisation is necessary to reach reasonable production costs.

Introduction

Aerogels, especially dry Aerogels, are a kind of materials with a high micro-porous structure, sometimes a nano-porous structure both with a very low bulk density. Silica Aerogel can be produced transparent with a high thermal resistance like organic insulation material. Aerogels from metal oxides have a high surface and are interesting for catalytic systems. In recent times Aerogels from renewable resources become more and more interest, especially from cellulose.

Around 1930 S. Kistler [1] started to produce Aerogels and beside silica-, alumina- and other metal oxide Aerogels he started as well to produce others from cellulose derivates.

NATEX started 2001 researching on Aerogels, but intense investigation was carried out within the Aerocell project supported under the 6th Framework Programme.

For each production step, shown underneath, different paths from the participating partners were used in order to find different kinds of Aerogels which can be used for the various applications.

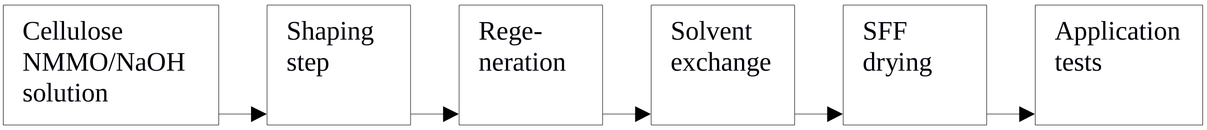

Figure 1: Schematic flow sheet for the Aerocellulose production

Figure 2: Starting material: pulp and 50 % NMMO solution – shaping – regenerated cellulose hydrogels – supercritical drying – Cellulose Aerogels. (Final published report EC project Aerocell 505888-1).

As a first step the wet Aerocell precursor gel has to be prepared and four different routes were investigated.

Cellulose-NMMO route prepared by Lenzing AG [2]

Cellulose up to concentrations between 0,3 - 5 % is dissolved directly into NMMO. To obtain a high porous material most of the concentrations is kept below 2 %. By adding other substances which are soluble in NMMO, composite materials can be produced. The heated and molten solution is transferred into the desired shape and gets solid after cooling down. After the anti-solvent process with water, a wet gel with different shapes is obtained.

Cellulose - NaOH route [3] prepared by CEMEF and Armines

Only cellulose with a low DP of 170 up to 500 can be solved in aqueous sodium hydroxide solutions. With such a relative low degree of polymerisation it is quite difficult to produce stable bodies and in some cases it is necessary to improve the solubility by adding urea. The gelation process starts by increasing the temperature, followed by the anti-solvent process with water. For larger bodies of several cm it is quite difficult to remove the NaOH out of the swollen wet gel.

Cellulose Ester route, prepared by CEP [4]

With this path partly cellulose acetate wet gels and partly cellulose acetate cross-linked with isocyanates can be produced.

Cellulose carbamate path prepared by Fraunhofer FhG-IAP [5]

The carbamate route was the main domain of Fraunhofer and includes four process steps. In the first step cellulose, NaOH and urea are kneaded into a viscous mass, afterwards the cellulose carbamate is dissolved in caustic soda at a reduced temperature (about -10°C). As Aerocells of carbamate are not so stable, higher cellulose concentration between 3 and 5 % has to be adjusted. For the gelation two ways are possible, one is the thermal precipitation and the other one is the chemical precipitation with sulphuric acid. In the last step all water soluble chemicals has to be removed by repeated washing with water, thereby obtaining a wet gel at a more or less neutral pH.

Solvent change

As already mentioned the solubility of water in supercritical CO_2 and CO_2 in water is very limited and the supercritical drying of water wet Aerogels causes a lot of capillary forces. Our drying tests with water wet Aerogels showed a complete destruction of the micro-porous structure and a volume shrinking of more than 60 %. The solubility of water in CO_2 is mainly dependent on the temperature, but higher processing than 150°C destroy the cellulose structure due to reducing the polymerisation grade and the pH. One way to avoid this problem is to replace the water by water mixable organic solvents. In several steps the water concentration is slowly reduced, consequently increasing thereby the one of the organic solvent. For large Aerogel bodies with a diameter of more than 7 cm this procedure needs several days. The reduction of water especially for Aerogels with small pores and higher density could be a very slow process.

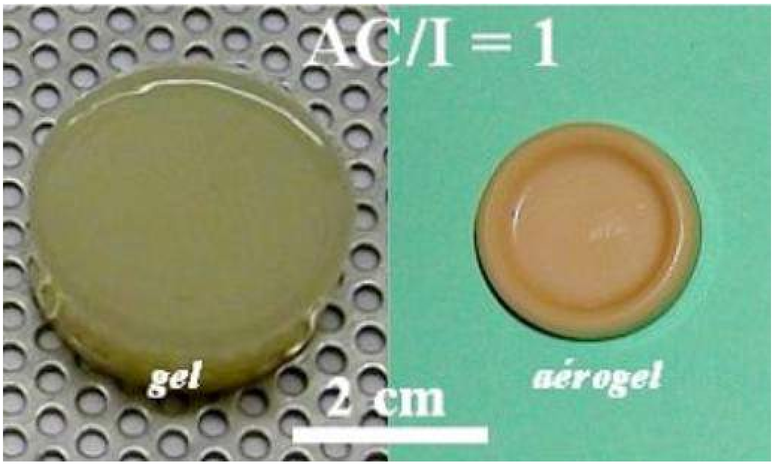

Figure 3: Volume shrinkage of an Acetogel from acetate (Archive Armines/Cemef)

To reduce the shrinking in the drying process the remaining water content should be less than 4 %, but some tests with 6 % showed acceptable results. Most of the samples are destroyed in case the water content is higher than 10 %. A lot of water solvent mixtures are obtained but the solvent can be recovered by means of distillation or in the future by an energy efficient process like pervaporation. This solvent change and the solvent recycling is the major energy consumer at the moment.

Supercritical drying

The substitution and replacement of the solvent molecules within the micro-porous structure by supercritical CO_2 is the basis for drying of Aerogels. As precondition it is necessary to use a solvent which is completely mixable with CO_2 or another dense gas. In the EC project only CO_2 was used as dense gas. If part of the liquid remains in the structure, e.g. if the water content is too high, capillary forces are created and destroying the structure.

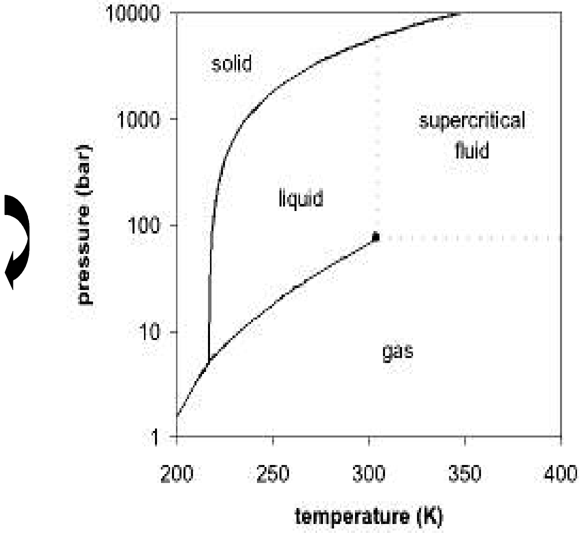

Figure 4: Phase diagram - principle of SC-drying

Currently the supercritical CO_2 drying is the best solution to avoid such capillary forces. It is also possible to increase the temperature of the organic solvent or water above the critical temperature by keeping the pressure above the critical pressure, but the water temperature has to be increased up to nearly 400°C. The SC drying process is a batch process and is executed in our modified CO_2 extraction plants. During the whole drying process it is at any time very important to avoid any surface tension between solvent and CO_2.

First of all the drying vessel is pressurized with CO_2 until the drying pressure is reached and the CO_2 diffuse into the solvent and a homogenous mixture of CO_2 and solvent is obtained within the solid structure. After starting a continuous CO_2 flow the mixture is more and more diluted and finally the solid structure is only filled with supercritical CO_2. After corresponding slow depressurization a dry porous structure is obtained.

Thermodynamic conditions for the drying routes

For most of the samples we used drying conditions of pressures between 90 to 250 bar and temperatures between 40 to 100°C, all depending on the kind of wet gel and the size of the samples.

To be sure that the mixture is always under supercritical conditions, knowledge about the phase

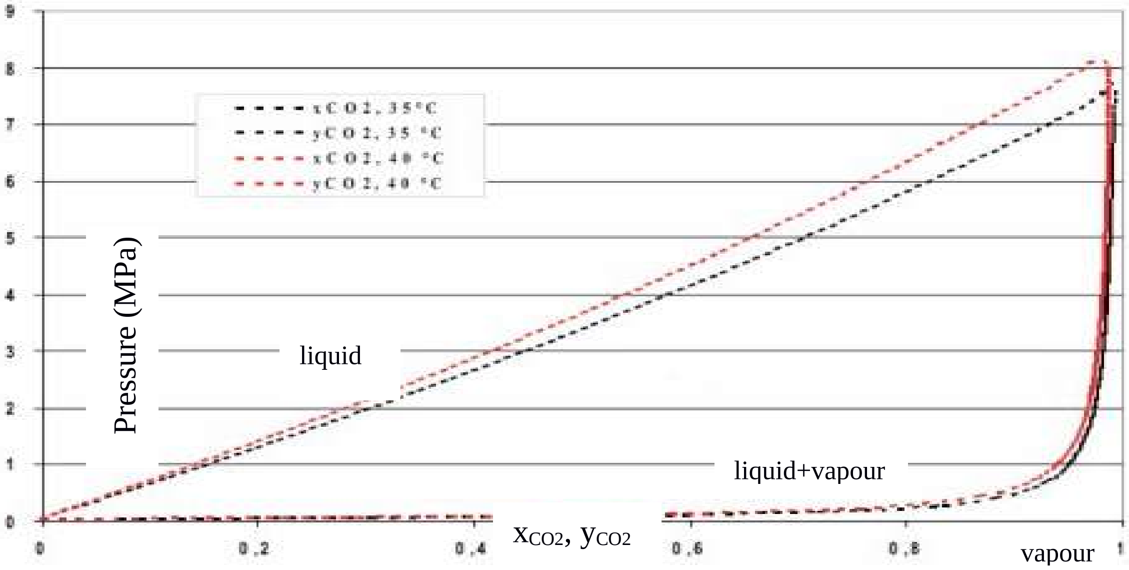

Figure 5: Binary phase diagram for the binary mixture acetone, CO_2, calculated by Fischer [6]

Experimental drying routes, laboratory plants

The drying tests were executed in different sized plants in the laboratory of NATEX. Most of the tests were made in the 5 l/1000 bar plant, some pre-tests in the 200 ml bench scale plant.

Figure 6: 5 l/1000 bar research unit (NATEX)

Figure 7: Divided basket (NATEX)

The samples loaded in baskets are inserted into the extractor. To avoid mechanical deformation during the loading, the basket – see Figure 7 - is divided into several trays and the bed height reduced. It is also important to keep the samples always covered with solvent, avoiding air drying which causes immediately shrinking.

It is quite difficult to determine the end of the drying process. To be sure that all solvent is removed from the samples, we installed an online measurement at the outlet of the extractor.

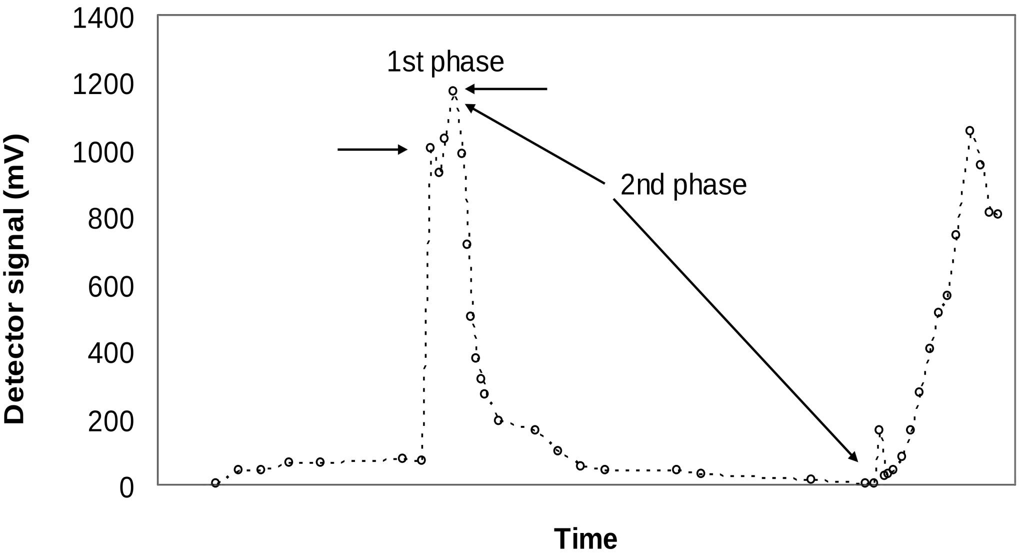

Figure 8: Online measurement of acetone concentration in CO_2

There is a high concentration at the beginning of the drying process due to the free available solvent around the Aerocell samples. After the first phase the solvent concentration decreases sharply and diffusion of solvent out of the pores commence. This diffusion period can last up to ten hours depending on the size of the micro-porous structure and the size of the sample (e.g. 8 cm). At the end the concentration increases again. We are not sure about this, but perhaps some still remaining solvent from the samples or solvent from dead ends of the plant is released during depressurization.

Figure 9: Pilot Plant for Aerocell drying.

High pressure vessel with quick acting closure and jacket heating

Design:

Pressure: 120/-1 bar

Temperature: 100/-10°C

Volume: 35 litres

After drying of numerous Cellulose Aerogels – from different starting materials - densities in a range between 0,014 to 0,5 kg/m³ and an internal surface between 50 to 420 m²/g were obtained. Typical micro-structures can be seen in Figure 10.

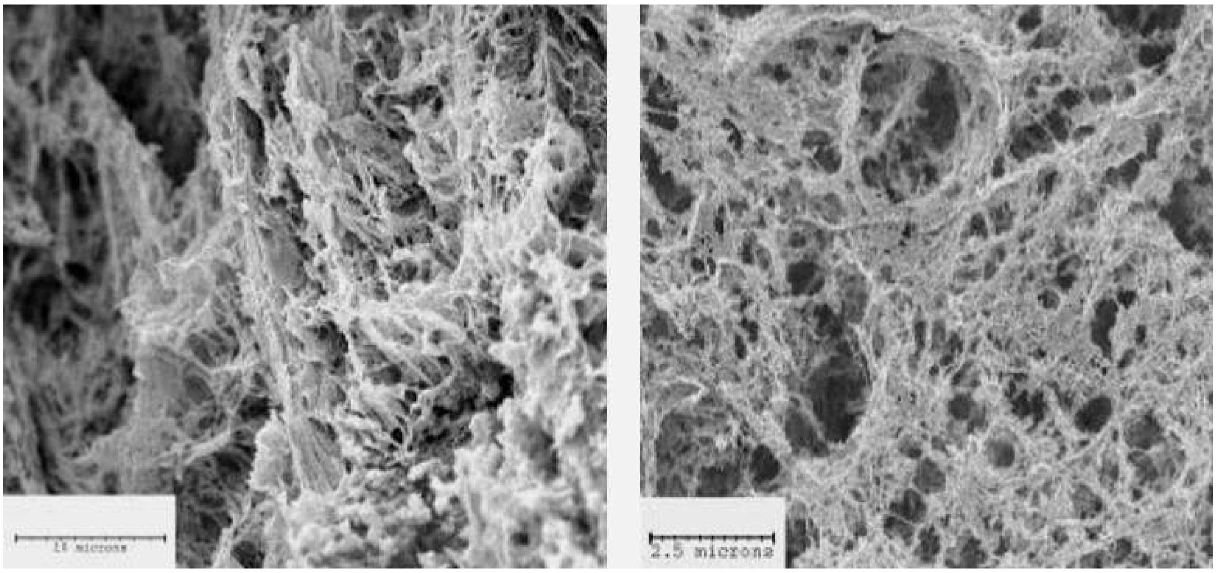

Figure 10: SEM images of Aerocellulose structures

Left: cylinder (scale 10 µm), Right: interior of a film (scale 2,5 µm). [7]

Some relations between production parameters and final obtained Aerogels can be seen in Table 1 [7] underneath.

Table 1: Correlation between production parameters and properties of Cellulose Aerogels

Increase of initial cellulose concentration	Increase density Lower total shrinkage
Regeneration in NMMO/water	Lower BET surface
Unbleached pulp	Lower density
Spheres by tripping into water by ambient temperature	Solid skin Fluffy core
Spheres by tripping into cold water	Complete solid particles
Spheres have a higher BET surface than cylinders	

Economics of SC drying

Based on the experimental results obtained from the laboratory and pilot plant economic calculations of different plant sizes were elaborated, using processing conditions with best results, i.e. drying at 120 bar and 50°C

A comparison between a compressor and pump driven process was elaborated. The result was that the energy consumption of the compressor process is in a range of about 50% less compared to the one using a circulation pump. The following diagrams are based on such a higher economic design.

Table 2 shows the basic data for the feasibility investigation, considering different plant sizes – ranging between 1 and 5 m³ payload volumes - and batch times between 5 and 9 hours.

Table 2: Basic data for the feasibility investigation

		1 x 1000 l	1 x 2000 l	1 x 3000 l	1 x 4000 l	1 x 5000 l
Production hours / year	hrs	8064 hrs				
Electrical energy	€/kWh	0,085				
Fuel	€/t	500				
CO_2	€/t	100				
Bulk density	kg/m³	20 - 50				
Depreciation	years	10 for the plant, 20 for land and building				
Import tax	%	0				
Interest	%	3% for 6 years				
Labor costs	€/h	400.000				
Capacity/ year	t/anno	20 - 50	40 - 100	60 - 150	80 - 200	100 - 250
TOTAL INVESTMENT	€	**3.000.000**	**3.500.000**	**4.250.000**	**4.650.000**	**4.900.000**
Start-up capital	€	150.000	175.000	212.500	232.500	245.000
Activated Charcoal	€	10.000	20.000	30.000	40.000	50.000
Spares / maintenance	€	30.000	30.000	30.000	30.000	30.000
OH, Office, insurance, etc.	€	15.000	15.000	15.000	15.000	15.000

Figure 11 shows the production costs for different plant sizes – between 1 and 5 m³ payload volumes – in dependence of the bulk density – chosen between 20 and 50 kg/m³ - and at a constant batch time of 8 hours. The production costs are between about 7 and 43 €/kg feed material.

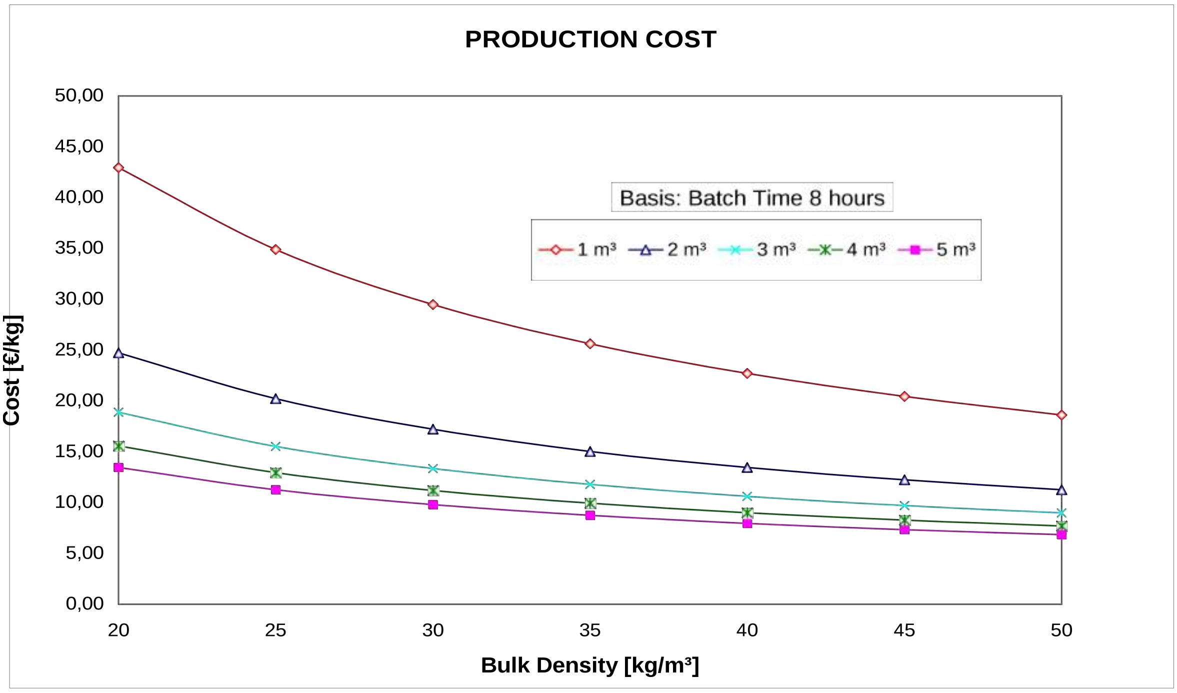

Figure 11: Production costs for different plant sizes

Figure 12 shows the influence of different batch times – between 5 and 9 hours – in dependence of the bulk density - chosen between 20 and 50 kg/m³ - and for a plant size of 5 m³ payload volume. The production costs are between about 5 and 15 €/kg feed material.

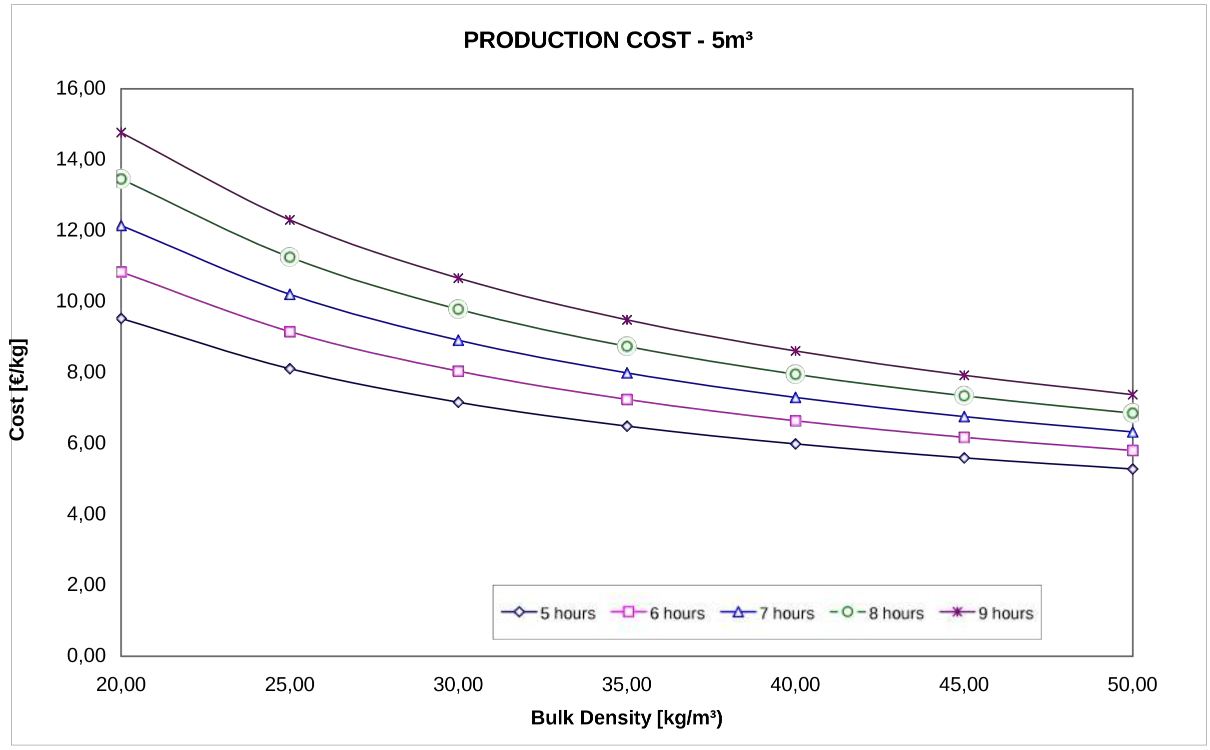

Figure 12: Production costs for different batch times

Application tests for Aerocellulose [7]

During the project around 400, but totally we produced around 600 different Aerocell samples. With the definition of standard drying processes and performed series of pilot tests a lot of experience and results were gained, made materials for application tests available and enabled feasibility studies. After several years of collecting results and experience corresponding cost efficient production methods for different kinds of Aerogels could be developed.

Packaging (investigated by company Novamont)

The usage of cellulose Aerogel as package material was one of the topics to be investigated. The developed Aerogel has good mechanical properties at a low density. Most of the samples have a bulk density between 18 - 45 kg/m³. A further advantage is that all cellulose Aerogels are highly biodegradable. Disadvantages are the low resilience (recovery of the original shape after deformation), the open structure of the Aerocell adsorbing immediately oil and water and of course the high price.

Cosmetics (investigated by company Cognis and other partners)

The goal was to use the small Aerocellulose particles as a powdered delivery system, to be loaded with active components and as well to use it in controlled release systems. The level of loading with liquids was not as good as on silicic acid, but further optimisation could result in an interesting product for the future, because of an increasing demand of silica free products.

Carbon Aerogels (several partners)

Around 100 samples were pyrolysed to produce Carbon Aerogels.

First the material was tested as basis for “Super Capacitors” and as well as electrodes in fuel cells. The results were not as good as expected and further developing work would be necessary.

The use of Carbon Aerogels as positive electrode in lithium batteries seems to be quite interesting. At the moment most of the electrodes are produced of carbon black powder with graphite agglomerated by a PTFE polymeric binder.

Ideal would be the production of monolithic, cylindrical blocks, which fits directly into the battery body. But it is very difficult to produce a precise cylindrical body. Gel preparation, shaping, solvent change, supercritical drying and finally pyrolyses, each step can cause shrinkage and deformation of the body. Even after optimisation of each step it was not possible to produce very precise bodies. Finally best results could be obtained with fibres of Carbon Aerogels winded in coils or used as fabrics.

Some problems, which could be solved after some tests, were to reach a good electrical contact from the electrical wire to the Carbon Aerogel. The loading and discharge profiles of prototype batteries are not as good as standard ones, but the main advantage is definitely the low weight of the Carbon Aerogel material which gives hopes for new applications.

LITERATURE:

[1] KISTLER, S. S. J. Phys. Chem. 1932, 36, 52.

[2] INNERLOHINGER, J., WEBER, H. K., KRAFT, G., Aerocellulose: Aerogels and aerogel-like materials made from cellulose, Macromolecular Symposia, 2006.

[3] GAVILLON, R., Préparation et caractérisations de matériau cellulosique ultra poreux, Thesis, Sophia Antipolis, 2007.

[4] FISCHER, F., RIGACCI, A., PIRARD, R., BERTHON-FABRY, S., ACHARD, P., Cellulose-based aerogels, Polymer, 47, 7636, 2006.

[5] PINNOW, M., FINK, H.-P., FANTER, C., KUNZE, J., Characterization of highly porous materials from cellulose carbamate, “Macromolecular Symposia” of Wiley VCH-Verlag GmbH, 2007

[6] FISCHER, thesis to obtain the degree Docteur de l’Ecole des Mines de Paris, « Synthèse et étude de matériaux nanostructurés a base d’acétate de cellulose pour applications énergétiques », Dec. 14th, 2006

[7] Published Final Activity Report AEROCELL, project no. 505888-1, “Aerocellulose and its Carbon Counterparts – Porous, Multifunctional Nano-Materials from Renewable Resources”, Feb. 5th, 2007

CO19

A NEW CONCEPT FOR AEROGEL DRYING PROCESS SCALE-UP

Ruiz-González F., Français E., Perrut M.
SEPAREX Champigneulles (France)
fruiz-gonzalez@separex.fr

ABSTRACT

Although their unique properties related to their uncommon high nano-porosity, aerogels have not yet widely developed as, until recently, they were considered prohibitively expensive. Large-scale applications (especially for building insulation where huge volumes are required at low cost) need optimization of the chemical recipes and components synthesis and development of a drying process adapted to such large-volume manufacture.

Based on our long experience of supercritical fluid processes and equipment, we propose a system to drastically cut cost of large-scale semi-batch processing consisting in several drying vessels operated in a way to recycling both the organic solvent and CO_2, decreasing significantly the process duration and the related energy consumption and manpower costs: This system is based on the concept of simulated moving bed, already implemented to move from the classical (batch) elution chromatography to a quasi-continuous chromatography with great benefits.

Introduction

Aerogels are prepared from gels, produced from organic monomers or inorganic salts or metal alkoxydes, or inorganic-organic precursors. A first step consists in preparation of a colloidal “sol” of the material in a solvent, which leads to a “gel” after a “maturation” time. The gel drying can be performed by venting the solvent above its critical point (generally high temperature) or, most commonly, by solvent exchange with a preferred solvent (CO_2) followed by supercritical venting (needing lower temperatures), the objective being to eliminate the solvent from the sol-gel without generating a two-phase system and related capillary forces. This is possible through compressing and heating the sol-gel above the critical pressure and temperature of the solvent (for CO_2 :Tc = 31°C, Pc = 7.4 MPa) and then by decompressing it to atmospheric pressure and cooling it to room temperature, maintaining the solvent in gas phase without any condensation as shown on Figure 1.

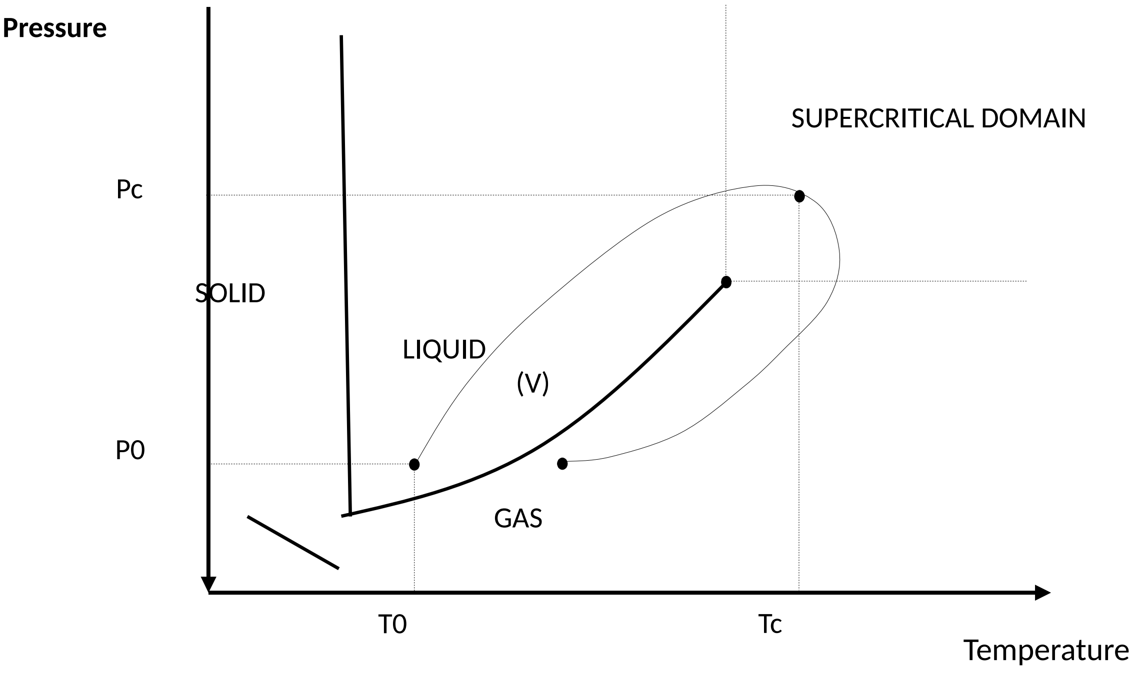

Figure 1: Supercritical drying procedure

Practically, for silica gels in ethanol, the supercritical drying using CO_2 is implemented as follows: The sol-gel is placed in a pressure vessel. The system is pressurized with CO_2 meanwhile it is gently heated and pressurized over the critical temperature and pressure.

Supercritical fluid $CO_2$is flushed through the vessel until ethanol has been totally removed from within the gel. Complete solvent substitution often needs several hours depending on the gel thickness. A slow release of CO_2 is then started until the pressure reach ambient pressure.

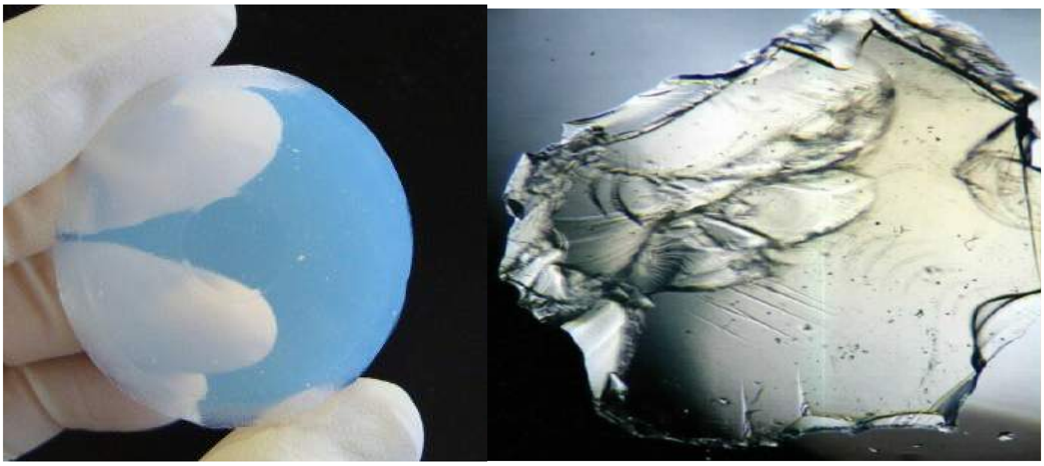

Figure 2: Examples of silica aerogel

Scale-up optimization system

The basic process as described earlier can be applied at lab or pilot-scale for process study and sample preparation, as no cost limitation has to be taken into account. This process is operated in batch mode, lasting from 12 h to several days depending on the aerogel type and size of aerogel pieces.

Obviously, such process cannot be scaled-up *as it is*, while leading to unacceptable costs related to drying duration, energy and fluid consumption and manpower and demanding a heavy investment on a high-pressure plant whose main parts are only used during part of time. Moreover, depressurization of large amounts of fluid leads to a significant cooling that is to be controlled to avoid aerogel structure degradation, what can be done by injection of heated air during the last depressurization step.

It is why we tried to design a process adapted to large-volume manufacture operated in semi-batch with optimal use of this expensive high-pressure equipment. We propose to use the concept of simulated moving bed that is familiar to the scientists working on chromatography processes, with the aim to replace a truly batch operation into a quasi-continuous one. For that purpose, the drying process has been also optimized leading to a suitable process.

The design relies on sharing the solvent exchange and supercritical drying in several steps that will be operated in parallel on several vessels. This sequential operation comprises n steps characterized by four parameters (pressure & temperature evolution CO_2 flow rate, step duration). One more step consists in unloading the aerogel and loading the sol-gel. So, this requires (n+1) similar pressure vessels that will be operated according to the complete sequence of (n+1) steps, with, at any moment, only one vessel operating in each of the steps.

To illustrate this sequential operation, we present on Figure 3 a basic curve in the (P, T) diagram.

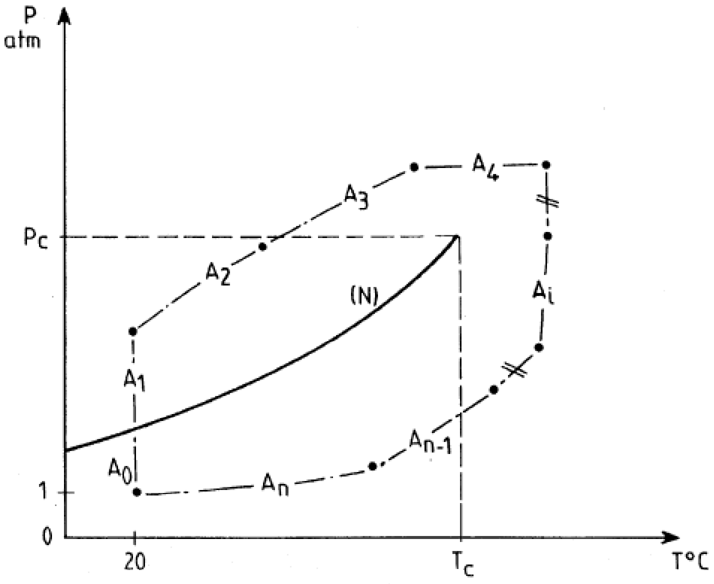

Figure 3: Sequential drying process

Obviously, the duration of each step has been set to be the same in order to avoid dead-times that would lead into capacity loss when each vessel operates in a given step. This permits to use only one CO_2 loop (reservoir, pump, recycle) always used at full capacity.

Process implementation

We present on Figure 4 an implementation of this process concept showing a flow sheet with 5 drying vessels (A0-A4), one liquid CO_2 pump (P), one air compressor (Co) to supply dry compressed air, 3 heat exchangers (R1-R3), 2 separators (S1-S2) to collect the organic solvent, a complex system of configuration valves (V) that manages the fluid circuits, and regulation valves (Pr) that control pressure inside each vessel. CO_2 is recycled through a condenser (C) and partly vented (Ve) or recompressed (D) prior to recycling.

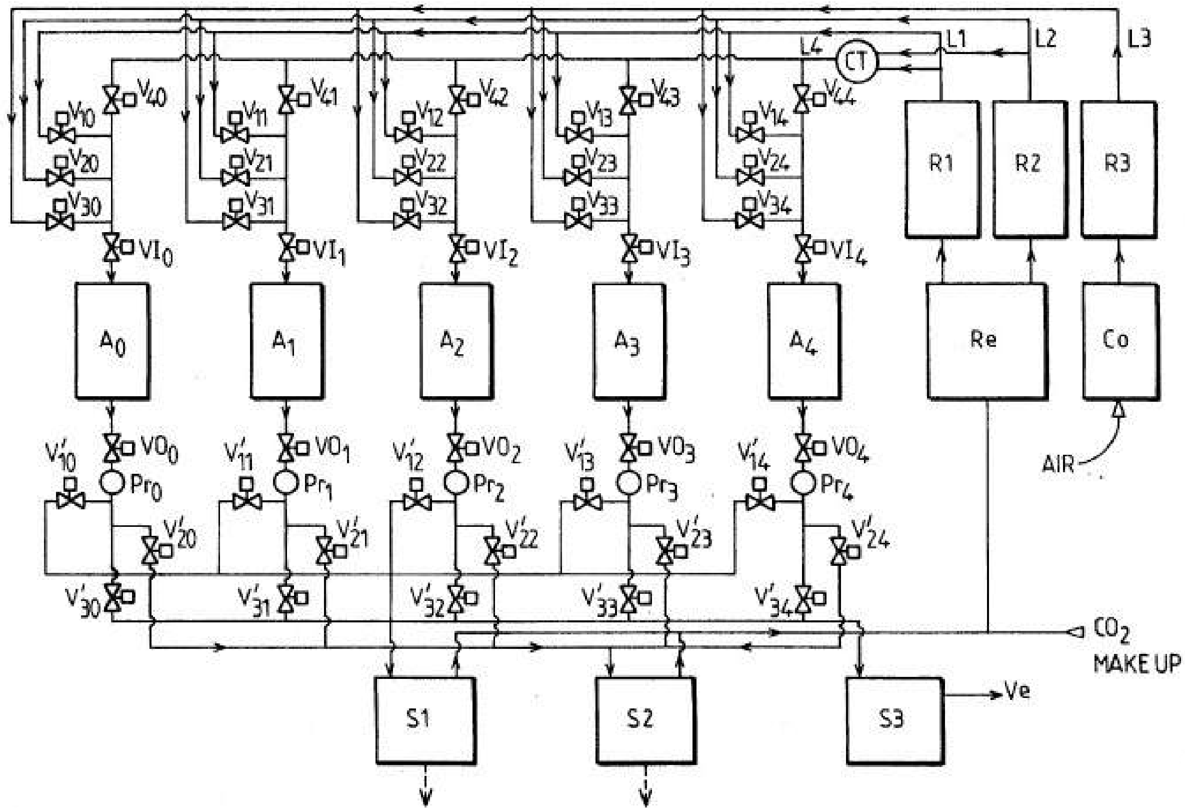

Figure 4: Process implementation system

Comparison between batch and sequential processes

Sol-gel drying procedure in a single autoclave can be transposed to the 5-autoclaves equipment with high savings of energy and time. The current recipe applied in a single-vessel can be split into 6 main steps as follows:

Step 1: Filling of the sol gel in the autoclave
Step 2: Pressurization
Step 3: Pressure and temperature increasing up to working conditions
Step 4: Drying step (solvent elimination)
Step 5: Gas withdrawal
Step 6: Aerogel recovery

The estimates of the duration of each step mentioned are based on experiments driven in our lab-scale unit. These values are necessary to define the sequences in the semi-continuous process.

The total duration of the complete process is about 450 min. considering that the five vessels are working at the same time, the optimal procedure is to use them during 450 / 5 = 90 min. Each step is operated in one (or two) vessel(s) as is described in Table 1.

Table 1. Example of process sequence.

	Vessel A_0	**Vessel A_1**	**Vessel A_2**	**Vessel A_3**	**Vessel A_4**
Sequence 1	½ S5 + S6 + S1 + S2	S5 + ½ S5	S4	S4	S2 + S3
Sequence 2	S2 + S3	½ S5+S6 +S1+S2	S5 + ½ S5	S4	S4
Sequence 3	S4	S2 + S3	½ S5+S6 +S1+S2	S5 + ½ S5	S4
Sequence 4	S4	4S5	S2 + S3	½ S5+S6 +S1+S2	S5 + ½ S5
Sequence 5	S5 + ½ S5	S4	S4	S2 + S3	½ S5+S6 +S1+S2

SN means step N

This procedure will transform a batch process into a semi continuous one with a frequency of 5 sequences. For each vessel, the steps conducted during the sequence n° N are identical to those of the n° N+5 sequence… For example, the sol-gel filling (S1) and the aerogel emptying (S6) will be done during each sequence in vessel A_0, then A_1, A_2, A_3, A_4 and A_0 again and so on…

The real durations in larger equipment have to be refined in order to fit the real drying requirements. That drastically depends on the aerogel type and size of piece, increasing from powder, granular to large monoliths.

Figure 5: Semi-industrial 170-litre SFD Unit

References

[1] Brinker C., Scherer G., *Sol-Gel Science: the physics and chemistry of sol-gel processing,* Academic Press, 1990.

[2] Ayern R. J., Jacobucci A., *Reviews in Chem. Eng*., 5, 1988, pp.158-193.

[3] Fricke J., Tillotson T., Aerogels: production, characterization, and applications, *Thin Solid Films* 297, 1997, pp. 212-223.

[4] Mulik S., Sotiriou-Leventis C., in *Aerogels Handbook of Advances in SolGel Derived Materials and Technologies* Series, M. A. Aegerter, N. Leventis, M. M. Koebel, Eds., Springer, 2011, pp. 251-286.

[5] Perrut M., Supercritical Fluid Applications: Industrial development and economic issues, *Ind. Eng. Chem. Res*., 39 (12), 2000, pp. 4531 - 4535.

[6] Perrut M, Français E., Process and equipment for drying polymeric aerogel in the presence of a supercritical fluid, US Patent 5,962,539, 1999.

Acknowledgements

For Aerogel R&D works, SEPAREX receives support from the European Union according programs AEROCOINs and AerSUS (FP7).

POSTERS

SEMINAR ON AEROGELS
Properties-Manufacture-Applications
6th – 7th December 2012
Université de Lorraine/**ENSIC - NANCY (France)**

LIST OF POSTERS

P01

A NOVEL CLASS OF HYDROPHOBIC CELLULOSE MATERIALS: LIGHTWEIGHT XEROCELLULOSE

Georg Pour[1], Arnaud Rigacci[2] and Tatiana Budtova[1]

1 - Center for Material Forming (CEMEF)[2], Mines ParisTech, UMR CNRS 7635
1, Rue Claude Daunesse, BP 207, 06 904 Sophia Antipolis Cedex, France
2 - Centre for Energy and Processes (CEP), Mines ParisTech,
1, Rue Claude Daunesse, BP 207, 06 904 Sophia Antipolis Cedex, France

INTRODUCTION

Nowadays the urge to find and create new alternatives for sustainable utilisation and use of renewable materials is greater than ever. In view of these circumstances cellulose, as renewable resource, is considered a promising material which could help to provide a possible solution for this quest we are facing momentarily. The development of novel cellulosic materials with high added value is thus of great interest.

Aerocellulose, an aerogel-like highly porous and ultra-light cellulose, is a new material recently developed in our laboratory[1,2]. Aerocellulose density is around 0.05-0.2 g/cm^3, with pore sizes varying from a few nanometres to a few microns and rather high specific surface of 200-300 m^2/g. It is prepared via cellulose dissolution followed by coagulation and drying with supercritical CO_2. Drying under supercritical conditions is needed to minimize pore collapse and cellulose densification. Potential Aerocellulose applications can vary from biomedical, pharmaceutical and cosmetics to thermal insulation and electrochemical (when pyrolysed)[3]. However, for some applications cellulose hydrophilicity may cause serious problems. Additionally, the process of drying via supercritical CO_2, even if very efficient, is rather time consuming, necessitates quite huge investment and could also present difficulties in terms of large scale utilisation if, for example, some continuous production of monolithic materials is required.

Within this paper we are introducing a brand new form of highly porous cellulose, so-called Xerocellulose, made from hydrophobically modified cellulose. Associated functionnalization allows drying under ambient pressure at room temperature without sample high contraction and thus avoiding drying in supercritical conditions. Furthermore, due to hydrophobisation, we were also able to reduce water vapours adsorption capacity significantly. The route of cellulose ambient-dried preparation and the influence of cellulose concentration and of degree of substitution (DS) on Xerocellulose density, morphology and water adsorption capacity will be presented and discussed.

MATERIAL AND METHODS

For the modification of the cellulose we have chosen microcrystalline cellulose Avicel® purchased from Sigma Aldrich (France) and used it without further purification. Solvents N, N-dimethylacetamide (DMAc), methanol (MeOH) and dimethylformamide (DMF) used for the reaction were purchased from Fisher Scientific whereas the reagents tritylchloride and LiCl were from Acros Organics and used without further purification. The cellulose dried in an oven at 80°C and solvents were dried with molecular sieves (3Å) over three days prior to the synthesis.

Cellulose modification is schematically presented in Figure 1: tritylchloride reacted with OH groups of the polysaccharide according to ref.4. The reaction was performed in LiCl/N,N-Dimethylacetamide. The reaction mixture of Avicel®, solvent and tritylchloride was stirred for 48h at elevated temperatures. The obtained modified cellulose was then dissolved in DMF and coagulated in methanol, washed in methanol and dried by evaporation at 40°C under primary

---

[2] Member of the European Polysaccharide Network of Excellence (EPNOE), www.epnoe.eu

vacuum . The most probable OH group which reacts with the tritylchloride is the hydroxyl group at carbon 6 of the anhydroglucose unit (Figure 1) because it is less sterically hindered in comparison with the other hydroxyl groups which enables the bulky tritylchloride to easily attack on this side. Additionally the choice of solvent is known to have an effect of the stereoselectivity[4].

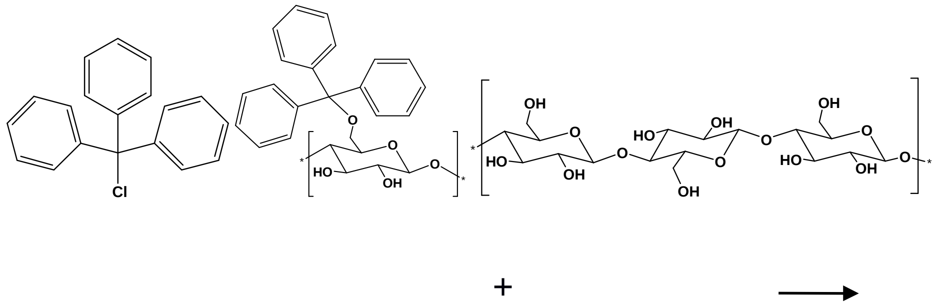

Figure 1: Reaction scheme of cellulose with tritylchloride according to ref.4

The Xerocellulose was prepared from dissolving modified cellulose in DMF, coagulation in the same anti-solvent (methanol) and further washing in ethanol. The samples were dried at room temperature under ambient conditions within two days.

IR spectroscopy was used to analyse the samples prepared in order to prove cellulose derivatisation. Xerocellulose morphology was studied by SEM (Zeiss supra 40 equipped with a Gemini® column). Apparent density was measured by accurately measuring sample dimensions and weight.

RESULTS

IR spectra of the initial (non-modified microcrystalline cellulose) and of two samples of modified cellulose with different degrees of substitution were performed. We could distinguish the spectra of the samples in respect to their different DS. The OH band decreased significantly and showed different intensity as well as new arising peaks for the aromatic functionalities appeared also varying in intensity due to different DS.

We obtained Xerocellulose samples with an increased hydrophobicity but at the same time maintaining low density properties like conventional Aerocellulose, within 0.2 – 0.3 g/cm^3. Xerocellulose morphology was significantly different in comparison to conventional cellulose. The Aerocellulose structure was more a fibre-like structure whereas the tritylcellulose network was formed by bigger “rose-shape” subunits which form a continuous porous network but more fragile and less flexible.

Via SEM we could also observe the difference in morphology of the samples in respect to their DS. Xerocellulose density strongly depends on the degree of substitution.

CONCLUSIONS

Using cellulose hydrophobisation in homogeneous conditions, we obtained brand new ambient-dried and lightweight cellulose so-called Xerocelluloses. Xerocellulose was made via dissolution-coagulation and evaporative drying in ambient conditions. This approach opens promising ways in making novel high-added-value hydrophobic cellulosic aerogel-like materials. For future big-scale applications avoiding drying super critically with CO_2 this could present an interesting alternative of producing light-weight porous cellulose material via a continuous processing route.

ACKNOWLEDGEMENT

The research leading to these results has received funding from the European Union Seventh Framework Programme (FP7/2007-2013) under grant agreement n° 260141 (AEROCOINS project).

REFERENCES

[1] Gavillon, R.; Budtova, T, *Biomacromolecules*, 2008, 9, 269-277.
[2] Sescousse, R.; Gavillon, R.; Budtova, T., *Carbohydrate Polymers*, 2011, 83, 1766-1774.
[3] Guilminot E., Gavillon R.,Chatenet M., Berthon-Fabry S, Rigacci A, Budtova T., *Journal of Power Sources*, 2008, 185, 717–726
[4] Camacho Gomez J.A., Erler U.W., Klemm D.O.; *Macromol. Chem. Phys.*, 1996, 197, 953

P02

FLEXIBLE PROCEDURE FOR THE PREPARATION OF ION-EXCHANGE METAL-DOPED CARBON AEROGELS

Kristiina Kreek[a]*

[a] Institute of Chemistry, Tallinn University of Technology, Akadeemia tee 15, Tallinn 12618, Estonia

E-mail: kristiina0005@gmail.com; Fax: +372 620 28 28

A method for preparing ion-exchange metal-doped carbon aerogels from 5-methylresorcinol (MR), 2,6-dihydroxy-4-methylbenzoic acid (dHMBA), which has an ion-exchange moiety and formaldehyde was developed. The aerogels doped with nickel, cobalt and copper were characterized by atom absorption spectroscopy, nitrogen adsorption analysis, transmission electron microscopy and X-ray diffraction.

Carbon aerogels exhibited high surface areas and pore volumes, which increased with the incorporation of metal species into the aerogels. The metal content in organic aerogels was found to be dependent on the MR/dHMBA molar ratio and was between 2.1-7.4 %, increasing with the increase of dHMBA content. The metal content in the prepared carbon aerogels was found to be up to 14.5%. Carbon aerogels contained metal nanoparticles and the size of nanoparticles was found to be dependent on the amount of dHMBA used during preparation.

We demonstrate that our method is suitable for preparing metal-doped carbon aerogels and that the proposed approach enables to control the metal content in aerogels and the size of nanoparticles in carbon aerogels.

INTRODUCTION

Carbon aerogels (CA) are obtained by the carbonization of organic aerogels (OA), which are prepared by drying a gel made through sol-gel polymerization. Due to their properties, such as low density, continuous porosity, high surface area and electrical conductivity, carbon aerogels are promising materials for several applications like catalyst support, adsorbent and electrode materials for supercapacitors [1-5]. Carbon aerogels are modified with metals in order to alter their structure and further expand their potential applications. Many researches, dealing with different methods used for metal doping, have been published [6-11]. Among those methods is the ion-exchange method developed by Baumann *et al.*, which involves the use of a compond for gel preparation that has an ion-exchange moiety capable of binding metal ions [11-19].

The goal of this work was to develop a method for preparing metal-doped aerogels by using precursors 5-methylresorcinol (MR) and 2,6-dihydroxy-4-methylbenzoic acid (dHMBA), which are by-products of the local oil-shale processing industry and have been previously studied for aerogel preparation [20-22]. The preparation of metal-doped aerogels was based on the ion-exchange method. The properties of the materials obtained will be analysed.

MATERIALS AND METHODS

Sample preparation

Metal-doped carbon aerogels were prepared similarly to those in the method described by Baumann [11]. The gels were prepared by adding dHMBA and 5-MR (molar ratios were the following: MR/dHMBA = 1, 3 or 9) to the solvent (70% acetonitrile and 30% distilled water). The molar ratio of the solvent (SOLV) to aromatic monomers (dHMBA and MR) was 35. Sodium acetate (SA) was added (dHMBA/SA = 1) and the mixture was stirred. After waiting 0.5 h, to allow all the acid to neutralize, formaldehyde (F) was added. The molar ratio of aromatic monomers (AM) to formaldehyde was 0.5. Finally sodium acetate was added as a catalyst (C) at a molar ratio of AM/C = 50.

Glass molds containing the solutions were sealed and the mixture was allowed to gel and cure at 40 °C for 7 days. The Na^+-doped gels obtained were orange and transparent. The gels were then soaked for 3 days in 0.1 M aqueous solutions of $CuCl_2$, $Co(NO_3)_2 \cdot 6H_2O$ and $Ni(NO_3)_2 \cdot 6H_2O$, respectively. Each time the solution was renewed after 24 h. After that the gels were washed by soaking them in water for 24 h, followed by solvent exchange with acetone which lasted 4 to 5 days. Acetone was changed after every 24 h.

The gels were dried with supercritical CO_2. The conditions used for drying were the following: the gel was introduced to liquid CO_2 at 200 bars and 25 ºC for 20 min, to fill the pores of the gel with liquid CO_2 and to mix it with acetone. The exit valve of the autoclave was then opened and the pressure inside the autoclave reduced to 100 bars, allowing the liquid CO_2 to flow through the gel at 100 bars and 25 ºC for 2 h in order to fill all the pores with liquid CO_2. Then the temperature was raised to 45 ºC to carry out supercritical extraction for 2 h, after which the autoclave was slowly depressurized to atmospheric pressure and then the temperature lowered to ambient temperature. Carbonization was performed in N_2 atmosphere by raising the temperature to 700 °C (2.5°C/min), from then on to 900 °C (5 °C/min) and was kept at that temperature for 1 h.

Characterization

The bulk densities of carbon aerogels were calculated by measuring the dimensions and mass of each monolithic sample. Elemental analyses were performed by a Spectra AA 220F flame atomic absorption spectrometer (AAS). Nitrogen adsorption analyses were performed using a Sorptometer KELVIN 1042 built by Costech International. Helium was used as a carrier gas, nitrogen as an adsorptive gas. Nitrogen adsorption data was taken at relative pressures from 0 to 1 and at liquid nitrogen temperature. The specific surface area (S_{BET}) was calculated according to the Brunauer-Emmet-Teller theory. The X-ray diffraction (XRD) pattern was recorded with a Rigaku Ultima IV diffractometer, using a line detector DtexUltra. Cu-K_α radiation was used with an Ni filter for removing K_β radiation. The recorded diffractograms were analysed by Rigaku PDXL software. Energy-filtered transmission electron microscopy (TEM) was carried out with Leo 912 Omega microscope at 120 kV, using a LaB_6 gun.

RESULTS AND DISCUSSION

In this work, a mixture of two aromatic monomers, along with formaldehyde, was used for aerogel preparation. Since out of the two aromatic monomers only dHMBA has an ion-exchange moiety (a carboxylic group) which binds metal ions, then the possibility of being able to vary the metal content in aerogels by changing the MR/dHMBA molar ratio was studied.

Figure 1 shows the copper content in organic aerogels prepared at different MR/dHMBA molar ratios. The molar ratio is expressed by the percent of dHMBA moles out of the moles of aromatic monomers (MR and dHMBA). It can be seen that with increasing the dHMBA percentage in organic aerogels, the copper content grows almost linearly. The theoretical content of copper in aerogels was calculated for comparison, according to the equation (1).

$$Cu\%_{theoretical} = \frac{m_{Cu}}{m_{MR} + m_{dHMBA} + m_{FA} + m_{Cu}} \times 100\% \qquad (1)$$

$$m_{Cu} = \frac{1}{2} \times \frac{m_{dHMBA}}{M_{dHMBA}} \times M_{Cu} \qquad (2)$$

M stands for the molar mass and m is the mass. While calculating the mass of copper present in the sample (equation (2)), it was assumed that two ions of sodium will be changed to one ion of copper during the ion-exchange process.

The experimentally found copper contents in aerogels are very similar to those calculated, but only a little higher. This could be due to some of the ions having been adsorbed on to the surface of the gel and not being washed out later with water or acetone. It could also be that the calculated total mass of aerogels was affected by other compounds that were present, but not included in the calculation or that the total mass of aerogels should have been smaller due to the formation of water during polymerization, which was later removed during solvent-exchange and therefore the total mass of aerogels was reduced by that amount.

The metal contents of carbon aerogels doped with Ni, Cu and Co are shown in Table 1. In the case of the aerogel prepared at molar ratio of MR/dHMBA=1, the copper content of both the organic and carbon aerogel was determined with AAS and was 7.4% and 14.5%, respectively. As expected, the copper content of the carbon aerogel was higher, due to the burnout of organic material during carbonization.

Table 1 also shows the densities and nitrogen adsorption analysis results for prepared aerogels. The densities of metal-doped organic aerogels were in the range of 0.48-0.66 g/cm^3 and those of carbon aerogels 0.98-1.23 g/cm^3, which is quite high compared to the aerogels prepared from 2,4-dihydroxybenzoic acid (dHBA) according to the ion-exchange method [14]. A possible explanation is that in our case we used higher solids content to prepare aerogels, which is known to cause higher densities for aerogels [23].

Nitrogen adsorption analysis results show that the surface areas and pore volumes of Ni, Co and Cu doped carbon aerogels are larger than those of the respective Na containing sample. Doping with the three transition metals used in this work therefore enabled to increase the surface area and pore volume of aerogels.

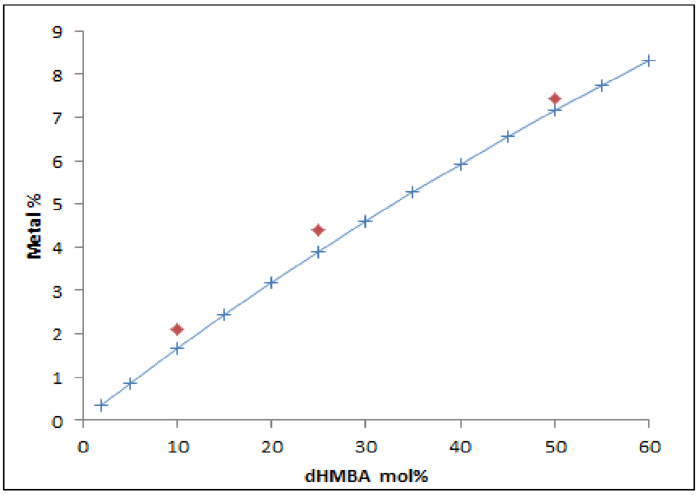

Figure 1. Copper content in organic aerogels prepared at different MR/dHMBA molar ratios. MR/dHMBA molar ratios are expressed by the percent of dHMBA moles out of the moles of AM (MR and dHMBA together). Symbols: lozenges – experimentally determined copper content; crosses (connected with lines) – calculated maximum copper content.

Table 1

Sample	OA, δ (g/cm^3)	CA, δ(g/cm^3)	S_{BET} (m^2/g)	V_{TOT} (mm^3/g)	metal (%)
Na	0,62	0,83	286	429	---
Ni	0,63	1,23	379	446	11
Cu	0,48	0,98	464	607	14,5
Co	0,66	1,10	519	610	10,7

The name of the sample shows the metal it contains. All the samples were prepared at a molar ratio of MR/dHMBA=1. OA is organic aerogel, CA is carbon aerogel. δ is the calculated density, S_{BET} is the BET surface area of carbon aerogel, V_{TOT} is the total pore volume of carbon aerogel and metal (%) is the percent of metal in the carbon aerogel.

X-ray diffraction pattern for a copper-doped carbon aerogel is shown in Figure 2. It can be seen that peaks corresponding to copper are present, therefore it can be concluded that copper ions must have reduced during carbonization. A peak corresponding to copper(I)oxide is also present, which could be due to either incomplete reduction of copper ions during carbonization or that some of the copper later oxidized.

.

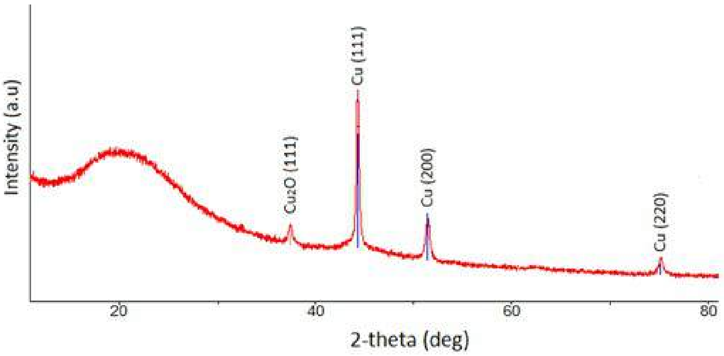

Figure 2. X-ray diffractogram of a copper-doped carbon aerogel prepared at a molar ratio of MR/dHMBA=1.

TEM pictures of copper-doped carbon aerogels are shown in Figure 3. The organic aerogel, which was soaked in a copper salt solution before drying, is depicted in Figure 3a. Copper nanoparticles cannot be seen in this case. When the same aerogel is carbonized then copper nanoparticles emerge (Figure 3b). Similar results for the aerogels prepared from dHBA have been reported earlier [11]. Figure 3c shows a carbon aerogel prepared at a smaller percentage of dHMBA present (the molar ratio of MR/dHMBA is higher). Since for that aerogel the metal content is lower, then the expected size of nanoparticles should also be smaller. This has been observed before by Baumann *et al.* [11]. Indeed, the diameters of nanoparticles were in the range of 5-60 nm, while in Figure 3b the estimated sizes were 5-130 nm. Besides having nanoparticles with larger diameters, the nanoparticles had also clustered together in the case of the aerogel prepared at a lower molar ratio of MR/dHMBA.

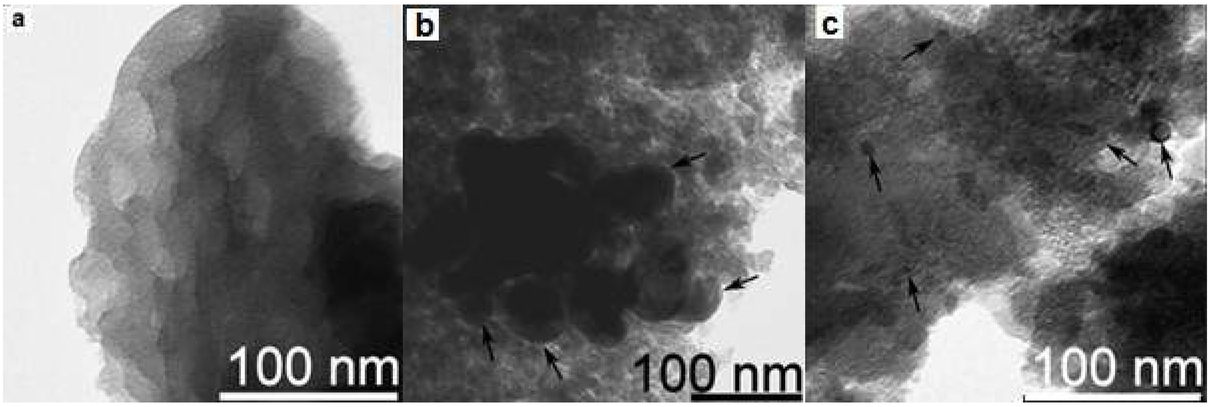

Figure 3. TEM pictures of metal doped aerogels. a - Cu-doped organic aerogel, MR/dHMBA=1; b - Cu-doped carbon aerogel, MR/dHMBA=1; c - Cu-doped carbon aerogel, MR/dHMBA=3.

CONCLUSION

With the use of 5-methylresorcinol (MR), 2,6-dihydroxy-4-methylbenzoic acid (dHMBA) and formaldehyde as monomers, ion-exchange metal-doped carbon aerogels were prepared and characterized. The doping of materials with Ni, Co and Cu resulted in carbon aerogels with higher surface areas and pore volumes than those of the respective Na doped sample. The specific surface areas of metal-doped carbon aerogels ranged from 380 to 520 m^2/g and pore volumes from 450 to 610 mm^3/g. Changing the molar ratio between MR and dHMBA enabled preparation of organic aerogels with copper content ranging from 2.1 to 7.4 %. The metal content of metal-doped carbon aerogels was up to 14.5 %. Carbon aerogels contained metal nanoparticles and their sizes also depended on the molar ratio of MR/dHMBA due to the influence of the latter on the metal content of aerogels.

ACKNOWLEDGEMENTS

The author would like to thank Mihkel Koel for support and advice throughout the research, Maria Kulp for performing elemental analyses, Mai Uibo for N_2-adsorption analyses, Arvo Mere for X-ray diffraction analyses and Krisztian Kordas for TEM pictures.

REFERENCES

[1] PEKALA, R. W., Journal of Materials Science., Vol. 24, **1989**, p. 3221

[2] TAMON, H., ISHIZAKA, H., MIKAMI, M., OKAZAKI, M., Carbon, Vol. 35, **1997**, p. 791

[3] PEKALA, R. W., FARMER, J. C., ALVISO, C. T., TRAN, T. D., MAYER, S. T., MILLER, J. M., DUNN, B., Journal of Non-Crystalline Solids, Vol. 225, **1998**, p. 74

[4] MORENO-CASTILLA, C., MALDONADO-HODAR, F. J., Carbon, Vol. 43, **2005**, p. 455

[5] MEENA, A. K., MISHRA, G. K., RAI, P. K., RAJAGOPAL, C., NAGAR, P. N., Journal of Hazardous Materials, Vol. 122, **2005**, p. 161

[6] MORENO-CASTILLA, C., MALDONADO-HODAR, F. J., RIVERA-UTRILLA, J., RODRIGUEZ-CASTELLON, E., Appied Catalysis A-General, Vol. 183, **1999**, p. 345

[7] MALDONADO-HODAR, F. J., FERRO-GARCIA, M. A., RIVERA-UTRILLA, J., MORENO-CASTILLA, C., Carbon, Vol. 37, **1999**, p. 1199

[8] BEKYAROVA, E., KANEKO, K., Advanced Materials., Vol. 12, **2000**, p. 1625

[9] BEKYAROVA, E., KANEKO, K., Langmuir, Vol. 15, **1999**, p. 7119

[10] MILLER, J. M., DUNN, B., Langmuir, Vol. 15, **1999**, p. 799

[11] BAUMANN, T. F., FOX, G. A., SATCHER, J. H., YOSHIZAWA, N., FU, R. W., DRESSELHAUS, M. S., Langmuir, Vol. 18, **2002**, p. 7073

[12] FU, R. W., BAUMANN, T. F., CRONIN, S., DRESSELHAUS, G., DRESSELHAUS, M. S., SATCHER, J. H., Langmuir, Vol. 21, **2005**, p. 2647

[13] STEINER, S. A., BAUMANN, T. F., KONG, J., SATCHER, J. H., DRESSELHAUS, M. S., Langmuir, Vol. 23, **2007**, p. 5161

[14] COTET, L. C., GICH, M., ROIG, A., POPESCU, I. C., COSOVEANU. V., MOLINS, E., DANCIU, V., Journal of Non-Crystalline Solids, Vol. 352, **2006**, p. 2772

[15] MARIE, J., BERTHON-FABRY, S., ACHARD, P., CHATENET, M., PRADOURAT, A., CHAINET, E., Journal of Non-Crystalline Solids, Vol. 350, **2004**, p. 88

[16] MARTINEZ, S., VALLRIBERA, A., COTET, C. L., POPOVICI, M., MARTIN, L., ROIG, A., MORENO-MANAS, M., MOLINS, E., New Journal of Chemistry., Vol. 29, **2005**, p. 1342

[17] CARROTT, P. J. M., MARQUES, L. M., RIBEIRO CARROTT, M. M. L., Microporous and Mesoporous Materials, Vol. 131, **2010**, p. 75

[18] MARQUES, L. M., CONCEICAO, F. L., CARROTT, M. M. L. R., CARROTT, P. J. M., Fuel Processing Technology, Vol. 92, **2011**, p. 229

[19] CARROTT, P. J. M., MARQUES, L. M., CARROTT, M. M. L. R., Microporous and Mesoporous Materials, Vol. 158, **2012**, p. 170

[20] PEREZ-CABALLERO, F., PEIKOLAINEN, A.-L., UIBU, M., KUUSIK, R., VOLOBUJEVA, O., KOEL, M., Microporous and Mesoporous Materials, Vol. 108, **2008**, p. 230

[21] PEIKOLAINEN, A.-L., PEREZ-CABALLERO, F., KOEL, M., Oil Shale, Vol. 25, **2008**, p. 348

[22] PEIKOLAINEN, A.-L, VOLOBUJEVA, O., AAV, R., UIBU, M., KOEL, M., Journal of Porous Materials, Vol. 19, **2012**, p. 230

[23] AL-MUHTASEB, S. A., RITTER, J. A., Advanced Materials, Vol. 15, **2003**, p. 101

P03

FLEXIBLE RF AND CARBON AEROGELS

Marina Schwan, Lorenz Ratke
Institut für Materialphysik im Weltraum, DLR Köln, 51170 Köln, Germany
Marina.Schwan@dlr.de

ABSTRACT

Organic resorcinol - formaldehyde (RF) aerogels dried under ambient conditions with a large resorcinol (R) to catalyst (C) ratio are usually hard and brittle with strength about 100 kPa and Young's-moduli in the range of 1-2 MPa. Their densities are in the range of 0.2 to 0.4 g/cm^3. We observe that under special conditions of aerogel preparation yield surprisingly flexible aerogels. They can be bent easily, similar to the well-known flexible silica aerogels. They have a low density about 0.06 g/cm^3, a very low elastic modulus of around 70 kPa and are elastically deformable by more than 40% in an almost reversible manner. The thermal conductivity of these aerogels is around 0.046 W/(mK). The flexible RF-aerogel shows a continuous network of particles with sizes of around 1 µm and pores of about 10 µm. Carbonization of the flexible RF aerogels leads to flexible carbon aerogel pieces.
This paper discusses the effect of resorcinol-water (R/W) molar ratio on the mechanical properties, pore structure and bulk density of flexible RF aerogels.

INTRODUCTION

Resorcinol-formaldehyde aerogels, first reported by Pekala [1], are organic aerogels which are synthesized by polycondensation of resorcinol with formaldehyde, building particles which form a three-dimensional network – a RF hydrogel is formed. Usually such a gel is dried supercritically with an organic solvent which is used to exchange the aqueous solution leading to low volume shrinkage, low bulk density and high surface area.
Various articles have reported the effects of pH [2], R/F, R/W molar ratios, concentration and type of catalyst [3], the drying routine [4] and the physical and chemical properties of the resulting RF aerogel [5]. To the best of our knowledge there is no report in the literature on the RF aerogels being flexible and not brittle.
The present paper describes a procedure to synthesize a flexible RF aerogel. In summary a high dilution of the components in the initial solution, a low R/C molar ratio and subcritical drying

results in a porous structure shown in Fig. 1, which astonishingly allows for an easy bending and compression: this aerogel is flexible.

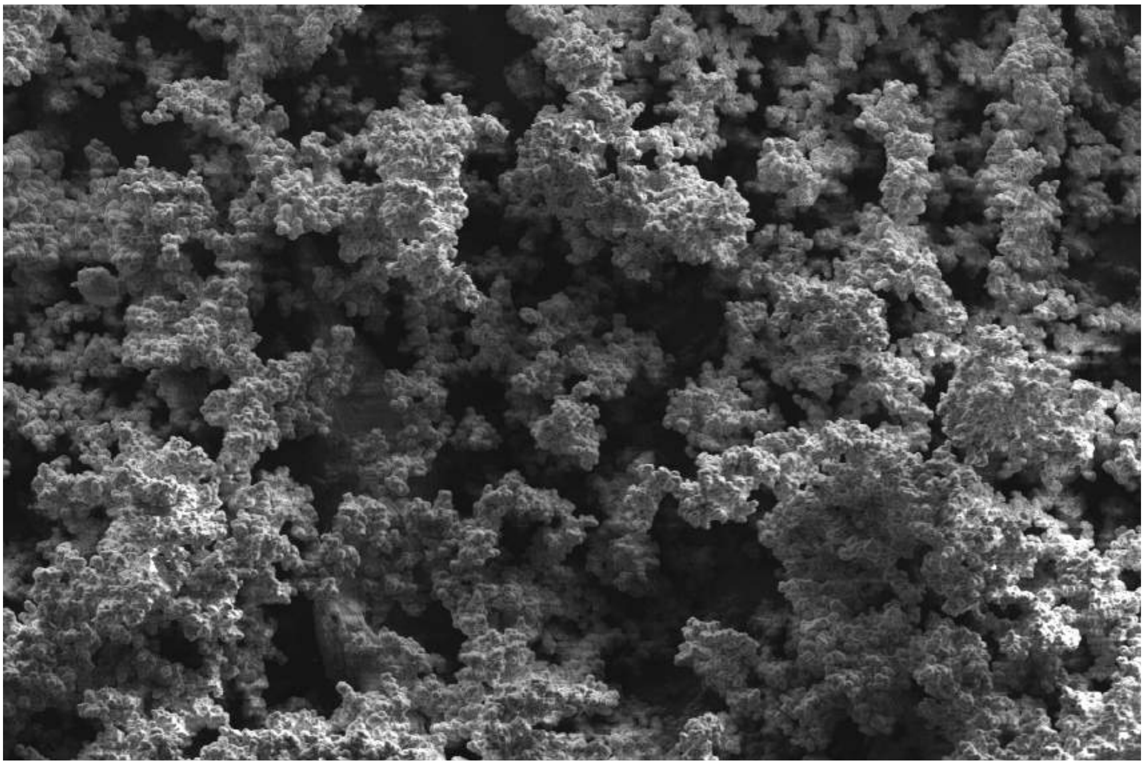

Figure 1: SEM pictures of a flexible RF aerogel

EXPERIMENTAL PROCEDURES

Materials and synthesis

The flexible RF aerogels have been produced by using resorcinol (R), formaldehyde (37% in water, stabilized with 10% methanol) (F), sodium carbonate (C) and nitric acid (2M). The gel solution was prepared from deionized water (W).

The resorcinol was dissolved in deionized water. The molar ratio R/W was varied in the range 0.005 to 0.013. After complete dissolution of resorcinol, formaldehyde was added to solution. The R/F molar ratio was fixed at 1:2. The solution was stirred and then sodium carbonate was added. The molar ratio R/C is 50:1. The gelation does not occur with R/C higher than 50. After further stirring the pH was adjusted in the range 5.4-5.6 with nitric acid. The solution was stirred, the container sealed and placed in an oven at 80°C for one week.

After 7 days the gelled solution changed its color from transparent to orange or orange brown. It was replaced from the oven and cooled to room temperature. The gel was washed 3 days with acetone and not dried supercritically but in an oven at 80°C. After 24h, the dry gel became orange – brown and flexible. Performing the transformation from a solution to a gel at a lower temperature, say 40°C, led to gels with a shrinkage of 40-50%. The material gelled at 80°C did not show measurable shrinkage. The dried gel was pyrolysed at 1000°C for 1 hour. The pyrolysed RF aerogel, called carbon aerogel, is also flexible but more brittle than RF-aerogel.

Characterization

Scanning electron micrographs (from Merlin, Zeiss) were used to determine the pore and particle size and also to study the structure of aerogels. The RF-samples were sputtered 45 sec with gold before imaging. The bulk densities were calculated by their mass to volume ratio. The thermal conductivity was determined by using HotDisk ™. The Young's modulus was determined in uniaxial compression tests with a Chatillon TCD200-SS Ametek machine. In this test cylindrical samples of 15-25 mm height were compressed up to 50% of their original height with a small piston (diameter 1mm). After some time the height was measured again and compared with the original height. The change in height versus load was plotted.

RESULTS AND DISCUSSION

Effect of R/W molar ratio on the mechanical properties and pore structure

The resorcinol/water molar ratio was studied in the range 0.005-0.013. For R/W 0.006-0.01 no shrinkage was observed, above and below this range the shrinkage is about 40-50%.

A high dilution of the initial solution (R/W=0.005) leads to non-flexible, compact aerogels with the bulk density of 0.35 g/cm^3, while the density of the aerogel with R/W = 0.006-0.01 is about 0.06-0.09 g/cm^3. The RF aerogels produced with R/W molar ratio 0.011-0.013 are corky with the bulk density 0.18-0.22 g/cm^3. The result is shown in the Fig. 2. The attributes "brittle", "flexible" and "corky" are used here from their haptic impression the aerogels make while handling.

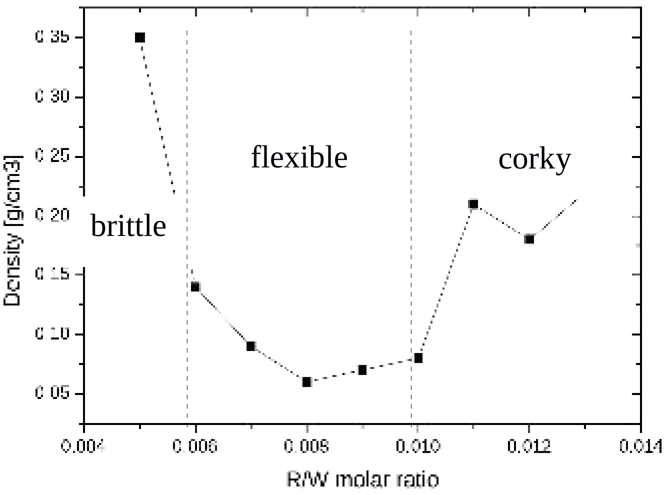

Figure 2: Effect of R/W molar ratio on the bulk density

The microstructure as seen with the SEM shows clear differences. The aerogels which are produced with R/W molar ratio 0.005 which are non-flexible show a nanostructure with particles about 50 nm and pores around 200 nm (Fig. 3a). The flexible aerogels with R/W molar ratio 0.007-0.009 show a coarse structure, with big particles around 1-2 µm. In addition, flexible aerogels have pores of about 5-20 µm, as showed in Figs. 3b-d. The corky aerogels with R/W molar ratio 0.011-0.013 also show a nanostructure, with small pores about 0.2-1µm (Fig. 3 e-f).

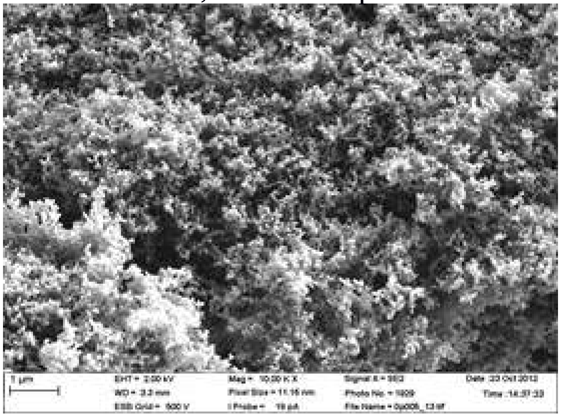

a R/W 0.005

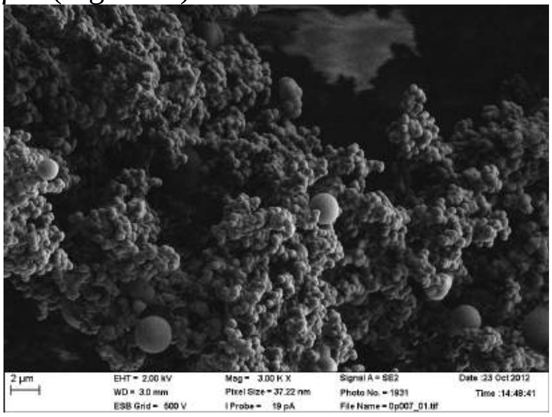

b R/W 0.007

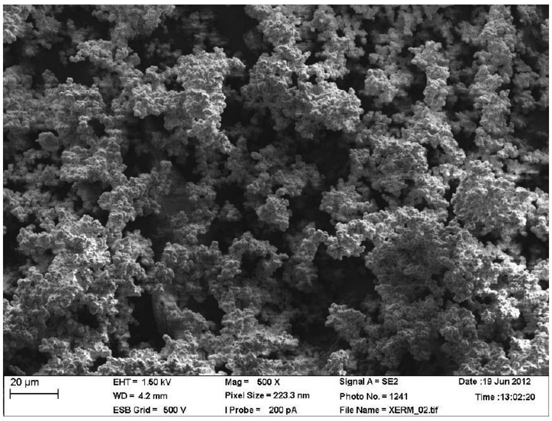

c R/W 0.008

d R/W 0.009

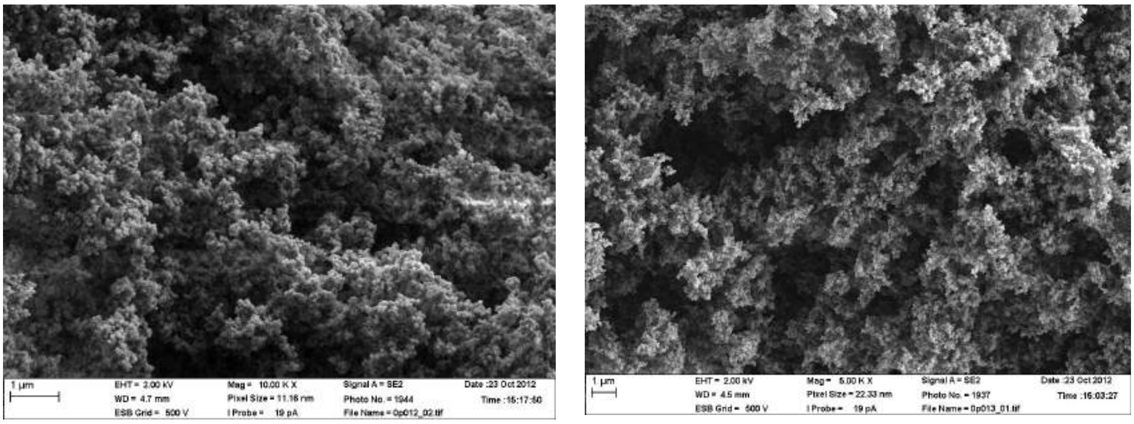

e R/W 0.012

f R/W 0.013

Figure 3: SEM pictures of flexible (b-d) and non-flexible (a, e, f) RF-aerogel produced with different R/W molar ratios

The response of the aerogels to a mechanical load is shown in the Fig. 4. The aerogels produced with R/W molar ratio 0.006-0.01 are flexible: they can be bent and deformed easily and reversibly like rubber. These aerogels endure up to 40% linear compression and then go back to 90% of their original height.

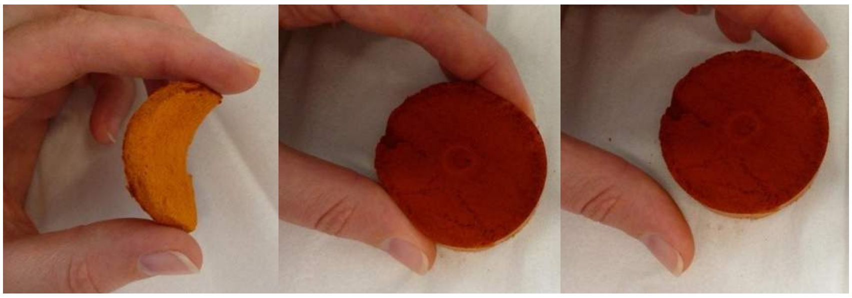

Figure 4: Flexible RF-Aerogele produced with R/W molar ratio 0.006-0.008

A stress-deflection curve typical for flexible RF aerogels (R/W = 0.006-0.01) is shown in Fig. 5a. At the beginning of the compression test the porous structure can be deformed linear elastically. The slop in this range was used to calculate Young's modulus. After a critical stress is reached the structure begins to collapse, cracks occur followed with a certain plateau in which the stress goes up and down. This plateau is an indicator for an elastic-brittle material with open pores [6]. With increased stress the pore walls touch, the densification begins.

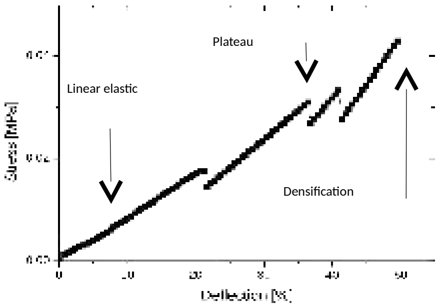

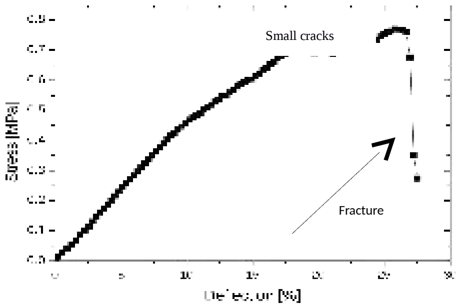

a

)

b)

Figure 5: Stress-deflection curve of (a) flexible RF and (b) non- flexible aerogels

Resorcinol-formaldehyde aerogels produced with R/W molar ratio 0.011-0.013 (Fig. 5b) show another type of stress-deflection curve which are typical for a hard, brittle material. The Fig. 5b shows a long linear elastic range. At a load of 0.45 MPa the slop decreases slightly, the sample begins to deform. The stress increases up to 0.75 MPa interrupted by small cracks at an almost constant average stress level. The sample eventually breaks.

The Young's modulus of resorcinol-formaldehyde aerogels, shown in Fig. 6, is related to R/W molar ratio. It has been observed that the Young's modulus of aerogels which are produced with R/W molar ratio 0.006-0.01 is 70-350 kPa. Outside of this R/W range the Young's modulus increased sharply up to 1300 kPa with R/W smaller than 0.006 and up to 4600 kPa with R/W higher than 0.01.

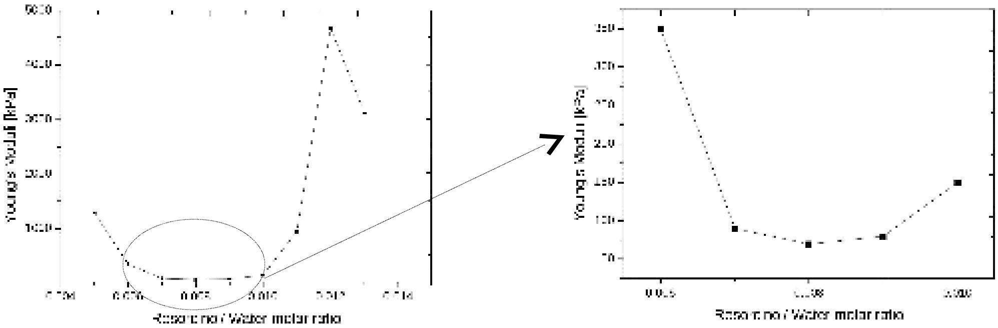

Figure 6: Effect of the Resorcinol/Water molar ratio on the Young's moduli

Keeping this in mind, we produced in the following aerogels without volume shrinkage, low Young's moduli and maximum flexibility, using an R/W molar ratio kept at 0.008.

Effect of pH on the bulk density

Figure 7 illustrates the bulk density at varying pH values. Solutions with an initial pH below 5.0 did no gel. A pH above 5.65 leads to hard, non-flexible RF aerogels with a bulk density 0.38-0.45 g/cm^3. Only in the pH range 5.05-5.65 flexible RF aerogels could be produced. It was observed that samples which were produced with pH 5.05-5.30 shrunk, compared to samples at pH 5.43-5.65 which had no shrinkage. The Fig. 7 shows that the bulk density of flexible aerogel without shrinkage is 0.06-0.09 g/cm^3.

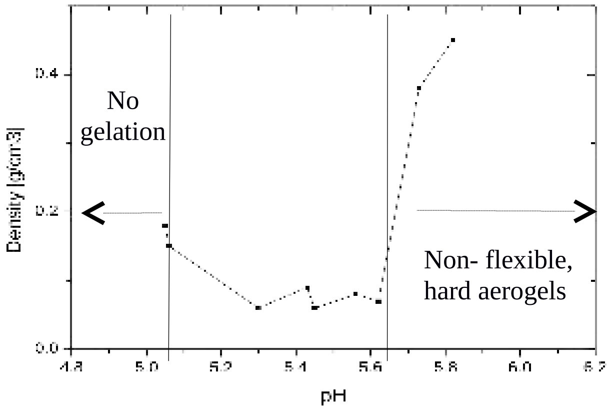

Figure 7: Effect of pH on the bulk density

CONCLUSIONS

It is clear that the water amount, R/C, R/F molar ratios and pH of the initial solution play an important role in synthesis of flexible resorcinol-formaldehyde aerogels. There is only a small window to produce flexible aerogel: R/C = 50, R/F = 0.5, R/W = 0.006-0.010 and pH 5.4-5.6. The flexible aerogels have a coarse structure with big pores, which allow a small movement of the walls in the structure without to destroying it. Resorcinol-formaldehyde aerogels, which are synthesized outside this window, showed no flexibility, high shrinkage and high density.
The central question – what is the origin of the flexibility of the resorcinol-formaldehyde aerogels – is left open. Further investigations to understand the relations between microstructure, process conditions and mechanical behavior are currently going on.

ACKNOWLEDGMENT

The authors gratefully acknowledge support Dr. M. Kolbe from DLR, Cologne for help with the SEM pictures.

REFERENCES

[1] Pekala R.W., J. of Mater. Science, Vol. 24, **1989**, 3221
[2] Lin C., Ritter J.A., Effect of synthesis pH on the structure of carbon xerogels. Carbon Vol. 35, **1997**, 1271
[3] Al Muhtaseb S.A., Ritter J.A. Preparation and properties of resorcinol-formaldehyde organic and carbon gels. Adv Mater., Vol. 15, **2003**,101
[4] Job N., Panariello F. Synthesis optimization of organic xerogels produced from convective air-drying of resorcinol-formaldehyde gels. J. Non-Cryst. Solids, Vol. 352, **2006**, 24
[5] Aegerter M. A., Leventis N., Koebel M. M. Aerogels Handbook, Springer New York, **2011**, 932, 813
[6] Gibson L.J., Ashby M.F., Cellular solids. Structure and properties, Cambridge University Press, Cambridge, UK, **2001**, 214, 509

P04

CITRIC ACID CATALYZED ORGANIC AEROGELS

Barbara Milow[*], Lorenz Ratke, Svenja Ludwig

Institut für Materialphysik im Weltraum, Deutsches Zentrum für Luft- und Raumfahrt (DLR),
51170 Köln, Germany, E-mail: barbara.milow@dlr.de, Fax: +49 2203 61768

Abstract

Organic aerogels based on resorcinol (R) and formaldehyde (F) using citric acid (CA) as a catalyst are synthesized via a sol-gel process and ambient pressure drying at a temperature of 80°C. The influence of the ratio resorcinol to catalyst (R/C) as well as variations of the mole fraction of water at constant ratio of R to F (R/F) on gelation time and the morphology of the monolithic aerogel samples is studied. The molar ratio of resorcinol to formaldehyde is kept at 1:1.3. The molar ratio of resorcinol to catalyst (R/C) is varied between 15 and 1429 and the molar ratio of resorcinol to water (R/W) is between 0.01 and 0.05. The process limits of the RF aerogels are established and the aerogels are characterized with respect to density, particle size and specific surface area.

Keywords:
Aerogel, sol-gel, citric acid, gelation time, ambient drying

1 Introduction

In the last decades a huge number of research papers have been published on the synthesis of so-called RF aerogels invented originally 1989 by Pekala [1]. Just a few papers report about acid-catalyzed RF aerogels [2, 3]. Until now these organic aerogels have a few commercial applications as for instance as a thermal insulation material for package purposes produced by American Aerogel® (Aerocore)[4]. The process of synthesizing organic aerogels is cost intensive compared to silica abased aerogels, mainly due to the comparable expensive resorcinol used. Investigations to reduce theses costs while receiving a product with improved properties are important, since these organic R/F aerogels are a basis for production of carbon aerogels via pyrolysis [5]. There are two major aspects to improve the manufacturing process: Reduction of gelation time and avoidance of supercritical drying.

It is known already for base catalyzed synthesis that the reduction of catalyst content leading to a large ratio R/C allows to substitute supercritical drying by ambient drying [5], however gelation time rises enormously. The use of acids to catalyze the jelling process accelerates the poly-condensation reaction of resorcinol-formaldehyde; it quickens the gelation time more than 15 times. In the literature [2] the effect of acetic acid is described as well as that of hydrochloric acid [3]. We employ in this study citric acid, since it is easy in handling, sustainable, well accepted and solid at room temperature.

2 Experimental procedures

1 Synthesis

The synthesis of the RF aerogels is performed by a sol-gel routine. The chemicals used are resorcinol (≤ 99%), aqueous solutions of formaldehyde (24 wt.-%) stabilized by methanol and citric acid (≤ 99%). They are all purchased from Merck Chemicals and used as received. The water used was deionized.

The solid resorcinol is filled into a beaker and dissolved in water during permanent stirring at room temperature (RT). After the dissolution is optically finished the solution is stirred for additional 15 minutes. Then the formaldehyde and the catalyst are added at once. The solution is stirred for another few minutes until the catalyst is dissolved and the solution is clear. Now the solution is put into closed polyethylene vessels and stored in a heating cabinet at 80 °C until gelation is finished. For drying the vessels are opened after 24 hours and the jelled bodies are kept in its vessels for 24 h at 80 °C. To reach weight stability the aerogels are dried for another 24 h at 40 °C in a vacuum chamber. The aerogels received are of light orange-ocher to dark-red-violet color.

2 Characterization

The pH-value of the synthesis is controlled by a pH-meter from Mettler Toledo. The duration of jelling is measured with a stopwatch. The density is measured using a methodology developed for irregular shaped open porous samples with GeoPyc® 1360 from Micromeritics®. The specific surface area is analyzed by Krypton gas adsorption at 77K using a BET analysis performed in a TriStar II 3020 from Micromeritics®. The microstructure of the samples is viewed with a scanning electron microscope (FE-SEM Merlin® from Zeiss) after coating the aerogels with a nanofilm of gold. The mechanical properties are determined in a compression test using a small scale testing machine (Chatillon TCD 200-SS).

3 Results and discussion

As known from Durairaj [6] the gelation time of the resorcinol-formaldehyde condensation is related to the pH-value. Therefore the control of the synthesis conditions by pH measurements is required. Aqueous solutions of the triprotic citric acid behave in a range of pH between 2.5 and 7.5 as a buffer. Pre-experiments are done to determine the dependence of the concentration of citric acid as a function of pH. In Figure 1 it is shown that in the range of 2.1 to 2.5 the value of pH can properly be adjusted by varying the concentration of the weak organic acid.

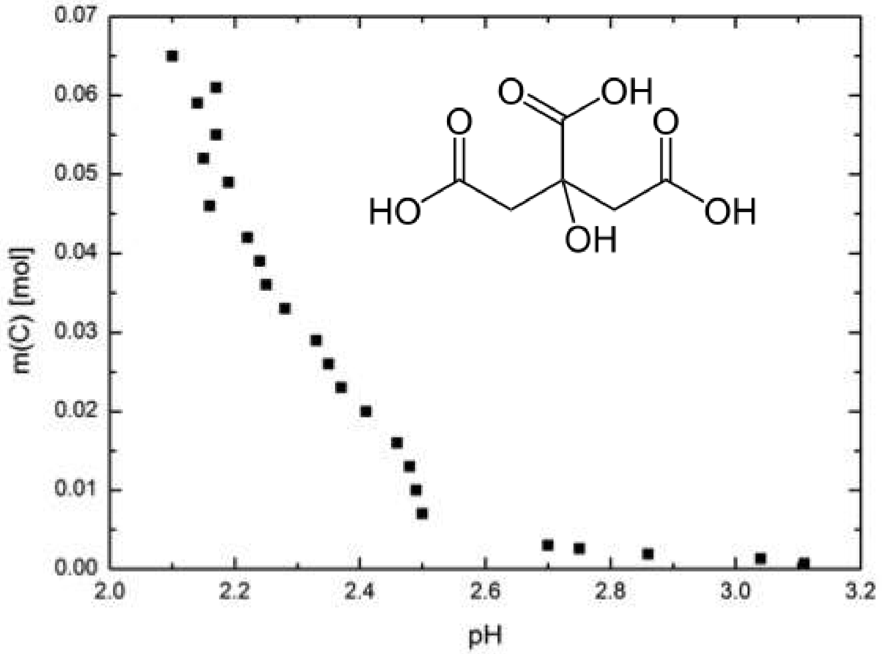

Figure 1: Relation between mole content of citric acid in the solutions and the pH-value.

The measured dependence of the gelation time on the value of pH and on the amount of catalyst used within the synthesis of RF aerogels is shown in Figure 2a and 2b. It fits to the expected results. The lower the catalyst concentration the slower is the sol-gel process with condensation and jelling (crosslinking). The dependence of gelation time on the catalyst concentration is not linear but as shown in Figure 2c using a logarithmic scale, as given by the value of pH, it is linear with a shift around pH 2.48 due to the triprotic nature of citric acid. Gelation does not occur if R/C is higher than 1500.

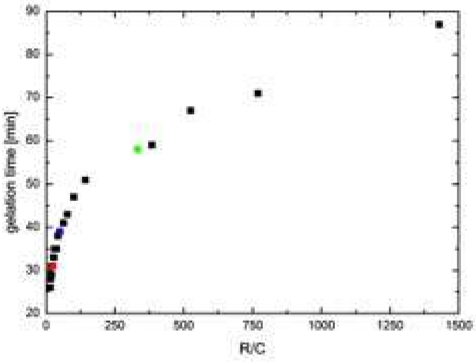

Figure 2a: Gelation time of RF gels in dependence on the R/C value, R/F = 0.77, R/W = 0.037.

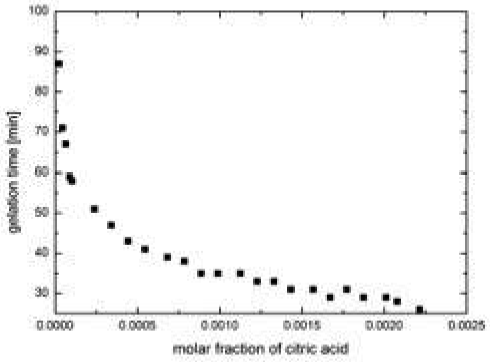

Figure 2b: Gelation time of RF gels in dependence on the mole fraction of citric acid, R/F = 0.77,

(Red square: sample A; blue square: sample B; green R/W = 0.037.
square: sample C, s. Table 1).

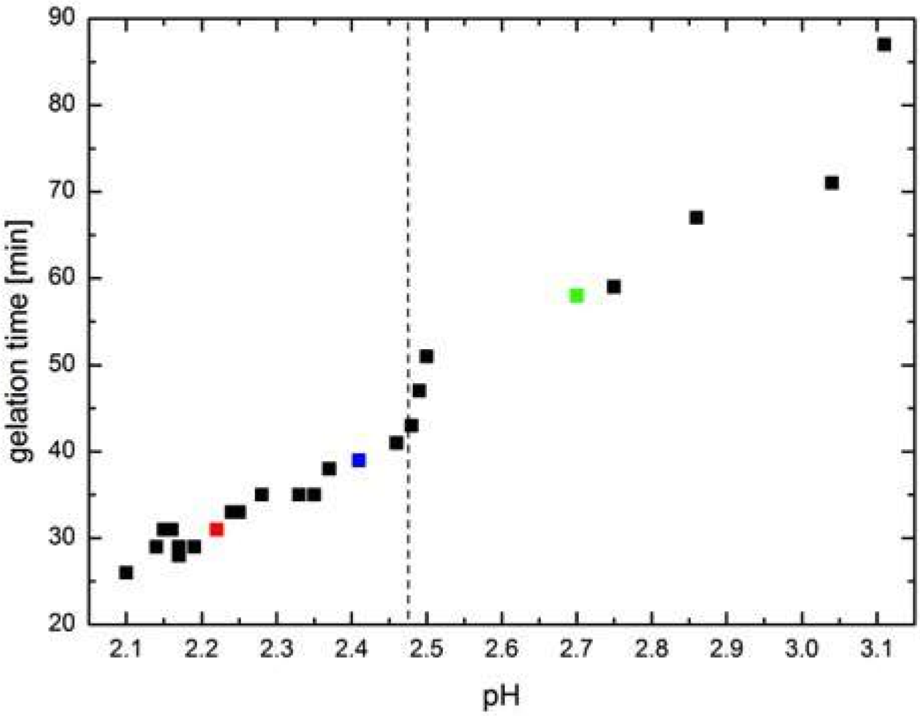

Figure 2c: Gelation time of RF gels in dependence of the value of pH, R/F = 0.77, R/W = 0.037.
(Red square: sample A, blue square: sample B, green square: sample C, s. Tab. 1).

Table 1: Selection of samples with catalyst concentration varied at constant R/F = 0.77 and R/W = 0.037.

sample	R/C	pH	Mole fraction of water	Mole fraction of citric acid	time of gelation [min]
A (🟥)	24	2.70	0.9202	1.43 E-03	31
B (🟦)	50	2.41	0.9209	6.82 E-04	39
C (🟩)	333	2.22	0.9214	1.02 E-04	58

To facilitate the comparison of the properties the mole fraction of water and citric acid are evaluated following equation 1:

(Eq. 1)

(Eq. 2)

In addition to the studies of the citric acid concentration a huge number of samples are synthesized to define the upper limit of dilution. Above 86 wt.-% of water jelling does not occur; the maximum porosity is consistent with a value of 86 %. The influence of the mole fraction of water on the gelation time is parabolic as shown in Figure 3.

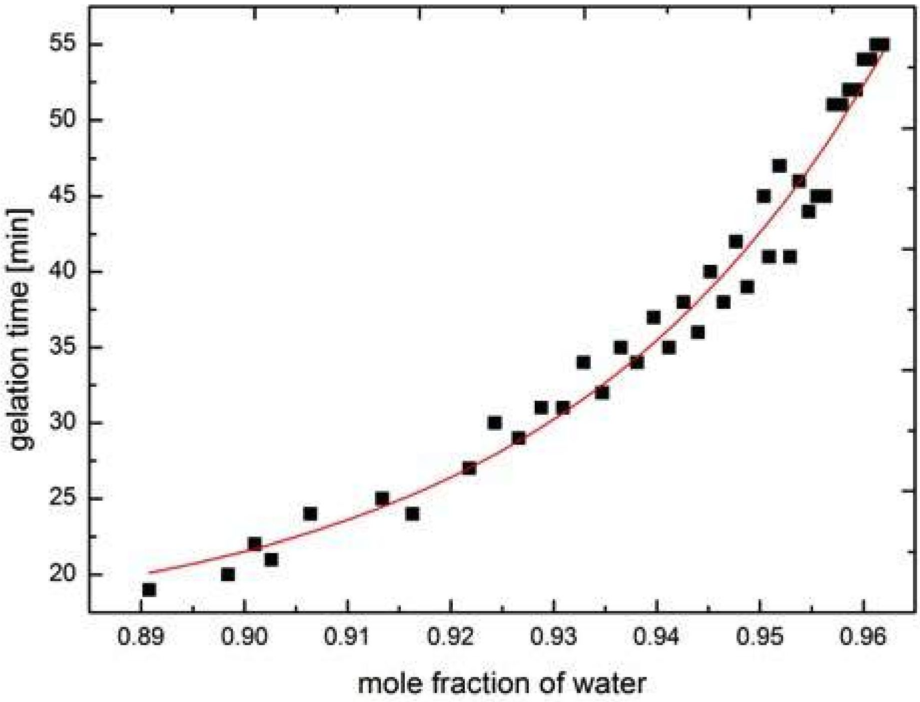

Figure 3: Gelation time of RF gels in dependence of the mole fraction of water, R/F = 0.77, R/C = 0.037.

The volume shrinkage during ambient drying at 80°C is calculated for a number of samples prepared with constant R/F and R/W by varying the amount of catalyst. The measured shrinkage in dependence of pH or mole fraction of citric acid can be described as a parabolic curve, shown in Figure 5a and 5b. The sample with 0.0013, pH = 2.28 (s. Figure 5: turquois quadrate) is neglected. The maximum volume shrinkage is between 25 and 29 %.

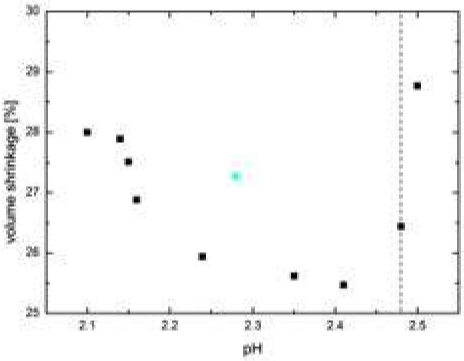

Figure 5a: Volume shrinkage in dependence of pH.

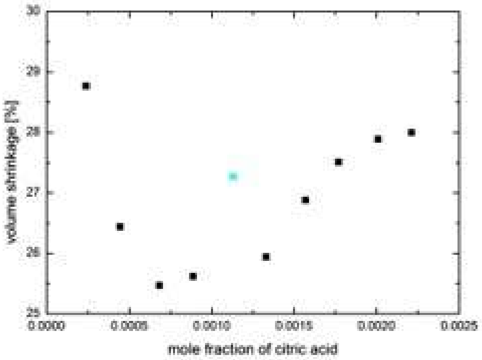

Figure 5b: Volume shrinkage in dependence of mole fraction of citric acid.

In addition the volume shrinkage is calculated keeping R/F and R/C constant while varying R/W. The effect measured is much more significant than for constant R/W. With an increasing sol dilution the maximum shrinkage exceeds and reaches 38%. Figure 6 shows the results of these measurements.

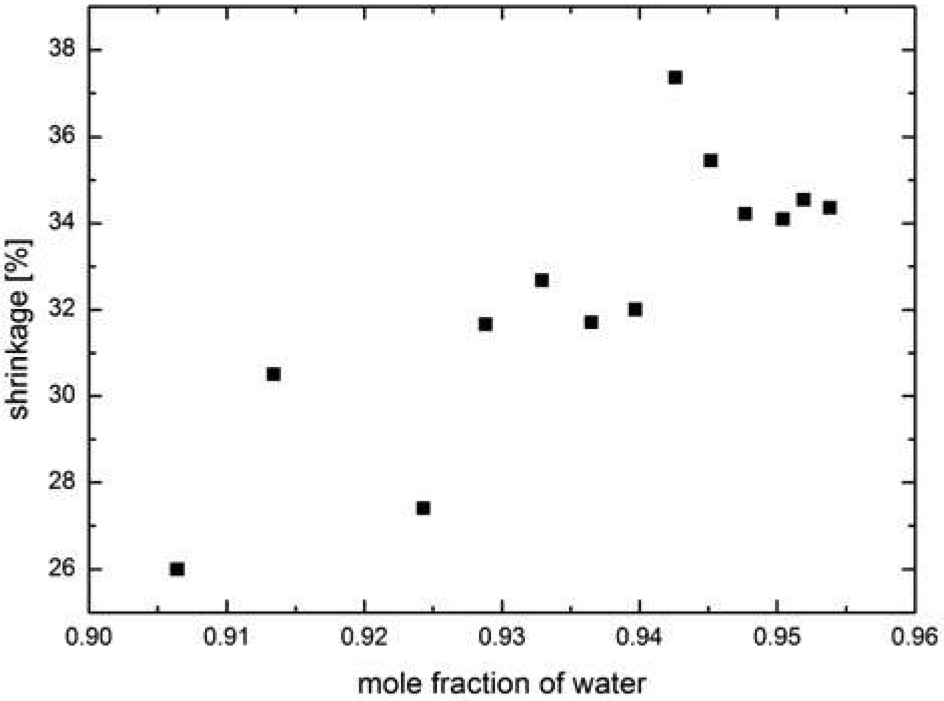

Figure 6: Volume shrinkage in dependence of the mole fraction of water (R/F = 0.77, R/C = 16.4, T_{drying} = 80°C).

The higher the concentration of catalyst and the higher the dilution of the sol the greater is the shrinkage of the RF aerogel samples. It is observed that the radial shrinkage of the samples is notably less (maximum 8%) than the shrinkage in height (maximum 34%).
Brandt et al. [4] synthesized carbon aerogels via an acetic acid catalyzed / subcritical drying route with R/C = 7.7, R/F = 0.5 and R/W = 0.019. They observed a linear shrinkage of only 2%, the resulting aerogel had a density of 240 kg/m³ and a specific inner surface area of 600 m²/g.
Also Reuß and Ratke [3] prepared subcritical dried, acid catalyzed RF aerogels using hydrochloric acid (R/C = 0.55, R/F = 0,75, variable R/W). Their densities are in the range of 410 to 218 kg/m³ and the BET surfaces are between 4.76 and 14.19 m²/g [5].

The RF aerogels described in this paper have a density between 357 and 144 kg/m³. In Figure 7 is shown that the dependence on the mole fraction of water is linear. For the black squares in Figure 7 the ratio of R/C = 16.4 is kept constant but for the red R/C is varied between 769 and 15.4. If the amount of catalyst is increased (decreasing mole fraction of water) the density increases, due to Figures 2c and 5 small amount of catalyst do not lead to poor aerogels.

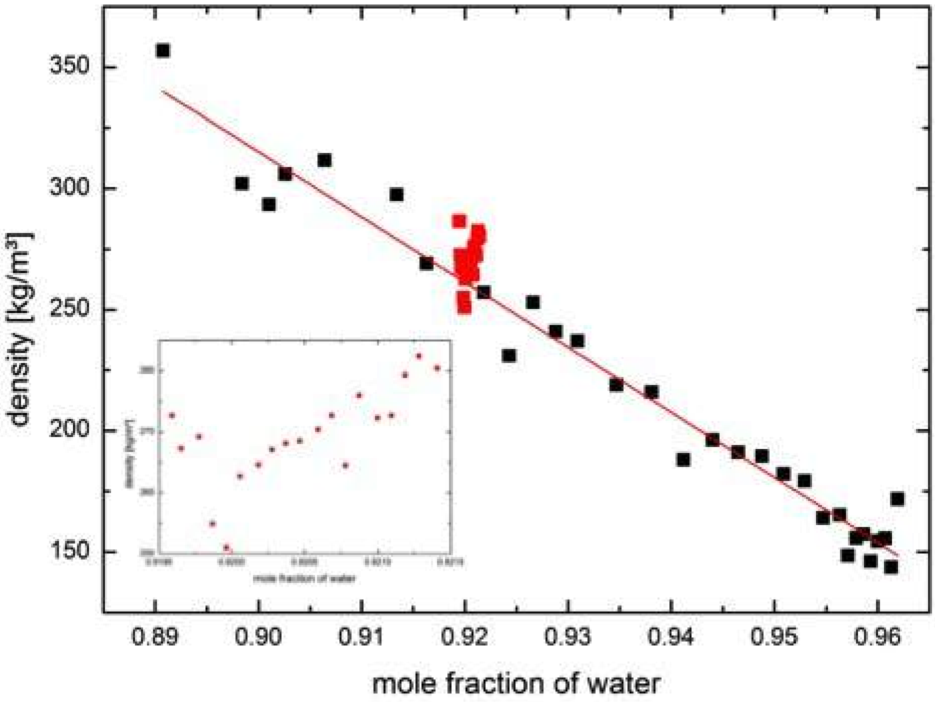

Figure 7: Dependence of the density on the mole fraction of water (R/F = 0.77, T_{drying} = 80°C, black quadrates: constant R/C = 16.4, red quadrates: constant R/W = 0.037).

The inner surface area is measured using krypton adsorption method because all citric acid catalyzed RF aerogels have small surfaces compared to those reported in the literature [2, 3] of acid catalyzed as well as sodium carbonate catalyzed [4] RF and carbon aerogels.

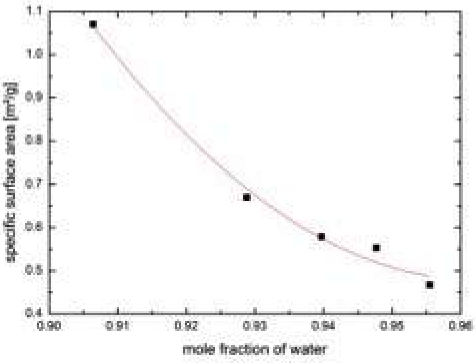

Figure 8a: Specific surface area (S_m) of RF aerogels as a function of mole fraction of water (R/F = 0.77, R/C = 16.4, T_{drying} = 80°C).

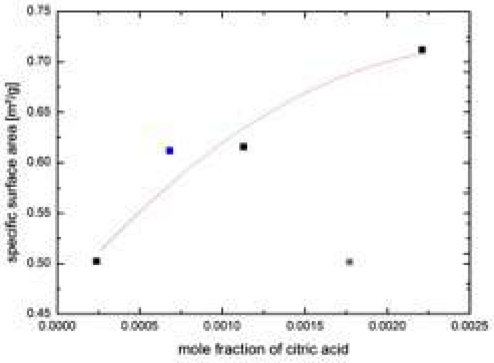

Figure 8b: Specific surface area (S_m) of RF aerogels as a function of mole fraction of citric acid (R/F = 0.77, R/W = 0.037, T_{drying} = 80°C, (blue square: sample B (s. Tab. 1), grey square: sample not involved in fitting).

Figure 8a and 8b show the specific surface area measured by krypton adsorption method in relation to the mole fraction of water and citric acid. As expected the inner surface area of the prepared aerogels decreases with increasing dilution of the precursor's solution as well as with decreasing concentration of catalyst. The decrease of the specific surface area with increasing amount of water is much bigger than the increase with an increasing mole fraction of citric acid. Even the molar ratio R/C is kept constant the influence of dilution cannot be neglected.

For better understanding and to neglect the density influence on the samples the mass dependent inner surface area (S_m) is transferred into the volume dependent specific surface area (S_V):

(Eq. 3)

In Figure 9a the data obtained are plotted against the mole fraction of water and in Figure 9b against the mole fraction of citric acid. The effect on the volume dependent specific surface area caused by the variation of the molar amount of water is much higher than by changes in the catalysts concentration.

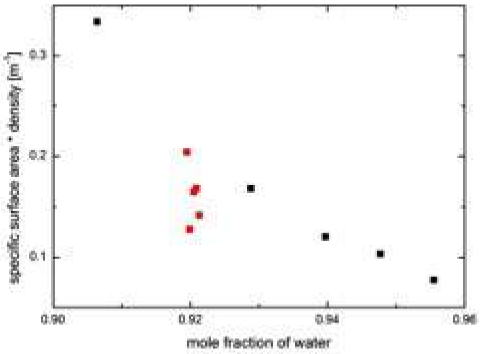

Figure 9a: Volume dependent specific surface area ($S_V = S_m \, x \, \rho$) of RF aerogels as a function of mole fraction of water (red square: amount of water is varied between R/W = 0.043 and 0.020, R/F = 0.77, R/C = 16.4, T_{drying} = 80°C, black squares: R/F = 0.77, R/W = 0.037, T_{drying} = 80°C).

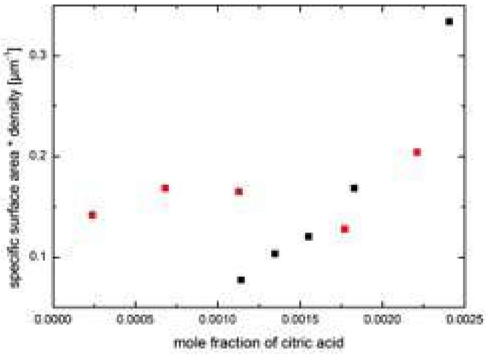

Figure 9b: Volume dependent specific surface area ($S_V = S_m \, x \, \rho$) of RF aerogels as a function of mole fraction of citric acid (red squares: amount of water is varied between R/W = 0.043 and 0.020, R/F = 0.77, R/C = 16.4, T_{drying} = 80°C, black squares: R/F = 0.77, R/W = 0.037, T_{drying} = 80°C).

S_V is reciprocally proportional to the diameter of the aerogel particles. As it is the ratio of surface area to volume (m^2/m^3) and it is supposed that the particles are spheres the radius of the particles can easily be calculated:

(Eq. 4)
(Eq. 5)

In Table 2 and 3 the evaluated values for the particle radii are listed beside other properties. The sizes fit well to the values received by the analysis of the structural texture by SEM (s. Figures 10a, b and c).

Table 2: Selection of samples with amount of water varied (R/F = 0.77, R/C = 16.4).

R/W	W/C	Mole fraction of water	Mole fraction of citric acid	Gelation time [min]	ρ [kg/m³]	S_m [m²/g]	S_V [µm²/µm³]	[µm]
0.043	381	0.9064	2.41 E-3	24	311.8	1.071	0.334	1.00
0.032	508	0.9288	1.83 E-3	31	241.0	0.670	0.169	1.97
0.027	606	0.9397	1.55 E-3	37	208.4	0.579	0.121	2.75
0.023	705	0.9477	1.34 E-3	42	186.9	0.553	0.103	3.24
0.020	836	0.9555	1.12 E-3	45	165.9	0.467	0.078	4.27

Table 3: Selection of samples with catalyst concentrations varied (R/F = 0.77, R/W = 0.037).

R/C	W/C	Mole fraction of water	Mole fraction of citric acid	Gelation time [min]	ρ [kg/m³]	S_m [m²/g]	S_V [µm²/µm³]	[µm]
143	3857	0.9213	2.39E-4	58	282.4	0.502	0.142	2.35
50 B (■)	1350	0.9209	6.82E-4	39	276.0	0.612	0.169	1.97
30.3	818	0.9205	1.13 E-3	35	268.5	0.616	0.165	2.02
19.2	519	0.9199	1.77 E-03	31	254.9	0.502	0.128	2.60
15.4	415	0.9195	2.21 E-3	26	286.5	0.712	0.204	1.63

The SEM pictures (s. Fig. 10a, 10b, 10c) of the citric acid catalyzed RF aerogel are compared with sodium carbonate catalyzed RF aerogel (s. Fig. 10d). The network of the acid-catalyzed RF aerogel is built of connected spherical particles of homogenous size. The necks between the particles are thin as if the aging period of the aerogel was very short. But for base-catalyzed aerogels the structural texture we found shows a different appearance: irregular shaped particles with heterogeneous size distribution are cross linked and built the network. This main difference can be explained by the two reaction mechanisms. As described by Mulik and Sotiriou-Leventis [5] the base-catalyzed gelation of RF aerogels follow an electrophilic attack of the formaldehyde on the catalytically deprotonated resorcinol (o-quinone methide intermediate) while the acid-catalyzed gelation follows a nucleophilic attack of the π-system of resorcinol on the protonated formaldehyde. Within the acid-catalyzed gelation mechanism “starting centers” - initial nucleus - are well distributed over the whole solution. The number of initial nucleus depends on the amount of catalyst and dilution. During the gelation process no new nuclei are built. Therefore the poly-condensation just leads to a homogeneous growth of the particles. While growing the particles connect and built their network. On the other hand base-catalysis leads to some initial nuclei which start growing, meanwhile new nucleus are built and start growing too, continuously growth and nucleation takes place in parallel and particles with various sizes are built. In addition aging seems to be a welcome structural reordering process (s. Figure 10d). The result is a much stronger and filigree RF aerogel particle network.

In addition we observed that the acid-catalysis is much faster and a more exothermal process (with hydrochloric acid or large amounts of citric acid the beakers heat up considerably). Until now kinetic studies are not really available and a detailed research on the kinetics of poly-condensation in acid and base catalyzed RF-aerogels would be necessary.

With increasing ratio of resorcinol to catalyst (R/C) the size of the spheres is larger and the number of spheres per volume unit is less. This is in agreement with the measured dependence of the inner surface area. Figure 9 shows two samples prepared under similar conditions. The particle radius of is around 2.5, 3 µm for R/C = 16.4, 18, and 6 µm for R/C = 333. The sizes of the particles compared to base catalyzed aerogels are much bigger.

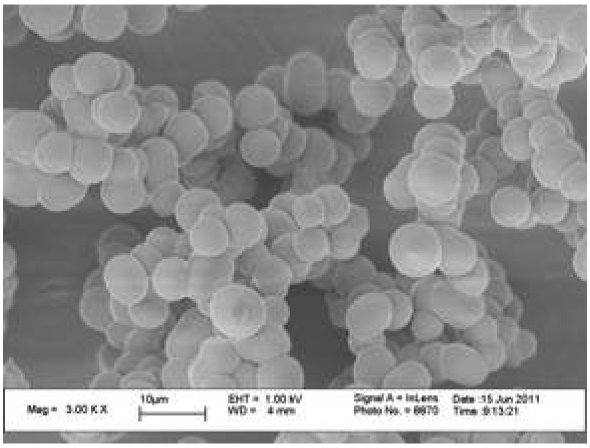

Figure 10a: SEM picture of RF Aerogel with R/F = 0.77, R/W = 0.023, R/C = 16,4, W/C = 705 (mole fraction of water = 0.9477) and T_{drying} = 80°C; r = 3 µm.

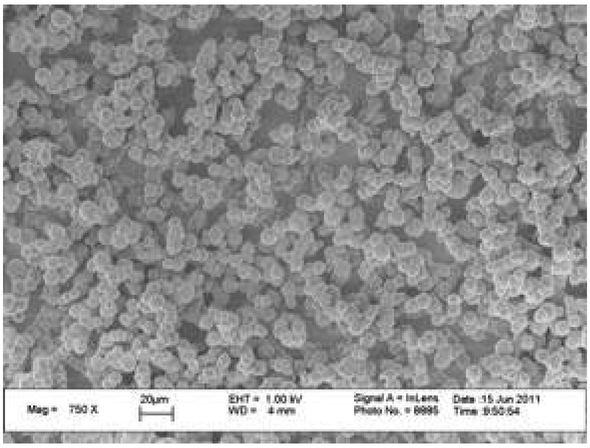

Figure 10b: SEM picture of RF Aerogel with R/F = 0.77, R/W = 0.037, R/C = 333, W/C = 9000 (mole fraction of water = 0.9214) and T_{drying} = 80°C; r = 6 µm.

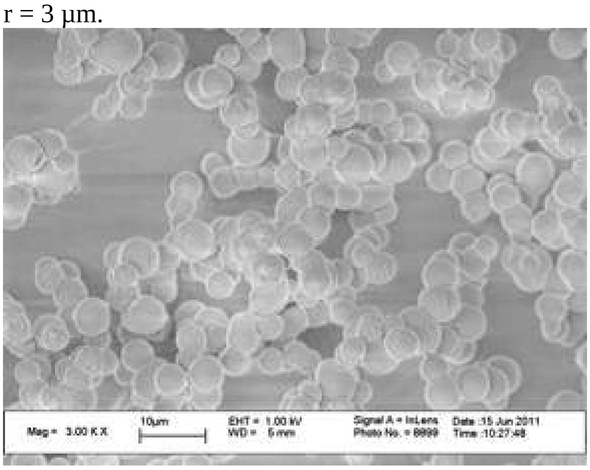

Figure 10c: SEM picture of RF Aerogel with R/F = 0.77, R/W = 0.037, R/C = 18, W/C = 491 (mole fraction of water = 0.9197) and T_{drying} = 80°C, r = 2.5 µm.

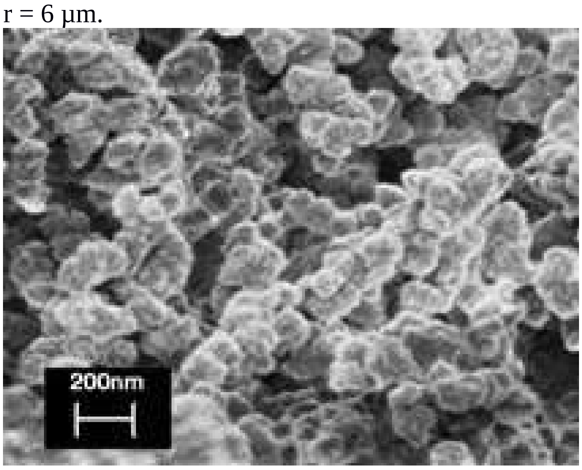

Figure 10d: SEM picture of RF Aerogel with R/F = 0.77, R/W = 0.039, R/C(Na_2CO_3) = 1500.

Conclusion and perspectives

The gelation of RF aerogels is much faster using citric acid as a catalyst. Within the limit of R/C < 150 and a minimum mole fraction of water of 0.96 RF aerogels are synthesized. Very low densities of $\rho < 150$ kg/m³ have been achieved. The specific surface area $S_m < 1.1$ m²/g is quiet small for aerogels and needs improvement. First results using a new reaction routine show exciting results and will be published soon.

Acknowledgements

We gratefully acknowledge the support by Micromeritics™.

References

[1] PEKALA, R. W., J Mater Sci 24, **1989,** 3221-3227.
[2] BRANDT, R., FRICKE, J., J Non-Cryst Solids 350, **2004**, 131-135.
[3] REUSS, M., RATKE, L., J Sol-Gel Sci Technol 47, **2008,** 74-80.
[4] http://americanaerogel.com/our-technology/aerogels/ (**15.11.2012**)
[5] AEGERTER, M. A., LEVENTIS, N., KOEBEL, M., “Aerogels Handbook”, **2011,** Springer New York.
[6] DURAIRAJ, R. B., “Resorcinol: Chemistry, Technology and Applications”, **2005**, Springer Berlin Heidelberg New York.

P05

CELLULOSE FIBER REINFORCED RF-AEROGELS

Jessica Laskowski*, Lorenz Ratke
Institut für Materialphysik im Weltraum, Deutsches Zentrum für Luft- und Raumfahrt, DLR, 51170 Köln, Germany
Jessica.Laskowski@dlr.de

ABSTRACT

Cellulose gels were synthesized in which the pore space was filled with resorcinol-formaldehyde (RF) aerogel solution. Three weight percent microcrystalline cellulose was dissolved in an aqueous calcium thiocyanate melt at 110 °C, which gelled on cooling building a nanofibrillar felt structure. The highly concentrated salt solution in the pore space is washed with ethanol until a test with Fe^{3+} ions does yield a colorless solution. After washing with formaldehyde (24%) the hydrogel was exposed to a resorcinol-formaldehyde solution while gelling. The RF solution had a molar ratio of resorcinol to water (R/W) of 0.04 and of resorcinol to formaldehyde (R/F) of 0.7. The molar ratio of resorcinol to catalyst sodium carbonate (R/C) used was 100, 500, 1000 or 1500. The composite gels prepared were dried supercritically and their nanostructure characterized by SEM. The aerogels were characterized by density, surface area, compression strength and thermal conductivity. Measurements of compression strength showed an anomalous behavior compared to those of pure cellulose aerogels.

INTRODUCTION

Nanoporous materials, such as organic aerogels, are increasingly important in various fields of technology. One of these materials is resorcinol-formaldehyde (RF) aerogel, which was developed by Pekala et al. [i] in 1987 and commences the research on organic aerogels. RF aerogels are synthesized via a polymerisation of resorcinol and formaldehyde in an aqueous solution with a particular pH-value which is initiated by a basic or acid catalyst like Na_2CO_3 [1] or acetic acid [ii]. Further research on RF aerogels enables ambient drying [iii] which is more commercial than the originally supercritical drying. Particularly an important application of RF is their pyrolysis to form carbon aerogels, which yields a property like electrical conductivity leading to applications as supercapacitors [iv] or battery electrodes [v].

- Cellulose is in addition an interesting organic material for aerogels especially because of being a re-growing biopolymer. The first cellulose aerogels were prepared by Tan et al. [vi] in 2001 by using cellulose acetate and de-esterifying. Jin et al. [vii] first described the synthesis with cellulose fibers three years later. They dissolute the polymers fibers in a calcium thiocyanate melt and the fibers build a nanofibrillar felt structure while cooling. After washing with ethanol the hydrogel obtained is dried supercritically with CO_2 to get an aerogel without shrinkage. Other methods are published in which the use of LiOH, urea and water [viii] is successfully applied. Typical properties of cellulose aerogels are a low density (10 – 350 kg/m³) and a high surface area (200 – 300 m²/g) [6, ix].

Developing new materials with improved properties like density (< 200 kg/m³), surface area (< 200 cm²/g), thermal conductivity (< 30 $mW(m \cdot K)^{-1}$) and compression strength (> 100 kPa) are desirable. We expect that using two components could be successful. Therefore the present investigation has the aim to prepare aerogel-composites with the incorporation of cellulose and RF. Up to now no information about composites of cellulose and RF is published.

MATERIAL AND METHODS

Chemicals

The chemicals used are calcium thiocyanate $Ca(SCN)_2$ 4 H_2O with a purity of 95 %, cellulose medium fibers with unknown purity and unknown degree of polymerisation, resorcinol (> 98 %) and sodium carbonate Na_2CO_3 with a purity of ≥ 99.8 % all were purchased from Sigma Aldrich. The 24 % formaldehyde solution (not buffered) used is from VWR and ethanol (denatured, 96 %) from Walter CMP GmbH & Co. KG. All chemicals were used as purchased.

Preparation of the cellulose-gel

20 g of $Ca(SCN)_2$ 4 H_2O are filled into a beaker and 3.15 mL deionized water and 0.695 g of cellulose are added. This amounts leads to a 59 wt% solution of $Ca(SCN)_2$ with 3 wt% cellulose. The suspension is heated up to 110 °C while stirring until the solution becomes clear and no cellulose fibers could be seen. We assume that at this point cellulose is completely dissolved. The hot solution is now filled fast into two sample-boxes and centrifuged for 30 seconds in order to remove air bubbles. The samples are than covered by ethanol to avoid crystallization on the surface of the sample noticeable as a thin skin on the surface. While cooling below 80 °C the dissolved cellulose fibers build a nanofibrillar felt structure. After 12 h these gels formed are released from the sample-boxes and are washed several times with ethanol to remove the salt from pore space. When the test with Fe^{3+} ions does yield a colorless solution the washing step is finished.

Preparation of the RF-solution

27.5 g of resorcinol are filled into a lockable vessel and 87.5 g of deionized water are added while stirring. If the solid is completely in solution 42.5 g of a 24 % formaldehyde solution and Na_2CO_3 as the catalyst are added still stirring. The amount of Na_2CO_3 depends on the molar ratio of resorcinol to catalyst (R/C) which was 100, 500, 1000 and 1500. The recipe used contains a molar ratio of resorcinol to water (R/W) of 0.04 and a molar ratio of resorcinol to formaldehyde (R/F) of 0.7.

Preparation of the cellulose fiber reinforced RF-aerogels

The cellulose gel synthesized is washed several times with a 24 % formaldehyde solution by exchanging the solvent in which the gel is stored. After the fifth time of daily exchange ethanol in the pore space supposed to be completely replaced by formaldehyde. The gel washed than is added in the freshly prepared RF-solution and the vessel is closed and stored at 40 °C. Thus the gel is exposed to the RF-solution while this gels. It is removed from solution when the gelation is close to the gelation point, where it has a very high viscosity. The gel is coated with a commercial foil and put into a sample-box to store the sample at 40 °C for final gelation and aging. After six days storage the sample is washed several times with ethanol and finally dried supercritically with the use of liquid carbon dioxide. The drying step was performed in an autoclave developed at DLR which is first filled with the gels in an ethanol bath and is closed carefully. The autoclave is then filled with liquid CO_2 until the samples are completely in liquid. The samples are washed regularly by venting the autoclave to a certain level and refill with CO_2 to remove ethanol from the sample pores. Finally the temperature and the pressure are increased above the critical point of CO_2 and the supercritical fluid is slowly discharged to finish the drying session.

Analyzing methods

The density of the samples was determined with the envelope density analyzer GeoPyc® 1360 from Micromeritics. The thermal conductivity was measured by the Hot Disc method with the thermal constants analyzer type TPS 2500. Furthermore the compression test was performed using the testing machine TCD 200-SS from Chatillon. Therefore rectangular samples were prepared with a lateral length of about 11 mm and a height depending on the synthesis. The specific surface area was measured by implement the BET method with the surface area analyzer Tristar II 3020 from Micromeritics using nitrogen adsorption. Finally the microstructure was examined with a field emission scanning electron microscope (FE-SEM) Merlin® from Carl Zeiss after coating the sample with a nanofilm of gold.

RESULTS

Typical cellulose fiber reinforced RF-aerogel synthesized is shown in figure 1. They were obtained after polishing the surface to remove from enveloping RF-aerogel to exclude an influence of pure RF-aerogel on measurements applied. Whereas cellulose aerogel appears colorless, the composites are brown caused by RF particles. Furthermore they are very stable in contrast to pure cellulose aerogels which are easily deformable with fingers. Compared to pure RF aerogels the reinforced materials are less brittle.

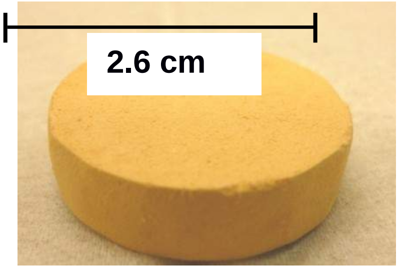

Figure 15: Photograph of a typical cellulose fiber reinforced RF-aerogel synthesized.

Usual density of cellulose aerogel measured is 65 kg/m^3. As expected, there is an increase in density, when their pores are filled with RF (table 1). The increase depends more or less on the RF-recipe that is the R/C value used but there is no linear relation. The density received varies between 180 and 335 kg/m^3. The radial shrinkage could have an influence on the results additionally, which decreases with higher R/C value used. The maximum shrinkage is with the molar ratio R/C of 100 and is about 19 %. Shrinkage is higher than for pure cellulose aerogel, which is 9 %.

The thermal conductivity obtained is higher than of pure cellulose aerogel (50 mW(m·K)$^{-1}$) and there might be a dependence of density what arise from the amount of RF. With the highest density (R/C 1000) a high thermal conductivity of 81 mW(m·K)$^{-1}$ is measured and vice versa (R/C 1500) with a result of 58 mW(m·K)$^{-1}$. Therefore, RF definitely causes a higher thermal conductivity.

Table 13 : Characteristics of cellulose aerogel and cellulose fibers reinforced RF-aerogels.

Material	R/C	Density ± 5 [kg/m^3]	Radial Shrinkage ± 2 [%]	Thermal Conductivity ± 4 [mW(m·K)$^{-1}$]
Cellulose	-	65	9	50
Cellulose + RF	100	300	19	61
Cellulose + RF	500	290	18	62
Cellulose + RF	1000	335	17	81
Cellulose + RF	1500	180	14	58

An anomalous behavior of synthesized reinforced materials occurs during the compression test (figure 2). Pure cellulose aerogels exhibit a classical deformation curve of a porous material: after the onset of irreversible deformation further deformation proceeds at almost constant stress. The reinforced materials show initially a deformation like the cellulose aerogel but at higher stress levels. The Young's modulus achieves values between 7 and 12 MPa which exceeds the Young's modulus of pure cellulose aerogel up to 94 %. After a critical amount of deformation a sharp transition to a new stress-compression curve with a much higher Young's modulus appears with R/C ratios 100, 500 and 1000 leading to yield strengths of more than 1 MPa compared to a few hundred kPa of pure cellulose aerogel or pure RF aerogels. Note that the transition is performed between a compression of 5 and 6 % respectively depending on the RF recipe.

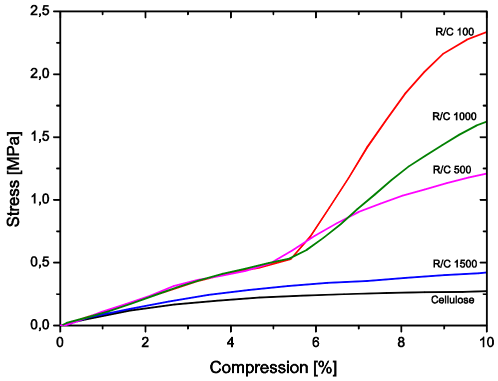

Figure 16: Stress-compression-curve of cellulose fibers reinforced RF-aerogels and cellulose aerogel.

Table 14: Young's modulus of cellulose and cellulose fibers reinforced RF-aerogels in compression section between 1 – 5 % (Young's modulus I) and between 5 to 10 % (Young's modulus II).

Material	R/C	Young's Modulus I ± 1.0 [MPa]	Young's Modulus II ± 2.0 [MPa]
Cellulose	-	6.3	-
Cellulose + RF	100	9.7	49.2
Cellulose + RF	500	12.2	20.7
Cellulose + RF	1000	11.2	27.7
Cellulose + RF	1500	7.0	-

The surface area measured by BET-method, whose isotherms are shown in figure 3 a, increase if RF with the R/C ratio of 100 is used combined to pure cellulose aerogels. In fact, the result double (table 3); the surface area obtained for pure cellulose aerogel is 166 m²/g and for the reinforced material is 342 m²/g. The small RF-particles apparently fill the cellulose pores and determine smaller pore diameters what was investigated by BJH-method (table 3). A higher R/C ratio like 1000 and 1500 indeed causes a surface decrease less than 100 m²/g and greater pore diameter. Bigger RF-particles are formed while gelling of the RF-solution with less amount of the catalyst. The big particles precipitate on cellulose fibers what induces smaller surface areas. Only the material with R/C ratio of 500 does not involve a change in results due to a balanced effect of superposing cellulose surface and building new surface area from RF particles. In summary figure 3 b shows the influence of R/C- value on the surface area which definitely decrease with higher R/C.

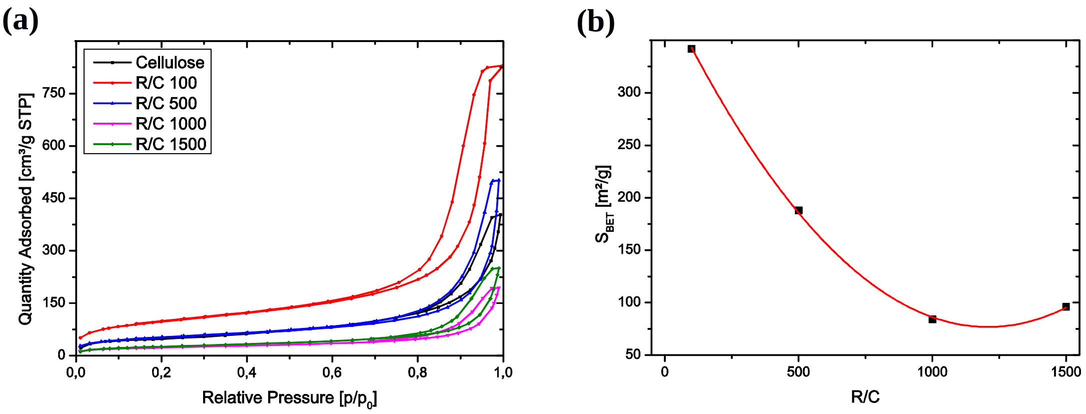

Figure 17: a N_2 sorption isotherm at 77 K of cellulose aerogel and of cellulose fibers reinforced materials (R/C 100 - R/C 1500) and **b** surface area as a function of R/C ratio.

The SEM pictures of materials synthesized furthermore reveal that RF diffuse into the pores of the cellulose hydrogel and settle on cellulose fibers (figure 4 b - d) what is indicated by small particles on the fibers. The content of RF-particles is inhomogeneous due to a faster gelation of the RF-solution than diffusion of RF-particles or molecules into the cellulose structure. The bigger RF-particles formed during the synthesis of the composite with the ratio R/C of 1500 (figure 4 e) did not have the ability to reach the core of the cellulose structure; therefore a typical cellulose nanostructure like figure 4 a was determined.

Table 15: Overview: BET- surface area S_{BET}, sorbed volume V_M and pore diameter of cellulose aerogel and cellulose fibers reinforced materials with different R/C ratio.

Material	R/C	S_{BET} ± 2 [m²/g]	V_M ± 2 [cm³/g] STP	Pore diameter ± 1 [nm]
Cellulose	-	166	38	16
Cellulose + RF	100	342	79	15
Cellulose + RF	500	188	43	22
Cellulose + RF	1000	84	19	20
Cellulose + RF	1500	96	22	20

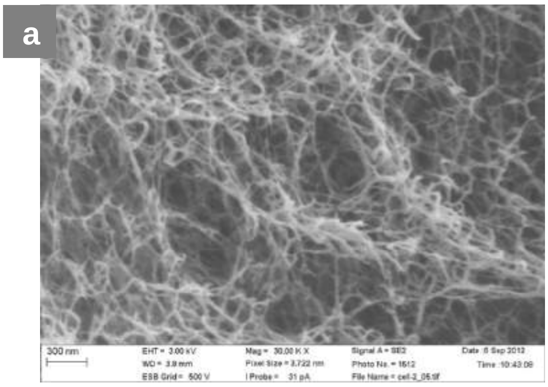

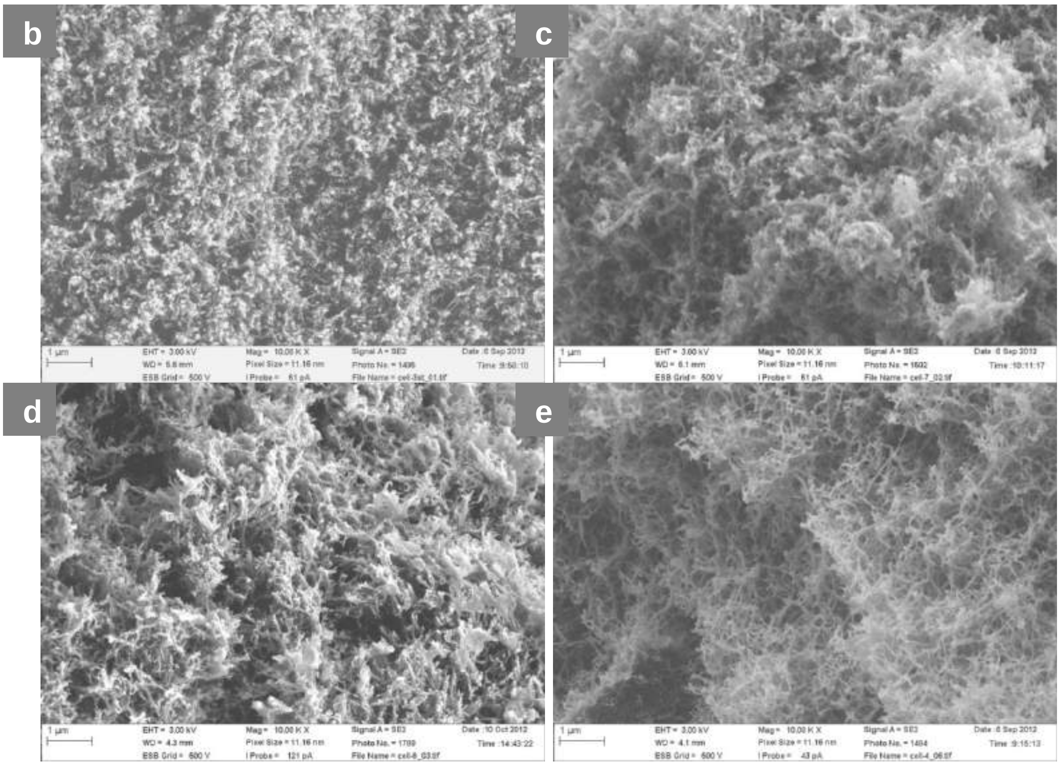

Figure 18: SEM pictures of a) cellulose aerogel and the cellulose fiber reinforced RF-aerogels with different R/C ratios of b) R/C 100, c) R/C 500, d) R/C 1000 and e) R/C 1500.

CONCLUSION

Cellulose fibers reinforced RF aerogels could be synthesized by immersing cellulose hydrogels into RF-solutions with different R/C ratios followed by supercritical CO$_2$ drying. The hydrogels were synthesized after a commonly used method [7, 9] in which 3 wt% cellulose is dissolute in a 59 wt% Ca(SCN)$_2$ melt. In this way, a novel type of RF-cellulose composites could be received. The RF-particles wet the cellulose fibers leading to an anomalous behavior in stress-compression test with high Young’s moduli in contrast to pure cellulose aerogel. The structure also causes improvements in surface area if high catalyst concentration is used (R/C = 100). Detailed studies of further RF-recipes with higher catalyst concentration (R/C < 100) will follow, as well an improved method to obtain homogeneous materials.

REFERENCES:

[] PEKALA, R. W., J. Mater. Sci., Vol. 24, **1989**, p. 3221.

[] BRANDT, R., et al., J. Porous Mater., Vol. 10, **2003**, p. 171.

[] BRANDT, R. FRICKE, J., J. Non-Cryst. Solids, Vol. 350, **2004**, p. 131.

[] MAYER, S.T., PEKALA, R.W., KASCHMITTER, J.L., J. Electrochem. Soc., Vol. 140, **1993**, p. 446.

[] SCHAEFER, D.W., KEEFER, K.D., Phys. Rev. Lett., Vol. 56, **1986**, p. 2199.

[] TAN, C., et al., Adv. Mater. Vol. 13, **2001**, p. 644.

[] JIN, H., et al., Colloids and Surfaces A: Physicochem. Eng. Aspects, Vol. 240, **2004**, p. 63.

[] CAI, J. et al., Chem. Sus. Chem., Vol. 1, **2008**, p. 149.

[] HOEPFNER, S., RATKE, L., MILOW, B., Cellulose, Vol. 15, **2008**, 15, p.121.

P06

SELF AND TRANSPORT DIFFUSION IN (AERO-) GELS

Martin Schormeyer, Stephan Braxmeier, Gudrun Reichenauer

Bavarian Center for Applied Energy Research (ZAE Bayern), Am Hubland, 97074 Würzburg, Germany

ABSTRACT

Transport of molecules and fluids in aero/xerogels as well as their gel precursors are important properties for both, material synthesis and applications.

Depending on the process under consideration self diffusion (concentration gradient at zero pressure gradient) and transport diffusion (total pressure gradient) have to be distinguished. We present experiment results for both situations:

> In-situ NMR was used to investigate the self diffusion coefficient during solvent exchange at ambient conditions as well as at high pressure in a CO_2 operated autoclave. The experiments reveal that the kinetics can be described by combining the self diffusion coefficient of the free fluid and the tortuosity of the pore network.
>
> Fluid transport was analyzed by performing quasi steady state gas permeation measurements at gas pressures in the average pressure range between 1000 and 10 mbar as well as sorption experiments with monitoring of the sorption kinetics. The investigations reveal that fluid transport is well described by Hagen-Poiseuille’s law unless the free path of the molecules exceeds the pore width (e.g. gas phase transport at ambient conditions in pore < 100 nm). In the later case, transport can be described by molecular diffusion; in addition, transport along a layer adsorbed at the large inner surface of the gel network plays a role, in particular, when the corresponding sorption isotherm in the related rel. pressure range exhibits a significant slope.

The transport mechanisms are contributing to the drying kinetics, both at ambient and high pressure conditions, and are also governing transport in all applications involving fluid transport (e.g. drug delivery, catalysis, thermal insulation, fluid separation and gas storage).

FORMATION OF SILICA MICROPARTICLES BY SAS PROCESS

A.Montes[a], **M. D. Gordillo**[a], **C. Pereyra**[a], **N. De la Rosa Fox**[b], **E. J. Martínez de la** Ossa[a]
[a]Department of Chemical Engineering and Food Technology,
[b]Department of Condensed Matter Physics
Faculty of Sciences, University of Cádiz
11510 Puerto Real (Cádiz), Spain
E-mail: antonio.montes@uca.es

Abstract

Silica microparticles are of great interest for several applications in areas such as medicine, biochemistry, colloidal chemistry and aerosol research. There are several methods to obtain these particles. In this work, the sol-gel method followed supercritical antisolvent (SAS) process was used to obtain these ones. A tetraethyl orthosilicate (TEOS) and water solution was dissolved in ethanol and then pumped into a vessel trough a nozzle (100 µm). The conditions inside the vessel were 120 bar and 313 K. The dissolution of the supercritical fluid in the organic solvent is accompanied by a large volume expansion and, consequently, a reduction in the liquid density, decreasing its solvent power, causing the supersaturation within the liquid mixture and finally the particles precipitation. All the experiments led to a successful precipitation of silica microparticles, in the micrometer range with a narrow particle size distribution. In all cases spherical morphology and no agglomeration was found.

Introduction

SAS process has been widely used for the last ten years in a variety of different fields: pharmaceuticals, explosives, polymers, colouring matter, superconductors, catalysts and inorganic compounds, among others [1-3]. Moreover, this process allows control of particle size distribution and morphology of silica particles. The sol-gel method, which is used to obtain aerogels, can also be used to precipitate SiO_2 microparticles using supercritical fluids (SCF). Given the specific properties of SCF, such as their high diffusivity as a consequence of their low viscosity and high density, the aforementioned fluids can provide a way to achieve nucleation of SiO_2 particles.

Therefore, a precursor solution made by mixing TEOS/water and ethanol was used to obtain SiO_2 microparticles.

However, very little is known about silica microparticles formation by SAS process. In this way, Chattopadhyay and Gupta [4] and Zhang et al [5] developed a method for precipitation of silica nanoparticles using $scCO_2$ acting as both an antisolvent and a reactant, where precipitation of silica nanoparticles was carried out using microemulsions of aqueous sodium silicate in organic solvents.

Therefore, the objective of this work is to achieve an effective silica precipitation at different sol aging times by SAS process. The precipitation of different aging sol was evaluated on silica particle size and morphology

Experimental section

Tetraethyl orthosilicate (TEOS) (≥ 99% purity) and ethanol (ETOH) (99.5% purity) were purchased from Sigma–Aldrich Chemical (Madrid, Spain). Carbon dioxide with a minimum purity of 99.8 % was supplied by Linde (Spain). Fourteen mL of TEOS and acid water mixture, with a molar ratio of 1:4 and pH=1 diluted in ethanol (total volume of 200 mL), was prepared. SAS process was carried out at different aging times (3, 8 and 21 days).

SAS experiment was carried out in a pilot plant developed by Thar Technologies® (model SAS 200). A schematic diagram of the equipment, described in detail in a previous work [6], is shown in Figure 1. The solution is dispersed in the fluid at high pressure by a nebulizer with an orifice diameter of 100 µm. Inside the precipitator the $scCO_2$ acts as an antisolvent promoting the precipitation of SiO_2 microparticles. Moreover, it is possible to adjust the optimum thermodynamic conditions for the process by studying vapour–liquid equilibrium data for the carbon dioxide + ethanol system [7]. Based on such data, the experiments were carried out at a pressure of 120 bar and a temperature of 313 K. All the experiments should therefore be performed above the mixture critical point (71.8 bar, 313K) of silica–ethanol–CO_2, in the miscible region. In line with usual practice with such ternary systems, the presence of silica does not affect the ethanol–CO_2 equilibrium, and therefore an EtOH–CO_2 pseudo-binary equilibrium is considered [8].

Scanning electron microscopy pictures of the powder precipitated on the wall of the vessel were obtained using a QUANTA 200 scanning electron microscope (SEM). Prior to analysis the samples were placed on carbon tape and then covered with a coating of gold using a sputter coater. The SEM images were processed using the image analysis software Scion Image (Scion

Corporation) to obtain the particle sizes. The mean particle size (PS) and coefficient of variation (CV) as measurement of the distribution width were calculated using StatGraphics Plus 5.1 software. Around 500 particles were counted to perform the analysis in each experiment.

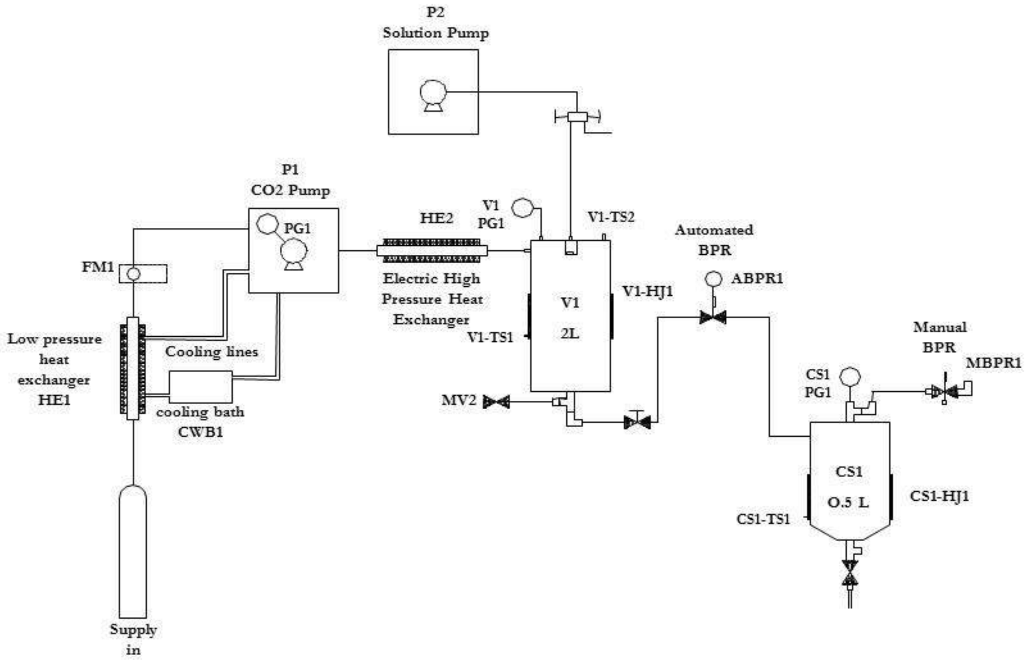

Figure 1. Schematic diagram of pilot plant SAS200

Results

All the experiment led to a successful precipitation of silica microparticles in the upper part of the vessel. Spherical morphology and no agglomeration appearance were obtained as can be shown in figure 2. De Marco et al. [9] observed a relative wide transition from a two-phase mixing flow to a single-phase mixing flow when the pressure was tuned near above the mixture critical point of ethanol and carbon dioxide. So the spherical microparticles formation can be attributed to micro-droplet drying [10], due to the operating conditions of this work there was not so far of mixture critical point and was situated into this two-phase mixing flow.

Figure 3. SEM images of powder precipitated by a) b) c) SAS process samples for 3, 8 and 21 aging days of the precursor solution

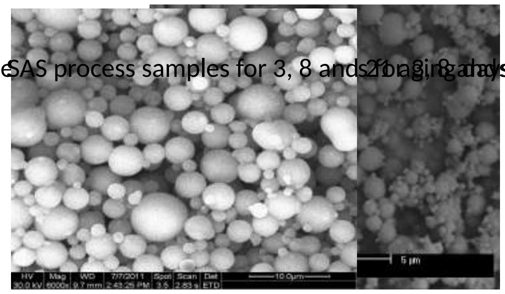

Figure 2. SEM images of powder precipitated by a) b) c) SAS process samples for 3, 8 and 21 aging days of the precursor solution respectively.

The samples display similar size distribution for the sol-gel aging periods of 3 and 8 days whereas significant size dispersion is observed for the 21 day-period (figure 3). Particle size is significantly decreased at 21 days. This can be explained because condensation is directly proportional to the concentration of solute, and the decrease of the condensation rate at lower concentrations, by delivery of water or alcohol along the time due to the own sol-gel process, tends to decrease the particle size [11].

	Lognormal distribution	
	MPS (μm)	C.V.
SAS (3 days)	2.47±1.27	0.51
SAS (8 days)	2.70±1.16	0.49
SAS (21 days)	0.99±0.86	0.86

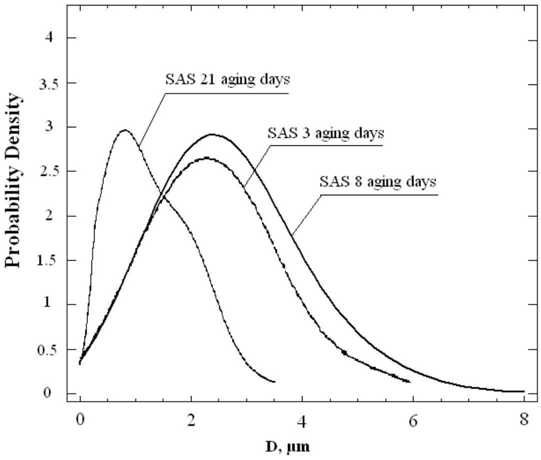

Figure 3. Particle size distribution (PSD), mean particle size (MPS) and coefficient of variation (C.V.) of samples obtained by SAS process.

Acknowledgements

We gratefully acknowledge the Spanish Ministry of Science and Technology (Project CTQ2010-19368) and the European Fund for Regional Development (FEDER) for financial support.

References

1. Teipel U., Kröber H., Krause H. H. (2001). Formation of Energetic Materials Using Supercritical Fluids. Propellants, Explosives, Pyrotechnics 26: 168-173.
2. Garay I., Pocheville A., Madariaga, L. (2010). Polymeric microparticles prepared by supercritical antisolvent precipitation. Powder Technology 197: 211–217.
3. Hsien-Tsung W., Ming-Jer L., Ho-mu, L. (2005). Nano-particles formation for pigment red 177 via a continuous supercritical anti-solvent process. J. Supercritical Fluids 33: 173–182.
4. Chattopadhyay P., Gupta, R. B. (2003). Supercritical CO_2-Based Formation of Silica Nanoparticles Using Water-in-Oil Microemulsions. Industrial& Engineering Chemistry Research 42: 465-472.
5. Zhang J., Liu, Z., Han B., Li, Z., Yang G., Li, J., Chen, J. (2006). Preparation of silica and TiO_2–SiO_2 core–shell nanoparticles in water-in-oil microemulsion using compressed CO_2 as reactant and antisolvent. J. of Supercritical Fluids 36: 194–201.
6. Tenorio, A., Gordillo, M. D., Pereyra, C. M., Martínez de la Ossa, E. M. (2007). Relative Importance of the Operating Conditions Involved in the Formation of Nanoparticles of Ampicillin by Supercritical Antisolvent Precipitation, Industrial& Engineering Chemistry Research 46: 114-123.

7 Secuianu, C., Feroiu, V., Geana, D. (2008). Phase behavior for carbon dioxide + ethanol system: Experimental measurements and modeling with a cubic equation of state, J. Supercritical Fluids 47:109–116.

8 Reverchon, E., Caputo, G., De Marco, I. (2003). Role of phase behaviour and atomization in the supercritical antisolvent precipitation, Industrial& Engineering Chemistry Research 42: 6406-6414.

9 De Marco, I., Knauer, O., Cice, F. , Braeuer, A., Reverchon, E. (2012). Interactions of phase equilibria, jet fluid dynamics and mass transfer during supercritical antisolvent micronization: The influence of solvents, Chemical Engineering Journal 203:71-80.

10 De Marco, I., Reverchon, E. (2011). Influence of pressure, temperature and concentration on the mechanisms of particle precipitation in supercritical antisolvent micronization, J. Supercritical Fluids 58: 295- 302.

11 Martin, A., Cocero, M. J. (2004). Numerical modeling of jet hydrodynamics, mass transfer, and crystallization kinetics in the supercritical antisolvent (SAS) process, J. Supercritical Fluids 32: 203-219.

i[] PEKALA, R. W., J. Mater. Sci., Vol. 24, **1989**, p. 3221.

ii[] BRANDT, R., et al., J. Porous Mater., Vol. 10, **2003**, p. 171.

iii[] BRANDT, R. FRICKE, J., J. Non-Cryst. Solids, Vol. 350, **2004**, p. 131.

iv[] MAYER, S.T., PEKALA, R.W., KASCHMITTER, J.L., J. Electrochem. Soc., Vol. 140, **1993**, p. 446.

v[] SCHAEFER, D.W., KEEFER, K.D., Phys. Rev. Lett., Vol. 56, **1986**, p. 2199.

vi[] TAN, C., et al., Adv. Mater. Vol. 13, **2001**, p. 644.

vii[] JIN, H., et al., Colloids and Surfaces A: Physicochem. Eng. Aspects, Vol. 240, **2004**, p. 63.

viii[] CAI, J. et al., Chem. Sus. Chem., Vol. 1, **2008**, p. 149.

ix[] HOEPFNER, S., RATKE, L., MILOW, B., Cellulose, Vol. 15, **2008**, 15, p.121.

P08

REGENERATION OF AIRCRAFT CABIN AIR USING AMINO FUNCTIONALIZED SILICA AEROGELS:
ADSORPTION OF CO2, H2O AND ETHANOL

K. Wörmeyer, I. Smirnova
[a]Hamburg-Harburg University of Technology, Institute of Thermal Separation Processes, Eißendorfer Str. 38, 21073 Hamburg, Germany

Abstract

One way to reduce the energy consumption and increase the passenger comfort of future aircraft is to increase the amount of recirculated air in the environmental control system (ECS). The increasing recirculation rates demand for the separation of passenger-emitted CO2 from the cabin air. For this task an adsorption process promises to be the most effective process, if a high performance adsorbent is used, possessing a high CO2 adsorption capacity at low partial pressures, the ability to adsorb moisture and

volatile organic compounds (e.g., ethanol). In addition, the regeneration of this material should be performed at mild temperatures and vacuum.

In this work, the applicability of amino functionalized silica aerogels as an adsorbent for this purpose is investigated. The high surface area, open pore structure, and high porosity of silica aerogels are promising characteristics for an adsorbent. Amino functionalization is applied to enhance the CO2 adsorption capacity of silica aerogels.

The effects of two different methods of aerogel functionalisation are investigated. Aminosilanes are introduced into the gel structure during gelation (Method 1) or after gelation by surface modification of the gel (Method 2). Aerogels are produced afterwards by supercritical drying with CO2. The produced materials are characterized by measuring CO2 adsorption isotherms in the range of 0.002 - 1 bar. Furthermore, the adsorption of CO2, H2O and ethanol from synthetic cabin air consisting of CO2 (500 - 4000 ppm): water (0-8500 ppm): ethanol (10 – 100 ppm): air is measured by breakthrough analysis. Additionally the aerogels are characterized by nitrogen adsorption isotherms (surface area, pore volume), FT-IR and elemental analysis.

The results show that the CO2 adsorption capacity can be increased by two orders of magnitude by amine modification and primarily depends on the amount of amines grafted to the silica structure of the aerogels. The produced aerogels exhibit a high CO2 adsorption capacity (5% (w/w) at 250 Pa, 0°C). They are also able to adsorb ethanol and water and they can be regenerated at 70°C and 250 mbar. An adsorber for future ECS with high recirculation rates was designed by modeling the adsorption process. The dimensions of this adsorber and the ECS with an increased recirculation air promise an enhanced energy efficiency of future aircraft.

P09

CHITIN PARTICLES ASSEMBLY INTO 3D STRUCTURES

Simone S. Silva[1,2], Ana Rita C. Duarte[1,2], João F. Mano[1,2] and Rui L. Reis[1,2]

[1] 3B's Research Group - Biomaterials, Biodegradables and Biomimetics, University of Minho, Headquarters of the European Institute of Excellence on Tissue Engineering and Regenerative Medicine, AvePark, 4806-909 Taipas, Guimarães, Portugal
[2] ICVS/3B's - PT Government Associate Laboratory, Braga/Guimarães, Portugal

Abstract

Hybrid materials have an immense potential for applications in a variety of advanced technologies, both as structural materials, as well as functional materials in biomedical applications. The sustainable development of hybrid materials is moving towards the use of green chemistry and clean technologies, namely by the use of natural polymers, sol-gel processes, ionic liquids (ILs) and supercritical fluids. In this work chitin-based hybrid 3D structures were prepared by particle agglomeration associating the use of an IL and a sol-gel process. Modified particles were produced dissolving chitin in an IL and precipitating the solution in a bath containing tetraethylorthosilicate/water/ethanol/hydrochloric acid.

Particle agglomeration was promoted by critical point drying as particles were loaded and pressed in a mould together with a gellan gum solution which enhanced the agglomeration and provided mechanical strength to the system. Chitin-based materials were characterized in terms of their structure by FTIR, crystallinity, morphological by scanning electron microscopy (SEM) and by micro-computed tomography. The mechanical properties were assessed in compression mode. The findings suggest that this strategy is feasible and advantageous to process hybrid chitin 3D matrices with both functional and structural characteristics that make then suitable for regenerative medicine applications.

P10

POLYMER-DERIVED SI-C AEROGELS

Emanuele Zera[1], Renzo Campostrini[1], Yigal Blum[2], Parakkulam Ramaswamy Aravind[3], Gian Domenico Soraru[1]

1. *Dept. of Materials Engineering, University of Trento,Trento, Italy*
2. *SRI International, Menlo Park, CA, USA*
3. *Inst. of Material Physics in Space,German Aerospace Research Centre, Köln, Germany*

ABSTRACT

SiC aerogels, due to the exceptional high temperature stability, even in harsh environments, could find application in different fields such as ultra-high temperature insulation materials, filters for chemical separation, catalyst supports etc. Unfortunately, synthesis of highly (meso)porous SiC is not an easy task: it can be obtained from organic-modified silica xerogels via high temperature carbothermal reduction or by casting liquid polycarbosilane into a sacrificial template.

We have recently shown that it is possible to crosslink a preceramic polymer (polysiloxane) into a highly diluted solution to produce a **pre**-ceramic aerogel which is then converted into the final ceramic SiOC aerogel upon a pyrolysis process in inert atmosphere at high temperature [1]. In the present work we apply this novel method to the synthesis of a polycarbosilane aerogel and to its pyrolythic conversion in the corresponding Si-C aerogel.

The crosslinking of the starting polycarbosilane (SMP-10 Starfire) is performed through hydrosilylation reaction in a highly diluted solution, using divinylbenzene (DVB) as crosslinker. The wet polycarbosilane network is supercritically dried using CO_2. Finally, the polymeric aerogel is fired in controlled atmosphere up to 1500°C. Si-C aerogels having a density as low as 0.17 g/cm^3, total porosity above 90 vol%, SSA of 500 m^2/g and a micro-meso pore volume of 0,60 cm^3/g have been obtained.

[1] G. D. Sorarù, F. Dalcanale, R. Campostrini, Amélie Gaston, Y. Blum, S. Carturan, P. R. Aravind, *Novel Polysiloxane and Polycarbosilane Aerogels via Hydrosilylation of Preceramic Polymers*, J. M

P11

AEROGEL DRYING EQUIPMENT

Ruiz-González F., Français E., Clavier JY.

SEPAREX Champigneulles (France)

ABSTRACT

Aerogel-like materials have been processed worldwide from laboratory to semi-industrial scale. However, both of them possess completely different and particular issues towards to obtain high quality crack-free Aerogels.

Therefore, this poster aims to define the most common issues for the two main supercritical drying processes as well as to report the most suitable solution for each of them:

High Temperature Supercritical Drying (HTSCD): The gelation solvent is pressurized and heated beyond its critical point and then directly vented slowly. Obviously, this requires relatively high temperature (i.e.